CZECH UNIVERSITY OF LIFE SCIENCES PRAGUE

Faculty of Agrobiology, Food and Natural Resources

Department of Soil Science and Soil Protection

Stable thallium isotope systematics in natural geosystems

Doctoral Thesis

Author: Ing. Kateřina Vejvodová

Supervisor: doc. RNDr. Aleš Vaněk, Ph.D.

Co-supervisor: doc. Ing. Ondřej Drábek, Ph.D.

Prague 2023

Declaration

I declare that the doctoral thesis “Stable thallium isotope systematics in natural geosystems” is my own work that I have conducted under the supervision of my supervisor doc. RNDr. Aleš Vaněk. All literature cited in this doctoral thesis are listed in the References.

In Prague on 14. 02. 2023

Ing Kateřina Vejvodová

Acknowledgements

I would like to thank my supervisor, doc. RNDr. Aleš Vaněk and co-supervisor doc. Ing. Ondřej Drábek, Ph.D, for all their patience, input, advice, constructive criticism and support throughout my Ph.D. You gave me the opportunity to explore a new field and I have learnt and grown a lot and am extremely grateful for this experience. I also want to thank everyone at the Department of Soil Science and Soil Protection for being a second family to me and for helping me throughout my journey. To my Soilmates, thank you for all the laughter and fun we have had, CPR will never be the same again. I would also like to thank the external group of people who have been part of the published works, without you, this would not have been possible.

Lastly, I would like to thank my family, partner and friends for whom I am eternally grateful. Thank you for supporting me throughout this crazy journey, being there to support my achievements and being a shoulder to cry on when things got too overwhelming. You have been my biggest supporters and without you, I would not have gotten to where I am now.

Table of Contents

1. Theory

1.1. Introduction

Sir William Crookes accidently discovered thallium (Tl) in 1861 when burning dust from a sulphuric acid industrial plant and observed a green spectral band. The name derives from 'thallos' which translated from Latinized Greek means a green shoot, a resemblance of the bright green spectral band observed by Crookes (Galván-Arzate and Santamaría, 1998). Thallium is a post-transition element with an atomic number of 81 and a mass of 204.37. It is an extremely toxic trace element, whose mobility, availability and bio-accessibility can lead to severe side effects to plants and animals (Galván-Arzate and Santamaría, 1998; Migaszewski and Gałuszka, 2021). It can also be classified as a heavy metal due to its density of 11.83 g/cm^3. In its purest form, Tl is found to be soft, odourless and tasteless, with a blue-white hue. Nevertheless, when it is found admixed with other substances, it can be found as yellow, colourless or white (Peter and Viraraghavan, 2005). The toxicity of Tl has been compared to that of Pb, Cd and in some cases, to Hg (Kemper and Bertram, 1991). Nevertheless, the attention given to Tl compared to that of other toxic elements is much less, especially in the past, mostly due the lack of technology with high precision Tl measurements. The development of a high precision (mass) spectrometer that could finally detect Tl in samples emerged in the end of the 20th century, thus creating and influx of research that focused on Tl in a wide range of environments and samples, and later on, focused on Tl isotopes. The research focused on Tl brought novel insights into its geochemistry, how the element behaves in different environmental compartments, and the factors that controls its mobility and isotopic fractionation, etc. The theory presented here within, looks at some of the discoveries that were made in the past two decades that were focused on Tl in industrial processes, and its behaviour in soils and plants and at the soil-plant interface(s).

1.2. Thallium toxicity

The Environmental Protection Agency classifies Tl as a priority pollutant. The approximate biological half-life of Tl is 3-8 days and is usually released from the body through urine (Zitko, 1975). That being said, Tl can enter the body via ingestion of contaminated food or via skin and mucous membranes and is then easily distributed throughout the body of animals and tends to

accumulate in the bones and central nervous system (Peter and Viraraghavan, 2005; Cvejtko et al., 2010). Thallium is believed to bind to sulfhydryl groups of proteins and mitochondrial membranes that lead to the inhibition of various enzyme reactions and causes Tl poisoning (Peter and Viraraghavan, 2005). Mulkey and Oehme (1993) suggested that the toxic effects of Tl were caused by the interaction with riboflavin, inhibition of cellular respiration, distribution of Ca homeostasis, and ligand formation with protein sulfhydryl groups. One of the proven methods of Tl toxicity is connected to the K-Tl relationship (described in section 1.4), where monovalent Tl can easily imitate the biological behaviour of K ions, and therefore substitutes K in the ATPase, pyruvate kinase, and stabilization of ribosomes (Peter and Viraraghavan, 2005). Signs of Tl poisoning were reported as vomiting, diarrhoea, hair loss, and distress to the nervous system and organs. In cases of acute Tl poisoning, people were observed to suffer from alopecia, gastroenteritis and polyneuropathy (Kazantzis, 2000). The organs that suffers the most from Tl intoxication are the central and peripheral nervous system (Kemper and Bertram, 1991). In one part of the world, where people suffer from chronic Tl toxicity, as a result of 350 years of mining, they show symptoms of headaches, abdomen/upper arm/thigh pain, anorexia, alopecia and in some cases, blindness (Zhang et al., 1998). In both cases of acute and chronic Tl toxicity, there have been cases that have led to death; however, this is usually not always the case thanks to successful therapies being developed in the second half of the 20th century.

1.3. Thallium uses

Since its discovery and up until the mid-20th century, there were 150 uses and applications of Tl listed in the cumulative index of 'Chemical Abstracts' (Peter and Viraraghavan, 2005). Such uses included the addition of Tl to rodenticides and insecticides, uses in the medical field to treat ringworms, syphilis, venereal diseases, malaria, and tuberculosis (Nriagu, 1998; Kazantzis, 2000). Consequently, the use of Tl in such cases is extremely dangerous due to Tl poisoning. Thallium salts were also used in many homicidal cases and in cases of illegal abortions (Kazantzis, 2000). Due to the detrimental health effects to many organs and especially the nervous system (Cvejtko et al., 2010), over time Tl was removed from such products and treatments. Currently, Tl is used in the manufacturing of semiconductor material, low-temperature thermometers, scintillation counter for radioactivity quantitation, low freezing alloys, antifriction alloys, low-melting special glasses, photocells, high-temperature superconductor materials, and/or cardiovascular imaging (Nriagu, 1998; Kazantzis, 2000; Karbowska, 2016; Belzile and Chen, 2017).

1.4. Thallium in the environment

Thallium has two oxidation states, monovalent and trivalent, however, in most environmental conditions, monovalent Tl is predominant (shown in Fig. 1) (Rader et al., 2018). In cases of extremely oxidising conditions, the formation of Tl(III) species could arise (Peter and Viraraghavan, 2005; Belzile and Chen, 2017; Migaszewski and Gałuszka, 2021). Examples of monovalent Tl are Tl_2O, Tl_2S and Tl_2SO_4, and trivalent Tl examples are Tl_2O_3, $TlCl_3$, and $Tl(OH)_3$ (Lin and Nriagu, 1999). The Goldschmidt geological classification of Tl is as a chalcophile. However, the chemistry of Tl allows it to display both chalcophilic and lithophilic behaviours, with the latter behaviour more predominant in the environment. The lithophilic behaviour of Tl, is mainly associated with its analogy to K, due to their similar ionic radii (1.59 Å for Tl and 1.51 Å for K), which has causes Tl to interfere with the K cycle.

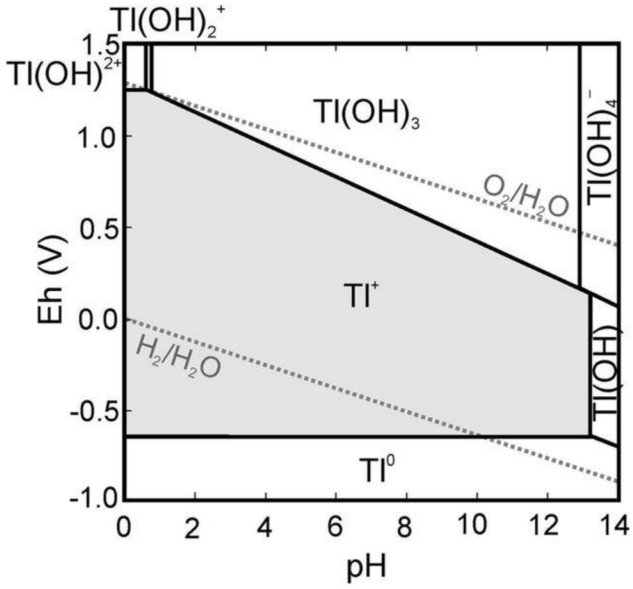

Figure 1. Eh-pH diagram of Tl-O-H systems (source: Migaszewski and Gałuszka, 2021; compiled from Davies et al., 2016 and Xu et al., 2019)

In the environment Tl is naturally found with a mean Tl concentration in the Earth's crust ranging between 0.1-1.7 mg/kg, usually associated with sulphides ores and in coal (Kazantzis, 2000). In silicates, Tl can range from 0.-2.0 mg/kg and in igneous rocks from 0.05-1.8 mg/kg, while in organic-rich shales Tl was found to reach concentrations up to 1000 mg/kg (Kazantzis, 2000; Kabata-Pendias and Pendias, 2011). A few places in the world identified having naturally high levels of Tl and were part of historic and in some cases, present day sulphide ore mining. Examples of such localities are Lanmuchang (China), Allchar (North Macedonia), Iron

Mountain (USA), Buus (Switzerland), Olkusz (Poland) and Tuscany (Italy) (Migaszewski and Gałuszka, 2021). Thallium can be found incorporated into the structure of minerals via redox reactions, sorption or substitution of cations (examples of minerals are listed in Table 1). Lorandite and Crookesite are minerals with extremely elevated concentrations of Tl, where Tl levels can reach up to 60% (Kazantzis, 2000).

In general, Tl is mostly associated with specific sulphides, namely pyrite (FeS_2), galena (PbS), sphalerite (ZnS), chalcopyrite ($CuFeS_2$), realgar (As_4S_4), specific Mn-oxides and silicates, such as biotite ($K(Mg,Fe)_3AlSi_3O_{10}(OH)_2$), muscovite ($KAl_2(AlSi_3O_{10})(OH)_2$), K-feldspar ($KAlSi_3O_8$), illite ($(K,H_3O)(Al,Mg,Fe)_2(Si,Al)_4O_{10}((OH)_2,(H_2O))$) and jarosite ($KFe_3(SO_4)_2(OH)_6$) (Nriagu, 1998; Kaplan and Mattigod, 1998; Peter and Viraraghavan, 2005; Karbowska, 2016; Garrido et al., 2020; Aguilar-Carrillo et al., 2020; Lin et al., 2020; Đorđević et al., 2021; Zhuang et al., 2021; Migaszewski and Gałuszka, 2021).

While the sources of Tl can be both geogenic and anthropogenic, geogenic inputs account for a small part of the overall inputs. Anthropogenic Tl was found with concentrations reaching up to thousands of mg/kg (Xiao et al., 2004; Cabala and Teper, 2007; Bačeva et al., 2014; Wei et al., 2020). The most important anthropogenic Tl sources in the environment include sulphide ore mining, ferrous and non-ferrous metallurgy, cement production and industrial coal combustion (Peter and Viraraghavan, 2005; Karbowska et al., 2018). Generally, in soils, geogenic Tl is usually found to be incorporated with aluminosilicates, whereas anthropogenic Tl is potentially more mobile in the soil (Al-Najar et al., 2005; Yang et al., 2005; Lin et al., 2020).

The fate of Tl can depend on a magnitude of factors ranging on the speciation of Tl, type of source(s), the sink(s), soil properties, plants, climate, and microorganisms. Plants can change the soil properties in the rhizosphere that can potentially (im)mobilise Tl, or uptake Tl. Changes in climate (including rainfall) can affect soil properties (eg. pH, OM content) and the leaching of elements. Microorganisms can also alter the soil properties, which can in turn affect the fate of Tl. An overview of the main geochemical processes that control Tl in the environment and the pathways from source to human can be seen in Fig. 2.

Table 1. Examples of Tl bearing minerals

Tl minerals	Chemical formula
Hutchinsonite	$TlPbAs_5S_9$
Lorandite	$TlAsS_2$
Urbanite	$TlAs_2SbS_5$
Crookesite	$Cu_7(Tl,Ag)Se_4$
Bernardite	$TlAs_5S_8$
Pierrotite	$Tl_2(Sb,As)_{10}S_{16}$
Carlinite	Tl_2S
Avicennite	Tl_2O_3
Jarosite	$KFe^{3+}_3(SO_4)_2(OH)_6$
Pharmacosiderite	$KFe_4(AsO_4)_3(OH)_4 \cdot H_2O$
Thalliomelane	$Tl(Mn^{4+}_{7.5}Cu^{2+}_{0.5})O_{16}$
Dorallcharite	$(Tl,K)Fe^{3+}_3(SO_4)_2(OH)_6$
Lanmuchangite	$TlAl(SO_4)_2 \cdot 12H_2O$
Ellisite	Tl_3AsS_3
Jankovicite	$Tl_5Sb_9(As,Sb)_4S_{22}$
Picotpaulite	$TlFe_2S_3$
Rebulite	$Tl_5Sb_5As_8S_{22}$
Simonite	$TlHgAs_3S_6$

Note: compiled from Balić-Žunić et al. (1994), Nraigu, (1998), Boev et al. (2001-2002), Daiyan et al., (2003), Herrmann et al. (2018), Aguilar-Carrillo et al. (2020), Đorđević et al. (2021), Gołębiowska et al. (2021), Zhao and Gu (2021) Migaszewski and Gałuszka, (2021).

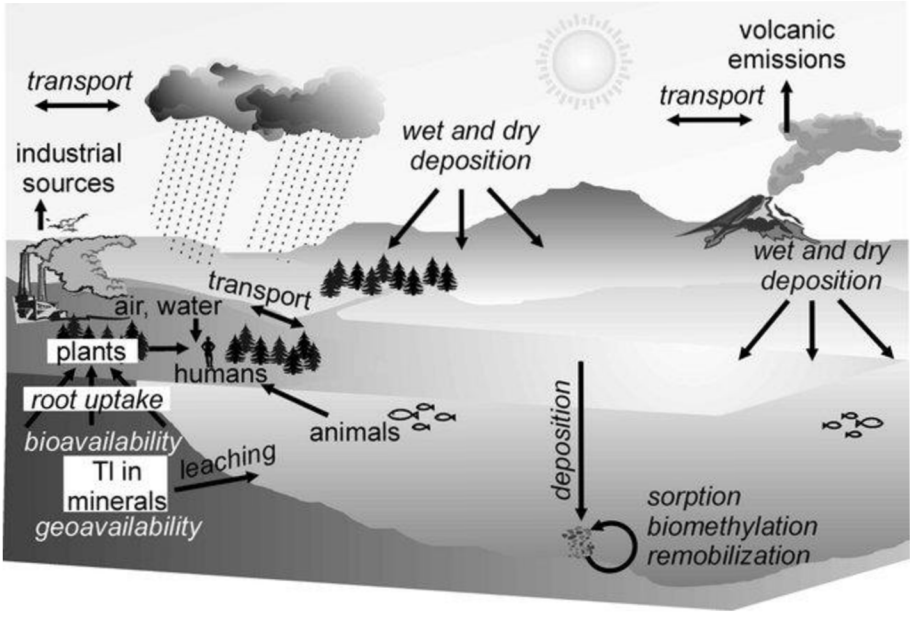

Figure 2. The main sources and geochemical processes that control Tl in the environment (source: Migaszewski and Gałuszka, 2021)

1.5. Stable Tl isotopes

1.5.1. Determination of Tl isotopic ratios

Thallium has two stable isotopes, with atomic masses of 203 and 205, with the abundances of ~30% and 70%, respectively (Fig. 3), and varying ratios in the environment, which are shown in Fig. 4 (Nielsen and Rehkämper, 2012; Nielsen et al., 2017).

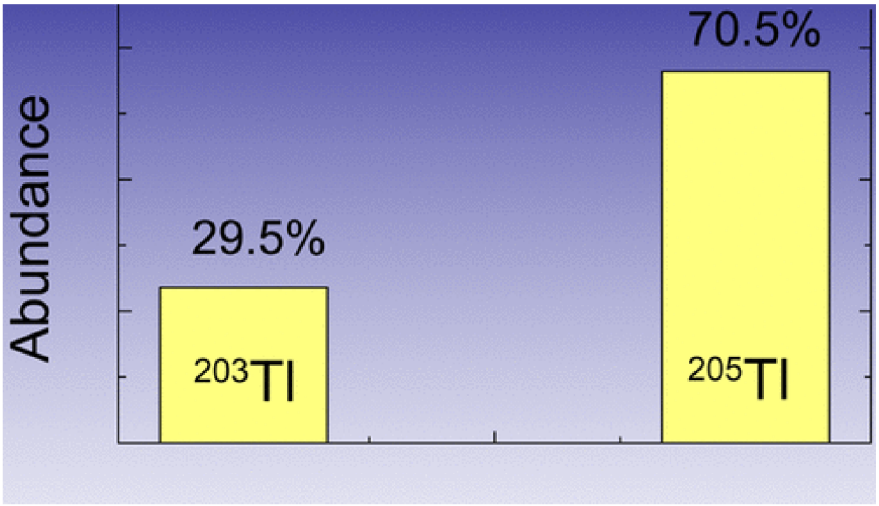

Figure 3. Abundance of stable Tl isotopes (source: Kersten et al., 2014)

Before the development of the multiple collector inductively coupled plasma mass spectrometry (MC-ICP-MS), Tl stable isotopes could not be precisely determined. The determination of Tl isotopes using thermal ionization mass spectrometry (TIMS) was not possible, due to its lack of precision and due to Tl only having two stable isotopes. It was only in the late 90s when Tl isotopes were first measured by Rehkämper and Halliday (1999) using multiple collector inductively coupled plasma mass spectrometry (MC-ICP-MS). The authors had created a novel chemical and mass spectrometric procedure that finally led to the measurements of Tl isotopes in environmental samples.

The high-precision MC-ICP-MS is capable of recognizing small variations in stable isotope compositions of Tl in different environmental samples. Once measured, the Tl isotopic ratio ($^{205}Tl/^{203}Tl$) in the sample is then calculated relative to the reference material NIST SRM 997 (National Institute of Standards and Technology) ($\varepsilon^{205}Tl = 0$). External normalization/standard sample bracketing (NIST SRM 997) is then used in order to eliminate the mass bias drift. The $^{208}Pb/^{206}Pb$ ratio is commonly used for internal correction of the raw $^{205}Tl/^{203}Tl$ ratio.

The isotope composition is then calculated using the following equation (eq.1):

Equation 1. Calculation of Tl isotope composition

$$\varepsilon^{205}Tl = 10^4 \times ({}^{205}Tl/{}^{203}Tl_{sample} - {}^{205}Tl/{}^{203}Tl_{NIST997})/({}^{205}Tl/{}^{203}Tl_{NIST997})$$

For Tl stable isotopes, the ε-notation (variations in parts per 10,000) is used because the Tl isotopic system was first created as a cosmochemical radiogenic isotope system (Nielsen and Rehkämper, 2012; Nielsen et al., 2017). The ε-notation also proves useful with regards to the variability of stable Tl isotope ratios, as data are presented usually as whole figures with only one decimal point. The ε-notation also allows for the comparison between terrestrial and cosmochemical data.

Before the samples can be measured precisely by the MC-ICP-MS, the sample must be subjected to a separation process where Tl must be isolated and any Pb in the sample must be removed in order to not interfere with any results. The separation process method has been described by Rehkämper and Halliday (1999). Nonetheless, with time, modifications have been made to the method (described in chapter 3.1.2) by Nielsen et al. (2004, 2007) and Baker et al. (2009). The separation processes for separating Tl from the sample matrix is dependent on trivalent Tl in acidic conditions to produce anionic complexes with halogens (Cl^- or Br^-) which can partition to anion exchange resins. Therefore, the samples must be prepared in oxidising conditions by adding water saturated in Br_2 to the digested samples, in order to make sure that all the present Tl is in the trivalent state. The Tl-rich sample is then washed with different acids until Br_2 is no longer present. The last step of the separation involves the removal of Tl from the resin using reducing agents (0.1 M HCl with dissolved SO_2 gas) (Nielsen et al., 2004, 2007; Baker et al., 2009; Nielsen and Rehkämper, 2012).

1.5.2. The use of Tl stable isotopes

The interest in Tl has led to the formation of an isotope-based source identification, allowing to distinguish the source and pathway of an element into the studied environment with the use of mixing models, especially in scenarios with more than one source. However, such mixing models cannot be used to provide data on the precise contributions of multiple anthropogenic sources, as sometimes more sources or processes can blur the source signals, making it harder to identify the exact source input. For more than two decades, Tl isotopes and isotopic

composition have been successfully studied in a range of different environments, including marine environments, soils, plants, and industrial wastes (Nielsen et al., 2004, 2005, 2006a, 2006b, 2006c, 2007, 2009, 2017; Rehkämper and Nielsen, 2004; Prytulak et al., 2013; Kersten et al., 2014; Vaněk et al., 2016, 2018, 2019, 2020, 2021, 2022; Vejvodová et al., 2020).

The aforementioned studies on Tl stable isotopes has provided an insight into Tl behaviour and its isotopic fractionation that it undergoes in different environmental compartments and related geochemical processes. This could help in our understanding, namely where Tl can come from or which type of mechanisms tend to affect its environmental/industrial cycles, etc. (Kersten et al., 2014; Wang et al., 2021). The environmental processes noted to cause variations in the isotopic ratios between environmental samples are evaporation/condensation, redox processes, dissolution/precipitation, adsorption/desorption, and biological cycling (Wiederhold, 2015; Vaněk et al., 2016; Liu et al., 2020a, 2020b). In soils and plants, Kersten et al. (2014) conducted the first study involving the use of Tl isotopes to provide useful insights into the origins (anthropogenic/geogenic) of Tl in soils and plants.

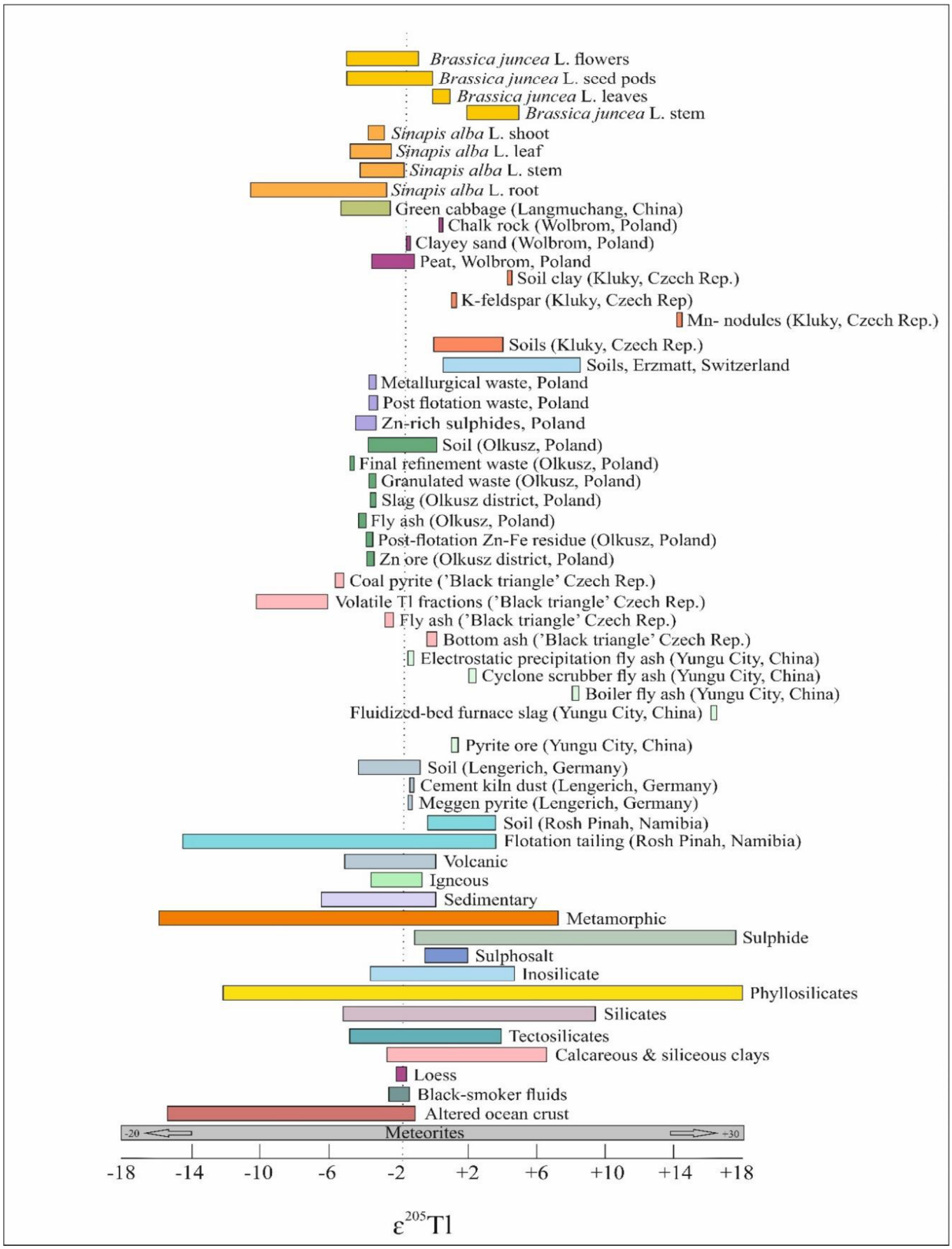

Figure 4. Thallium isotopic variations in different geological/industrial reservoirs. The dashed line $\varepsilon^{205}Tl = -2$ depicts the Tl isotopic composition of the Earth's mantle. Adapted and modified from Kersten et al. (2014) with added data compiled from new publications (found in section 7.5)

1.5.3. Stable Tl isotopic fractionation

Isotopic fractionation refers to the 'relative partitioning of the heavy (^{205}Tl) and light (^{203}Tl) isotopes between two coexisting phases (or rocks, solutions, etc.) in a natural system' (Tiwari et al., 2015).

Mass-dependent isotopic fractionation of Tl isotopes may be controlled by both equilibrium and kinetically driven processes; the processes are shown in Fig. 5 (Wiederhold, 2015). Kinetic processes are unilateral reactions that are induced by different reaction rates between the light and heavy isotopes, where the lighter isotope commonly assigns faster reaction rates than that of the heavier one. The remaining reactants (if any) of such processes are isotopically heavier. If no reactant remains, then the reaction displays no isotopic effects or fractionation (Tiwari et al., 2015). Examples of kinetically driven processes are evaporation and diffusion. On the other hand, equilibrium driven processes occur when the two phases can react with forward and backward reactions until an 'equilibrium' is achieved. The isotopic enrichment is controlled by energy difference in the environments where the reaction takes place and reaches isotopic equilibrium. In stronger bonding environments, the compounds are usually enriched with heavy isotopes (Wiederhold, 2015).

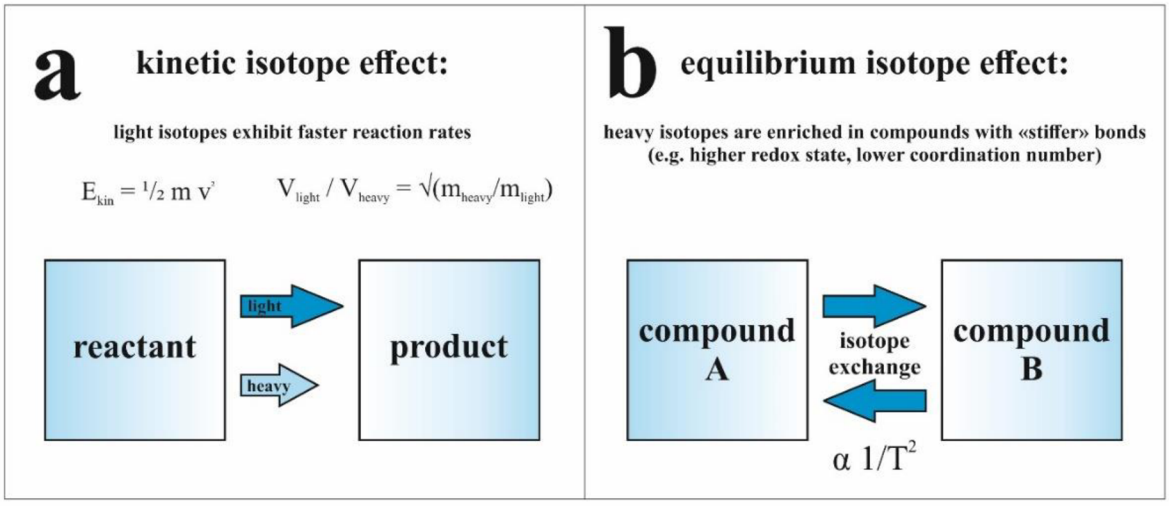

Figure 5. A schematic illustration of kinetic and equilibrium stable isotope fractionation (source: Wiederhold, 2015). E_{kin}= kinetic isotope effect of an element; m = isotopic mass; v = velocity; T = temperature

Rayleigh models are used to determine the factors that control fractionation in different processes or to quantify magnitude of transformation based on the isotope data. The Rayleigh model is typically used to explain the change of isotope ratios in reactions that are unidirectional and incomplete.

Thallium isotopic fractionation can be controlled by redox conditions and bonding environments. For example, in a highly oxidising environment, Tl(I) can oxidise to Tl(III), which is found to lead to the enrichment of ^{205}Tl isotope in Mn(III,IV)-oxides (especially birnessite ($K_4Mn_{14}O_{27}\cdot 9H_2O$)) and ferromanganese nodules and crusts, however, Fe(III)-oxides probably do not significantly sorb Tl or even isotopically redistribute it (Peacock and Moon, 2012). Higher ε^{205}Tl values observed by Rader et al. (2018) in sulphides indicate that the presence of covalent bonds and high oxidation states could favour ^{205}Tl.

1.6. Thallium isotopes in industrial wastes

High temperature processes can potentially volatilize Tl compounds, therefore, processes that are associated with, for example, coal combustion, cement production and mining and smelting activities are potential sources of Tl contamination. Such processes can lead to the mobilization of an estimate of 2000-5000 tons of Tl per year (Galván-Arzate and Santamaria, 1998; Kazantzis, 2000; Peter and Viraraghavan, 2005; Antón et al., 2012; Xiao et al., 2012; Kersten et al., 2014; Vaněk et al., 2016). The reason for elevated levels of Tl mobilization is the high concentrations of Tl in coal and sulphides.

The Tl isotopic ratios of each of the individual waste materials are usually unique. Even when studying sulphides, each sulphide from a different region potentially has its own unique Tl isotopic signature, due to different compositions and processing. The high temperature processing that most waste materials are subjected to could result in significant Tl isotope fractionation; however, this is not always the case.

Several studies have looked at slags, fly ashes, Tl-rich ores and more, providing some understanding how Tl fractionates throughout the material processing. Vaněk et al. (2018) studied waste samples from a Zn smelter and found fly ash to be isotopically lighter with ε^{205}Tl -4.1 compared to the slag (ε^{205}Tl -3.3). These results were similar to a previous study that investigated products from coal combustion, where the fly ash was also found to be isotopically lighter (ε^{205}Tl ~ -2.5 to -2.8) compared to bottom ash (ε^{205}Tl ~ 0.0) (Vaněk et al., 2016). The addition of pyrite in coal feed as well as the high temperatures the materials are processed at could be a leading influencer of the emissions of lighter Tl fractions. Vaněk et al. (2016) concluded that such a process is mainly controlled by kinetic fractionation; the same study also demonstrated through a model thermo-desorption experiment using sulphides that around 1% of Tl volatilized at 700°C (ε^{205}Tl -6.2), 4% at 900°C (ε^{205}Tl -10.3), and at 300-900°C there was 78% of Tl condensate (ε^{205}Tl -6.2).

A study by Liu et al. (2020) predicted that the Rayleigh-type fractionation controlled Tl isotopes during pyrite smelting in sulphuric acid production, where great Tl isotopic fractionation was observed between the pyrite ore (ε^{205}Tl ~+1.3) and the waste materials (ε^{205}Tl ~-1.1 to +16.2). The Rayleigh-type fractionation demonstrates the evolution of stable isotopic ratios during 'incomplete unidirectional reactions within a closed system' through fractional distillation (Wiederhold, 2015). It has been suggested that the high temperature causes ^{203}Tl isotope to enter the vapour phase, leaving the ^{205}Tl isotope to become enriched in the slags, through processes of evaporation and condensation leading to isotopic fractionation, with kinetic isotope fractionation as a possible controlling factor (Liu et al., 2020a). During the processing of industrial material, the different temperatures in the different parts of the processing lead to the evaporation/condensation of Tl that accumulates in the different phases, the temperatures also cause Tl isotope fractionation that causes an isotopic variability of the different fly ash samples and waste materials. The reducing particle sizes throughout the processing of materials also leads to an increase in sorption capacity for volatile Tl, thereby enriching fly ash in ^{203}Tl isotopes, while ^{205}Tl isotopes remain enriched in the slag (Chen et al., 2013; Liu et al 2020a).

In a paper written by Zhou et al. (2022), studying Pb-Zn smelting, they observed significant variations in Tl isotopic composition of the raw material (Pb-Zn ore) (ε^{205}Tl -0.87) and different waste materials (ranging from ε^{205}Tl -4.62 to +1.12), these large variations attribute to the possibility of Tl isotopic fractionation during the entire smelting processes. The combination of the results and the application of the Rayleigh fractionation model proved the enrichment of ^{205}Tl isotopes in the waste slags and that volatile fractions formed during high-temperature processes were enriched in the ^{203}Tl isotope (Zhou et al., 2022). However, such fractionation is not always the case, as shown by the results of Vaněk et al. (2018).

1.7. Thallium and Tl isotopes in soil

The Tl presence in soils is attributed to the mineralogy of the parent material, it is generally present as monovalent Tl and can be relatively mobile (depending on soil mineralogy) (Kabata-Pendias and Pendias, 2011). The bioavailability and mobility of Tl is dependent on the soil mineralogy, where the presence of Mn(III,IV)-oxides decreases Tl mobility and Ca-carbonates potentially increasing Tl mobility. Another controlling factor can be the soil pH and quantity and quality of organic matter (OM) present in the soil; lower soil pH can lead to decreased stability of secondary Tl phases which can in turn mobilize Tl, and increased OM in soils has a tendency to accumulate Tl (Grösslová et al., 2015).

The first ever study about Tl isotopes in soils was conducted by Kersten et al. (2014), who laid the foundation for the application of stable Tl isotope ratios as a source fingerprint. Their study produced results showing two Tl pools: one with high Tl concentrations and heavy isotope composition (ε^{205}Tl >-1.0) and one with low Tl concentrations and light Tl isotope compositions (ε^{205}Tl <-3.0). Such results indicate that the heavier Tl isotope composition represents Tl from anthropogenic origins and the lighter compositions from geogenic origins.

In several soils rich in geogenic Tl, an enrichment in ^{205}Tl in the middle zone of the profile was linked to a continuous mobilization and immobilization of Tl that was controlled by the redox cycles involving the parent material and soil forming processes (Rehkämper et al., 2004; Nielsen et al., 2013; Vaněk et al., 2020). The isotopically heavier fractions mobilized during the weathering of Tl(III)-containing phases and systematic redox changes probably led to the enrichment of ^{205}Tl into other phases, such as illite, where Tl(I) was the prevailing Tl form (Vaněk et al., 2020). Figure 6 shows an overview of Tl cycling in soil under the influence of Mn-oxides and clay minerals.

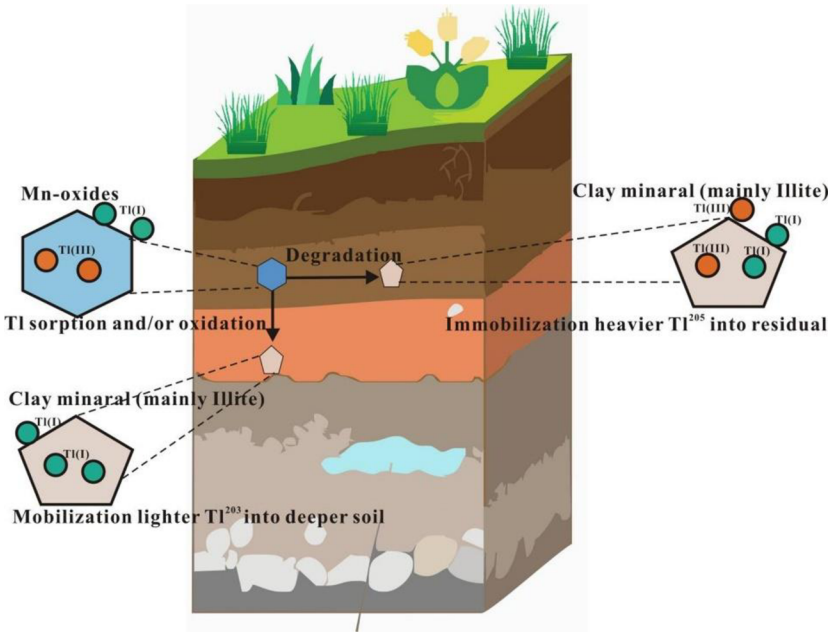

Figure 6. Systematic Mn-oxide degradation Tl cycling in soil (source: Zhong et al., 2022)

Grösslová et al. (2018) observed different soil profiles from an area contaminated with dust from flotation tailings (Zn-Pb ore deposits) and noticed that total Tl concentrations and presence of ^{205}Tl isotope decreased with depth (0.5 to 7.6 mg/ kg Tl; ε^{205}Tl ~-0.4 to +3.8). The upper soil layers displayed a resemblance to the flotation wastes (13 to 27 mg/kg Tl; ε^{205}Tl ~+6.1 to +6.3), therefore confirming the anthropogenic influence on the soil contamination. Liu et al. (2022)

saw similar results, where the Tl isotopic ratio matched with the waste materials of a nearby Pb-Zn smelter. The isotopic compositions of acid wastes (result of removal of SO_2 gas) (ε^{205}Tl -4.6), background sediments (ε^{205}Tl +1.3) and smelter slag (ε^{205}Tl +1.1) (Liu et al., 2020a; Zhou et al., 2022) indicate that the wastes play a major role in Tl input to the sediments (profiles ranging from ε^{205}Tl -3.8 to +2.4).

However, in some cases, there are both anthropogenic and geogenic sources of Tl into the soils, which can clearly be seen when observing the Tl isotopic compositions or soils, bedrocks, and waste materials. A study by Vaněk et al. (2018) displayed variations in the Tl isotope signature between the upper and lower horizons, with ε^{205}Tl increasing with depth. The soil profile depicted two Tl pools: anthropogenic and geogenic, with a higher predominance of the anthropogenic pool.

1.8. Thallium and Tl isotopes in plants

The Brassica family are proven hyper-accumulators of Tl, while mustard plants and Brake fern also showed Tl accumulating abilities (Xiao et al., 2004; Krasnodębska-Ostręga et al., 2008, 2012; Jia et al., 2013; Holubík et al., 2020; Wei et al., 2020). The species that have been studied and proven to translocate Tl are *Sinapis alba* L., *Iberis intermedia* L., *Brassica napus* L., *Biscutella laevigata* L., *Brassica oleracea* L. *var. capitata* L. (Tremel et al., 1997; Xiao et al., 2004; Al-Najar et al., 2003, 2005; Scheckel et al., 2004, 2007; Krasnodębska-Ostręga et al., 2012; Jia et al., 2013; Grösslová et al., 2015; Ning et al., 2015; Liu et al., 2017, 2020b; Vaněk et al., 2010, 2011, 2013, 2015, 2019, 2020; Holubík et al. 2020, 2021).

In several studies plants were observed to preferentially uptake of Tl compared to that of Hg and As. Reasons behind such results could be because of the affinity Tl has to K, where Tl is mistaken for K during uptake, higher bioaccessibility of Tl in (Xiao et al., 2004; Grösslová et al., 2015; Rader et al., 2019). Higher concentration of Tl in plants can be explained by the high Tl levels around the plant rhizosphere, with the mobility controlled by many factors including water, pH, organic matter, mineralogy, speciation and cation exchange capacity.

The predominance and plant availability of Tl(I) in soils leads to the accumulation of the lighter Tl isotope by plants, with possible fractionation during translocation from roots to above ground biomass (Kersten et al., 2014; Vaněk et al., 2019). The pioneering study by Kersten et al. (2014) on Tl isotopes in plants showed an enrichment of light Tl isotopes in the soil-root interface, but that there was further fractionation along the translocation pathway from the roots (ε^{205}Tl -2.5)

to the young leaves (ε^{205}Tl -5.4). However, Vaněk et al. (2019) observed the opposite Tl isotope shifts, where translocation lead to heavier Tl isotopes in the shoots (ε^{205}Tl <-2.5) compared to the roots (ε^{205}Tl <-5.9). A possible explanation for the heavier Tl isotopes in the above ground biomass could be due to the role of K^+ in the Tl cycle, Tl(I) complexation by specific organic ligands or association with S-coordinated Tl(I) (Vaněk et al., 2019).

Rader et al. (2018) studied Indian mustard plants and observed heavier Tl isotope in the beginning stages of plant growth (ε^{205}Tl ~+2.5) compared to later stages, such as flowering (ε^{205}Tl ~-0.2 to -1.8). The results allow to observe the level of translocation that occurs within the plant during plant growth, with biological processes that occur during the plant development controlling the isotopic patterns (Rader et al., 2019).

The clear differences between the Tl isotopic compositions in plants display the heterogeneity of the behaviour and fractionation of Tl, and stress the influence of the growing medium, Tl concentrations and origins in the growing medium, and the plant species.

1.9. Thallium in organic environments

Peats are well known scavengers of trace elements, being one of best archives for atmospheric depositions (Cabala et al., 2013; Shotyk and Krachler, 2004; Smieja-Król et al., 2015, 2019). Little is known about Tl in peatlands, with even less information concerning Tl isotopic behaviour. Studies have shown that Tl is immobile in peat, allowing researchers to predict the sources of Tl into the peat (Shotyk and Krachler, 2004). The lack of Tl in the bottom layer of the peat indicates little to no influence of the mineral dissolution on Tl concentrations in the peat profile. High enrichment factors of Tl can only be associated with anthropogenic deposition from the industrial periods, which is usually in the older layers of the peat profile, where Tl is immobile. Smieja-Król et al. (2015) observed Tl immobilization within the peat profile through precipitation of sulphide and due to strong correlations between Tl and Zn, Tl co-precipitated with Zn.

Trends in Tl concentrations and enrichments along with sample dating in peats clearly correlate with the industrials activities occurring within the time frame, thanks to the peat's ability to preserve Tl within the layers. Mihaljevič et al. (2020) have confirmed such data, where Tl values within a peat profile significantly increased during periods of industrial activities in the mid 20th century and then decreased due to cleaner technologies.

2. Hypotheses and aims

2.1. Hypotheses

(I) There is a link between Tl soil chemistry/soil processes and Tl isotopic fractionation. Thallium isotopic signatures can be used as a proxy for redox controlled processes in soil.

(II) Thallium has limited mobility in peat profiles. Therefore, peat/organic environments can potentially be used as an archive for monitoring historical/atmospheric Tl deposition.

(III) Stable Tl isotopic ratios in sulphides and materials derived by high temperature sulphide processing can potentially be used for tracing sources of Tl contamination, i.e., in cases where the signatures between anthropogenic and geogenic Tl significantly differ.

2.2. Aims

The aim of this thesis is to obtain a clearer and more comprehensive set of information on the behaviour and interactions of stable T1 isotopes within the natural geosystems. The focus is on understanding the geochemical cycle of Tl and tracing Tl contamination using stable Tl isotopic ratios ($^{205}Tl/^{203}Tl$). The following aims were set in place:

(I) Understanding the key controls of Tl behaviour in soils

Fulfilled in the published paper in section 7.1.

(II) Tracing Tl contamination and stable Tl isotopes in soils and peat bog deposits

Fulfilled in the published papers in sections 7.1 and 7.2.

(III) Assessment of the role of peat constituents in post-depositional Tl dynamics

Fulfilled in the published papers in sections 7.2 and 7.4.

(IV) Verification of Tl geochemistry in a peat bog - A model experiment

Fulfilled in the published paper in section 7.4.

(V) Assessment of the behaviour of stable Tl isotopes throughout metallurgical processes

Fulfilled in the published paper in section 7.3.

3. Methodology

The study area focuses on one study area within Czech Republic and one study area in Poland. The study area in Czech Republic is Kluky and the study area in Poland is located in the districts of Miasteczko Ślaskie and Olkusz. Kluky, located in Southern Bohemia, is characterized by moderate Tl concentrations in soils derived from Tl-rich Paleozoic granites. The Miasteczko Ślaskie and Olkusz districts, in the Silesia–Krakow region (Poland) can be briefly characterized by historical mining and processing of Zn–Pb ores. Extreme concentrations of Tl and other trace elements were observed in the forest floor humus or the upper soil layers at the site (Cabala & Teper, 2007; Vaněk et al., 2013) and up to 30 mg/kg for Tl was detected in the peat layers (Cabala et al., 2013; Smieja-Król & Bauerek, 2015). A set of Zn-rich sulphide concentrates and selected processing wastes were obtained from a hydrometallurgy of Zn that were obtained from a MVT ('The Mississippi Valley'-type) deposit located in Olkusz, Poland, Lisheen, Ireland and Pinargozu, Turkey, that were processed in a Boleslaw Zn smelter in Poland.

To understand the relationship between peat matter, sulphide weathering and Tl release, a model pot experiment was set up (details can be found in the published work in chapter 4.4). Store bought peat was used throughout the experiment and sulphide waste material from the Boleslaw Zn smelter was placed into double layered polyamide bags (NITEX 03-1/1, Sefar AG, Switzerland; 3 × 3 cm inner bag and 5 × 5 cm outer bag, mean mesh size of 1 cm) and placed 1 cm below the peat surface. The pots were fit with a Rhizon pore water samplers (Rhizosphere Research Products, the Netherlands) to collect pore water samples. The pots were subjected to watering with either synthetic rainwater or deionized water to maintain 70% of water holding capacity. Pore water samples were collected using a surgical needle and a 9mL vacuum collection test tube (Vacuette, Greiner Bio-One GmbH) after 1, 2, 3, 4, 6, 8 and 12 weeks.

3.1. Characteristics of soils, peat and waste materials

3.1.1. Sample characterisation

In Table 2, an overview of the analyses done on all soil, peat and waste samples can be found. The analysis were done in accordance to the cited methodologies and detailed descriptions can be found within the published papers in chapter 7. Many of the analyses were done in replicates in order to ensure the accuracy of the results obtained. Certified reference materials ensured the quality control of the chemical analyses; detailed data are presented in individual published

papers. Soil and peat samples were collected according to soil horizons and peat layers, as well as parent material and other soil fractions. Waste samples from the Zn smelter included waste materials ranging from ZnS concentrates, sludges and smelter feed.

Table 2. An overview of physiochemical analysis conducted on soils, peat and waste material

Physicochemical		
	Method	**Sample**
pH	H_2O (1/5 v/v) (Handylab pH 11 multimeter, Schott, Germay) KCl (1/5 v/v) (Handylab pH 11 multimeter, Schott, Germay)	S, P
Total C/S	CNS analyser (Flash, 2000; Thermo Fisher Scientific, Germany)	S, P
Cation exchange capacity (CEC)	Sodium acetate method (Bower et al., 1954), AAS (280FS, Varian, Australia) $BaCl^2$ extraction (ISO 11260:1994), ICP-OES (Thermo Scientific iCAP 7000)	S, P
Acid oxalate extractable	0.2 M ammonium oxalate/oxalic acid (Pansu and Gautheyrou, 2006), ICP-OES (Thermo Scientific iCAP 7000)	S
Total elemental concentration	Digestion in mixture of acids (HNO_2, HCl, HF), Q-ICP-MS (Xseries II, Thermo Scientific, Germany)	S, P, W
Exchangeable fraction	1M NH_4NO_3 (1/10 S/L ratio, ICP-OES (Thermo Scientific iCAP 7000)	S, P
Particle size distribution	Sedimentation process (Gee and Bauder, 1986)	S
Ash content	Combustion of 1g sample at 550 °C	P
Age dating	^{210}Pb γ spectroscopy (Canberra DSA 2000 multichannel analyser) ^{14}C (EnvironMICADAS compact tandem accelerator)	P
Mineralogical		
	Method	**Sample**
Identify sample composition/mineralogy	X-ray diffraction (XRD) (X'Pert Pro diffractometer, PANalytical, the Netherlands)	S, W
Images	Scanning electron microscopy (SEM) (Tescan Vega, Czech Rep.)	W
Quantitative microanalysis	Electron probe microanalysis (EPMA) (JEOL JXA-8530F, Japan)	W
Tl speciation	X-ray absorption near edge structure (XANES) spectroscopy (Tl L_{III}-edge, SUL-X beamline)	W

Note: S- soil, P- peat, W- waste material

3.1.2. Isotopic analysis and measurement

In order to determine Tl isotopic ratios within a sample, the Tl must be isolated from the dissolved sample matrix. The sample undergoes a three-stage chromatographic separation involving an anion exchange resin (Bio-Rad AG1-X8, 200–400 mesh, Cl^-cycle) that was adapted from the procedure described by Baker et al. (2009). The procedure involves evaporating and then re-dissolving the sample in 0.1 M HCl. Afterwards, Br_2 was added to the sample solution so that the reagent had a final concentration of 1% (v/v) and the sample was left overnight in order for Tl(I) to oxidise to Tl(III). The chromatography uses resin-filled columns with different reagent mixtures and volumes flowing through it, as such:

i) 5 × 1 mL 0.1 M HCl-SO_2 + 5 × 1 mL 0.1 M HCl, resin cleaning
ii) 5 × 2 mL 0.1 M HCl-1% Br_2, resin treatment; sample loading (0.1 M HCl-1%Br_2)
iii) 10 × 2 mL 0.01 M HCl-1% Br_2
iv) 6 × 2 mL 0.5 M HNO_3-1% Br_2
v) 6 × 2 mL 2 M HNO_3-1% Br_2
vi) 6 × 2 mL 0.1 M HCl-1% Br_2
vii) 15 × 2 mL 0.1 M HCl-SO_2, Tl/Pb fraction elution

The obtained Tl/Pb fraction was evaporated and re-dissolved in 200 µL 0.1 M HCl-1% Br_2 (> 12 h), in preparation for the next part of Tl purification. For the second and third chromatographic stage, a PP 1.2-mL micro-column filled with 250 µL of resin was used. Resin cleaning and treatment, as well as sample loading were performed in the same way, with corresponding lower volumes of individual reagent mixtures. Once the final Tl fraction was obtained, the Tl sample was typically evaporated and diluted in 5 mL 2% HNO_3. Thallium and Pb concentrations were monitored after sample dissolution and throughout the Tl separation. Chemicals of ultrapure and suprapure quality (Merck, Germany), and deionized water (MilliQ$^+$, Millipore, USA) were used for the separation techniques.

Multi-collector inductively coupled plasma mass spectrometry (MC-ICP-MS) (Neptune Plus, Thermo Scientific, Germany) with a desolvating nebulizer (Aridus II, CETAC, USA) was used to determine the Tl isotope ratios. All the solutions were measured in 3 runs (50 cycles each). External normalization/standard sample bracketing (NIST SRM 997) was employed to eliminate the mass bias drift. The $^{208}Pb/^{206}Pb$ ratio was used for internal correction of the raw $^{205}Tl/^{203}Tl$ ratios. The Tl isotopic composition was calculated using the following equation with ε notation relative to NIST SRM 997 (Eq. 1, found in section 1.5.1).

4. Discussion

4.1. The key controls of Tl fractionation in soils

While it is understood that any changes in soil properties can affect an element and the fractionation that it may undergo, there are certain properties that have a greater influence than others. Therefore, it is important to understand the behaviour of Tl in soils and investigate the main influencing factors on its mass-dependant isotopic fractionation. There are several geochemical factors that may influence Tl enrichments in soils; two observed factors that controlled Tl enrichment in soils were the presence of micaceous clays (due to K-Tl analogy) and Mn-oxides (due to systematic degradation). Our results showed that an enrichment of isotopically heavier Tl in the middle (A/B) profile zone attributed to the larger abundance of ^{205}Tl in the illite clay (3 mg/kg Tl; ε^{205}Tl ~ +4.6) and Mn-oxide nodules (5 mg/kg Tl; ε^{205}Tl +8.2 to +14, respectively) present in the sample, which underwent redox-reactions (Fig. 7). However, out of the two, the presence of Mn-oxides and its systematic degradation was the main controlling factor for Tl enrichments and fractionation. The relationship between Tl and Mn-oxides and the associated positive effects have been observed by several researchers, especially in ocean (Rehkämper et al., 2002, 2004; Peacock and Moon, 2012; Kersten et al., 2014; Vaněk et al., 2016; 2018; Howarth et al., 2018).

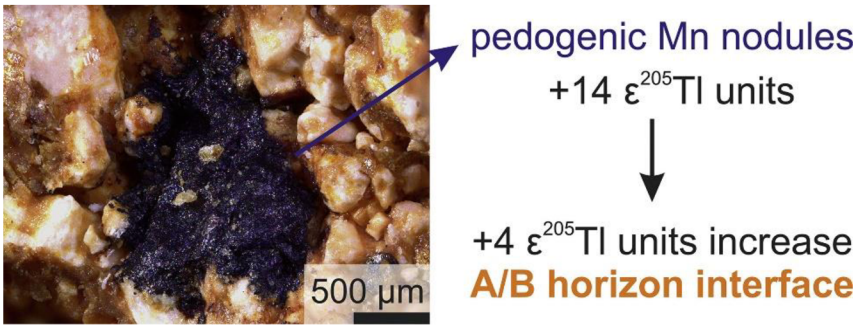

Figure 7. Optical micrograph of Mn-oxide-rich nodule and isotopic composition of the Mn-oxide and the A/B soil horizon

Our results have demonstrated a clear similarity to a previous work by Vaněk et al. 2020, where enrichments of ^{205}Tl in the middle profile were attributed to the presence of Mn(III,IV)-oxide nodules. Manganese oxides are enriched in ^{205}Tl isotopes due to the oxidative Tl sorption. The suggested reasoning behind the fractionation caused by Mn-oxides is the shifts in Tl(I)-Tl(III) (Wiederhold, 2015; Rader et al., 2018). The results also contribute to current research on Mn-

oxides, proving the influence of Mn-oxides on Tl mobility and fractionation in soils. An array of studies have proven the significant role of Mn-oxides on Tl isotope fractionation, where a shift in Tl(I)-Tl(III) or vice versa is the key factor in the isotopic fraction of Tl in soils (Nielsen et al., 2013; Kersten et al. 2014; Wiederhold, 2015; Vaněk et al., 2016, 2018; Howarth et al., 2018; Rader et al., 2018; Vejvodová et al., 2020).

Our results from the published paper in section 7.1 intended to fulfil the first aims: 'Understanding the key control of Tl in soils' and 'tracing Tl contamination and stable Tl isotopes in soils and peat bog deposits'. As mentioned above, the results provided two key controls on Tl: the presence of micaceaous clays and Mn-oxides. The use of Tl isotopes also helped in identifying the source of Tl in the soil.

4.2. Fractionation of Tl in sulphide and industrial processing

The current research covers various waste materials from different high-temperature processes, including ore roasting and coal burning, majority of which confirm the occurrence of Tl fractionation (Liu et al., 2020a). Despite the difference in the waste materials and by-products, the research agrees that during high temperature processing, partial Tl isotopic fractionation can occur, where slags and bottom ash are enriched in ^{205}Tl isotope, while fly ash is enriched in light Tl isotopes, due to kinetic fractionation processes (Vaněk et al., 2016). However, results from the publication in section 7.3 depict otherwise. From a set Tl-rich sulphide concentrates and wastes from a hydrothermal Zn extraction, insignificant Tl isotopic variations between the initial smelter feed- sulphide concentrates and the waste materials were found (despite large variations in Tl concentrations). The results, therefore, show minimum Tl isotopic effects in terms of a total industrial process. Vaněk et al. (2018) observed similar results where there were large differences in Tl concentrations between the waste samples, however, there was minimal isotopic fractionation. This points to little or no influence of gangue mineralization on the Tl isotopic compositions and that the processing of the sulphide ores leads to insignificant Tl isotopic fractionation in that case.

A comparison of ores studied (Table 3.) shows that ores tend to have their own Tl isotopic signature, which is based upon many factors including deposit type, sulphide melt, temperature and original matrix.

Our published paper found in section 7.3 aided in fulfilling the aim to "assessment of the behaviour of stable Tl isotopes throughout metallurgical processes". The paper provided

valuable insights into the fractionation, or lack of fractionation of Tl throughout the metallurgical processes.

Table 3. Examples of Tl isotopic signatures of waste materials

Waste type	ε^{205}Tl	Source
ZnS concentrate	-3.47 to -4.40	Vaněk et al. (2021)
Pyrite ore	+1.3	Liu et al. (2020a)
Meggen pyrite	-0.4	Kersten et al. (2014)
Ore-stage pyrite	-1.3	Wickham et al. (2014)
Tl-rich coal pyrite	-5.5	Vaněk et al. (2016)
Flotation tailings	+6.2	Grösslová et al. (2018)
Sphalerite	-2.7	Hettman et al. (2014)
Galena	-1.4	Hettman et al. (2014)

4.3. Mobility and fractionation of Tl in a peat profile

4.3.1. Thallium isotopic variations in a contaminated peatland

It is understood from previous research, that Tl is immobile in organic environments like peat (Shotyk and Krachler, 2004; Smieja-Król et al., 2015). Our results presented in section 7.2 confirm the conservative behaviour of Tl within a peat profile, similar to the behaviours of Pb, and opposite to the mobile Zn. The results of Tl and Pb in the peat reflect the history of atmospheric deposition; however, Tl in the peat seems to be more affected by geogenic sources compared to Pb (inferred from calculated element enrichments). The Tl isotopic ratios display a correlation with the local anthropogenic Tl as well as the geogenic Tl. Interestingly, the results showed little to no fractionation within the profile, and confirmed the use of Tl isotopes as a tracer for source apportionment, as we could identify both geogenic and anthropogenic pools. The absence of isotopic fractionation indicated no Tl sorption onto the peat organic matter nor to biological processes, and that no redox Tl(I)-Tl(III) shifts occurred. In our sulphides study and the peatlands paper (section 7.3 and 7.2, respectively), we were able to determine the isotopic compositions of different waste materials from a Zn smelter, which was used to trace the sources of Tl within the peat profile. The variations in Tl isotopic ratios in the peat samples were in accordance with the major local anthropogenic sources and background Tl isotopic values of the study area.

Nonetheless, regarding Tl isotopic behaviour within a peat profile, there are no other known publications for comparison.

The published paper found in section 7.2 was designed to "trace Tl contamination and stable isotopes in soils and peat bog deposits" and for the "assessment of the role of peat constituents in post-depositional Tl dynamics". The paper fulfilled these aims by providing novel data on the behaviour of Tl in peatlands and the use of Tl isotopes to understand the source and the stability of Tl in a peat profile.

4.3.2. Thallium reactivity in an organic environment

In peatlands and our model pot experiment, we observed the conservative nature of Tl. Surprisingly, Tl was less conservative than Pb. Our results showed that Sphalerite (ZnS) was the less stable Tl-containing sulphide compared to galena (PbS) and pyrite (FeS_2) within the peat environment, and was responsible for Tl mobilization into the peat. Increased Tl concentrations in the pore solutions were connected to increased Tl leaching from the ZnS. Interestingly, Zn concentrations remained stable and was leached from ZnS at a much lower rate than Tl, while being more mobile. The mobility of the elements followed as such Zn>Tl>Pb (Fig. 8). Increased mobility of Zn in peat profiles was confirmed by our results in section 7.2 and by Weiss et al., 2007. While the conservative nature of Pb in peat was mentioned by Mihaljevič et al. (2006); Shotyk and Krachler (2004); Shotyk et al. (2017); Smieja-Król et al. (2015).

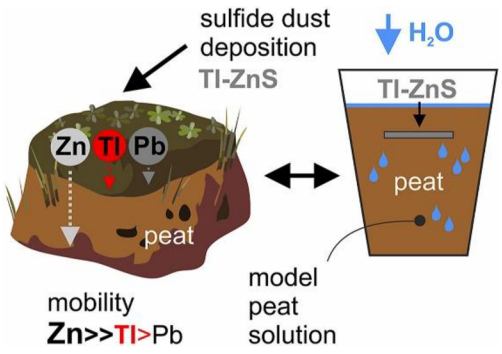

Figure 8. Graphical representation of the mobility of Tl, Zn and Pb in peat

Samples that were treated with synthetic rainwater (SRW) led to increased elemental mobility. Sphalerite degradation and ultimate release of Tl and Zn are strongly influenced by pH (acid promoted and oxidative leaching) (Robson et al., 2014). Thallium in the peat showed lower

concentration gradients in the topmost segment compared to the control, and SRW promoted the vertical migration of both Tl and Zn. Elevated Tl in peat pore solutions also displays very low levels of Tl retention by peat (at least in the short term) (Jacobson et al., 2005a). The possibility of Tl(I) to form complexes with organic ligands of fulvic/humic acids are low (Nriagu, 1998), therefore explaining the vertical migration of Tl in the peat profile under acid rain influence. However, while Tl did not show any complexations with peat organic matter in our studies, Jacobson et al., (2005b) observed approximately 15% of Tl(I) to form complexes with organic compounds. Therefore, the conservative nature of Tl is attributed to Tl mainly associating with exchange sites of the organic matter (Vaněk et al., 2013, 2016, 2018).

The aims of the paper in section 7.4 were "verification of Tl geochemistry in a peat bog- A model experiment" and "assessment of the role of peat constituents in post-depositional Tl dynamics". The paper clearly fulfilled the aims by depicting the behaviour of Tl released from ZnS and the implications of acid rain on Tl and other PTE mobility within peatlands. As described above, the paper also describes the influence of the peat properties (pH, organic matter content) on the mobility of Tl.

4.4. The use of Tl isotopes for source identification

The use of Tl isotopes for source apportionment has been investigated by a handful of researchers. Kersten et al. (2014) published the first paper about Tl isotopes in soils and successfully used Tl isotopes in source identification. Since then, publications on a similar topic gradually increased, eg. Grösslová et al. (2018), Vaněk et al. (2018, 2020, 2021), Liu et al. (2020) and Zhou et al. (2022).

The results compiled from all the mentioned research provide a database on Tl isotopic compositions of a range of materials and indicate the potentials and success of using Tl isotopes to determine the source of Tl into the environment. The data shows the heterogeneity between different materials and their Tl isotopic composition, ranging from light to heavy Tl isotopes (Fig. 9). Nevertheless, it has also indicated the complications that can arise and could potentially 'blur' the source signals. Such complications include the influence of soil properties, geochemical processes (sorption, precipitation) and the processing methods of waste materials in the case of anthropogenic contamination. The reason these changes could potentially affect the isotopic composition of a sample is because they lead to changes in the primary isotopic data, making it harder to trace. For example, the waste materials from Poland (Section 3, 4.2 and 7.3) showed little to no Tl isotopic fractionation, which can make it difficult to precisely

pinpoint the source of Tl in the environment, especially in areas with naturally high Tl background concentrations.

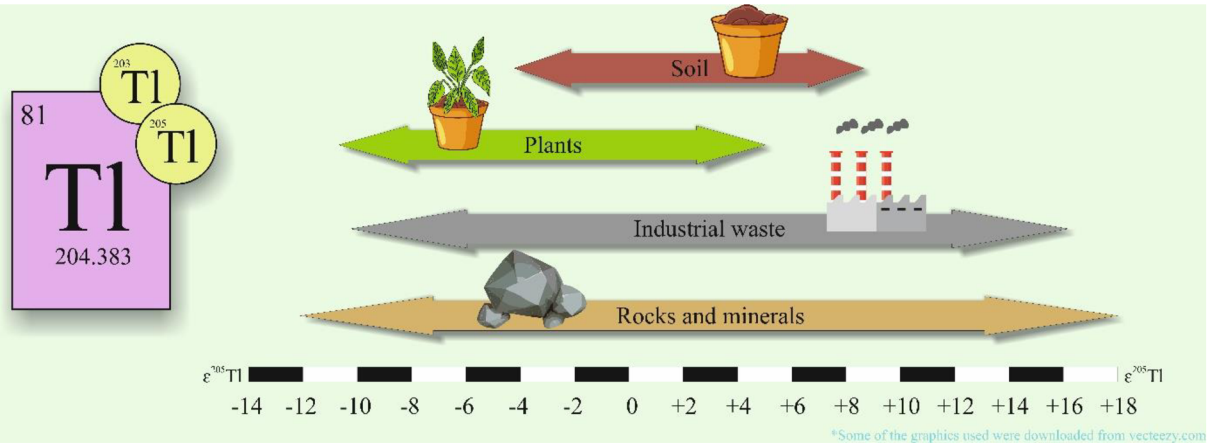

Figure 9. Overview of the range of Tl isotopic compositions in various materials.

5. Conclusions

The dissertation focused on an understanding of the behaviour of Tl and Tl isotopic systematics in various geosystems. This involved studying Tl in soils, peats and industrial processes. The dissertation focuses on answering theories about the key controls of Tl in soil, the mobility and stability of Tl in organic environments, and efficiency of Tl isotopes in source apportionment and understanding Tl behaviour.

The key controls of Tl mobility and fractionation in soils is attributed to the presence of micaceous clays (mainly illite) and Mn-oxides in the soil profile. The behaviour between Mn-oxides and Tl has been studied before, and the results continue to validate the role of Mn-oxides in Tl enrichments and isotopic fractionation in soils. Continuous degradation of Mn-oxides and the redox reactions that occur with Tl, play a role in Tl enrichments. Thallium isotopic data was able to be used as a proxy for redox reactions in soils and to further confirm the specific sources of Tl within different horizons.

In organic environments, Tl continues to behave conservatively, however, to a lesser extent than Pb, and shows no isotopic fractionation occurring within a peat profile, thus making it a suitable archive for monitoring trends of Tl deposition. Nonetheless, when organic environments (especially contaminated) are affected by acid rain, sphalerite is less stable than other sulphides, and in turn controls the Tl fluxes into the peat. The increased acidity of organic environments also leads to increased Tl mobility.

While most (but not all) of the research has shown that high temperature processes should lead to some isotopic fractionation, the research presented in this dissertation proves that while this may be case in many situations, it is not the rule. In such cases, the use of Tl isotopes to distinguish specific waste materials as a source of contamination can become tricky and more complicated.

The results show the use and application of Tl isotopes in a range of geosystems, while providing new knowledge on the behaviour of Tl and Tl fractionation within the pedosphere.

6. References

Aguilar-Carrillo, J., Herrera-García, L., Reyes-Domínguez, I. A., Gutiérrez, E. J. (2020). Thallium (I) sequestration by jarosite and birnessite: Structural incorporation vs surface adsorption. Environ Pollut. 257, 113492. https://doi.org/10.1016/j.envpol.2019.113492

Al-Najar, H., Schilz, R., Römheld, V. (2003). Plant availability of thallium in the rhizosphere of hyperaccumulator plants: a key factor for assessment of phytoextraction. Plant Soil. 249, 97-105. https://doi.org/10.1023/A:1022544809828

Al-Najar, H., Kaschl, A., Schulz, R., Römheld, V. (2005). Effect of thallium fractions in the soil and pollution origins on Tl uptake by hyperaccumulator plants: a key factor for the assessment of phytoextraction. Int J Phytoremediat. 7, 55-67. https://doi.org/10.1080/16226510590915837

Antón, M.A.L., Spears, D.A., Somoano, M.D., Tarazona, M.R.M. (2012). Thallium in coal: Analysis and environmental implications. Fuel. 105, 13-18. https://doi.org/10.1016/j.fuel.2012.08.004

Bačeva, K., Stafilov, T., Šajn, R., Tănăselia, C., Makreski, P. (2014). Distribution of chemical elements in soils and stream sediments in the area of abandoned Sb-As-Tl Allchar mine, Republic of Macedonia. Environ Res. 133, 77-89. https://doi.org/10.1016/j.envres.2014.03.045

Baker, R.G.A., Rehkämper, M., Hinkley, T.K., Nielsen, S.G., Toutain, J.P. (2009). Investigation of thallium fluxes from subaerial volcanism- Implication for the present and past mass balance of thallium in the oceans. Geochem Cosmochim Ac. 73, 6340-6359. https://doi.org/10.1016/j.gca.2009.07.014

Balić-Žunić, T., Moëlo, Y., Lončar, Ž., Micheelsen, H. (1994). Dorallcharite Tl0.8K0.2Fe3(SO4)2(OH)6, a new member of the jarosite-alunite family. Eur J Mineral. 6, 255-264. https://doi.org/10.1127/ejm/6/2/0255

Boev, B., Bermanec, V., Serafimovski, T., Lepitkova, S., Mikulčić, S., Soufek, M., Jovanovski, G., Stafilov, T., Najdoski, M. (2001-2002). Allchar mineral assemblage. Geol Maced. 15-16, 1-23.

Bower, C.A., Reitemeier, R.F., Fireman, M. (1954). Exchangeable cation analysis of saline and alkali soils. Soil Sci. 73, 251-262. https://doi.org/10.1097/00010694-195204000-00001

Belzile, N., Chen, Y. (2017). Thallium in the environment: A critical review focused on natural waters, soils, sediments and airborne particles. Appl Geochem. 84, 218-243. https://doi.org/10.1016/j.apgeochem.2017.06.013

Cabala, J., Teper, L. (2007). Metalliferous constituents of rhizosphere soils contaminated by Zn-Pb mining in southern Poland. Water Air Soil Poll. 178, 351-362. https://doi.org/10.1007/s11270-006-9203-1

Cabala, J., Smieja-Król, B., Jablonska, M., Chrost, L. (2013). Mineral components in a peat deposit: looking for signs of early mining and smelting activities in Silesia-Cracow region (Southern Poland). Environ. Earth Sci. 69, 2559-2568. https://doi.org/10.1007/s12665-012-2080-6

Chen, Y.H., Wang, C.L., Liu, J., Wang, J., Qi, J.Y., Wu, Y.J. (2013). Environmental exposure and flux of thallium by industrial activities utilizing thallium-bearing pyrite. Sci China Earth Sci. 56, 1502-1509. https://doi.org/10.1007/s11430-013-4621-6

Cvjetko, P., Cvjetko, I., Pavlica, M. (2010). Thallium toxicity in humans. Arh Hig Rada Toksikol. 61, 111-119. https://doi.org/10.2478/10004-1254-2010-1976

Daiyan, C., Guanxin, W., Zhenxi, Z., Yuming, C. (2003). Lanmuchangite, a new thallium (hydrous) sulphate from Lanmuchang, Guizhou Province, China. Chin J Geochem. 22, 185-192. https://doi.org/10.1007/BF02831529

Davies, M., Figueroa, L., Wildeman, T., Bucknam, C. (2016). The oxidative precipitation of thallium al alkaline pH for treatment of mining influenced water. Mine Water Environ. 35, 77-85. https://doi.org/10.1007/s10230-015-0349-1

Đorđević, T., Drahota, P., Kolitsch, U., Majzlan, J., Peřestá, S., Kiefer, S., Stöger-Pollach, M., Tepe, N., Hofmann, T., Mikuš, T., Tasev, G., Serafimovski, T., Boev, I., Boev, B. (2021). Synergetic Tl and As retention in secondary minerals: An example of extreme arsenic and thallium pollution. Appl Geochem. 135, 105114. https://doi.org/10.1016/j.apgeochem.2021.105114

Galván-Arzate, S., Santamaría, A. (1998). Thallium toxicity. Toxicol Lett. 99, 1-13. https://doi.org/10.1016/S0378-4274(98)00126-X

Gee, G.W., Bauder, J.W. (1986). Particle-size analysis. In: Klute, A. (Ed.), Methods of Soil Analysis. Part I: Physical and Mineralogical Methods. American Society of Agronomy-Soil Science Society of America, Madison, WI, pp. 383-411.

Garrido, F., Garcia-Guinea, J., Lopez-Arce, P., Voegelin, A., Göttlicher, J., Mangold, S., Almendros, G. (2020). Thallium and co-genetic trace elements in hydrothermal Fe-Mn deposits of Central Spain. Sci Total Environ. 717, 137162. https://doi.org/10.1016/j.scitotenv.2020.137162

Gołębiowska, B., Pieczka, A., Zubko, M., Voegelin, A., Göttlicher, J., Rzepa, G. (2021). Thalliomelane, $TlMn_{7.5}^{4+}Cu_{0.5}^{2+}O_{16}$, a new member of the coronadite group from the preglacial oxidation zone at Zalas, southern Poland. Am Mineral. 106, 2020-2027. https://doi.org/10.2138/am-2021-7577

Grösslová, Z., Vaněk, A., Mihaljevič, M., Ettler, V., Hojdová, M., Zádorová, T., Pavlů, L., Penížek, V., Vaněčková, B., Komárek, M., Chrastný, V., Ash, C. (2015). Bioaccumulation of thallium in a neutral soil as affected by solid-phase association. J Geochem Explor. 159, 208-212. https://doi.org/10.1016/j.gexplo.2015.09.009

Grösslová, Z., Vaněk, A., Oborná, V., Mihaljevič, M., Ettler, V., Trubač, J., Drahota, P., Penížek, V., Pavlů, L., Sracek, O., Kříbek, B., Voegelin, A., Göttlicher, J., Drábek, O., Tejnecký, V., Houška, J., Mapani, B., Zádorová, T. (2018). Thallium contamination of desert soil in Namibia: Chemical, mineralogical and isotopic insights. Environ Pollut. 239, 272-280. https://doi.org/10.1016/j.envpol.2018.04.006

Herrmann, J., Voegelin, A., Palatinus, L., Mandold, S., Majzlan, J. (2018). Secondary Fe-As-Tl mineralization in soils near Buus in the Swiss Jura Mountains. J. Mineral. 30, 887-898. https://doi.org/10.1127/ejm/2018/0030-2766

Hettmann, K., Marks, M.A.W., Kreissig, K., Zack, T., Wenzel, T., Rehkämper, M., Jacob, D.E., Markl, G. (2014). The geochemistry of Tl and its isotopes during magmatic and hydrothermal processes: The peralkaline Ilimaussaq complex, southwest Greenland. Chem Geol. 366, 1-13. https://doi.org/10.1016/j.chemgeo.2013.12.004

Holubík, O., Vaněk, A., Mihaljevič, M., Vejvodová, K. (2020). Higher Tl bioaccessibility in white mustard (hyper-accumulator) grown under the soil than hydroponic conditions: A key factor for the phytoextraction use. J Environ Manage. 255, 109880. https://doi.org/10.1016/j.jenvman.2019.109880b

Holubík, O., Vaněk, A., Mihaljevič, M., Vejvodová, K. (2021). Thallium uptake/tolerance in a model (hyper)accumulating plant: Effect of extreme contaminant loads. Soil Water Res. 16, 129-135. https://doi.org/10.17221/167/2020-SWR

Howarth, S., Prytulak, J., Little, S.H., Hammond, S.J., Widdowson, M. (2018). Thallium concentration and thallium isotope composition of lateritic terrains. Geochem Cosmochim Ac. 239, 446-462. https://doi.org/10.1016/j.gca.2018.04.017

Jacobson, A.R., McBride, M.B., Baveye, P., Steenhuis, T.S. (2005a). Environmental factors determining the trace-level sorption of silver and thallium to soils. Sci. Total Environ. 345, 191–205. https://doi.org/10.1016/j.scitotenv.2004.10.027

Jacobson, A.R., Klitzke, S., McBride, M.B., Baveye, P., Steenhuis, T.S. (2005b). The desorption of silver and thallium from soils in the presence of a chelating resin with thiol functional groups. Water Air Soil Pollut 160, 41–54. https://doi.org/10.1007/s11270-005-3860-3

Jia, Y., Xiao, T., Zhou, G., Ning, Z. (2013). Thallium at the interface of soil and green cabbage (Brassica oleracea L. var. capitata L.): soil-plant transfer and influencing factors. Sci Total Environ. 450-451, 140-147. https://doi.org/10.1016/j.scitotenv.2013.02.008

Kabata-Pendias, A., Pendias, H. (2011). Trace elements in soils and plants. CRC Press, Boca Raton.

Kaplan, D.I., Mattigod, S.V. (1998). Aqueous geochemistry of thallium, in: Nriagu, J.O. (Ed.), Thallium in the Environment, vol 2. Wiley & Sons, New York, pp. 15-29.

Karbowska, B. (2016). Presence of thallium in the environment: sources of contaminations, distribution and monitoring. Environ Monit Assess. 188, 1-19. https://doi.org/10.1007/s10661-016-5647-y

Karbowska, B., Rębiś, T., Milczarek, G. (2018). Electrode modified by reduced graphene oxide for monitoring of total thallium in grain products. Int J Environ Res Public Health. 15, 653. https://doi.org/10.3390/ijerph15040653

Kazantzis, G. (2000). Thallium in the environment and health effects. Environ Geochem Hlth. 22, 275-280. https://doi.org/10.1023/A:1006791514080

Kemper, F.H., Bertram, H.P. (1991). Thallium. In: Metals and their compounds in the environment: occurrence, analysis, and biological relevance. New York: Weinheim, 1227-1241.

Kersten, M., Xiao, T., Kreissig, K., Brett, A., Coles, B.J., Rehkämper, M. (2014). Tracing anthropogenic thallium in soil using stable isotope compositions. Environ Sci Technol. 48, 9030-9036. https://doi.org/10.1021/es501968d

Krasnodębska-Ostręga, B., Sadowska, M., Ostrowska, S. (2012). Thallium speciation in plant tissue-Tl(III) found in Sinapis alba L. grown in soil polluted with tailing sediment containing thallium minerals. Talanta. 93, 326-329. https://doi.org/10.1016/j.talanta.2012.02.042

Lin, T.S., Nriagu, J. (1999). Thallium speciation in the Great Lakes. Environ Sci Technol. 33, 3394-3397. https://doi.org/10.1021/es9810960

Lin, J., Yin, M., Wang, J., Liu, J., Tsang, D.C.W., Wang, Y., Lin, M., Li, H., Zhou, Y., Song, G., Chen, Y. (2020). Geochemical fractionation of thallium in contaminated soils near a large-scale Hg-Tl mineralised area. Chemosphere. 239, 124775. https://doi.org/10.1016/j.chemosphere.2019.124775

Liu, J., Luo, X., Wang, J., Xiao, T., Chen, D., Sheng, G., Yin, M., Lippold, H., Wang, C., Chen, Y. (2017). Thallium contamination in arable soils and vegetables around steel plant-A newly-found significant source of Tl pollution in South China. Environ Pollut. 224, 445-453. https://doi.org/10.1016/j.envpol.2017.02.025

Liu, J., Yin, M., Xiao, T., Zhang, C., Tsang, D.C.W., Bao, Z., Zhou, Y., Chen, Y., Luo, X., Yuan, W., Wang, J. (2020a). Thallium isotopic fractionation in industrial process of pyrite smelting and environmental implications. J Hazard Mater. 384, 121378. https://doi.org/10.1016/j.jhazmat.2019.121378

Liu, J., Wei, X., Zhou, Y., Tsang, D.C.W., Bao, Z., Yin, M., Lippold, H., Yuan, W., Wang, J., Feng, Y., Chen, D. (2020b). Thallium contamination, health risk assessment and source apportionment in common vegetables. Sci Total Environ. 703, 135547. https://doi.org/10.1016/j.scitotenv.2019.135547

Liu, J., Ouyang, Q., Wang, L., Wang, J., Zhang, Q., Wei, X., Lin, Y., Zhou, Y., Yuan, W., Xiao, T. (2022). Quantification of smelter-derived contributions to thallium contamination in river sediments: Novel insights from thallium isotope evidence. J. Hazard. Mater. 424, 127594. https://doi.org/10.1016/j.jhazmat.2021.127594

Mihaljevič, M., Zuna, M., Ettler, V., Šebek, O., Strnad, L., Goliáš, V. (2006). Lead fluxes, isotopic and concentration profiles in a peat deposit near a lead smelter (Příbram, Czech Republic). Sci. Total Environ. 372, 334–344. https://doi.org/10.1016/j.scitotenv.2006.09.019

Mihaljevič, M., Vojtech, E., Vaněk, A. (2020). Historical thallium deposition trends as recorded in peat bogs- examples from Czech sites with contrasting pollution histories. EGU General Assembly, Online, EGU2020-3376. https://doi.org/10.5194/egusphere-egu2020-3376

Migaszewski, Z.M., Gałuszka, A. (2021). Abundance and fate of thallium and its stable isotopes in the environment. Rev *Environ Sci* Bio. 20, 5-30. https://doi.org/10.1007/s11157-020-09564-8

Mukley, J.P., Oehme, F.W. (1993). A review of thallium toxicity. Vet Hum Toxicol. 35, 445-453.

Nielsen, S.G., Rehkämper, M., Baker, J., Halliday, A.N. (2004). The precise and accurate determination of thallium isotope compositions and concentrations for water samples by MC-ICPMS. Chem Geol. 204, 109-124. https://doi.org/10.1016/j.chemgeo.2003.11.006

Nielsen, S.G., Rehkämper, M., Porcelli, D., Andersson, P., Halliday, A.N., Swarzenski, P.W., Latkoczy, C., Günther, D. (2005). Thallium isotope composition of the upper continental crust and rivers – An investigation of the continental sources of dissolved marine thallium. Geochem Cosmochim Ac. 19, 2007-2019. https://doi.org/10.1016/j.gca.2004.10.025

Nielsen, S.G., Rehkämper, M., Halliday, A.N. (2006a). Large thallium isotopic variations in iron meteorites and evidence for lead-205 in the early solar system. Geochem Cosmochim Ac. 70, 2643-2657. https://doi.org/10.1016/j.gca.2006.02.012

Nielsen, S. G., Rehkämper, M., Norman, M.D., Halliday, A.N., Harrison, A.N. (2006b). Thallium isotopic evidence for ferromanganese sediments in the mantle source of Hawaiian basalts. Nature. 439, 314-314. https://doi.org/10.1038/nature04450

Nielsen, S. G., Rehkämper, M., Teagle, D.A.H., Butterfield, D., Halliday, A.N. (2006c). Hydrothermal fluid fluxes calculated from the isotopic mass balance of thallium in the ocean crust. Earth planet Sc Lett. 251, 120-133. https://doi.org/10.1016/j.epsl.2006.09.002

Nielsen, S.G., Rehkämper, M., Brandon, A.D., Norman, M.D., Turner, S., O'Reilly, S.Y. (2007). Thallium isotopes in Iceland and Azores lavas- Implications for the role of altered crust and mantle geochemistry. Earth planet Sc Lett. 264, 332-345. https://doi.org/10.1016/j.epsl.2007.10.008

Nielsen, S.G., Mar-Gerrison, S., Gannoun, A., LaRowe, D., Klemm, V., Halliday, A.N., Burton, K.W., Hein, J.R. (2009). Thallium isotope evidence for a permanent increase in marine organic carbon export in the early Eocene. Earth planet Sc Lett. 278, 297-307. https://doi.org/10.1016/j.epsl.2008.12.010

Nielsen, S.G., Rehkämper, M. (2012). Thallium isotopes and their application to problems in earth and environmental science, in: Baskaran, M., (Ed.), Handbook of Environmental Isotope Geochemistry: Advances in Isotope Geochemistry, Part 2. Springer, Berlin, pp. 247-269.

Nielsen, S.G., Wasylenki, L.E., Rehkämper, M., Peacock, C.L., Xue, Z., Moon, E.M. (2013). Towards an understanding of thallium isotope fractionation during adsorption to manganese oxides. Geochem Cosmochim Ac. 117, 252-265. https://doi.org/10.1016/j.gca.2013.05.004

Nielsen, S.G., Rehkämper, M., Prytulak, J. (2017). Investigation and Application of Thallium Isotope Fractionation. Rev Mineral Geochem. 82, 759-798. https://doi.org/10.2138/rmg.2017.82.18

Ning, Z., He, I., Xiao, T., Márton, L. (2015). High accumulation and subcellular distribution of thallium in green cabbage (Brassica Oleracea L. Var Capitata L). Int J Phytoremediat, 17. 1097-1104. https://doi.org/10.1080/15226514.2015.1045133

Nriagu, J. (1998). Thallium in the Environment. Wiley, New York.

Pansu, M., Gautheyrou, J. (2006). Handbook of Soil Analysis: Mineralogical, Organic and Inorganic Methods. Springer-Verlag, Berlin, Heidelberg, Germany.

Peacock, C.L., Moon, E.M. (2012). Oxidative scavenging of thallium by birnessite: Explanation for thallium enrichment and stable isotope fractionation in marine ferromanganese precipitates. Geochem Cosmochim Ac. 84, 297-313. https://doi.org/10.1016/j.gca.2012.01.036

Peter, A.L.J., Viraraghavan, T. (2005). Thallium: a review of public health and environmental concerns. Environ Int. 31, 493-501. https://doi.org/10.1016/j.envint.2004.09.003

Prytulak, J., Nielsen, S.G., Plank, S.G., Plank, T., Barker, M., Elliott, T. (2013). Assessing the utility of thallium and thallium isotopes for tracing subduction zone inputs to the Mariana arc. Chem Geol. 345, 139-149. https://doi.org/10.1016/j.chemgeo.2013.03.003

Rader, S.T., Mazdab, F.K., Barton, M.D. (2018). Mineralogical thallium geochemistry and isotope variations from igneous, metamorphic, and metasomatic systems. Geochem Cosmochim Ac. 243, 42-65. https://doi.org/10.1016/j.gca.2018.09.019

Rader, S.T., Maier, R.N., Barton, M.D., Mazdab, F.K. (2019). Uptake and fractionation of thallium by *Brassica juncea* in geogenic thallium-amended substrate. Environ Sci Technol. 53, 2441-2449. https://doi.org/10.1021/acs.est.8b06222

Rehkämper, M., Halliday, A.N. (1999). The precise measurement of Tl isotopic compositions by MC-ICPMS: application to the analysis of geological materials and meteorites. Geochem Cosmochim Ac. 63, 935-944. https://doi.org/10.1016/S0016-7037(98)00312-3

Rehkämper, M., Frank, M., Hein, J.R., Porcelli, D., Halliday, A., Ingri, J., Liebetrau, V. (2002). Thallium isotope variations in seawater and hydrogenetic, diagenetic, and hydrothermal ferromanganese deposits. Earth Planet Sc Lett. 197, 65-81. https://doi.org/10.1016/S0012-821X(02)00462-4

Rehkämper, M., Frank, M., Hein, J.R., Halliday, A. (2004). Cenozoic marine geochemistry of thallium deduced from isotopic studies of ferromanganese crusts and pelagic sediments. Earth Planet Sc Lett. 219, 77-91. https://doi.org/10.1016/S0012-821X(03)00703-9

Rehkämper, M., Nielsen, S.G. (2004). The mass balance of dissolved thallium in the oceans. Mar. Chem. 85, 125-139. https://doi.org/10.1016/j.marchem.2003.09.006

Robson, T.C., Braungardt, C.B., Rieuwerts, J., Worsfold, P. (2014.) Cadmium contamination of agricultural soils and crops resulting from sphalerite weathering. Environ. Pollut. 184, 283–289. https://doi.org/10.1016/j.envpol.2013.09.001

Scheckel, K.G., Lombi, E., Rock, S.A., McLaughlin, M.J. (2004). In Vivo synchrotron study of thallium speciation and compartmentation in Iberis Intermedia. Environ Sci Technol. 38, 5059-5100. https://doi.org/10.1021/es049569g

Scheckel, K.G., Hamon, R., Jassogne, L., Rivers, M., Lombi, E. (2007). Synchrotron X-ray absorption-edge computed microtomography imaging of thallium compartmentalization in Iberis intermedia. Plant Soil. 290, 51-60. https://doi.org/10.1007/s11104-006-9102-7

Shotyk, W., Krachler, M. (2004). Atmospheric deposition of silver and thallium since 12370 ^{14}C years BP recorded by a Swiss peat bog profile, and comparison with lead and cadmium. J. Environ. Monit. 6, 427–433. https://doi.org/10.1039/b315084b

Shotyk, W., Appleby, P.G., Bicalho, B., Davies, L.J., Froese, D., Grant-Weaver, I., Magnan, G., Mullan-Boudreau, G., Noernberg, T., Pelletier, R., Shannon, B., van Bellen, S., Zaccone, C. (2017). Peat bogs document decades of declining atmospheric contamination by trace metals in the Athabasca bituminous sands region. Environ. Sci. Technol. 51, 6237–6249. https://doi.org/10.1021/acs.est.6b04909

Smieja-Król, B., Janeczek, J., Bauerek, A., Thorseth, I.H. (2015). The role of authigenic sulfides in immobilization of potentially toxic metals in the Bagno Bory wetland, southern Poland. Environ. Sci. Pollut. Res. 22, 15495–15505. https://doi.org/10.1007/s11356-015-4728-8

Smieja-Król, B., Bauerek, A. (2015). Controls on trace-element concentrations in the pore waters of two Sphagnum-dominated mires in southern Poland that are heavily polluted by atmospheric deposition. J. Geochem. Explor. 151, 57–65. https://doi.org/10.1016/j.gexplo.2015.01.010

Smieja-Król, B., Fiałkiewicz-Kozieł, B., Michalska, A., Krzykawski, T., Smołka-Danielowska, D. (2019). Deposition of mullite in peatlands of southern Poland: implications for recording large-scale industrial processes. Environ. Pollut. 250, 717–727. https://doi.org/10.1016/j.envpol.2019.04.077

Tiwari, M., Singh, A.K., Sinha, D.K. (2015). Chapter 3- Stable Isotopes: Tools for understanding past climatic conditions and their applications in chemostratigraphy. Chemostratigraphy, 65-92. https://doi.org/10.1016/B978-0-12-419968-2.00003-0

Tremel, A., Masson, P, Garroud, H., Donard, O.F.X., Baize, D., Mench, M. (1997). Thallium in French agrosystems-II. Concentration of thallium in field-grown rap and some other plant species. Enviorn Pollut. 97, 161-168. https://doi.org/10.1016/S0269-7491(97)00060-2

Vaněk, A., Komárek, M., Chrastný, V., Bečka, D., Mihaljevič, M., Šebek, O., Panušková, G., Schusterová, Z. (2010). Thallium uptake by white mustard (Sinapis alba L.) grown on moderately contaminated soils- Agro-environmental implications. J Hazard Mater. 182, 303-308. https://doi.org/10.1016/j.jhazmat.2010.06.030

Vaněk, A., Komárek, M., Vorkurková, P., Mihaljevič, M., Šebek, O., Panušková, G., Chrastný, V., Drábek, O. (2011). Effect of Illite and birnessite on thallium retention and bioavailability in contaminated soils. J Hazard Mater. 191, 170-176. https://doi.org/10.1016/j.jhazmat.2011.04.065

Vaněk, A., Chrastný, V., Komárek, M., Penížek, V., Teper, L., Cabala, J., Drábek, O. (2013). Geochemical position of thallium in soils from a smelter-impacted area. J. Geochem. Explor. 124, 176-182. https://doi.org/10.1016/j.gexplo.2012.09.002

Vaněk, A., Grösslová, Z., Mihaljevič, M., Ettler, V., Chrastný, V., Komárek, M., Tejnecký, V., Drábek, O., Penížek, V., Galušková, I., Vaněčková, B., Pavlů, L., Ash, C. (2015). Thallium contamination of soils/vegetation as affected by sphalerite weathering: a model rhizospheric experiment. J Hazard Mater. 283, 148-156. https://doi.org/10.1016/j.jhazmat.2014.09.018

Vaněk, A., Grösslová, Z., Mihaljevič, M., Trubač, J., Ettler, V., Teper, L., Cabala, J., Rohovec, J., Zádorová, T., Penížek, V., Pavlů, L., Holubík, O., Němeček, K., Houška, J., Drábek, O., Ash, C. (2016). Isotopic tracing of thallium contamination in soils affected by emissions from coal-fired power plants. Environ Sci Technol. 50, 9864-9871. https://doi.org/10.1021/acs.est.6b01751

Vaněk, A., Grösslová, Z., Mihaljevič, M., Ettler, V., Trubač, J., Chrastný, V., Penížek, V., Teper, L., Cabala, J., Voegelin, A., Zádorová, T., Oborná, V., Drábek, O., Holubík, O., Houška, J., Pavlů, L., Ash, C. (2018). Thallium isotopes in metallurgical wastes/ contaminated soils: a novel tool to trace metal source and behavior. J Hazard Mater. 343, 78-85. https://doi.org/10.1016/j.jhazmat.2017.09.020

Vaněk, A., Holubík, O., Odborná, V., Mihaljevič, M., Trubač, J., Ettler, V., Pavlů, L., Vokurková, P., Penížek, V., Zádorová, T., Voegelin, A. (2019). Thallium stable isotope fractionation in white mustard: Implications for metal transfers and incorporation in plants. J Hazard Mater. 369, 521-527. https://doi.org/10.1016/j.jhazmat.2019.02.060

Vaněk, A., Voegelin, A., Mihaljevič, M., Ettler, V., Trubač, J., Drahota, P., Vaňková, M., Oborná, V., Vejvodová, K., Penížek, V., Pavlů, L., Drábek, O., Vokurková, P., Zádorová T., Holubík, O. (2020). Thallium stable isotope ratios in naturally Tl-rich soils. Geoderma. 364, 114183. https://doi.org/10.1016/j.geoderma.2020.114183

Vaněk, A., Vejvodová, K., Mihaljevič, M., Ettler, V., Trubač, J., Vaňková, M., Goliáš, V., Teper, L., Sutkowska, K., Vokurková, P., Penížek, V., Zádorová T., Drábek, O. (2021). Thallium and lead variations in a contaminated peatland: A combined isotopic study from a mining/smelting area. Environ Pollut. 290, 117973. https://doi.org/10.1016/j.envpol.2021.117973

Vaněk, A., Vejvodová, K., Mihaljevič, M., Ettler, V., Trubač, J., Vaňková, M., Teper, L., Cabala, J., Sutkowska, K., Voegelin, A., Göttlicher, J., Holubík, O., Vokurková, P., Pavlů, L., Galušková, I., Zádorová T. (2022). Evaluation of thallium isotopic fractionation during the metallurgical processing of sulphides: an update. J Hazard Mater. 424, Part A, 127325. https://doi.org/10.1016/j.jhazmat.2021.127325

Vejvodová, K., Vaněk, A., Mihaljevič, M., Ettler, V., Trubač, J., Vaňková, M., Drahota, P., Vorkurková, P., Penížek, V., Zádorová, T., Tejnecký, V., Pavlů, L., Drábek, O. (2020). Thallium isotopic fractionation in soil: the key controls. Environ Pollut. 265, Part A, 114822. https://doi.org/10.1016/j.envpol.2020.114822

Wang, L., Jin, Y., Weiss, D.J., Schleicher, N.J., Wilcke, W., Wu, L., Guo, Q., Chen, J., O'Connor, D., Hou, D. (2021). Possible application of stable isotope compositions for the identification of metal sources in soil. J Hazard Mater. 407, 124812. https://doi.org/10.1016/j.jhazmat.2020.124812

Wei, X., Zhou, Y., Tsang, D.C.W., Song, L., Zhang, C., Yin, M., Liu, J., Viao, T., Zhang, G., Wang, J. (2020). Hyperaccumulation and transport mechanism of thallium and arsenic in brake ferns (*Pteris vittata* L.): A case study from mining area. J Hazard Mater. 388, 121756. https://doi.org/10.1016/j.jhazmat.2019.121756

Weiss, D.J., Rausch, N., Mason, T.F.D., Coles, B.J., Wilkinson, J.J., Ukonmaanaho, L., Arnold, T., Nieminen, T.M. (2007). Atmospheric deposition and isotope biochemistry of zinc in ombrotrophic peat. Geochem. Cosmochim. Acta. 71, 3498-3517. https://doi.org/10.1016/j.gca.2007.04.026

Wickham, K. (2014). Thallium Isotope Implications for the Metalliferous Source of Carlin-Type Gold Deposits in Northern Nevada. Master's Thesis, University of Nevada, Reno, NV, USA.

Wiederhold, J.G. (2015). Metal stable isotope signatures as tracers in environmental geochemistry. Environ Sci Technol. 49, 2606-2624. https://doi.org/10.1021/es504683e

Xiao, T., Guha, J., Boyle, D., Liu, C.Q., Chen, J. (2004). Environmental concerns related to high thallium levels in soils and thallium uptake by plants in southwest Guizhou, China. Sci Total Environ. 318, 223-244. https://doi.org/10.1016/S0048-9697(03)00448-0

Xiao, T., Yang, F., Li, S., Zheng, B., Ning, Z. (2012). Thallium pollution in China: A geo-environmental perspective. Sci Total Environ. 421-422, 51-58. https://doi.org/10.1016/j.scitotenv.2011.04.008

Xu, H., Luo, Y., Wang, P., Zhu, J., Yang, Z., Liu, Z. (2019). Removal of thallium in water/wastewater: a review. Water Res. 165, 114981. https://doi.org/10.1016/j.watres.2019.114981

Yang, C., Chen, Y., Peng, P., Li, C., Chang, X., X, C. (2005). Distribution of natural and anthropogenic thallium in the soils in an industrial pyrite slag disposing area. Sci Total Environ. 341, 159-172. https://doi.org/10.1016/j.scitotenv.2004.09.024

Zhang, Z., Zhang, B., Long, J., Zhang, X., Chen, G. (1998). Thallium pollution associated with mining of thallium deposits. Sci China, Ser D. 41, 75-81. https://doi.org/10.1007/BF02932424

Zhao, F., Gu, S. (2021). Secondary sulfate minerals from thallium mineralized areas: Their formation and Environmental signifikance. Minerals. 11, 855. https://doi.org/10.3390/min11080855

Zhong, Q., Qi, J., Liu, J., Wang, J., Lin, K., Ouyang, Q., Zhang, X., Wei, X., Xiao, T., El-Naggar, A., Rinklebe, J. (2022). Thallium isotopic compositions as tracers in Environmental studies: A review. Environ. Int. 162, 107148. https://doi.org/10.1016/j.envint.2022.107148

Zhou, Y., He, H., Wang, J., Liu, J., Lippold, H., Bao, Z., Wang, L., Lin, Y., Fang, F., Huang, Y., Jiang, Y., Xiao, T., Yuan, W., Wei, X., Tsang, D.C.W. (2022). Stable isotope fractionation of thallium as novel evidence for its geochemical transfer during lead-zinc smelting activities. Sci Total Environ. 803, 150036. https://doi.org/10.1016/j.scitotenv.2021.150036

Zhuang, W., Liu, M., Song, J., Ying, S. C. (2021). Retention of thallium by natural minerals: A review. Sci Total Environ. 777, 146074. https://doi.org/10.1016/j.scitotenv.2021.146074

Zitko, V. (1975). Toxicity and pollution potential of thallium. Sci Total Environ. 4, 185-192. https://doi.org/10.1016/0048-9697(75)90039-X

7. Published works

7.1. Thallium isotopic fractionation in soil: the key controls

Vejvodová, K., Vaněk, A., Mihaljevič, M., Ettler, E., Trubač, J., Vaňková, M., Drahota, P., Vokurková, P., Penížek, V., Zádorová, T., Tejnecký, V., Pavlů, L., Drábek, O. (2020). Thallium isotopic fractionation in soil: the key controls. Environmental Pollution, 265, 114822.

7.2. Thallium and lead variations in a contaminated peatland: A combined isotopic study from a mining/smelting area

Vaněk, A., Vejvodová, K., Mihaljevič, M., Ettler, V., Tubač, J., Vaňková, M., Goliáš, V., Teper, L., Cabala, J., Sutkowska, K., Vokurková, P., Penížek, V., Zádorová, T., Drábek, O. (2021). Thallium and lead variations in a contaminated peatland: A combined isotopic study from a mining/smelting area. Environmental Pollution, 290, 117973.

7.3. Evaluation of thallium isotopic fractionation during the metallurgical processing of sulphides: An update

Vaněk, A., Vejvodová, K., Mihaljevič, M., Ettler, V., Tubač, J., Vaňková, M., Teper, L., Cabala, J., Sutkowska, K., Voegelin, A., Göttlicher, J., Holubík, O., Vokurková, P., Pavlů, L., Galušková, I., Zádorová, T. (2021). Evaluation of thallium isotopic fractionation during the metallurgical processing of sulphides: An update. Journal of Hazardous Materials, 424, 127325.

7.4. Effect of peat organic matter on sulphide weathering and thallium reactivity: Implications for organic environments

Vejvodová, K., Vaněk, A., Spasić, M., Mihaljevič, M., Ettler, V., Vaňková, M., Drahota, P., Teper, L., Vokurková, P., Pavlů, L., Zádorová, T., Drábek, O. (2022). Effect of peat organic matter on sulphide weathering and thallium reactivity: Implications for organic environments. Chemosphere, 299, 134380.

7.5. Understanding stable Tl isotopes in industrial processes and the environment: A review

Vejvodová, K., Vaněk, A., Drábek, O., Spasić, M. (2022). Understanding stable Tl isotopes in industrial processes and the environment: A review. Journal of Environmental Management, 315, 115151.

7.1. Thallium isotopic fractionation in soil: the key controls

Vejvodová, K., Vaněk, A., Mihaljevič, M., Ettler, E., Trubač, J., Vaňková, M., Drahota, P., Vokurková, P., Penížek, V., Zádorová, T., Tejnecký, V., Pavlů, L., Drábek, O. (2020). Thallium isotopic fractionation in soil: the key controls. Environmental Pollution, 265, 11482

Environmental Pollution 265 (2020) 114822

Contents lists available at ScienceDirect

Environmental Pollution

journal homepage: www.elsevier.com/locate/envpol

Thallium isotopic fractionation in soil: the key controls☆

Kateřina Vejvodová [a], Aleš Vaněk [a, *], Martin Mihaljevič [b], Vojtěch Ettler [b], Jakub Trubač [b], Maria Vaňková [b], Petr Drahota [b], Petra Vokurková [a], Vít Penížek [a], Tereza Zádorová [a], Václav Tejnecký [a], Lenka Pavlů [a], Ondřej Drábek [a]

[a] Department of Soil Science and Soil Protection, Faculty of Agrobiology, Food and Natural Resources, Czech University of Life Sciences Prague, Kamýcká 129, 165 00, Praha 6, Czech Republic
[b] Institute of Geochemistry, Mineralogy and Mineral Resources, Faculty of Science, Charles University, Albertov 6, 128 00, Praha 2, Czech Republic

ARTICLE INFO

Article history:
Received 20 April 2020
Received in revised form
13 May 2020
Accepted 14 May 2020
Available online 15 May 2020

Keywords:
Thallium
Isotope
Fractionation
Mn-oxide
Illite

ABSTRACT

We studied the key geochemical and mineralogical factors that could affect the fractionation of stable thallium (Tl) isotopes in soil. A set of grassland soil samples enriched in geogenic Tl in combination with selected Tl-containing mineral materials from the Czech Republic (Kluky) were investigated for this purpose. The results demonstrate significant incorporation of Tl in pedogenic (specific) Mn-oxide, which led to a large accumulation of the heavy ^{205}Tl isotope (~+14 ε^{205}Tl units), presumably resulting from oxidative Tl sorption. Consequently, we concluded that the Mn-oxide-controlled Tl uptake is the primary cause of the observed ^{205}Tl enrichment in the middle profile zone, at the A/B soil horizon interface, with up to +4 of ε^{205}Tl. Furthermore, our results displayed a clear relationship between the Tl isotopic fractionation degree and the Mn-oxide soil concentration ($R^2 = 0.6$), as derived from the oxalate-extractable data. A combination of soil and mineralogical considerations suggests that ^{205}Tl enrichment in respective soil samples is also partly due to the Tl present in micaceous clay minerals, mainly illite, which is the predominant pedogenic Tl host phase. In line with our previous results, this Tl behavior can be inferred from systematic Mn-oxide degradation and the associated Tl (enriched in ^{205}Tl) cycling in the studied soils and thus, presumably in the redoximorphic soils in general.

1. Introduction

The geochemistry of thallium (Tl) is complex and poorly understood in some respects. This is mainly due to the combination of the lithophilic (in analogy to K) and chalcophilic properties of Tl and the associated contrasting effects (Peter and Viraraghavan, 2005). In general, the variations of stable Tl isotopes (^{205}Tl and ^{203}Tl) may indicate specific chemical processes or chemical alterations of Tl in soils (Howarth et al., 2018; Kersten et al., 2014; Nielsen et al., 2017; Vaněk et al., 2016, 2018). On the other hand, our recent results (Vaněk et al., 2020) demonstrate that Tl isotopic patterns may not necessarily reflect Tl speciation or mineralogical association in the soil but could even indicate redox-driven Tl cycling due to soil formation (or rock weathering). In naturally Tl-rich soils at Buus (Switzerland), we observed exceptionally highly positive ε^{205}Tl factors in the B soil horizons (~+8), up to 7 units higher relative to the local bedrock or altered Tl ore (Vaněk et al., 2020). Illite and possibly other micaceous clay minerals have been shown to be predominant Tl-containing phases, for which, however, any isotopic fractionation attributable to "secondary" Tl uptake is unlikely, i.e., principally due to the charge equilibrium for Tl sorption. Therefore, the preliminary conclusion was that this ^{205}Tl enrichment resulted from systematic (long-term) Tl mobilization and immobilization cycles involving Tl(I)↔Tl(III) shifts, although with no specific link to the actual speciation data.

In the southern part of the Czech Republic (approximately 80 km S of Prague), near the village Kluky, is an area with elevated background levels of Tl in the soils (Vaněk et al., 2009). This geochemical anomaly is a result of Paleozoic granites containing silicate minerals enriched in Tl. In local soils, muscovite and/or illite, K-feldspar in combination with secondary Mn-oxide(s) were found to be major phases hosting Tl (Vaněk et al., 2009).

This study was performed to characterize the key geochemical and mineralogical factors that may affect the fractionation of stable Tl isotopes in soils. For this purpose, a complete (fully-developed)

☆ This paper has been recommended for acceptance by Bernd Nowack.

* Corresponding author.
E-mail address: vaneka@af.czu.cz (A. Vaněk).

https://doi.org/10.1016/j.envpol.2020.114822
0269-7491/

soil profile was sampled at Kluky. All soil samples were tested for their physicochemical and mineralogical properties, Tl chemical fractionation (using simple extractions) and stable Tl isotopic ratios. In addition, the soil data were supplemented with the Tl isotopic data on different Tl-containing (reference) materials, which correspond to various pedogenic stages of Tl.

2. Materials and methods

2.1. Soil sampling

The study area (Kluky) can be found in Fig. 1. Except for the geogenic origin of Tl, there is no evidence for any important anthropogenic Tl inputs in the area (Vaněk et al., 2009). All soil and reference Tl-containing samples (namely, bedrock, K-feldspar, soil clay and Mn-oxide-rich nodules) were collected from a well-developed grassland soil profile (GPS coordinates: N 49.305443; E 14.232777) (Fig. 1). The soil profile was properly sampled from a ~1 × 1-m-wide pit (Fig. 1). All soil samples were dried, sieved to the ≤2-mm fraction and homogenized. In relation to the redoximorphic nature of local soils, the studied soil profile was characterized as an Eutric Stagnic Cambisol (Loamic, Ochric), according to FAO. The clay material was isolated by an accurate (time-dependent) sedimentation of soil particles in H_2O suspension (≥24 h) (Gee and Bauder, 1986) and the Mn-oxide material, forming nodules (and coatings), was separated manually.

2.2. Soil properties

The soil pH was measured in both H_2O and KCl solutions (1:5, v/v). The total carbon/sulfur concentrations (TC, TS) were measured by a CNS analyzer (Flash, 2000; Thermo Scientific, Germany). For the soil cation exchange capacity (CEC), the method of $BaCl_2$ saturation (0.1 M) was used (ISO 11260:1994). The acid oxalate extraction (0.2 M ammonium oxalate/oxalic acid at pH 3) was performed to quantify the approximate amount of amorphous/poorly-crystalline Fe-oxides/Mn-oxides and the associated Tl content (Pansu and Gautheyrou, 2006). The soil extraction with 1 M NH_4NO_3 was conducted to quantify the exchangeable soil Tl concentration, i.e., at the 1:2.5 ratio (2 h). For the particle size distribution and the content of soil clay, an accurate (time-dependent) sedimentation was used (Gee and Bauder, 1986).

X-ray diffraction (XRD) (X'Pert Pro X-ray diffractometer, the Netherlands) was used to identify all bulk sample, soil clay and oxide mineralogy, i.e., under the following analytical conditions: CuKα radiation, 40 kV, 30 mA, step scanning at 0.01°/200 s in the range 5–70° 2θ, in combination with X'Pert HighScore software 1.0 and the JCPDS PDF-2 database.

In order to measure major and trace element concentrations in soil, bedrock and mineral samples, a finely-ground mass of 0.2–0.5 g was dissolved in a mixture of $HF/HNO_3/H_2O_2$ (Merck, Germany) in 60-mL PTFE beakers (Savillex, USA) (48 h, 150 °C). All the concentrations were determined in three replicates using a combination of inductively coupled plasma optical emission and quandrupole-based mass spectrometers (ICP-OES; Q-ICP-MS – iCAP 6500, Thermo Scientific, UK; Q-ICP-MS, Xseries II, Thermo Scientific, Germany). The SRM 2711 (NIST, USA) was employed for the quality control (Table S1, Supplementary Material).

2.3. Thallium isolation

The Tl solutions were obtained by separation using two-stage chromatography employing Bio-Rad AG1-X8 (an anion exchange resin; 200–400 mesh; Cl^- cycle), with HBr absent for the whole procedure. The obtained Tl-rich fractions were evaporated and dissolved in 0.1 M HCl (after the first stage of extraction) and then the whole process was repeated to obtain Tl solutions containing no Pb. Complete information about the Tl isolation in the dissolved samples or specific soil extracts is available in our previous publications (Grösslova et al., 2018; Vaněk et al., 2016, 2018, 2020).

2.4. Thallium isotope measurement

Complete information about the determination of Tl isotopic ratios in all the studied samples, as well as the analytical conditions, being consistent with Prytulak et al. (2013), are described in detail in the Supplementary Material.

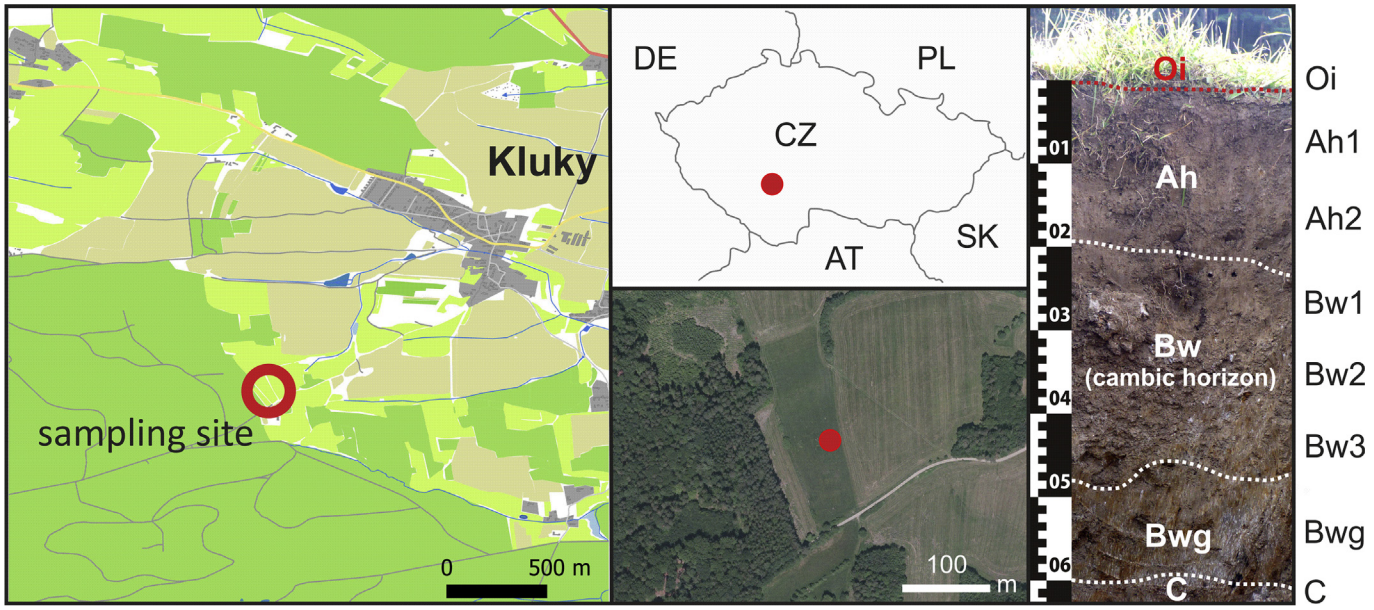

Fig. 1. The soil sampling site (GPS coordinates: N 49.305443; E 14.232777) and the studied grassland soil profile (Eutric Stagnic Cambisol, Loamic, Ochric) with the Paleozoic granite as a bedrock.

3. Results and discussion

3.1. Soil characterization

The physicochemical properties of the individual soil samples are given in Table 1. The soil profile can be described by a medium portion of the clay fraction (10–21%) (loam or sandy loam, FAO), medium to increased CEC (i.e., in relation to sandy soils), with maximum values in the bottom soil horizons (Bw3, Bwg, C) (~30 cmol (+)/kg), and a slightly acidic pH range (~5.5 in H_2O solution). Regarding the TC contents, the organic and organo-mineral horizons (Oi, Ah) accounted for 1–25%, in contrast to the low TC levels in the mineral horizons (≤0.4%). In accordance with the redoximorphic feature of the soil profile (Fig. 1), we observed a peak in the oxalate-extractable Fe and Mn concentrations at the Ah/Bw horizon interface, suggesting local enrichment in readily degradable Fe/Mn-oxides (Table 1).

The mineralogy of the bulk samples according to XRD was dominated by quartz (SiO_2), K-feldspar and plagioclase ($KAlSi_3O_8$, $NaAlSi_3O_8$) (Fig. 2). The minor phases were muscovite ($K,Al_2(AlSi_3O_{10})$ $(F,OH)_2$) or illite ($(K,H_3O)Al_2(Si,Al)_4O_{10}(OH)_2$), amphibole ($Ca_2(Mg,Fe,Al)_5(Si,Al)_8O_{22}(OH)_2$) and chlorite ($(Mg,Al)_6(Si,Al)_4O_{10}(OH)_8$). The analysis of the sample of soil clay revealed the presence of illite, kaolinite ($Al_2Si_2O_5(OH)_4$), chlorite and mixed-layered chlorite/smectite (Fig. 2). In the isolated Mn-bearing nodules, XRD indicated the presence of amorphous (poorly-crystalline) Mn-oxide (AMO) (Fig. 2). Considering the earlier data on the speciation of Fe and Mn oxides in the Kluky soils using the voltammetry of microparticles (VMP) (Vaněk et al., 2009), Mn(III,IV)-oxide aggregated with specific Fe(III)-oxides, ferrihydrite and goethite ($5Fe_2O_3 \cdot 9H_2O$, α-FeOOH), all represent the major pool of soil oxides (Fig. S1, Supplementary Material). The peak potential (E) of the Mn-oxide, however, did not correspond to common Mn(III,IV)-oxide typical for soils, which generally have the E ~0.5 V vs. SCE (Vaněk et al., 2009). An analogous E was reported only for pyrolusite (β-MnO_2) (Bakardjieva et al., 2000), which, however, is usually absent in soils (O'Reilly and Hochella, 2003).

3.2. Thallium concentrations and extractability in the soil profile

The vertical trends of total, oxalate-extractable and exchangeable Tl concentrations and proportions in the studied soils are presented in Table 1 and Fig. 3. The soil profile demonstrated a gradual increase in the total Tl concentration with a peak in the Bwg horizon (3 mg/kg), followed by a significant decline for the C horizon (parent material) and the bedrock sample (≤2 mg/kg). This pattern, which in turn, did not correspond to any data on "labile" Tl fractions, makes it possible to tentatively infer the dynamics of Tl processes (including the redox-controlled processes) and associated migration and/or redistribution effects during pedogenesis. For example, the vertical distribution of clay particles and its maximum in the Bwg horizon (21%) indicate that soil Tl enrichment may be due to clay/illite accumulation within the soil profile (Vaněk et al., 2020; Voegelin et al., 2015; Wick et al., 2018), in accordance with the Tl concentration for the separated clay fraction (3.4 mg/kg) (Table 1).

Although the concentrations of both exchangeable and oxalate-extractable Tl fractions were generally low (0.02–0.05 mg/kg), corresponding to only of ~1–4% of the total soil Tl, there was a distinct peak in the subsurface Ah2 horizon, which resembled the patterns of oxalate-extractable Mn (and Fe) (Table 1, Fig. 3). In combination with the mineralogical data, our results point to a low mobility of Tl, which can correspond to Tl incorporated into silicate phases, presumably the mica-type/clay minerals, such as illite (or eventually to K-feldspar) and in parallel to the association of minor Tl amounts with secondary soil oxides (Aguilar-Carrillo et al., 2018; Gomez-Gonzalez et al., 2015; Grösslova et al., 2018; Jakubowska et al., 2007; Liu et al., 2016, 2019; Vaněk et al., 2009, 2020; Voegelin et al., 2015; Wick et al., 2018). Due to the very low Tl sorption efficiencies of Fe(III)-oxides (Jacobson et al., 2005; Vaněk et al., 2010, Vaněk, 2012), the detected Mn(III,IV)-oxide is assumed to dominate the retention of oxalate-extractable soil Tl (Table 1, Figs. 2 and 3) (see sections below). If we consider that the majority of the Mn released in the oxalate extraction (~25 g/kg) (Table 1) corresponds to the Mn-oxide itself with ~8–9 mol Mn/kg (~450 g Mn/kg) (Vaněk et al., 2010; Wick et al., 2019), without any redistribution effects, the approximate Mn-oxide concentration in the tested nodules accounts for only ~5% of the total solid (nodule) composition (Fig. 2). The molar Tl_{oxal}/Mn_{oxal} ratios in this sample and in the individual soil horizons spanned a small range of ~0.00002–0.00005 (mol/mol) (Table 1). These values indicate relatively stable Tl loadings of the Mn-oxide in all the tested

Table 1
Physicochemical characteristics and total (Tl_{TOT}), oxalate-extractable (Tl_{oxal}) and exchangeable (Tl_{exch}) Tl concentrations and Tl isotopic signatures ($\varepsilon^{205}Tl$) in the studied soil and selected Tl-containing samples (bedrock, K-feldspar, soil clay, Mn-oxide-rich nodules) and the standard reference material.

Sample/	Depth	pH		clay	TC	TS	CEC	Al_{oxal}	Fe_{oxal}	Mn_{oxal}	Tl_{oxal}	Tl_{oxal}/Mn_{oxal}	Tl_{TOT}	Tl_{exch}	$\varepsilon^{205}Tl \pm 0.7$
Soil Horizon	(cm)	H_2O	KCl	(%)	(%)		(cmol+/kg)	(mg/kg)				(mol/mol)	(mg/kg)	(mg/kg)	
Oi	1–0	–	–	–	25.3	0.42	–	–	–	–	–	–	0.62 ± 0.14	–	+1.96
Ah1	0–10	5.4	4.5	11.3	3.8	0.10	19.3	1220	4730	314	0.02	0.00002	1.29 ± 0.06	0.02	+1.25
Ah2	10–20	5.5	4.4	10.4	0.9	0.02	15.8	1110	4800	397	0.03	0.00002	1.32 ± 0.02	0.05	+4.03
Bw1	20–30	5.6	4.4	15.7	0.3	0.01	14.5	1080	5390	427	0.04	0.00002	1.51 ± 0.14	0.04	+3.72
Bw2	30–40	5.6	4.3	15.5	0.2	0.02	13.3	792	4350	303	0.03	0.00002	1.83 ± 0.02	0.04	+3.48
Bw3	40–50	5.9	4.1	17.1	0.3	0.01	30.0	892	4250	261	0.03	0.00003	2.65 ± 0.28	0.03	+2.69
Bwg	50–60	5.6	4.0	21.4	0.4	0.01	35.8	808	4120	175	0.03	0.00004	2.95 ± 0.16	0.04	+0.02
C	60–	5.5	4.0	–	0.1	0.01	31.5	881	4320	151	0.03	0.00005	1.99 ± 0.10	0.04	+1.52
Bedrock/granite		–	–	–	–	–	–	–	–	–	–	–	1.34 ± 0.08	–	+1.60
K-feldspar		–	–	–	–	–	–	–	–	–	–	–	2.12 ± 0.12	–	+1.39
Soil clay		–	–	–	–	–	–	–	5870	593	0.10	0.00004	3.35 ± 0.20	–	+4.57
Mn-oxide nodules		–	–	–	–	–	–	1750	8590	25,600	1.91	0.00002	–	–	+14.4*
Mn-oxide nodules		–	–	–	–	–	–	–	–	–	–	–	4.98 ± 0.40	–	(+8.17)
AGV-2		–	–	–	–	–	–	–	–	–	–	–	0.27 ± 0.02	–	−3.10

The total Tl concentrations (2 SD level, n = 3); the data on oxalate-extractable and exchangeable Tl/metal fractions (n = 3, RSD <10%). The $\varepsilon^{205}Tl$ results: universal error ±0.7 $\varepsilon^{205}Tl$ (2 SD). *The $\varepsilon^{205}Tl$ value for the Mn-oxide nodules – the oxalate extract; the $\varepsilon^{205}Tl$ value in the brackets – totally digested sample. CEC: cation exchange capacity; TC: total carbon; TS: total sulfur; –: not determined.

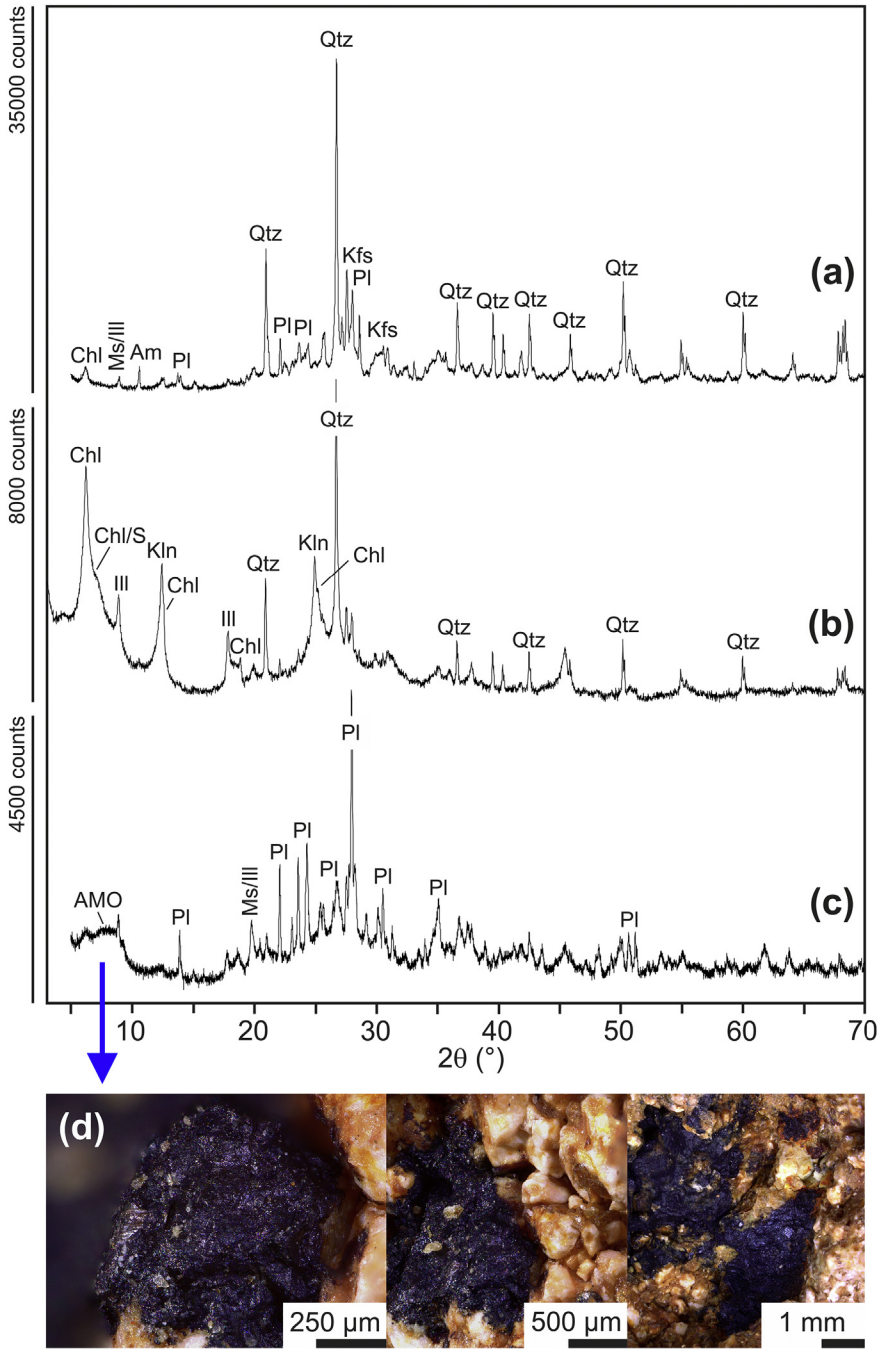

Fig. 2. X-ray diffraction patterns of the bulk soil sample (mixed Bw horizon) (a), the separated soil clay (b), and the Mn-oxide-rich nodules (c). Mineral abbreviations: Am, amphibole; AMO, amorphous manganese oxide; Chl, chlorite; Chl/S, mixed-layered chlorite/smectite; Ill, illite; Kfs, K-feldspar; Kln, kaolinite; Ms/Ill, muscovite and/or illite; Pl, plagioclase; Qtz, quartz. Identification of mixed-layered chlorite/smectite is based on the ethylene glycol solvation. Optical micrographs of Mn-oxide-rich nodules and coatings (d).

samples, as well as minimum changes (if any) in the oxide speciation or Tl sorption efficiency over the entire soil profile. The calculated model Tl loading for such a Mn-oxide with ~40 mg Tl/kg oxide thus indicates a medium level of Tl saturation (Vaněk et al., 2020; Voegelin et al., 2015; Wick et al., 2019). Nevertheless, the predicted oxide-associated Tl load is much lower (of one/two orders) compared to soils developed from rocks that host Tl in some type of sulfide mineralization (Hermann et al., 2018; Karbowska et al., 2014; Vaněk et al., 2020; Voegelin et al., 2015; Xiao et al., 2004, 2012). This is because the weathering of Tl-containing sulfides is characterized by large Tl fluxes, accompanied by extreme loads and Tl incorporation into the newly-formed pedogenic phases. Thallium(I)- and also Tl(III)-containing oxides and sulfates represent typical alteration products (avicennite, birnessite, jarosite, etc.) (Aguilar-Carrillo et al., 2018; Garrido et al., 2020; Gomez-Gonzalez et al., 2015; Hermann et al., 2018; Voegelin et al., 2015; Xiao et al., 2004).

3.3. Thallium isotopic signatures in the soil profile

The Tl isotopic results in our soils and the Tl-containing (reference) samples are shown in Table 1 and Fig. 3. The soil profile

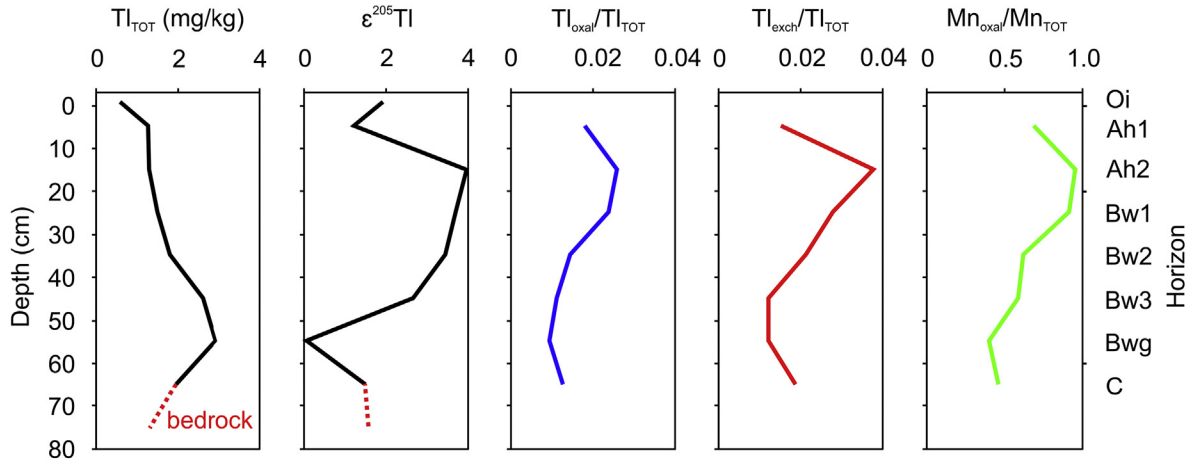

Fig. 3. Vertical patterns of total Tl concentrations (Tl_{TOT}), Tl isotopic signatures ($\varepsilon^{205}Tl$) and the proportions of oxalate-extractable and exchangeable Tl or Mn fractions relative to total element concentrations in the studied soil profile. All concentration data correspond to mean values (n = 3).

showed a significant variability in the Tl isotopic signature. We identified a positive peak in the middle zone of the profile, between the Ah2 and Bw horizons, with the $\varepsilon^{205}Tl$ factors of +3.5 to +4. The Tl signatures in the uppermost and the bottom soil horizons (Oi, Ah1, Bwg, C), by contrast, showed markedly lighter Tl ($\varepsilon^{205}Tl$ ~0 to +2), similar to that of the bedrock ($\varepsilon^{205}Tl$ +1.6) or local K-feldspar ($\varepsilon^{205}Tl$ +1.4). The observed Tl isotopic data for the Oi or Ah horizons did not indicate any trend that could be attributed to enhanced ^{203}Tl uptake by vegetation, as could be possibly expected (Kersten et al., 2014). The Tl isotopic fractionation effects which may be responsible for the highly negative $\varepsilon^{205}Tl$ values in the biomass are generally related to Tl uptake from more significant Tl pools in soil/soil solution (Rader et al., 2019; Vaněk et al., 2019), i.e., where important Tl fluxes potentially take part in biogeochemical processes.

The bedrock/feldspar $\varepsilon^{205}Tl$ factors can be thought as a primary Tl isotopic reference, which is related to Tl present in aluminosilicates, mainly K-phyllosilicates and feldspars (Vaněk et al., 2009). These Tl isotopic records were consistent with the $\varepsilon^{205}Tl$ patterns reported by Rader et al. (2018) for a large set of hydrothermal silicate minerals. The increase in $\varepsilon^{205}Tl$ in the samples of soil clay (+4.6) and bulk Mn-oxide nodules (+8.2) (Table 1) suggests significant Tl isotopic shift due to the alteration of soil Tl as affected by pedogenesis, where redox-driven Tl cycling presumably plays a key role. Conversely, the rapid decrease in $\varepsilon^{205}Tl$ (~0) in the Bwg horizon is in accordance with the presence of the isotopically heavier Tl fraction in the overlying layers (Ah2, Bw1, Bw2), indicating preferential leaching of the lighter ^{203}Tl isotope and its subsequent sorption by pedogenic phases in the bottom soil horizon (Bwg) (Fig. 3).

3.4. Key geochemical processes controlling Tl isotopic fractionation in soil

By combining the $\varepsilon^{205}Tl$ soil data with the trends in oxalate-extractable and exchangeable Tl (and Mn) fractions, we attributed the heavy Tl isotopic enrichment in the soil to preferential sorption of the ^{205}Tl isotope by the Mn-oxide (Fig. 3). Another evidence for the heavy Tl isotopic shift is provided by a linear (positive) relationship (R^2 = 0.6) between the 1/Mn (extracted in the oxalate solution) and the Tl isotopic records determined for all the soil horizons and the soil clay sample (Fig. 4), indicative of the Mn-oxide-induced fractionation of Tl isotopes. This type of expression displays the relationship between the degree of the Tl isotopic

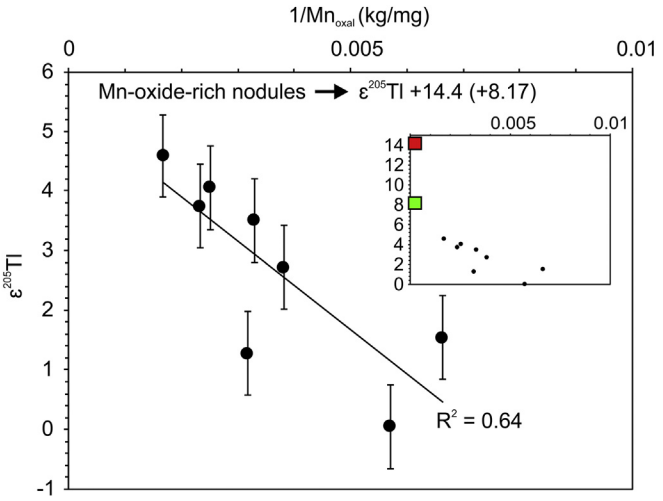

Fig. 4. Thallium isotopic signatures of the soil horizons and the separated soil clay as a function of inverse oxalate-extractable Mn concentrations. Red and green squares in the inset depict Tl isotopic signatures of the oxalate extract and the dissolved sample of the Mn-oxide-rich nodules, respectively. The linear function and the R^2 value were obtained using only soil and clay sample data. An universal error of ±0.7 (2 SD) is assigned to the Tl isotopic soil data. The Mn data correspond to the mean values (n = 3). (For interpretation of the references to colour in this figure legend, the reader is referred to the Web version of this article.)

fractionation and the Mn-oxide concentration in the soil. Although the affinity of Tl to Mn-oxides in soils/sediments and associated positive isotopic effects have been mentioned several times (Howarth et al., 2018; Kersten et al., 2014; Peacock and Moon, 2012; Rehkämper et al., 2002, 2004; Vaněk et al., 2016, 2018), Tl(III) species are probably the dominant source of heavy ^{205}Tl isotope enrichment, if present in the alteration product (Schauble, 2007). Nielsen et al. (2013) documented a significant accumulation of the sorbed ^{205}Tl-rich fraction onto the surface of model K-birnessite, where the degree of fractionation equaled as much as 1.0015. This phenomenon was demonstrated mainly for the oxidative Tl sorption, being in accordance with the X-ray absorption data obtained by Wick et al. (2019). Thallium could also be fixed by Mn-oxides normally, i.e., absent Tl oxidation (Nielsen et al., 2013; Vaněk et al., 2010); however, this type of Tl sorption should not cause significant fractionation of Tl isotopes (Nielsen et al., 2013; Schauble, 2007).

Since the Mn-oxide nodules exhibit large ε^{205}Tl factors of ~+14 and + 8 for the oxalate extract and totally digested sample (Table 1), respectively, they fall within the range of high ε^{205}Tl records observed in modern sedimentary (seawater or terrestrial) crusts/nodules rich in Fe and Mn oxides; they typically span a range of ~+10 to +15 (Nielsen et al., 2017; Rehkämper et al., 2002, 2004). We assume that the oxidative Tl sorption by the Mn-oxide in our soils is the major process related to the retention of the oxalate-extractable soil Tl. In that case, it can be estimated that the cumulative ε^{205}Tl shift for the bulk soil samples and the soil clay would reach "only" ~+0.3 and ~+0.8 (in maximum), respectively. However, if we use the clay sample as a reference (ε^{205}Tl +4.6) for the mass balance estimation, the resulting calculated model Tl isotopic shift for the clay fraction in the individual soil horizons would account for up to +1 ε^{205}Tl unit, which corresponds to 10–21% of the total soil particle distribution. Taking into account the oxalate-extractable Tl and Mn concentrations in the clay sample (0.1 mg/kg), it is evident that an appropriate part of the isotopic signature, although unquantified, reflects the ε^{205}Tl of authigenic Mn-oxide (~+14), thus being a clay constituent (Table 1).

It should be noted that Tl adsorption onto clay minerals is not associated with any reduction and oxidation reactions. As a simple process linked with the monovalent Tl(I)–K(I) ion exchange it should not exhibit a significant Tl isotopic effect (Schauble, 2007). The role of Mn-oxide in the Tl isotopic fractionation has been proven and it is clearly the key factor that controls the isotope dynamics in the studied soils. However, model calculations (using oxide-related Tl isotopic shifts) and the limited Tl amount present in the oxide fraction (oxalate-extractable Tl concentration) suggest that the bulk Tl isotopic variations may be affected by clay minerals, mainly illite. Since illite presumably dominates quantitative Tl sorption in the studied soils, the origin of the increased ε^{205}Tl values observed in the respective Ah and Bw horizons should, at least to some degree, inherit the isotopic signature of the Mn-oxide. In our opinion, the isotopically heavy Tl could also enter into the structure of K-phyllosilicates, considering systematic redox Tl cycling typical for the redoximorphic soils. Continuous ^{205}Tl enrichment in Mn-oxide(s), their degradation accompanied by the mobilization/immobilization of the relatively heavier Tl isotope fraction due to abrupt (cyclic) Eh decline, for instance in a H_2O-saturated soil profile, can be reasonably assumed. Although, this would apparently happen at low Tl(I) fluxes and/or limited Tl-silicate loadings. In other words, the capturing of Tl by pedogenic silicates as a mechanism itself would not be the direct control for the accumulation of the heavy isotopic fraction. Our previous study on the Tl geochemical anomaly at Buus (Switzerland) demonstrates that this is most likely the cause of the positive anomalies in ε^{205}Tl factors in the B soil horizons, unrelated to Tl speciation patterns (Vaněk et al., 2020).

4. Conclusions

This study combines an accurate detection of stable Tl isotope ratios with Tl data from chemical extractions, physicochemical and mineralogical analyses conducted in Tl-containing soils and selected mineral (reference) materials. The results show that Tl incorporation in the pedogenic Mn(III,IV)-oxide, forming nodules, led to a substantial enrichment in the ^{205}Tl isotope, corresponding to ~+14 ε^{205}Tl units. As such, this is probably due to oxidative Tl sorption. Overall, we conclude that Mn-oxide-controlled Tl uptake is the primary cause of the enrichment in ^{205}Tl observed in the middle profile zone, at the A/B soil horizon interface, accounting for up to +4 of ε^{205}Tl for bulk samples. In addition, our results document a relationship between the Tl isotopic fractionation degree and the soil Mn-oxide concentration, as can be simply derived from the oxalate-extractable data. By combining soil and mineralogical data, we suggest that ^{205}Tl enrichment in respective soil horizons is partly due to Tl present in specific clay phases, i.e., mainly illite, as inferred from the redoximorphic nature of the tested soil samples, and the systematic (redox-driven) Mn-oxide degradation and Tl (enriched in ^{205}Tl) cycling.

CRediT authorship contribution statement

Kateřina Vejvodová: Methodology, Data curation, Investigation, Writing - original draft. **Aleš Vaněk:** Conceptualization, Supervision, Data curation, Methodology, Investigation, Writing - review & editing. **Martin Mihaljevič:** Methodology, Investigation. **Vojtěch Ettler:** Writing - review & editing. **Jakub Trubač:** Methodology. **Maria Vaňková:** Methodology, Data curation, Writing - review & editing. **Petr Drahota:** Methodology, Investigation. **Petra Vokurková:** Methodology. **Vít Penížek:** Methodology, Visualization. **Tereza Zádorová:** Methodology. **Václav Tejnecký:** Methodology, Visualization. **Lenka Pavlů:** Methodology. **Ondřej Drábek:** Methodology.

Acknowledgements

This work was funded by the Czech Science Foundation (Project GAČR 20-08717S) and the European Regional Development Fund (Project CZ.02.1.01/0.0/0.0/16_019/0000845). Charles University team received institutional funding from the Centre for Geosphere Dynamics (UNCE/SCI/006). Part of the equipment used for this study was purchased from the Operational Programme Prague – Competitiveness (Project CZ.2.16/3.1.00/21516). Dr. Madeleine Štulíková (a native speaker) is thanked for revision of the English manuscript. Finally, we would also like to thank the Editor Prof. Bernd Nowack (Swiss Federal Laboratories for Materials Science and Technology) and the anonymous reviewers for their valuable comments which helped to improve the original manuscript version.

Appendix A. Supplementary data

Supplementary data to this article can be found online at https://doi.org/10.1016/j.envpol.2020.114822.

References

Aguilar-Carrillo, J., Herrera, L., Gutiérrez, E.J., Reyes-Domínguez, I.A., 2018. Solid-phase distribution and mobility of thallium in mining-metallurgical residues: environmental hazard implications. Environ. Pollut. 243, 1833–1845. https://doi.org/10.1016/j.envpol.2018.10.014.

Bakardjieva, S., Bezdička, P., Grygar, T., Vorm, P., 2000. Reductive dissolution of microparticulate Mn oxides. J. Solid State Electrochem. 4, 306–313. https://doi.org/10.1007/s100089900104.

Garrido, F., Garcia-Guinea, J., Lopez-Arce, P., Voegelin, A., Göttlicher, J., Mangold, S., Almendros, G., 2020. Thallium and co-genetic trace elements in hydrothermal Fe-Mn deposits of Central Spain. Sci. Total Environ. 717, 137162. https://doi.org/10.1016/j.scitotenv.2020.137162.

Gee, G.W., Bauder, J.W., 1986. Particle-size analysis. In: Klute, A. (Ed.), Methods of Soil Analysis. Part I: Physical and Mineralogical Methods. American Society of Agronomy-Soil Science Society of America, Madison, WI, pp. 383–411.

Gomez-Gonzalez, M.A., Garcia-Guinea, J., Laborda, F., Garrido, F., 2015. Thallium occurrence and partitioning in soils and sediments affected by mining activities in Madrid province (Spain). Sci. Total Environ. 536, 268–278. https://doi.org/10.1016/j.scitotenv.2015.07.033.

Grösslová, Z., Vanek, A., Oborná, V., Mihaljevic, M., Ettler, V., Trubac, J., Drahota, P., Penízek, V., Pavlu, L., Sracek, O., Kríbek, B., Voegelin, A., Göttlicher, J., Ondrej, D., Tejnecký, V., Houska, J., Mapani, B., Zádorová, T., 2018. Thallium contamination of desert soil in Namibia: chemical, mineralogical and isotopic insights. Environ. Pollut. 239, 272–280. https://doi.org/10.1016/j.envpol.2018.04.006.

Hermann, J., Voegelin, A., Palatinus, L., Mangold, S., Majzlan, J., 2018. Secondary Fe-as-Tl mineralization in soils near Buus in the Swiss jura mountains. Eur. J. Mineral 30, 887–898. https://doi.org/10.1127/ejm/2018/0030-2766.

Howarth, S., Prytulak, J., Little, S.H., Hammond, S.J., Widdowson, M., 2018. Thallium

concentration and thallium isotope composition of lateritic terrains. Geochem. Cosmochim. Acta 239, 446–462. https://doi.org/10.1016/j.gca.2018.04.017.
Jacobson, A.R., McBride, M.B., Baveye, P., Steenhuis, T.S., 2005. Environmental factors determining the trace-level sorption of silver and thallium to soils. Sci. Total Environ. 345, 191–205. https://doi.org/10.1016/j.scitotenv.2004.10.027.
Jakubowska, M., Pasieczna, A., Zembrzuski, W., Swit, Z., Lukaszewski, Z., 2007. Thallium in fractions of soil formed on floodplain terraces. Chemosphere 66, 611–618. https://doi.org/10.1016/j.chemosphere.2006.07.098.
Karbowska, B., Zembrzuski, W., Jakubowska, M., Wojtkowiak, T., Pasieczna, A., Lukaszewski, Z., 2014. Translocation and mobility of thallium from zinc–lead ores. J. Geochem. Explor. 143, 127–135. https://doi.org/10.1016/j.gexplo.2014.03.026.
Kersten, M., Xiao, T., Kreissig, K., Brett, A., Coles, B.J., Rehkämper, M., 2014. Tracing anthropogenic thallium in soil using stable isotope compositions. Environ. Sci. Technol. 48 (16), 9030–9036. https://doi.org/10.1021/es501968d.
Liu, J., Wang, J., Chen, Y., Xie, X., Qi, J., Lippold, H., Luo, D., Wang, C., Su, L., He, L., Wu, Q., 2016. Thallium transformation and partitioning during Pb – Zn smelting and environmental implications. Environ. Pollut. 212, 77–89. https://doi.org/10.1016/j.envpol.2016.01.046.
Liu, J., Yin, M., Luo, X., Xiao, T., Wu, Z., Li, N., Wang, J., Zhang, W., Lippold, H., Belshaw, N.S., Feng, Y., Chen, Y., 2019. The mobility of thallium in sediments and source apportionment by lead isotopes. Chemosphere 219, 864–874. https://doi.org/10.1016/j.chemosphere.2018.12.041.
Nielsen, S.G., Wasylenki, L.E., Rehkämper, M., Peacock, C.L., Xue, Z., Moon, E.M., 2013. Towards an understanding of thallium isotope fractionation during adsorption to manganese oxides. Geochem. Cosmochim. Acta 117, 252–265. https://doi.org/10.1016/j.gca.2013.05.004.
Nielsen, S.G., Rehkämper, M., Prytulak, J., 2017. Investigation and application of thallium isotope fractionation. Rev. Mineral. Geochem. 82, 759–798. https://doi.org/10.2138/rmg.2017.82.18.
O'Reilly, S.E., Hochella, M.F., 2003. Lead sorption efficiencies of natural and synthetic Mn and Fe-oxides. Geochem. Cosmochim. Acta 67, 4471–4487. https://doi.org/10.1016/S0016.7037(03)00413-7.
Pansu, M., Gautheyrou, J., 2006. Handbook of Soil Analysis: Mineralogical, Organic and Inorganic Methods. Springer-Verlag, Berlin, Heidelberg, Germany.
Peacock, C.L., Moon, E.M., 2012. Oxidative scavenging of thallium by birnessite: explanation for thallium enrichment and stable isotope fractionation in marine ferromanganese precipitates. Geochem. Cosmochim. Acta 84, 297–313. https://doi.org/10.1016/j.gca.2012.01.036.
Peter, A.L.J., Viraraghavan, T. Thallium, 2005. A review of public health and environmental concerns. Environ. Int. 31 (4), 493–501. https://doi.org/10.1016/j.envint.2004.09.003.
Prytulak, J., Nielsen, S.G., Plank, T., Barker, M., Elliot, T., 2013. Assessing the utility of thallium and thallium isotopes for tracing subduction zone inputs to the Mariana arc. Chem. Geol. 345, 139–149. https://doi.org/10.1016/j.chemgeo.2013.03.003.
Rader, S.T., Mazdab, F.K., Barton, M.D., 2018. Mineralogical thallium geochemistry and isotope variations from igneous, metamorphic, and metasomatic systems. Geochem. Cosmochim. Acta 243, 42–65. https://doi.org/10.1016/j.gca.2018.09.019.
Rader, S.T., Maier, R.M., Barton, M.D., Mazdab, F.K., 2019. Uptake and fractionation of thallium by *Brassica juncea* in a geogenic thallium-amended substrate. Environ. Sci. Technol. 53 (5), 2441–2449. https://doi.org/10.1021/acs.est.8b06222.
Rehkämper, M., Frank, M., Hein, J.R., Porcelli, D., Halliday, A., Ingri, J., Liebetrau, V., 2002. Thallium isotope variations in seawater and hydrogenetic, diagenetic, and hydrothermal ferromanganese deposits. Earth Planet Sci. Lett. 197, 65–81. https://doi.org/10.1016/S0012-821X(02)00462-4.
Rehkämper, M., Frank, M., Hein, J.R., Halliday, A., 2004. Cenozoic marine geochemistry of thallium deduced from isotopic studies of ferromanganese crusts and pelagic sediments. Earth Planet Sci. Lett. 219, 77–91. https://doi.org/10.1016/S0012-821X(03)00703-9.
Schauble, E.A., 2007. Role of nuclear volume in driving equilibrium stable isotope fractionation of mercury, thallium, and other very heavy elements. Geochem. Cosmochim. Acta 71, 2170–2189. https://doi.org/10.1016/j.gca.2007.02.004.
Vaněk, Aleš, et al., 2012. Effect of low-molecular-weight organic acids on the leaching of thallium and accompanying cations from soil - A model rhizosphere solution approach. Journal of Geochemical Exploration 112, 212–217. https://doi.org/10.1016/j.gexplo.2011.08.010.
Vaněk, A., Chrastný, V., Mihaljevič, M., Drahota, P., Grygar, T., Komárek, M., 2009. Lithogenic thallium behavior in soils with different land use. J. Geochem. Explor. 102, 7–12. https://doi.org/10.1016/j.gexplo.2008.10.004.
Vaněk, A., Grygar, T., Chrastný, V., Tejnecký, V., Drahota, P., Komárek, M., 2010. Assessment of the BCR sequential extraction procedure for thallium fractionation using synthetic mineral mixtures. J. Hazard Mater. 176, 913–918. https://doi.org/10.1016/j.jhazmat.2009.11.123.
Vaněk, A., Grösslová, Z., Mihaljevič, M., Trubač, J., Ettler, V., Teper, L., Cabala, J., Rohovec, J., Zádorová, T., Penížek, V., Pavlů, L., Holubík, O., Němeček, K., Houška, J., Drábek, O., Ash, C., 2016. Isotopic tracing of thallium contamination in soils affected by emissions from coal-fired power plants. Environ. Sci. Technol. 50 (18), 9864–9871. https://doi.org/10.1021/acs.est.6b01751.
Vaněk, A., Grösslová, Z., Mihaljevič, M., Ettler, V., Trubač, J., Chrastný, V., Penížek, V., Teper, L., Cabala, J., Voegelin, A., Zádorová, T., Oborná, V., Drábek, O., Holubík, O., Houška, J., Pavlů, L., Ash, C., 2018. Thallium isotopes in metallurgical wastes/contaminated soils: a novel tool to trace metal source and behavior. J. Hazard Mater. 343, 78–85. https://doi.org/10.1016/j.jhazmat.2017.09.020.
Vaněk, A., Holubík, O., Oborná, V., Mihaljevič, M., Trubač, J., Ettler, V., Pavlů, L., Vokurková, P., Penížek, V., Zádorová, T., Voegelin, A., 2019. Thallium stable isotope fractionation in white mustard: implications for metal transfers and incorporation in plants. J. Hazard Mater. 369, 521–527. https://doi.org/10.1016/j.jhazmat.2019.02.060.
Vaněk, A., Voegelin, A., Mihaljevič, M., Ettler, V., Trubač, J., Drahota, P., Vaňková, M., Oborná, V., Vejvodová, K., Penížek, V., Pavlů, L., Drábek, O., Vokurková, P., Zádorová, T., Holubík, O., 2020. Thallium stable isotope ratios in naturally Tl-rich soils. Geoderma 364, 114183. https://doi.org/10.1016/j.geoderma.2020.114183.
Voegelin, A., Pfenninger, N., Petrikis, J., Majzlan, J., Plötze, M., Senn, A.C., Mangold, S., Steininger, R., Göttlicher, J., 2015. Thallium speciation and extractability in a thallium- and arsenic-rich soil developed from mineralized carbonate rock. Environ. Sci. Technol. 49 (9), 5390–5398. https://doi.org/10.1021/acs.est.5b00629.
Wick, S., Baeyens, B., Marques Fernandes, M., Voegelin, A., 2018. Thallium adsorption onto illite. Environ. Sci. Technol. 52 (2), 571–580. https://doi.org/10.1021/acs.est.7b04485.
Wick, S., Peña, J., Voegelin, A., 2019. Thallium sorption onto manganese oxides. Environ. Sci. Technol. 53 (22), 13168–13178. https://doi.org/10.1021/acs.est.9b04454.
Xiao, T., Guha, J., Boyle, D., Liu, C.Q., Chen, J., 2004. Environmental concerns related to high thallium levels in soils and thallium uptake by plants in southwest Guizhou, China. Sci. Total Environ. 318, 223–244. https://doi.org/10.1016/S0048-9697(03)00448-0.
Xiao, T., Yang, F., Li, S., Zheng, B., Ning, Z., 2012. Thallium pollution in China: a geo-environmental perspective. Sci. Total Environ. 421–422, 51–58. https://doi.org/10.1016/j.scitotenv.2011.04.008.

7.2. Thallium and lead variations in a contaminated peatland: A combined isotopic study from a mining/smelting area

Vaněk, A., Vejvodová, K., Mihaljevič, M., Ettler, V., Tubač, J., Vaňková, M., Goliáš, V., Teper, L., Cabala, J., Sutkowska, K., Vokurková, P., Penížek, V., Zádorová, T., Drábek, O. (2021). Thallium and lead variations in a contaminated peatland: A combined isotopic study from a mining/smelting area. Environmental Pollution, 290, 117973

Environmental Pollution 290 (2021) 117973

Contents lists available at ScienceDirect

Environmental Pollution

journal homepage: www.elsevier.com/locate/envpol

Thallium and lead variations in a contaminated peatland: A combined isotopic study from a mining/smelting area☆

Aleš Vaněk [a,*], Kateřina Vejvodová [a], Martin Mihaljevič [b], Vojtěch Ettler [b], Jakub Trubač [b], Maria Vaňková [b], Viktor Goliáš [b], Leslaw Teper [c], Katarzyna Sutkowska [c], Petra Vokurková [a], Vít Penížek [a], Tereza Zádorová [a], Ondřej Drábek [a]

[a] Department of Soil Science and Soil Protection, Faculty of Agrobiology, Food and Natural Resources, Czech University of Life Sciences Prague, Kamýcká 129, 165 00, Praha 6, Czech Republic

[b] Institute of Geochemistry, Mineralogy and Mineral Resources, Faculty of Science, Charles University, Albertov 6, 128 00, Praha 2, Czech Republic

[c] Institute of Earth Sciences, Faculty of Natural Sciences, University of Silesia, Bedzinska 60, 41-200, Sosnowiec, Poland

ARTICLE INFO

Keywords:
Deposition
Contamination
Isotopes
Peat
Mobility

ABSTRACT

Vertical profiles of Tl, Pb and Zn concentrations and Tl and Pb isotopic ratios in a contaminated peatland/fen (Wolbrom, Poland) were studied to address questions regarding (i) potential long-term immobility of Tl in a peat profile, and (ii) a possible link in Tl isotopic signatures between a Tl source and a peat sample. Both prerequisites are required for using peatlands as archives of atmospheric Tl deposition and Tl isotopic ratios as a Tl source proxy. We demonstrate that Tl is an immobile element in peat with a conservative pattern synonymous to that of Pb, and in contrast to Zn. However, the peat Tl record was more affected by local geogenic source(s), as inferred from the calculated element enrichments. The finding further implies that Tl was largely absent from the pre-industrial emissions (>~250 years BP). The measured variations in Tl isotopic ratios in respective peat samples suggest a consistency with major local source(s) of anthropogenic Tl (ε^{205}Tl between ~ -3 and −4), as well as with background Tl isotopic values in the study area (ε^{205}Tl between ~0 and −1), in line with detected $^{206}Pb/^{207}Pb$ ratios (1.16–1.19). Therefore, we propose that peatlands can be used for monitoring trends in Tl deposition and that Tl isotopic ratios can serve to distinguish Tl sources. However, given that the studied fen has a particularly complicated geochemistry (attributed to significant environmental changes in its history), it seems that ombrotrophic peatland(s) could be better suited for this type of Tl research.

1. Introduction

Due to their organic nature, peatlands behave as efficient scavengers of trace elements from the atmosphere (e.g., Cabala et al., 2013; De Vleeschouwer et al., 2009, 2020; Farmer et al., 2006; Fiałkiewicz-Kozieł et al., 2018, 2020; Kylander et al., 2005; Shotyk et al., 1992, 1996, 1998, 2001, 2016a, 2017; Shotyk and Krachler, 2004; Smieja-Król and Bauerek, 2015; Smieja-Król et al., 2015, 2019; Weiss et al., 1999, 2002, 2007). Regarding pollutant capture in peatlands, both physical and chemical mechanisms of binding have to be considered. This is a result of the gradual degradation of dust microparticles accompanied by element leaching and retention onto the organic matter (OM) or even coprecipitation (Cabala et al., 2013; Smieja-Król et al., 2010, 2015). There are a number of studies on trace element variations in peat profiles which demonstrate that peatlands (both bogs and fens), due to their sedimentary character, can be used to trace changes in atmospheric deposition, albeit with some limitations for specific elements and environmental conditions (Mihaljevič et al., 2006; Novak et al., 2008; Novak and Pacherova, 2008; Shotyk et al., 2000; Zuna et al., 2011, 2012). In general, peatlands cannot serve as efficient archives for elements which are mobile and tend to migrate through the peat layers (Smieja-Król and Bauerek, 2015; Weiss et al., 2007).

To our knowledge, there is only limited information about the geochemistry of thallium (Tl) in peatlands (Shotyk and Krachler, 2004; Shotyk et al., 2017; Smieja-Król et al., 2015), in fact, nothing is known about the behavior of its isotopes in this geosystem. In Upper Silesia in southern Poland there are several smaller peatlands. One of them is situated at Wolbrom, a town that has been subjected to long-term

☆ This paper has been recommended for acceptance by Yong Sik Ok.

* Corresponding author.
E-mail address: vaneka@af.czu.cz (A. Vaněk).

https://doi.org/10.1016/j.envpol.2021.117973
Received 28 April 2021; Received in revised form 8 July 2021; Accepted 12 August 2021
Available online 20 August 2021

deposition of trace elements, including Tl, caused by sulfide ore mining/processing. This type of activity is among the most significant local/global sources of anthropogenic Tl in the environment (e.g., Aguilar-Carrillo et al., 2018; Garrido et al., 2020; Gomez-Gonzalez et al., 2015; Lis et al., 2003; Liu et al., 2016, 2019, 2020a, 2020b; Lukaszewski et al., 2018; Wang et al., 2018, 2021; Xiao et al., 2004a, 2004b, 2012).

In this study, we report combined Tl, Pb and Zn concentrations and the Tl and Pb isotopic data from two contaminated peat profiles so that the following fundamental questions can be addressed. (i) Is Tl immobile in peat in the long term? (ii) Do Tl isotopes fractionate over post-depositional dust alteration and/or Tl adsorption? (iii) Do peatlands behave as efficient archives of atmospheric Tl pollution – can Tl isotopic signatures serve as proxies for Tl sources in peat, i.e., similar to Pb?

2. Experimental

2.1. Study site characterization and peat sampling

The studied peatland is situated at Wolbrom, a town in Upper Silesia (Silesian–Kraków region), southern Poland (GPS coordinates: N 50.376220, E 19.780626) (Fig. 1). The area is relatively small (~1000 × 500 m), it is characterized by a mean annual temperature of ~7 °C and ~700 mm/year precipitation. The botanical analysis revealed numerous remains of *Carex* and *Phragmites* species (e.g., *Carex rostrata* and *Phragmites australis*), proving that the peatland is a fen (Pawełczyk et al., 2017). However, due to recent urbanization in Wolbrom (Fig. 1), the original fen vegetation suffers from degradation in several habitats; alder and birch in combination with *Molinietalia* communities or *Nardo-Callunetea* swards represent the prevailing secondary plant species (Latałowa and Nalepka, 1987). The total peat thickness is up to 260 cm and the peat is generally assigned a good stability (Pawełczyk et al., 2017). Tudyka and Pazdur (2012) report that the oldest peat sections at Wolbrom date back to ~9900 BC.

The Wolbrom peatland has been contaminated by atmospheric fallout rich in trace elements including Zn, Pb and Tl, due to nearby mining/processing of Tl-rich Zn–Pb sulfide ores (ZnS and PbS; MVT deposit type) at Olkusz, situated ~20 km SW (Fig. 1). Being operational since 1952, the local Boleslaw Zn plant (primary/secondary Zn smelter) is considered the prevailing modern source of Tl/trace element contamination in the area (Cabala and Teper, 2007; Vaněk et al., 2011, 2013). Nevertheless, mining-related activities and even metal-containing dust loads derived from local flotation tailing dams both have to be considered as a decades-long source of Tl remobilization/deposition (Jakubowska et al., 2007; Karbowska et al., 2014; Lis et al., 2003; Lukaszewski et al., 2018). Furthermore, it should be noted that first metal extractions in the region, mainly silver and lead, are documented by archeologists and date back to both Roman and medieval periods (Bodnar and Rozmus, 2004; Cabala et al., 2013; Rozmus, 2014).

In this study, we sampled one complete peat profile (0–110 cm, à 2 cm, 55 samples) and one shallow profile (0–40 cm, à 2 cm, 20 samples) from ~0.5 × 1 m-wide pits in November 2019 (Fig. 1). The latter (incomplete) profile was sampled for comparison, so that the concentration trends of trace elements for the contaminated section could have been verified. The samples were stored in PE bags, then dried to a constant weight and properly homogenized in the laboratory. The underlying mineral layers (rocks) bordering the peat column, represented by Quaternary clayed sand (120–150 cm) and Cretaceous (Turonian) chalk rock (≥150 cm), were sampled by drilling. It should be emphasized that we revealed a marked compaction of peat during core sampling and that was the reason why we decided to collect peat samples manually.

For the isotopic tracing of Tl and Pb, we used the isotopic records from respective industrial and natural samples (Table 1). These materials involve: (i) massive Pb ore (PbS) (adopted from Vaněk et al., 2011); (ii) Zn ore concentrate (ZnS) from the Olkusz mine, produced by flotation; (iii) Reflot – Zn/Pb ore concentrate (ZnS + PbS), produced by mine waste recycling (flotation); (iv) modern fly ash and slag – waste materials derived from Zn roasting/Waelz technology (Boleslaw Zn plant), i.e., by roasting different recyclable Zn-rich materials (adopted from Vaněk et al., 2018); (v) modern granulated waste – a complex mixture of materials from pyro- and hydrometallurgy (adopted from Vaněk et al., 2018); (vi) Larox sludge – waste from the wet filtration of $ZnSO_4$ electrolyte within the hydrometallurgical process. This material is a waste product from the initial feed, which consists of ~50% of local ZnS (Olkusz mine). At this point it should be noted that old processing wastes are not available, therefore we could study only the available modern materials. As far as the geogenic Tl is concerned, the isotopic data relating to the underlying rocks were used as a background reference (Table 1).

2.2. Peat properties

The soil pH (active and potential) was measured in H_2O/KCl

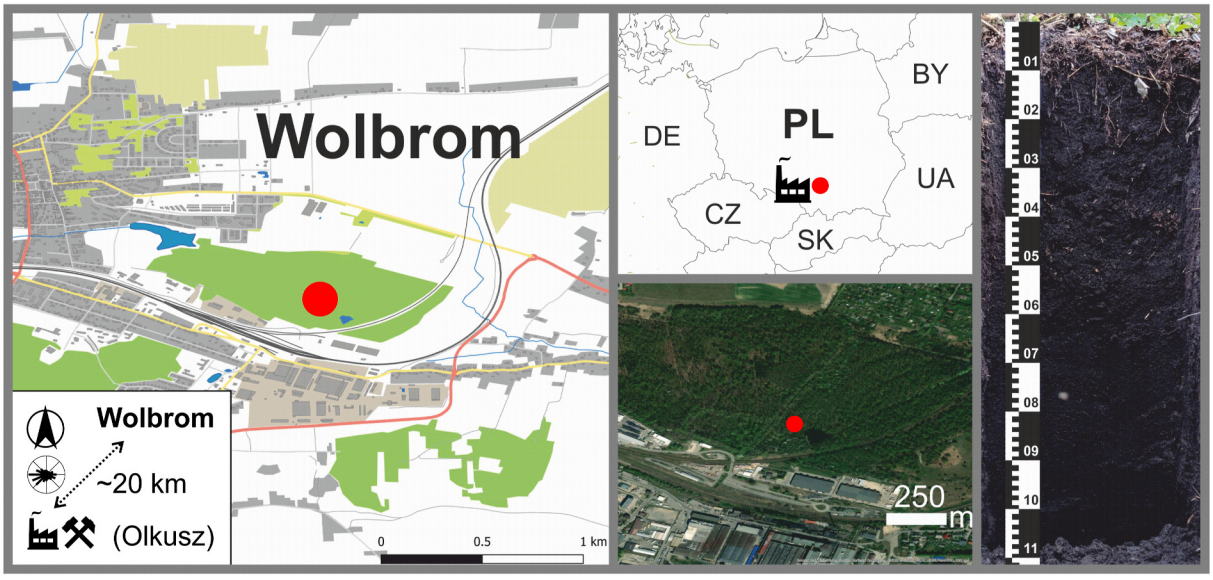

Fig. 1. The peat sampling site (GPS coordinates: N 50.376220, E 19.780626); the studied peat profile.

Table 1
The physicochemical properties, total and exchangeable Tl concentrations (Tl_{TOT}, Tl_{EXCH}) and the Tl and Pb isotopic signatures (in $\varepsilon^{205}Tl$, $^{206}Pb/^{207}Pb$) in peat samples (≤40 cm) from the main/complete peat profile (0–110 cm), the underlying mineral layers/rocks (≥120 cm) and the reference ore/waste materials.

Sample/ Layer	Depth (cm)	Age Date	pH H_2O	pH KCl	Density (g/cm^3)	LOI (%)	TC* (%)	TS*	CEC (cmol+/kg)	Tl_{TOT} (mg/kg)	Tl_{EXCH}* (mg/kg)	$\varepsilon^{205}Tl$ ±0.7	$^{206}Pb/^{207}Pb$
1	0–2	2016 ± 4 AD	4.3	4.2	–	74.3	40.7	0.5	99	0.71*	0.11	–	1.1792
2	2–4	2009 ± 5 AD	4.2	3.9	0.21	76.9	38.7	0.5	96	0.72	0.12	–	1.1759
3	4–6	2004 ± 5 AD	3.8	3.8	0.21	75.2	38.2	0.5	96	0.76	0.13	−3.09	1.1742
4	6–8	1998 ± 6 AD	3.9	3.8	0.25	72.7	36.9	0.5	96	0.84	0.11	−2.30	1.1641
5	8–10	1991 ± 7 AD	4.2	3.8	0.25	74.0	37.3	0.5	93	0.80*	0.12	−2.78	1.1712
6	10–12	1981 ± 8 AD	4.1	3.8	0.29	–	36.9	0.5	95	0.82	–	−3.57	1.1658
7	12–14	1971 ± 10 AD	4.3	3.9	0.29	–	38.6	0.5	103	0.72	–	−3.16	1.1707
8	14–16	1962 ± 12 AD	4.5	4.1	0.29	–	38.5	0.5	98	0.51	–	–	1.1651
9	16–18	1954 ± 13 AD	4.8	4.3	0.29	–	40.3	0.5	98	0.41	–	–	1.1706
10	18–20	1946 ± 14 AD	4.8	4.3	0.29	–	40.3	0.6	102	0.48	–	–	1.1773
11	20–22	–	4.9	4.3	0.28	–	39.2	0.6	96	0.48	–	–	1.1750
12	22–24	–	4.9	4.4	0.28	–	42.5	0.6	103	0.36	–	–	1.1750
13	24–26	–	4.9	4.4	0.28	–	42.3	0.6	107	0.30	–	–	1.1768
14	26–28	–	4.9	4.4	0.28	–	44.0	0.7	112	0.29	–	–	1.1741
15	28–30	–	5.0	4.5	0.28	–	45.5	0.7	111	0.25	–	–	1.1699
16	30–32	–	5.0	4.5	0.26	–	40.7	0.6	110	0.45	0.04	–	1.1761
17	32–34	–	5.0	4.5	0.26	–	42.8	0.7	111	0.39	0.03	–	1.1749
18	34–36	–	4.9	4.4	0.26	–	42.0	0.7	100	0.41	0.02	−1.06	1.1760
19	36–38	–	4.9	4.5	0.26	–	43.4	0.7	91	0.35	0.02	−1.25	1.1751
20	38–40	300 ± 90 BC	5.1	4.5	0.26	–	41.1	0.7	109	0.42*	0.02	−1.59	1.1693
Clayey sand	120–150	Quaternary	–	–	–	–	–	–	–	0.12 ± 0.06#	–	−1.47	1.1893
Chalk rock (bedrock)	150-	Turonian	–	–	–	–	–	–	–	0.21 ± 0.10#	–	+0.47	1.1856
Massive Pb ore (PbS)		–	–	–	–	–	–	–	–	–	–	–	1.173
Zn ore concentrate (ZnS)		–	–	–	–	–	–	–	–	70.1 ± 12.8#	–	−4.40	–
Reflot (ZnS + PbS)		–	–	–	–	–	–	–	–	94.8 ± 3.6#	–	−4.20	–
Fly ash (Zn metallurgy, roasting)		–	–	–	–	–	–	–	–	15.0 ± 1.0#	–	−4.09	1.174
Slag (Zn metallurgy, roasting)		–	–	–	–	–	–	–	–	1.19 ± 0.60#	–	−3.31	–
Granulated waste (Zn metallurgy)		–	–	–	–	–	–	–	–	322 ± 110#	–	−3.60	–
Larox sludge (Zn metallurgy)		–	–	–	–	–	–	–	–	122 ± 0	–	−3.63	–

The $\varepsilon^{205}Tl$ data assign an estimated error (±0.7, 2 SD) which is based on our long-term external reproducibility for the SRM AGV-2 (Andesite, USGS, USA). *The data depict means (n = 3; RSD ≤10%). #The Tl concentrations depict means (n = 3; ±2 SD). LOI: loss on ignition. –: not determined. Reflot – a concentrate produced by mine waste recycling (flotation). The isotopic data in Pb ore, fly ash, slag and granulated waste were adopted from Vaněk et al. (2011, 2018). See the SM section for details.

solutions (v/v ratio, 1/5). The ash content (loss of ignition) was determined by combusting 1 g of peat at 550 °C (expressed as % of the dry weight sample). The total carbon and sulfur concentrations (TC, TS) were determined using a CNS analyzer (Flash, 2000; Thermo Scientific, Germany). The soil cation exchange capacity (CEC) was determined on the basis of sodium acetate method (Bower et al., 1954). For the determination of exchangeable Tl fraction in peat, representing the potentially labile Tl pool, a 1 M NH_4NO_3 extraction solution was used (S/L ratio, 1/10, 2 h).

Total Zn, Pb, Tl, Fe, Mn and Sc concentrations in peat samples, rocks and ore/waste materials were determined using Q-ICP-MS Xseries II (Thermo Scientific, Germany); a total mass of ≤0.5 g of a finely-ground sample was digested in a mixture of HNO_3, HCl and HF (3/1/1 ratio, ≤20 mL, ~200 °C, 3 h, ±5 mL H_2O_2) (Merck, Germany) using a microwave system (Multiwave 5000, Anton Paar, Austria). The obtained solutions were evaporated and redissolved in 2% HNO_3 (25 mL) before further use or analysis. An analogous dilution was used for the exchangeable Tl determination. Scandium concentrations were determined by Q-ICP-MS using a single Sc calibration prior to the measurement. All mineral and selected peat samples (no. 1, 5 and 20) were 3-times replicated. This data, in combination with data obtained for the SRM 2711 (Montana Soil, NIST, USA) (Table S1, Supplementary Material, SM) were used for the quality control (QC) of concentration measurements (Tl, Zn, Pb).

^{210}Pb γ spectrometry was used for age dating of the uppermost peat layers (≤20 cm). A Canberra DSA 2000 multichannel analyzer controlled by GENIE 2000 software was used to determine the specific activities of ^{210}Pb, ^{226}Ra and ^{137}Cs isotopes. Selected peat samples from the deeper layers (≥40 cm) were dated by the ^{14}C technique using an EnvironMICADAS compact tandem accelerator. Detailed information about both $^{210}Pb/^{14}C$-dating methods is available in the SM section.

2.3. Thallium and Pb isotopic analyses

The determination of Tl isotopic ratios preceded Tl isolation. For this purpose, a two-stage chromatographic separation employing the Bio-Rad AG1-X8 (an anion exchange resin, 200–400 mesh, Cl^- cycle) was conducted, i.e., without utilizing HBr. For detailed information about the Tl isolation from sample solutions refer to Grösslová et al., 2018; Vaněk et al. (2016), 2018, 2020. Detailed information about the

measurement of Tl isotopic ratios using MC-ICP-MS Neptune Plus (Thermo Scientific, Germany), including the analytical conditions similar to those described in e.g. Prytulak et al. (2013, 2017), and the respective QC (Table S2, SM), are shown in the SM section. The Tl isotopic composition was calculated using the following equation with ε notation relative to NIST SRM 997 (Eq. (1)):

$$\varepsilon^{205}Tl = \frac{{}^{205}Tl/{}^{203}Tl_{sample} - {}^{205}Tl/{}^{203}Tl_{NIST997}}{{}^{205}Tl/{}^{203}Tl_{NIST997}} \times 10^4 \quad (1)$$

The Pb isotopic ratios ($^{206}Pb/^{207}Pb$) were determined using Q-ICP-MS. Solutions were diluted to ~20 μg Pb/L prior to analysis. The mass bias correction was performed using standard-sample bracketing with the SRM 981 (Common lead, NIST, USA). The accuracy of the measurements was controlled using the SRM AGV-2 (Andesite, USGS, USA) with $^{206}Pb/^{207}Pb$ = 1.2085 ± 0.0006 and $^{208}Pb/^{206}Pb$ = 2.0415 ± 0.0013. More information about the analytical conditions for the determination of Pb isotopes is available in Vaněk et al. (2011) and Zuna et al. (2011).

3. Results and discussion

3.1. Trace element concentrations in peat

The concentration trends of Zn, Pb and Tl in the studied peat profiles are shown in Fig. 2 and listed in Tables 1, S3 and S4 (SM). Both deep and shallow profiles identically exhibit significant accumulation of all trace elements in the interval of ~0–40 cm, with the highest concentrations within the uppermost peat (0–16 cm), corresponding to layers formed earlier than 1962 (±12), as dated by the ^{210}Pb method. The question that arises here is to which degree the contribution of recent biomass (e.g., decayed roots/leaves) could have affected our ^{210}Pb data. However, in view of temporal emission data for Boleslaw Zn plant and the data on local Zn–Pb ore production (at Olkusz), in combination with the absence of peat disturbance according to the ^{210}Pb, there is a match in trace element stratigraphy in the studied peat columns, with a peak between the 1960s and the mid 1980s (Liszka and Świć, 2004) (Fig. 2, Table S3, S4, SM). The finding is also consistent with trace element records in the surface layers of different ombrotrophic bogs in southern Poland, mostly attributed to ore mining/processing activities, or extensive coal mining/industrial burning, or due to the general development of local industry (Fiałkiewicz-Kozieł et al., 2018; Smieja-Król and Bauerek, 2015; Smieja-Król et al., 2010, 2015, 2019). Despite the fact that we do not have exact data on historical mining-/smelting-derived Tl emissions in the Wolbrom area, a similar trend as for Zn and Pb is inferred (Lis et al., 2003; Vaněk et al., 2011, 2013). Given the high concentrations of Tl/trace elements in the 0-10-cm peat section (≥1991) (Tables 1, S3, SM), continuing ore mining or more likely dust/trace element remobilization from the adjacent flotation tailing dams are assumed to be the primary cause (Cabala and Teper, 2007; Jakubowska et al., 2007; Karbowska et al., 2014; Lis et al., 2003).

The peat interval of 0–50 cm covers the peat age of more than the last 5000 years. Due to their position in the age-depth model, samples 20 (38–40 cm) and 26 (50–52 cm), ^{14}C-dated 300 BC and 3720 BC respectively, do reflect an ancient hiatus (Fig. S1, SM). The event, which was first revealed by Pawełczyk et al. (2017) in the Wolbrom fen, could be related to specific environmental changes such as a low water table in that time (Pawełczyk et al., 2017). In addition, we assume that increased concentrations of trace elements in the respective peat zone (38–52 cm) (Fig. 2, Tables 1, S3, S4, SM) result from the hiatus as well, reflecting the

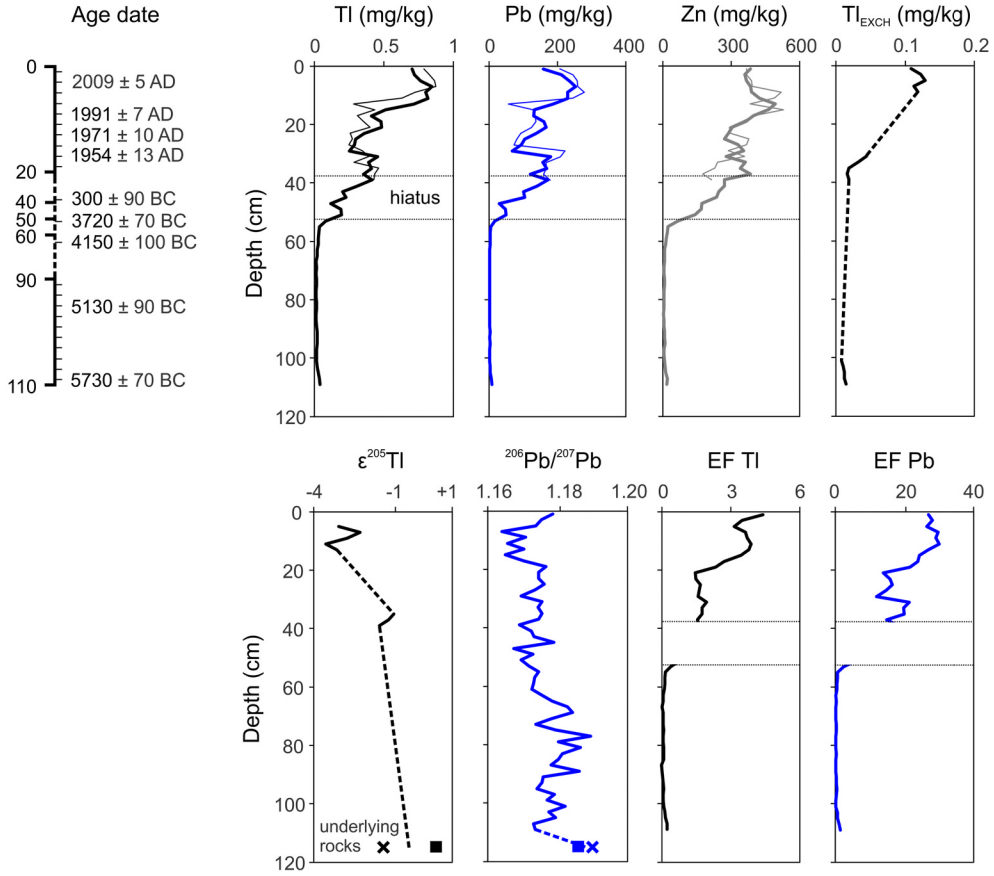

Fig. 2. The depth-dependent evolution of Tl, Pb and Zn concentrations, the exchangeable Tl fraction, the Tl and Pb isotopic signatures (in $\varepsilon^{205}Tl$, $^{206}Pb/^{207}Pb$) and corresponding enrichment factors of Tl and Pb in the studied peat profiles. Dashed lines indicate approximations between the measured samples. Narrow lines for Tl, Pb and Zn concentrations depict trends obtained within the shallow/incomplete peat profile (0–40 cm). See the SM section for details.

decline in OM accumulation, caused by a limited plant growth in that time. Due to the minimum rate of sediment formation (Fig. S1, SM) we were not able to distinguish/quantify the potential effect of pre-Roman mining/processing of local ores (Bodnar and Rozmus, 2004; Rozmus, 2014).

The relatively high concentrations of trace elements in peat samples above the hiatus (≤38 cm) were attributed to a combined effect of historical ore mining/processing at Olkusz. Archeologists document that the area acts as a mining/smelting center (mainly for Pb and Ag ores) within both the Roman and medieval periods (Bodnar and Rozmus, 2004; Cabala et al., 2013; Rozmus, 2014). It is probable that the deposition of trace elements in the area further accelerated with the start of industrial revolution (~250 years BP), which, however, we were not able to link with the peat concentration data, due to the absence of peat dating for this time interval.

To estimate the anthropogenic enrichment of trace elements, we used the Sc concentration for element normalization and local bedrock ratio M/Sc as a geogenic (background) reference (Table S3, SM). The enrichment factor (EF) was calculated as (Eq. (2)):

$$EF = [M/Sc]_{sample} \Big/ [M/Sc]_{bedrock} \quad (2)$$

This approach was chosen with regard to generally increased background concentrations of trace elements in the study area, and thus a less informative value of Sc for the average Earth crust (if used).

Similar to their concentrations, the maximum EFs for both Pb (≤30) and Tl (≤4) (Fig. 2, Table S3, SM), were found in the uppermost peat (0–16 cm), indicative of extensive mining and processing of local ores and even post-mining effects over the course of the second half of 20th century until the present time. In line with Pb concentrations, significant Pb enrichments, starting with EF = 15, were found above the hiatus (≤38 cm), again in line with historical mining/processing of local ores. In contrast, systematically low EF values of Tl (≤4) in combination with Tl concentrations of 0.3–0.8 mg/kg recorded for the same peat section, imply the importance of the introduction of natural (geogenic) Tl into the peatland (Table S3, SM). In other words, the EF values from the range of ≤0.5–1.0 suggest that the vast majority of Tl entered peat naturally (soil erosion, rock weathering, etc.). However, this can be promoted by agricultural tillage (Shotyk et al., 2001), i.e., due to soil/rock dust mobilization and deposition. Such a prediction is possibly supported by matching Tl concentrations in the underlying rock samples (0.1–0.2 mg/kg) or the low amount of exchangeable Tl fraction in the middle profile zone (≤0.04 mg/kg), as well as the isotopic proxies (Fig. 2, Tables 1, S5, SM).

3.2. Trace element mobility in peat

When viewing the highest concentrations of trace elements, a vertical shift of Zn (~4 cm) relative to Pb/Tl can be observed in the uppermost peat (0–16 cm) (Tables S3, S4, SM). Similarly, in the deeper peat (~30 cm) an increased Zn concentration was observed alongside declining Pb/Tl concentrations. As such, this supports the anticipated vertical migration of Zn in the peat profile (Weiss et al., 2007) in line with low peat pH values (~4) (Table 1) and generally "less active behaviors" of Pb and Tl (e.g., Shotyk et al., 1996; Shotyk and Krachler, 2004; Zuna et al., 2011). Although we did not investigate the peat pore waters at the sampling site, the formation of strong Zn complexes with mobile fulvic acids associated with small-size colloidal particles could promote its migration (Novak and Pacherova, 2008). Lead, by contrast, tends to occur in large colloids and it readily forms stable complexes with humic acids (Gao et al., 1999), likely promoting its immobility in peat. Although, Shotyk et al. (2016b) report that some part of the total Pb can be mobilized in peat and enter the peat pore water, on an example of different bogs the authors highlight that less than 0.01% of total Pb is labile (soluble), making the potential for Pb migration very small.

As far as Tl is concerned, there is no evidence on the formation of stable/strong complexes with any simple organic compounds, fulvic or humic acids (Jacobson et al., 2005; Nriagu, 1998). This implies that Tl (if previously mobilized) is possibly adsorbed more simply, following the non-specific/specific reactions onto the OM. The association of Tl with the –SH functional groups can further promote its fixation (Nriagu, 1998). Shotyk and Krachler (2004) report that Tl in bogs exhibits a comparable pattern to Pb (and Ag), supporting the theory that Tl is immobile in peat. Our evidence for the proposed Pb/Tl analogy, as well as a general stability of Tl in the studied peatland is provided by a significant positive relationship ($R^2 = 0.95$) between their concentrations (Fig. S2, SM). The question that arises here is, what could be the role of K^+ and/or NH_4^+ in exchangeable Tl sorption, reflecting comparable ion chemistry and allowing their competition or potentially specific (stronger) Tl fixation (Vaněk et al., 2012).

In general, we do not expect significant mobilization of trace elements in the underlying mineral formations and their migration upward in the fen. This behavior seems to be negligible for Pb and Tl and only limited for Zn, as inferred by the concentration comparison at the rock-peat interface (Table S3, SM).

3.3. Thallium isotopic variability in peat

The Tl isotopic data found in the peat profile, the underlying rocks and the industrial samples are shown in Fig. 2 and listed in Tables 1 and S5 (SM).

Given the overall variability in the studied industrial samples (~1 ε^{205}Tl) involving local Zn/Pb ores and different waste materials from both roasting/Waelz (fly ash, slag) and hydrometallurgical technologies (granulated waste, Larox sludge) derived from primary and recyclable Zn-rich materials (Table 1), generally small Tl isotopic fractionation is assumed for a complex industrial process (Vaněk et al. (2018). Such an isotopic homogeneity is quite surprising, at least in view of a wide range of Tl concentrations (1–300 mg/kg) (Table 1) or a large variability in Tl isotopic ratios in different solid wastes from pyrite roasting, yielding ~17 ε^{205}Tl units (from −1 to +16), as reported by Liu et al. (2020a). Therefore, our results are similar to data by Kersten et al. (2014), who indicate even the absence of Tl isotopic fractionation for a high-temperature process, albeit in relation cement production. The authors revealed an analogy in the isotopic signature in Tl-rich FeS_2, co-combusted FeS_2 roasting waste (as an additive) and emitted cement kiln dust (CKD), all featuring ε^{205}Tl ~0.

Our peat profile exhibits an apparent isotopic variability with ε^{205}Tl yielding the range of −3.6 and −1.1. Importantly, we identified only negative ε^{205}Tl values (≥-3.6) in the uppermost peat (0–14 cm, ≥1971). Therefore, these values are quite similar to the isotopic signatures found in local ore and/or metallurgical samples (ε^{205}Tl from −3.3 to −4.4), which correspond to the potential source(s) of historical Tl contamination in the area (Table 1). Regarding these findings, there is evidence to suggest that detectable Tl contamination is entering the peat via the isotopically light Tl (enriched in ^{203}Tl) (Fig. 2).

By contrast, in the 34–40 cm peat-profile section we identified a clear shift toward the isotopically-heavy Tl (enriched in ^{205}Tl) (ε^{205}Tl ≥ -1.6) (Fig. 2). By combining this data with generally low EFs for Tl and a missing isotopic link with the reference ores and metallurgical wastes (Table 1), we assume that the peat signatures reflect the introduction of geogenic Tl. Besides the isotopic similarity with the underlying rocks (ε^{205}Tl −1.5 and + 0.5, respectively) (Table 1), the proposed geogenic origin of Tl in the deeper peat is further supported by a model isotopic segregation according to source reservoirs (Fig. S3, SM). Since we did not detect either vertical Tl shift(s) in the studied profiles, suggesting its immobility in peat, or any indication for specific Tl(I) complexation onto the OM, the Tl isotopic fractionation in peat is not very probable. Although in relation to Cu, Bigalke et al. (2010) attributed specific fixation of Cu onto humic compounds to the accumulation of the isotopically heavy fraction of Cu, accompanied by the isotopically light Cu

mobilization/migration.

At this point, it should be highlighted that the introduction and/or recycling of Tl via its uptake by peat vegetation, i.e., due to the K-channel and/or –SH containing compounds in plants (e.g., Kersten et al., 2014; Rader et al., 2019; Vaněk et al., 2019) cannot explain variations in Tl distribution in the studied peatland. The deep peat layers (≥60 cm), absent of contamination, are very low in Tl (~0.01 mg/kg); this is much less in comparison with the underlying rocks (≥0.12 mg/kg) (Table S3, SM). This finding allows us to neglect the biological Tl uptake as a potential source of Tl isotopic fractionation toward the isotopically light Tl in the surface/subsurface peat (Vaněk et al., 2019).

3.4. Lead isotopic variability in peat

The Pb isotopic ratios ($^{206}Pb/^{207}Pb$) determined in the studied peat profile, underlying rocks and selected materials referring to anthropogenic and geogenic Pb are shown in Fig. 2 and listed in Tables 1 and S5 (SM).

The vertical $^{206}Pb/^{207}Pb$ profile shows apparently less radiogenic Pb in the 0-40-cm peat section, yielding 1.1641–1.1792, relative to the deeper peat samples (1.1722–1.1906) (Table S5, SM). Given the overall isotopic variations within the profile, the data strongly suggest that extensive mining and processing of local Zn/Pb ores, including post-mining effects in the second half of 20th century, are the primary cause for a $^{206}Pb/^{207}Pb$ decline in the uppermost peat (<16 cm) (Fig. 2). Such a prediction is favored by similar signatures for local galena and fly ash samples (1.173 and 1.174, respectively), mimicking the model (modern) sources of anthropogenic Pb in the area (Vaněk et al., 2011). This data in combination with $^{206}Pb/^{207}Pb$ values measured in the underlying rocks (1.1856 and 1.1893, respectively), points further to an introduction of only geogenic Pb in peat pre-dating ~4000 BC (~≥60 cm). The trend where Pb is less radiogenic for all modern, industrial and pre-industrial periods (De Vleeschouwer et al., 2009; Fiałkiewicz-Kozieł et al., 2018, 2020; Mihaljevič et al., 2006; Novak et al., 2008; Shotyk et al., 2000; Weiss et al., 2002) and becomes progressively more radiogenic downwards in the peat (higher in $^{206}Pb/^{207}Pb$) is best distinguishable for a complete peat profile (Fig. 2, Table S5, SM). Overall, the obtained Pb isotopic data (indicative of Pb mixing between two reservoirs but with a predominance of the anthropogenic pool), are in good agreement with both element and EF systematics of Pb in the studied peat profile (Table S3, SM), as well as with $^{206}Pb/^{207}Pb$ ratios observed in various peatlands in southern Poland (Fiałkiewicz-Kozieł et al., 2018, 2020).

3.5. Limitations of the use of stable Tl isotopes for source tracing in peatlands

If we use the Fe and Mn concentration data or the depth-dependent evolution of Mn/Fe ratio in the studied peat profile (Fig. S4, SM) as proxies for the redox-driven effects, variations reflecting environmental changes in the studied peatland are apparent. For example, the increased Fe and Mn concentrations and a high Mn/Fe ratio in the depth of ~10 cm can be related to modern oxidation of the OM just below the peat surface. Similarly, small peaks in Mn concentration and Mn/Fe ratio observed at ~50 cm can imply an old oxidation event in the peatland (Fig. S4, SM), which could be linked with the identified hiatus. Cabala et al. (2013), who studied the origin of metallic phases in peat, show that both Fe/Mn-oxides can readily form, following for example the breakdown of metal-organic complexes. Furthermore, the oxidation process can be caused by a low water-table level, an interaction of oxygenated meteoric waters within the surface/subsurface peat section, or even an interaction of peat with oxidizing groundwater (Cabala et al., 2013). On examples of laterite profiles, Howarth et al. (2018) report peaks in Fe-oxide concentrations accompanied by positive $\varepsilon^{205}Tl$ values, which trace the paleowater tables. For Tl, numerous studies suggest that the precipitation of secondary Tl-containing phases in sedimentary systems, mainly of specific Mn-oxides (e.g., hexagonal birnessite) and associated oxidative Tl uptake (Peacock and Moon, 2012; Voegelin et al., 2015; Wick et al., 2019, 2020), is a major control mechanism for isotopically-heavy Tl enrichments (Fe/Mn-oxide containing sedimentary crusts, precipitates, soil nodules, etc.) (Nielsen et al., 2013, 2017; Ostrander et al., 2019; Owens et al., 2017; Rehkämper et al., 2002, 2004; Schauble, 2007).

Although we did not observe any indications for vertical Tl migration and Tl isotopic fractionation in the studied peatland, cyclic changes in pH and/or redox could result in partial Tl leaching and subsequent preferential Tl enrichment in specific peat layers, accompanied by oxidative Tl sorption. For instance, this Tl behavior has recently been observed in the redoximporhic soils (Vaněk et al., 2020; Vejvodová et al., 2020). Therefore, if these processes take place in a peatland, they could limit the use of Tl isotopic ratios as proxies for anthropogenic/geogenic Tl sources. To gain further insights into this issue, and to verify the conservative feature of Tl, combined Tl isotopic and mineralogical micro-scale studies are required in peatlands with marked oxide accumulations and/or in peat samples enriched in Fe/Mn-oxides (e.g., Smieja-Król et al., 2010, 2015).

4. Conclusions

This study presents vertical patterns of Tl, Pb and Zn concentrations and stable Tl and Pb isotopic ratios from a historically contaminated peatland/fen (Wolbrom, Poland). The following major conclusions were made:

(i) Thallium is characterized as an immobile element in peat which mirrors the conservative pattern of Pb, in contrast to Zn which has a tendency to migrate. Both Tl and Pb reflect the history of atmospheric deposition. However, the peat Tl record is more affected by local geogenic sources, relative to Pb, as inferred from calculated (anthropogenic) element enrichments. Overall, this finding indicates that pre-industrial anthropogenic emissions (>~250 years BP) were generally low in Tl, confirming the observation of e.g. Shotyk and Krachler (2004).

(ii) The measured variations in Tl isotopic ratios (in $\varepsilon^{205}Tl$) in peat samples suggest a link with the local source(s) of anthropogenic Tl and the background Tl isotopic values in the study area. Furthermore, we did not detect Tl isotopic fractionation in peat samples, which if present, could be ascribed to Tl-rich dust alteration and/or Tl sorption onto the peat OM during the post-depositional residence time in peat, or even to biological processes. The finding is indicative of the absence of redox Tl(I)–Tl(III) shift(s), being previously proposed as a key control for Tl isotopic fractionation in sediments/soils, etc.

(iii) The obtained stable Tl isotopic data show a consistency with the $^{206}Pb/^{207}Pb$ ratios, which further support the potential use of Tl isotopic ratios as proxies for Tl sources in peatlands. However, given the complicated geochemistry of the studied fen, we propose to focus further research on well-preserved Tl-contaminated ombrotrophic peatlands.

Declaration of competing interest

The authors declare that they have no known competing financial interests or personal relationships that could have appeared to influence the work reported in this paper.

Acknowledgements

This study was funded by the projects of the Czech Science Foundation (GAČR 20-08717S) and the European Regional Development Fund (CZ.02.1.01/0.0/0.0/16_019/0000845). Charles University authors also received institutional funding from the UNCE/SCI/006

project and the Polish authors were supported by the University of Silesia (WNP/INoZ/2020-ZB32). We would also like to thank the Editor Prof. Yong Sik Ok and the anonymous reviewers for their valuable comments which helped to improve the quality of the original manuscript version. Christopher Ash is thanked for English editing.

Appendix A. Supplementary data

Supplementary data to this article can be found online at https://doi.org/10.1016/j.envpol.2021.117973.

Author contributions

Vaněk Aleš: Methodology, Data Processing, Paper Preparation/Editing. Kateřina Vejvodová: Peat Analyses. Martin Mihaljevič: Isotope Analyses, Paper Preparation/Editing. Vojtěch Ettler: Data Interpretation, Paper Preparation/Editing. Jakub Trubač: Isotope Analyses, Dating. Maria Vaňková: Data Processing, Paper Editing. Viktor Goliáš: Dating. Leslaw Teper: Sampling; Data Interpretation, Paper Editing. Katarzyna Sutkowska: Sampling. Petra Vokurková: Peat Analyses. Vít Penížek: Sampling. Tereza Zádorová: Data Processing. Ondřej Drábek: Peat Analyses.

References

Aguilar-Carrillo, J., Herrera, L., Gutiérrez, E.J., Reyes-Domínguez, I.A., 2018. Solid-phase distribution and mobility of thallium in mining-metallurgical residues: environmental hazard implications. Environ. Pollut. 243, 1833–1845. https://doi.org/10.1016/j.envpol.2018.10.014.

Bigalke, M., Weyer, S., Wilcke, W., 2010. Copper isotope fractionation during complexation with insolubilized humic acid. Environ. Sci. Technol. 44 (14), 5496–5502. https://doi.org/10.1021/es1017653.

Bodnar, R., Rozmus, D., 2004. Wczesnośredniowieczne ślady hutnictwa w Dąbrowie Górniczej-Łośniu oraz na obszarach pogranicznych. In: Rozmus, D. (Ed.), Archeologiczne I Historyczne Ślady Górnictwa I Hutnictwa Na Terenie Dąbrowy Górniczej I Okolic. Księgarnia Akademicka Kraków, pp. 9–60, 2004 (in Polish).

Bower, C.A., Reitemeier, R.F., Fireman, M., 1954. Exchangeable cation analysis of saline and alkali soils. Soil Sci. 73 (4), 251–262. https://doi.org/10.1097/00010694-195204000-00001.

Cabala, J., Teper, L., 2007. Metalliferous constituents of rhizosphere soils contaminated by Zn-Pb mining in southern Poland. *Water*. Air and Soil Pollution 178, 351–362. https://doi.org/10.1007/s11270-006-9203-1.

Cabala, J., Smieja-Król, B., Jablonska, M., Chróst, L., 2013. Mineral components in a peat deposit: looking for signs of early mining and smelting activities in Silesia-Cracow region (Southern Poland). Environ. Earth Sci. 69, 2559–2568. https://doi.org/10.1007/s12665-012-2080-6.

De Vleeschouwer, F., Fagel, N., Cheburkin, A., Pazdur, A., Sikorski, J., Matielli, N., Renson, V., Fialkiewicz, B., Piotrowska, N., Le Roux, G., 2009. Anthropogenic impacts in North Poland over the last 1300 years - a record of Pb, Zn, Cu, Ni and S in an ombrotrophic peat bog. Sci. Total Environ. 407, 5674–5684. https://doi.org/10.1016/j.scitotenv.2009.07.020.

De Vleeschower, F., Baron, S., Cloy, J.M., Enrico, M., Ettler, V., Fagel, N., Kempter, H., Kylander, M., Li, C., Longman, J., Martinez-Cortizas, A., Marx, S., Mattielli, N., Mighall, T., Nieminen, T.M., Piotrowska, N., Pontevedra-Pombal, X., Pratte, S., Renson, V., Shotyk, W., Shuttleworth, E., Sikorski, J., Stromsoe, N., Talbot, J., von Scheffer, C., Weiss, D., Zaccone, C., Le Roux, G., 2020. Comment on: "A novel approach to peatlands as archives of total cumulative spatial pollution loads fromatmospheric deposition of airborne elements complementary to EMEP data: priority pollutants (Pb, Cd, Hg)" by Ewa Miszczak, Sebastian Stefaniak, Adam Michczyński, Eiliv Steinnes and Irena Twardowska. Sci. Total Environ. 737, 138699. https://doi.org/10.1016/j.scitotenv.2020.138699.

Farmer, J.G., Graham, M.C., Yafa, C., Cloy, J.M., Freeman, A.J., MacKenzie, A.B., 2006. Use of 206Pb/207Pb ratios to investigate the surface integrity of peat cores used to study the recent depositional history and geochemical behaviour of inorganic elements in peat bogs. Global Planet. Change 53, 240–248. https://doi.org/10.1016/j.gloplacha.2006.03.006.

Fiałkiewicz-Kozieł, B., Łokas, E., Gałka, M., Kołaczek, P., De Vleeschouwer, F., Le Roux, G., Smieja-Król, B., 2020. Influence of transboundary transport of trace elements on mountain peat geochemistry (Sudetes, Central Europe). Quat. Sci. Rev. 230, 106162. https://doi.org/10.1016/j.quascirev.2020.106162.

Fiałkiewicz-Kozieł, B., De Vleeschouwer, F., Mattielli, N., Fagel, N., Palowski, B., Pazdur, A., Smieja-Król, B., 2018. Record of Anthropocene pollution sources of lead in disturbed peatlands from Southern Poland. Atmos. Environ. 179, 61–68. https://doi.org/10.1016/j.atmosenv.2018.02.002.

Gao, K.Z., Pearce, J., Jones, J., Taylor, C., 1999. Interaction between peat, humic acid and aqueous metal ions. Environ. Geochem. Health 21, 13–26. https://doi.org/10.1023/A:1006592627852.

Garrido, F., Garcia-Guinea, J., Lopez-Arce, P., Voegelin, A., Göttlicher, J., Mangold, S., Almendros, G., 2020. Thallium and co-genetic trace elements in hydrothermal Fe-Mn deposits of Central Spain. Sci. Total Environ. 717, 137162. https://doi.org/10.1016/j.scitotenv.2020.137162.

Gomez-Gonzalez, M.A., Garcia-Guinea, J., Laborda, F., Garrido, F., 2015. Thallium occurrence and partitioning in soils and sediments affected by mining activities in Madrid province (Spain). Sci. Total Environ. 536, 268–278. https://doi.org/10.1016/j.scitotenv.2015.07.033.

Grösslová, Z., Vanek, A., Oborná, V., Mihaljevič, M., Ettler, V., Trubač, J., Drahota, P., Penizek, V., Pavlů, L., Sracek, O., Kribek, B., Voegelin, A., Göttlicher, J., Ondrej, D., Tejnecký, V., Houska, J., Mapani, B., Zádorová, T., 2018. Thallium contamination of desert soil in Namibia: chemical, mineralogical and isotopic insights. Environ. Pollut. 239, 272–280. https://doi.org/10.1016/j.envpol.2018.04.006.

Howarth, S., Prytulak, J., Little, S.H., Hammond, S.J., Widdowson, M., 2018. Thallium concentration and thallium isotope composition of lateritic terrains. Geochem. Cosmochim. Acta 239, 446–462. https://doi.org/10.1016/j.gca.2018.04.017.

Jacobson, A.R., McBride, M.B., Baveye, P., Steenhuis, T.S., 2005. Environmental factors determining the trace-level sorption of silver and thallium to soils. Sci. Total Environ. 345, 191–205. https://doi.org/10.1016/j.scitotenv.2004.10.027.

Jakubowska, M., Pasieczna, A., Zembrzuski, W., Swit, Z., Lukaszewski, Z., 2007. Thallium in fractions of soil formed on floodplain terraces. Chemosphere 66, 611–618. https://doi.org/10.1016/j.chemosphere.2006.07.098.

Karbowska, B., Zembrzuski, W., Jakubowska, M., Wojtkowiak, T., Pasieczna, A., Lukaszewski, Z., 2014. Translocation and mobility of thallium from zinc–lead ores. J. Geochem. Explor. 143, 127–135. https://doi.org/10.1016/j.gexplo.2014.03.026.

Kersten, M., Xiao, T., Kreissig, K., Brett, A., Coles, B.J., Rehkämper, M., 2014. Tracing anthropogenic thallium in soil using stable isotope compositions. Environ. Sci. Technol. 48 (16), 9030–9036. https://doi.org/10.1021/es501968d.

Kylander, M.E., Weiss, D.J., Martínez Cortízas, A., Spiro, B., Garcia-Sanchez, R., Coles, B. J., 2005. Refining the pre-industrial atmospheric Pb isotope evolution curve in Europe using an 8000 year old peat core from NW Spain. Earth Planet Sci. Lett. 240, 467–485. https://doi.org/10.1016/j.epsl.2005.09.024.

Latałowa, M., Nalepka, D., 1987. A study of the late-glacial and holocene vegetational history of the Wolbrom area (Silesian-Cracovian upland). Acta Palaeobot. 27, 75–115.

Lis, J., Pasieczna, A., Karbowska, B., Zembrzuski, W., Lukaszewski, Z., 2003. Thallium in soils and stream sediments of a Zn-Pb mining and smelting area. Environ. Sci. Technol. 37, 4569–4572. https://doi.org/10.1021/es0346936.

Liszka, J., Świć, E., 2004. Dzieje Wydarzenia Ludzie. Zakłady Górniczo-Hutnicze „Bolesław". S. A., Bukowno, Poland (in Polish).

Liu, J., Wang, J., Chen, Y., Xie, X., Qi, J., Lippold, H., Luo, D., Wang, C., Su, L., He, L., Wu, Q., 2016. Thallium transformation and partitioning during Pb − Zn smelting and environmental implications. Environ. Pollut. 212, 77–89. https://doi.org/10.1016/j.envpol.2016.01.046.

Liu, J., Yin, M., Luo, X., Xiao, T., Wu, Z., Li, N., Wang, J., Zhang, W., Lippold, H., Belshaw, N.S., Feng, Y., Chen, Y., 2019. The mobility of thallium in sediments and source apportionment by lead isotopes. Chemosphere 219, 864–874. https://doi.org/10.1016/j.chemosphere.2018.12.041.

Liu, J., Yin, M., Xiao, T., Zhang, C., Tsang, D.C.W., Bao, Z., Zhou, Y., Chen, Y., Luo, X., Yuan, W., Wang, J., 2020a. Thallium isotopic fractionation in industrial process of pyrite smelting and environmental implications. J. Hazard Mater. 384, 121378. https://doi.org/10.1016/j.jhazmat.2019.121378.

Liu, J., Wei, X., Zhou, Y., Tsang, D.C.W., Bao, Z., Yin, M., Lippold, H., Yuan, W., Wang, J., Feng, Y., Chen, D., 2020b. Thallium contamination, health risk assessment and source apportionment in common vegetables. Sci. Total Environ. 703, 135547. https://doi.org/10.1016/j.scitotenv.2019.135547.

Lukaszewski, Z., Jakubowska, M., Zembrzuski, W., 2018. The mobility of thallium from bottom soil of the Silesian-Cracowian zinc-lead ore deposit region (Poland). J. Geochem. Explor. 184, 11–16. https://doi.org/10.1016/j.gexplo.2017.10.009.

Mihaljevič, M., Zuna, M., Ettler, V., Šebek, O., Strnad, L., Goliáš, V., 2006. Lead fluxes, isotopic and concentration profiles in a peat deposit near a lead smelter (Příbram, Czech Republic). Sci. Total Environ. 372, 334–344. https://doi.org/10.1016/j.scitotenv.2006.09.019.

Nielsen, S.G., Wasylenki, L.E., Rehkämper, M., Peacock, C.L., Xue, Z., Moon, E.M., 2013. Towards an understanding of thallium isotope fractionation during adsorption to manganese oxides. Geochem. Cosmochim. Acta 117, 252–265. https://doi.org/10.1016/j.gca.2013.05.004.

Nielsen, S.G., Rehkämper, M., Prytulak, J., 2017. Investigation and application of thallium isotope fractionation. Rev. Mineral. Geochem. 82, 759–798. https://doi.org/10.2138/rmg.2017.82.18.

Novak, M., Pacherova, P., 2008. Mobility of trace metals in pore waters of two Central European peat bogs. Sci. Total Environ. 394, 331–337. https://doi.org/10.1016/j.scitotenv.2008.01.036.

Novak, M., Erel, Y., Zemanova, L., Bottrell, S.H., Adamova, M., 2008. A comparison of lead pollution record in Sphagnum peat with known historical Pb emission rates in the British Isles and the Czech Republic. Atmos. Environ. 42, 8997–9006. https://doi.org/10.1016/j.atmosenv.2008.09.031.

Nriagu, J.O., 1998. Thallium in the Environment. John Wiley & Sons, Inc., New York, USA.

Ostrander, C.M., Nielsen, S.G., Owens, J.D., Kendall, B., Gordon, G.W., Romaniello, S.J., Anbar, A.D., 2019. Fully oxygenated water columns over continental shelves before the Great Oxidation Event. Nat. Geosci. 12 (3), 186–191. https://doi.org/10.1038/s41561-019-0309-7.

Owens, J.D., Nielsen, S.G., Horner, T.J., Ostrander, C.M., Peterson, L.C., 2017. Thallium-isotopic compositions of euxinic sediments as a proxy for global manganese-oxide

burial. Geochem. Cosmochim. Acta 213, 291–307. https://doi.org/10.1016/j.gca.2017.06.041.

Pawełczyk, F., Chróst, L., Magiera, T., Michczyński, A., Sikorski, J., Tudyka, K., Zajac, E., 2017. Radiocarbon and lead-210 age-depth model and trace elements concentration in the Wolbrom fen (S Poland). Geochronometria 44, 40–48. https://doi.org/10.1515/geochr-2015-0046.

Peacock, C.L., Moon, E.M., 2012. Oxidative scavenging of thallium by birnessite: explanation for thallium enrichment and stable isotope fractionation in marine ferromanganese precipitates. Geochem. Cosmochim. Acta 84, 297–313. https://doi.org/10.1016/j.gca.2012.01.036.

Prytulak, J., Nielsen, S.G., Plank, T., Barker, M., Elliot, T., 2013. Assessing the utility of thallium and thallium isotopes for tracing subduction zone inputs to the Mariana arc. Chem. Geol. 345, 139–149. https://doi.org/10.1016/j.chemgeo.2013.03.003.

Prytulak, J., Brett, A., Webb, M., Plank, T., Rehkämper, M., Savage, P.S., Woodhead, J., 2017. Thallium elemental behavior and stable isotope fractionation during magmatic processes. Chem. Geol. 448, 71–83. https://doi.org/10.1016/j.chemgeo.2016.11.007.

Rader, S.T., Maier, R.M., Barton, M.D., Mazdab, F.K., 2019. Uptake and fractionation of thallium by *Brassica juncea* in a geogenic thallium-amended substrate. Environ. Sci. Technol. 53 (5), 2441–2449. https://doi.org/10.1021/acs.est.8b06222.

Rehkämper, M., Frank, M., Hein, J.R., Porcelli, D., Halliday, A., Ingri, J., Liebetrau, V., 2002. Thallium isotope variations in seawater and hydrogenetic, diagenetic, and hydrothermal ferromanganese deposits. Earth Planet Sci. Lett. 197, 65–81. https://doi.org/10.1016/S0012-821X(02)00462-4.

Rehkämper, M., Frank, M., Hein, J.R., Halliday, A., 2004. Cenozoic marine geochemistry of thallium deduced from isotopic studies of ferromanganese crusts and pelagic sediments. Earth Planet Sci. Lett. 219, 77–91. https://doi.org/10.1016/S0012-821X(03)00703-9.

Rozmus, D., 2014. Wczesnośredniowieczne Zagłębie Hutnictwa Srebra I Ołowiu Na Obszarach Obecnego Pogranicza Śląska I Małopolski (Druga Połowa XI–XII/XIII Wiek). Early Medieval District of Silver and Lead Metallurgy in the Frontier Areas of Upper Silesia and Little Poland (Second Half of the 11th-12th/13th Centuries). Księgarnia Akademicka Kraków, p. 321pp (in Polish).

Schauble, E.A., 2007. Role of nuclear volume in driving equilibrium stable isotope fractionation of mercury, thallium, and other very heavy elements. Geochem. Cosmochim. Acta 71, 2170–2189. https://doi.org/10.1016/j.gca.2007.02.004.

Shotyk, W., Nesbitt, H.W., Fyfe, W.S., 1992. Natural and anthropogenic enrichments of trace metals in peat profiles. Int. J. Coal Geol. 20, 49–84. https://doi.org/10.1016/0166-5162(92)90004-G.

Shotyk, W., Cheburkin, A.K., Appleby, P.G., Fankhauser, A., Kramers, J.D., 1996. Two thousand years of atmospheric arsenic, antimony, and lead deposition recorded in an ombrotrophic peat bog profile, Jura Mountains, Switzerland. Earth Planet Sci. Lett. 145, E1–E7. https://doi.org/10.1016/S0012-821X(96)00197-5.

Shotyk, W., Weiss, D., Appleby, P.G., Cheburkin, A.K., Frei, R., Gloor, M., Kramers, J.D., Reese, S., Van Der Knaap, W.O., 1998. History of atmospheric lead deposition since 12,370 14C yr BP from a peat bog, Jura Mountains, Switzerland. Science 281, 1635–1640. https://doi.org/10.1126/science.281.5383.1635.

Shotyk, W., Blaser, P., Grünig, A., Cheburkin, A.K., 2000. A new approach for quantifying cumulative, anthropogenic, atmospheric lead deposition using peat cores from bogs: Pb in eight Swiss peat bog profiles. Sci. Total Environ. 249, 281–295. https://doi.org/10.1016/S0048-9697(99)00523-9.

Shotyk, W., Weiss, D., Kramers, J.D., Frei, R., Cheburkin, A.K., Gloor, M., Reese, S., 2001. Geochemistry of the peat bog at Etang de la Gruère, Jura Mountains, Switzerland, and its record of atmospheric Pb and lithogenic trace metals (Sc, Ti, Y, Zr, and REE) since 12,370 ^{14}C yr BP. Geochem. Cosmochim. Acta 65, 2337–2360. https://doi.org/10.1016/S0016-7037(01)00586-5.

Shotyk, W., Krachler, M., 2004. Atmospheric deposition of silver and thallium since 12 370 ^{14}C years BP recorded by a Swiss peat bog profile, and comparison with lead and cadmium. J. Environ. Monit. 6, 427–433. https://doi.org/10.1039/b315084b.

Shotyk, W., Appleby, P.G., Bicalho, B., Davies, L., Froese, D., Grant-Weaver, I., Krachler, M., Magnan, G., Mullan-Boudreau, G., Noernberg, T., Shannon, B., van Bellen, S., Zaccone, C., 2016a. Peat bogs in northern Alberta, Canada reveal decades of declining atmospheric Pb contamination. Geophys. Res. Lett. 43, 9964–9974. https://doi.org/10.1002/2016GL070952.

Shotyk, W., Rausch, N., Nieminen, T.M., Ukonmaanaho, L., Krachler, M., 2016b. Isotopic Composition of Pb in peat and porewaters from three contrasting ombrotrophic bogs in Finland: evidence of chemical diagenesis in response to acidification. Environ. Sci. Technol. 50, 9943–9951. https://doi.org/10.1021/acs.est.6b01076.

Shotyk, W., Appleby, P.G., Bicalho, B., Davies, L.J., Froese, D., Grant-Weaver, I., Magnan, G., Mullan-Boudreau, G., Noernberg, T., Pelletier, R., Shannon, B., van Bellen, S., Zaccone, C., 2017. Peat bogs document decades of declining atmospheric contamination by trace metals in the Athabasca bituminous sands region. Environ. Sci. Technol. 51, 6237–6249. https://doi.org/10.1021/acs.est.6b04909.

Smieja-Król, B., Fiałkiewicz-Kozieł, B., Palowski, B., 2010. Heavy metal behaviour in peat – a mineralogical perspective. Sci. Total Environ. 408, 5924–5931. https://doi.org/10.1016/j.scitotenv.2010.08.032.

Smieja-Król, B., Bauerek, A., 2015. Controls on trace-element concentrations in the pore waters of two *Sphagnum*-dominated mires in southern Poland that are heavily polluted by atmospheric deposition. J. Geochem. Explor. 151, 57–65. https://doi.org/10.1016/j.gexplo.2015.01.010.

Smieja-Król, B., Janeczek, J., Bauerek, A., Thorseth, I.H., 2015. The role of authigenic sulfides in immobilization of potentially toxic metals in the Bagno Bory wetland, southern Poland. Environ. Sci. Pollut. Res. 22, 15495–15505. https://doi.org/10.1007/s11356-015-4728-8.

Smieja-Król, B., Fiałkiewicz-Kozieł, B., Michalska, A., Krzykawski, T., Smołka-Danielowska, D., 2019. Deposition of mullite in peatlands of southern Poland: implications for recording large-scale industrial processes. Environ. Pollut. 250, 717–727. https://doi.org/10.1016/j.envpol.2019.04.077.

Tudyka, K., Pazdur, A., 2012. ^{14}C Dating with the ICELS liquid scintillation counting system using fixed-energy balance counting window method. Radiocarbon 54, 267–273. https://doi.org/10.2458/azu_js_rc.v54i2.15832.

Vaněk, A., Chrastný, V., Teper, L., Cabala, J., Penížek, V., Komárek, M., 2011. Distribution of thallium and accompanying metals in tree rings of Scots pine (*Pinus sylvestris* L.) from a smelter-affected area. J. Geochem. Explor. 108, 73–80. https://doi.org/10.1016/j.gexplo.2010.10.006.

Vaněk, A., Komárek, M., Chrastný, V., Galušková, I., Mihaljevič, M., Šebek, O., Drahota, P., Tejnecký, V., Vokurková, P., 2012. Effect of low-molecular-weight organic acids on the leaching of thallium and accompanying cations from soil – a model rhizosphere solution approach. J. Geochem. Explor. 112, 212–217. https://doi.org/10.1016/j.gexplo.2011.08.010.

Vaněk, A., Chrastný, V., Komárek, M., Penížek, V., Teper, L., Cabala, J., Drábek, O., 2013. Geochemical position of thallium in soils from a smelter-impacted area. J. Geochem. Explor. 124, 176–182. https://doi.org/10.1016/j.gexplo.2012.09.002.

Vaněk, A., Grösslová, Z., Mihaljevič, M., Trubač, J., Ettler, V., Teper, L., Cabala, J., Rohovec, J., Zádorová, T., Penížek, V., Pavlů, L., Holubík, O., Němeček, K., Houška, J., Drábek, O., Ash, C., 2016. Isotopic tracing of thallium contamination in soils affected by emissions from coal-fired power plants. Environ. Sci. Technol. 50 (18), 9864–9871. https://doi.org/10.1021/acs.est.6b01751.

Vaněk, A., Grösslová, Z., Mihaljevič, M., Ettler, V., Trubač, J., Chrastný, V., Penížek, V., Teper, L., Cabala, J., Voegelin, A., Zádorová, T., Oborná, V., Drábek, O., Holubík, O., Houška, J., Pavlů, L., Ash, C., 2018. Thallium isotopes in metallurgical wastes/contaminated soils: a novel tool to trace metal source and behavior. J. Hazard Mater. 343, 78–85. https://doi.org/10.1016/j.jhazmat.2017.09.020.

Vaněk, A., Holubík, O., Oborná, V., Mihaljevič, M., Trubač, J., Ettler, V., Pavlů, L., Vokurková, P., Penížek, V., Zádorová, T., Voegelin, A., 2019. Thallium stable isotope fractionation in white mustard: implications for metal transfers and incorporation in plants. J. Hazard Mater. 369, 521–527. https://doi.org/10.1016/j.jhazmat.2019.02.060.

Vaněk, A., Voegelin, A., Mihaljevič, M., Ettler, V., Trubač, J., Drahota, P., Vaňková, M., Oborná, V., Vejvodová, K., Penížek, V., Pavlů, L., Drábek, O., Vokurková, P., Zádorová, T., Holubík, O., 2020. Thallium stable isotope ratios in naturally Tl-rich soils. Geoderma 364, 114183. https://doi.org/10.1016/j.geoderma.2020.114183.

Vejvodová, K., Vaněk, A., Mihaljevič, M., Ettler, V., Trubač, J., Vaňková, M., Drahota, P., Vokurková, P., Penížek, V., Zádorová, T., Tejnecký, V., Pavlů, L., Drábek, O., 2020. Thallium isotopic fractionation in soil: the key controls. Environ. Pollut. 265, 114822. https://doi.org/10.1016/j.envpol.2020.114822.

Voegelin, A., Pfenninger, N., Petrikis, J., Majzlan, J., Plötze, M., Senn, A.C., Mangold, S., Steininger, R., Göttlicher, J., 2015. Thallium speciation and extractability in a thallium- and arsenic-rich soil developed from mineralized carbonate rock. Environ. Sci. Technol. 49 (9), 5390–5398. https://doi.org/10.1021/acs.est.5b00629.

Wang, Z., Zhang, B., Jiang, Y., Li, Y., He, C., 2018. Spontaneous thallium (I) oxidation with electricity generation in single-chamber microbial fuel cells. Appl. Energy 209, 33–42. https://doi.org/10.1016/j.apenergy.2017.10.075.

Wang, J., Wang, L., Wang, Y., Tsang, D.C.W., Yang, X., Beiyuan, J., Yin, M., Xiao, T., Jiang, Y., Lin, W., Zhou, Y., Liu, J., Wang, L., Zhao, M., 2021. Emerging risks of toxic metal(loid)s in soil-vegetables influenced by steel-making activities and isotopic source apportionment. Environ. Int. 146, 106207. https://doi.org/10.1016/j.envint.2020.106207.

Weiss, D., Shotyk, W., Appleby, P.G., Kramers, J.D., Cheburkin, A.K., 1999. Atmospheric Pb deposition since the Industrial Revolution recorded by five Swiss peat profiles; enrichment factors, fluxes, isotopic composition, and sources. Environ. Sci. Technol. 33, 1340–1352. https://doi.org/10.1021/es980882q.

Weiss, D., Shotyk, W., Boyle, E.A., Kramers, J.D., Appleby, P.G., Cheburkin, A.K., 2002. Comparative study of the temporal evolution of atmospheric lead deposition in Scotland and eastern Canada using blanket peat bogs. Sci. Total Environ. 292, 7–18. https://doi.org/10.1016/s0048-9697(02)00025-6.

Weiss, D.J., Rausch, N., Mason, T.F.D., Coles, B.J., Wilkinson, J.J., Ukonmaanaho, L., Arnold, T., Nieminen, T.M., 2007. Atmospheric deposition and isotope biogeochemistry of zinc in ombrotrophic peat. Geochem. Cosmochim. Acta 71, 3498–3517. https://doi.org/10.1016/j.gca.2007.04.026.

Wick, S., Peña, J., Voegelin, A., 2019. Thallium sorption onto manganese oxides. Environ. Sci. Technol. 53 (22), 13168–13178. https://doi.org/10.1021/acs.est.9b04454.

Wick, S., Baeyens, B., Fernandes, M.M., Göttlicher, J., Fischer, M., Pfenninger, N., Plötze, M., Voegelin, A., 2020. Thallium sorption and speciation in soils: role of micaceous clay minerals and manganese oxides. Geochem. Cosmochim. Acta 288, 83–100. https://doi.org/10.1016/j.gca.2020.07.037.

Xiao, T., Guha, J., Boyle, D., Liu, C.Q., Chen, J., 2004a. Environmental concerns related to high thallium levels in soils and thallium uptake by plants in southwest Guizhou, China. Sci. Total Environ. 318, 223–244. https://doi.org/10.1016/S0048-9697(03)00448-0.

Xiao, T., Guha, J., Boyle, D., Liu, C.Q., Zheng, B., Wilson, G.C., Rouleau, A., Chen, J., 2004b. Naturally occurring thallium: a hidden geoenvironmental health hazard? Environ. Int. 30, 501–507. https://doi.org/10.1016/j.envint.2003.10.004.

Xiao, T., Yang, F., Li, S., Zheng, B., Ning, Z., 2012. Thallium pollution in China: a geo-environmental perspective. Sci. Total Environ. 421–422, 51–58. https://doi.org/10.1016/j.scitotenv.2011.04.008.

Zuna, M., Mihaljevič, M., Šebek, O., Ettler, V., Handley, M., Navrátil, T., Goliáš, V., 2011. Recent lead deposition trends in the Czech Republic as recorded by peat bogs and tree rings. Atmos. Environ. 45, 4950–4958. https://doi.org/10.1016/j.atmosenv.2011.06.007.

Zuna, M., Ettler, V., Šebek, O., Mihaljevič, M., 2012. Mercury accumulation in peatbogs at Czech sites with contrasting pollution histories. Sci. Total Environ. 424, 322–330. https://doi.org/10.1016/j.scitotenv.2012.02.049.

7.3. Evaluation of thallium isotopic fractionation during the metallurgical processing of sulphides: An update

Vaněk, A., Vejvodová, K., Mihaljevič, M., Ettler, V., Tubač, J., Vaňková, M., Teper, L., Cabala, J., Sutkowska, K., Voegelin, A., Göttlicher, J., Holubík, O., Vokurková, P., Pavlů, L., Galušková, I., Zádorová, T. (2021). Evaluation of thallium isotopic fractionation during the metallurgical processing of sulphides: An update. Journal of Hazardous Materials, 424, 127325.

Journal of Hazardous Materials 424 (2022) 127325

Contents lists available at ScienceDirect

Journal of Hazardous Materials

journal homepage: www.elsevier.com/locate/jhazmat

Evaluation of thallium isotopic fractionation during the metallurgical processing of sulfides: An update

Aleš Vaněk [a,*], Kateřina Vejvodová [a], Martin Mihaljevič [b], Vojtěch Ettler [b], Jakub Trubač [b], Maria Vaňková [b], Leslaw Teper [c], Jerzy Cabala [c], Katarzyna Sutkowska [c], Andreas Voegelin [d], Jörg Göttlicher [e], Ondřej Holubík [a], Petra Vokurková [a], Lenka Pavlů [a], Ivana Galušková [a], Tereza Zádorová [a]

[a] Department of Soil Science and Soil Protection, Faculty of Agrobiology, Food and Natural Resources, Czech University of Life Sciences Prague, Kamýcká 129, 165 00 Praha 6, Czech Republic
[b] Institute of Geochemistry, Mineralogy and Mineral Resources, Faculty of Science, Charles University, Albertov 6, 128 00 Praha 2, Czech Republic
[c] Institute of Earth Sciences, Faculty of Natural Sciences, University of Silesia, Bedzinska 60, 41-200 Sosnowiec, Poland
[d] Eawag, Swiss Federal Institute of Aquatic Science and Technology, Ueberlandstrasse 133, CH-8600 Duebendorf, Switzerland
[e] Institute for Photon Science and Synchrotron Radiation, Karlsruhe Institute of Technology, KIT Campus North, Hermann-von-Helmholtz-Platz 1, D-76344 Eggenstein-Leopoldshafen, Germany

ARTICLE INFO

Editor: Yang Deng Cyden

Keywords:
Waste
Metallurgy
Isotopic Fractionation
Speciation

ABSTRACT

In this study, we report combined Tl isotopic and Tl mineralogical and speciation data from a set of Tl-rich sulfide concentrates and technological wastes from hydrometallurgical Zn extraction. We also present the first evaluation of Tl isotopic ratios over a cycle of sulfide processing, from the ore flotation to pyro- and hydrometallurgical stages. The results demonstrate that the prevailing Tl form in all samples is Tl(I), without any preferential incorporation into sulfides or Tl-containing secondary phases, indicating an absence of Tl redox reactions. Although the Tl concentrations varied significantly in the studied samples (~9–280 mg/kg), the overall Tl isotopic variability was small, in the range of −3.1 to −4.4 ± 0.7 (2σ) ε^{205}Tl units. By combining present ε^{205}Tl results with the trends first found for a local roasting plant, it is possible to infer minimum Tl isotopic effects throughout the studied industrial process. As a result, the use of Tl isotopic ratios as a source proxy may be complicated or even impossible in areas with naturally high/extreme Tl background contents. On the other hand, areas with two or more isotopically contrasting Tl sources allow for relatively easy tracing, i.e., in compartments which do not suffer from post-depositional isotopic redistributions.

1. Introduction

Thallium (Tl) is a toxic trace element (metal) included in the US EPA list of priority toxic pollutants (Kazantzis, 2000). Because of its acute and chronic toxicity for most living organisms (comparable to e.g. Hg or Cd) (John Peter and Viraraghavan, 2005), Tl can be thought as one of the most dangerous elements in the environment. Since metal sulfides tend to accumulate Tl (e.g., FeS_2 and ZnS), their mining, metallurgical processing and co-processing (mine waste recycling) all represent potential pathways of Tl entry into the environment (Kazantzis, 2000; Xiao et al., 2004, 2012; John Peter and Viraraghavan, 2005; Jakubowska et al., 2007; Karbowska et al., 2014; Gomez-Gonzalez et al., 2015; Liu et al., 2016, 2019; Aguilar-Carrillo et al., 2018; Garrido et al., 2020; Wei et al., 2021; Ning et al., 2021). Thallium may occur in K-silicates (K-feldspars, micas) or may specifically be adsorbed by micaceous clay minerals (mainly illite), mostly reflecting ion Tl(I)-K(I) exchange reactions. Furthermore, Tl-containing sulfide and oxide associations, including Tl(III) forms, are reported as important Tl pools or sinks in the environment (Fe-Zn sulfide deposits, Fe-Mn crusts/nodules, etc.) (Tremel et al., 1997; Jović, 1998; Jacobson et al., 2005a, 2005b; Vaněk et al., 2011, 2013; Voegelin et al., 2015; Nielsen et al., 2017). It should be noted that Tl has two stable isotopes (^{205}Tl and ^{203}Tl) with average abundances of ~70% and ~30%, respectively. Despite recent achievements in Tl isotope geochemistry in Earth and environmental sciences (Grösslová et al., 2018; Howarth et al., 2018; Nielsen et al., 2013, 2017, Ostrander et al., 2019, 2020; Owens et al., 2017; Peacock and Moon,

* Corresponding author.
E-mail address: vaneka@af.czu.cz (A. Vaněk).

https://doi.org/10.1016/j.jhazmat.2021.127325
Received 9 July 2021; Received in revised form 20 September 2021; Accepted 20 September 2021
Available online 24 September 2021

2012; Prytulak et al., 2013, 2017, Rader et al., 2018, 2019, Rehkämper et al., 2002, 2004, Vaněk et al., 2016, 2018, 2019, 2020, 2021; Vejvodová et al., 2020, etc.), still very little is known about the behavior of stable Tl isotopes during industrial activities. For example, we do not know to what degree Tl isotope fractionation can take place during metallurgical sulfide processing, involving all the stages such as ore flotation, pyrometallurgy as well as hydrometallurgy. The only available Tl isotopic data and related effects are known for different waste materials from specific high-temperature operations (ore roasting, coal burning) – various fly ashes/dusts, slags, etc. (Vaněk et al., 2016, 2018; Liu et al., 2020). The major findings can be summarized as follows: (i) partial Tl isotopic fractionation can potentially take place during high-temperature activities, with isotopically lighter Tl present in fly ash relative to remaining slag or bottom ash (enriched in heavy ^{205}Tl isotope); (ii) the volatile Tl fractions present in gas/vapor phases tend to be enriched in light ^{203}Tl isotope, probably due to its higher reaction rate during evaporation (Vaněk et al., 2016, 2018).

However, to be able to assess the behavior/fate of Tl stable isotopes throughout the metallurgical processes, the isotopic signatures of the feed treatment or final/base metal solution refinement(s) are clearly yet to be determined. In this study, we report combined Tl isotopic and Tl mineralogical and speciation data from a set of Tl-rich sulfide concentrates and technological wastes from hydrometallurgical Zn extraction. We attempt to answer the following fundamental questions: (i) How does the hydrometallurgical process influence complex Tl chemistry, i.e., what are major smelter-derived Tl-containing phases? (ii) Do changes in Tl chemistry reflect the changes in Tl isotopic composition in metallurgical wastes? (iii) To what degree can Tl isotopes be redistributed during a complete industrial cycle (pyro- and hydrometallurgy) relative to the primary Tl source (ore)?

The work follows our earlier Tl isotopic research from a roasting/Waelz technology (Vaněk et al., 2018) and it offers new insights into stable Tl isotope signatures in source materials of anthropogenic origin, which can potentially be used to assess industrial Tl inputs in the environment.

2. Experimental

2.1. Ore and processing waste samples

A set of Zn-rich sulfide concentrates and selected processing wastes (sludges) from the hydrometallurgy of Zn were investigated in this work. All studied samples originate from specific (MVT – "the Mississippi Valley"-type) sulfide deposits located in Europe and Asia (Olkusz, Poland; Lisheen, Ireland; Pinargozu, Turkey) and were simultaneously processed in the Boleslaw Zn smelter (southern Poland) in November 2020. Detailed information about the samples, their location within the industrial process (Fig. S1), sample mineralogy and chemistry are given in the Supplementary Material section.

2.2. Mineralogical characterization and Tl speciation

The phase compositions of the studied samples were determined by X-ray diffraction analysis (XRD) (X'Pert Pro diffractometer, PANalytical, the Netherlands) under the following conditions: CuKα radiation at 40 kV (30 mA), 2 theta range of 5–80°, counting time of 150 s per step (step of 0.02°). The obtained diffraction patterns were processed using X'Pert High Score Plus 3.0 software, in combination with a Crystallography Open Database (COD) (Gražulis et al., 2012). Selected ore/waste samples (1, 4, and 6) were studied using scanning electron microscopy (SEM) and electron probe microanalysis (EPMA). A JEOL JXA-8530F (JEOL, Japan) electron probe microanalyzer with a field emission gun as an electron source and an energy dispersion spectrometer (EDS) (JEOL JED-2300F) was used. This instrument was also used for quantitative microanalysis. The EPMA operating conditions, calibration standards and detection limits are reported in Table S1 (Supplementary Material).

To gain information on Tl speciation, the samples with the highest Tl concentrations (to eliminate Fe, As, Sb etc. interferences, if present) were analyzed by X-ray absorption near edge structure (XANES) spectroscopy (Tl L_{III}-edge, SUL-X beamline) at the Synchrotron Radiation Source, Karlsruhe Institute of Technology (KIT, Germany). These measurements were performed in fluorescence mode at room temperature. The BCR sequential extraction method was applied to the studied samples as well, using the procedure properly described in Vaněk et al. (2010). The reason was to better assess the role of major Tl-host phases in a complex process of Tl uptake (coprecipitation).

2.3. Element concentrations

Samples were air-dried (to a constant weight) prior to Tl/element concentration measurement. A sample aliquot of 0.2 g was dissolved in a mixture of concentrated HNO_3/HF (Merck Ultrapure, Germany) (2:1 ratio, ~20 mL, total volume) and then diluted in 2% HNO_3 (50 mL). PTFE beakers (60-mL, Savillex, USA) and a ceramic plate (150–200 °C, 48 h) were utilized throughout this step. Concentrations of Tl, Zn, Pb, and Fe in the individual solutions were determined using Q-ICP-MS (Xseries II, Thermo Scientific, Germany) in a triplicate approach. Standard reference material 2711 (Montana Soil, NIST, USA) was used for the QC of quantitative Tl analysis (Table S2, Supplementary Material).

2.4. Thallium isolation

A two-step chemical separation of Tl with Bio-Rad AG1-X8 resin in the Cl^- form without utilizing HBr was used (Supplementary Material). The technique is analogical with those used within our previous studies (Vaněk et al., 2016, 2018, 2019, 2020; Grösslová et al., 2018; Vejvodová et al., 2020).

2.5. Thallium isotope measurement

Detailed information about the measurement of Tl isotopic ratios using MC-ICP-MS Neptune plus (Thermo Scientific, Germany), including the analytical conditions similar to those described in e.g., Prytulak et al., (2013, 2017), and the respective QC (Table S3), are shown in the Supplementary Material Section.

3. Results and discussion

3.1. Thallium phase associations by XRD and EPMA

The XRD analysis indicated that the phase composition of the studied concentrates is dominated by sphalerite (ZnS) and pyrite (FeS_2) with minor proportion of other sulfides, secondary sulfates (anglesite, $PbSO_4$; plumbojarosite, $PbFe_6(SO_4)_4(OH)_{12}$; susannite, $Pb_4(SO_4)(CO_3)_2(OH)_2$) and gangue phases such as quartz (SiO_2), dolomite ($CaMg(CO_3)_2$) or calcite ($CaCO_3$) (Fig. S2). In contrast, metallurgical sludges are mainly composed of a spinel-family oxide (franklinite, $ZnFe_2O_4$), sphalerite and sulfates such as plumbojarosite, anglesite and gypsum ($CaSO_4.2\ H_2O$) (Fig. S2). The EPMA data indicate that high concentrations of EPMA-detectable Tl are found in all the sulfides: 0.03–0.09 wt% in sphalerite, 0.04–0.07 wt% in pyrite and 0.20 wt% in galena (Table S4). Given the high proportion of sphalerite (Fig. 1 and S2), this phase is the dominant carrier of Tl in the concentrates, in line with measured Zn concentrations (Table 1). Thallium was also detected in mixtures of secondary Pb phases, where it is probably mainly bound in plumbojarosite, with Tl concentrations in the range 0.06–0.20 wt% (Table S5). Interestingly, high Tl amounts were also found in franklinite (0.12–0.28 wt% Tl) and in gypsum (0.30 wt% Tl) in the Larox sludge sample (Table S6). We assume that this can be a result of Tl coprecipitation with secondary metallurgical phases as a function of Tl concentration in the reaction media, pH, temperature, etc. However, passive Tl sorption can

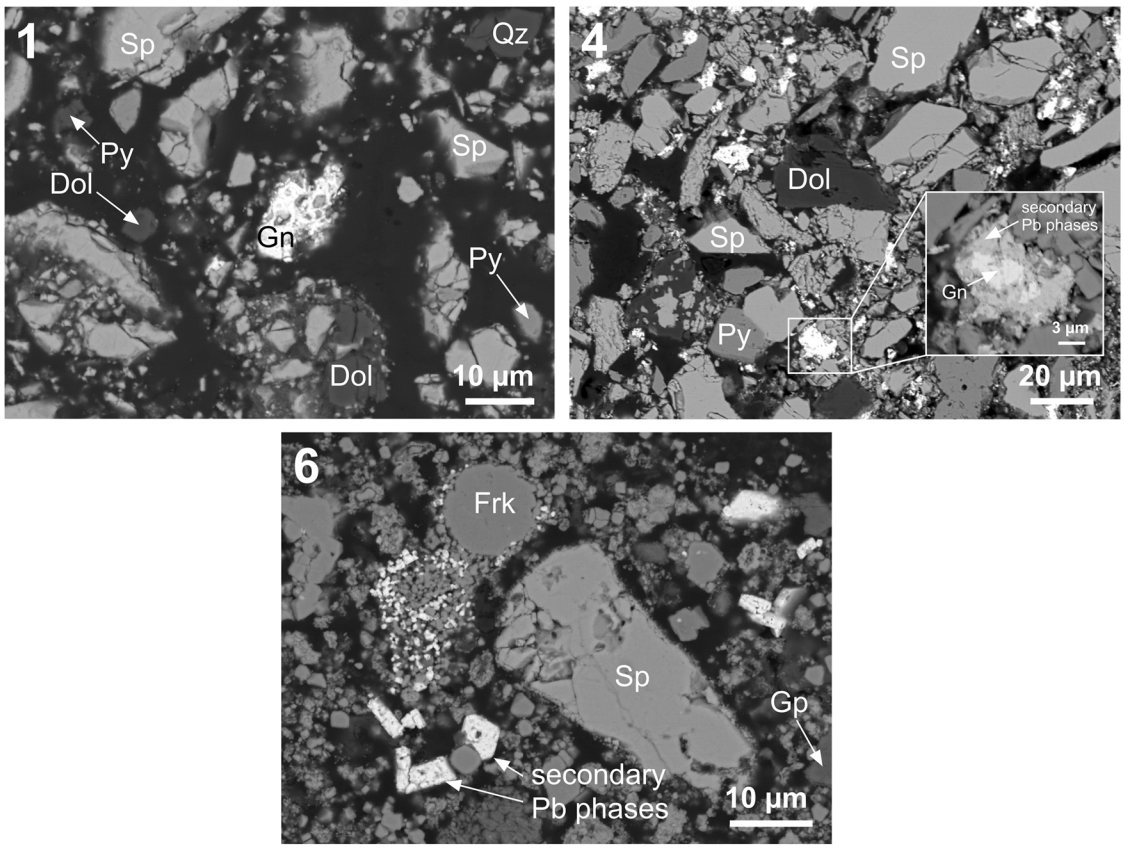

Fig. 1. Scanning electron micrographs in back-scattered electrons (SEM-BSE) of selected sulfide concentrates (no. 1 and 4) and a metallurgical waste/sludge (no. 6). Fragments of sphalerite, pyrite and galena associated with the gangue dolomite and quartz (1 – Lisheen, Ireland); fragments of sphalerite, pyrite and gangue dolomite with residues of galena grains altered to a mixture of secondary Pb phases (4 – Olkusz, Poland); fragments of sphalerite, franklinite and gypsum associated with a mixture of Pb-rich secondary weathering products (6 – Larox sludge). Phase abbreviations: Dol – dolomite ($CaMg(CO_3)_2$); Frk – franklinite ($ZnFe_2O_4$); Gn – galena (PbS); Gp – gypsum ($CaSO_4.2\,H_2O$); Py – pyrite (FeS_2); Sp – sphalerite (ZnS); Qz – quartz (SiO_2).

also be promoted by Tl(I) retention in exchangeable K-exchanged positions/layers, for instance, in oxide or sulfate precipitates (Vaněk et al., 2010).

3.2. *Thallium speciation by XANES spectroscopy*

The Tl L_{III}-edge XANES spectra of selected ore and metallurgical samples (1, 2, 6 and 7) are compared to reference spectra in Fig. 2. In general, the quality of the sample spectra is not ideal because of spectral interferences and fluorescence attenuation caused by the very high levels of Zn, Pb and As in the samples. Nevertheless, the spectra most closely resemble to the spectra of Tl(I)-aqueous or Tl(I)-sulfide (lorandite), indicating that most Tl is monovalent Tl(I). Due to the limited quality of the sample spectra, the lack of reference spectra for other potential Tl(I) phases, and limited spectral characteristics, our data do not allow to further constrain the speciation of Tl(I) in metallurgical samples. Only for the Larox sludge, do the spectral characteristics suggest that a fraction of the Tl(I) may be incorporated in jarosite, as would be consistent with the literature (Dutrizac, 1997). Regarding the absence of clearly detectable levels of Tl(III), this finding is in agreement with the generally low stability of trivalent Tl(III) species, which start to degrade at relatively low temperatures (~150 °C, $TlCl_3$) as they generally have only limited/low thermal stability (Holleman et al., 1995; Phillips and Perry, 1995; Lide, 2009). Moreover, the formation of Tl(III) species could only be favored under highly oxidative conditions, otherwise Tl(I) species tend to dominate (Vaněk et al., 2016).

Although the reliability of the BCR sequential extraction in the determination of Tl sources is generally not much high (Vaněk et al., 2010), its combination with all the Tl speciation and mineralogical data allowed us to draw the following key conclusions (Table S7). With the exception of samples 6 and 7 (Larox and Dorr sludges), the samples showed a good geochemical stability, as the majority of Zn and Pb, including Tl, was associated with the oxidizable and residual fractions (Table S7). This finding indicates the dominant role of sulfides in the total process of Tl retention, as well as only limited role of sulfide weathering in Tl release. On the other hand, there is clear evidence for the formation of Tl-containing precipitates (oxides, sulfates) in metallurgical wastes with marked Tl solubility within the acid-extractable and reducible fractions (Table S7). This behavior strengthens the conclusion that Tl can significantly be mobilized during hydrometallurgical Zn extraction, or the metallurgy of sulfides in general.

3.3. *Thallium concentrations and isotopic variability in sulfide concentrates*

Thallium concentrations in the studied concentrates varied substantially, from 8.6 mg/kg (sample 2) to 169 mg/kg (sample 1) (Table 1). All samples are identical in their origin, as they originate from the low-T sulfide mineralizations (<200 °C) of the Mississippi Valley type (MVT) (Supplementary Material). Monovalent Tl, as a relatively conservative trace element with a chemistry similar to K, tends to accumulate in "late" hydrothermal fluids from which it can preferentially enter the specific low/medium-T mineral associations, including sulfides (Hettmann et al., 2014).

The Tl isotopic variability observed in the concentrate samples, expressed as ε^{205}Tl, ranged from −3.4 to −4.4 (±0.7). The finding suggests quite uniform isotopic compositions. Considering the ε^{205}Tl value of −3.9 in the post-flotation waste (sample 5) derived from the

Table 1
Thallium/element concentrations and Tl isotopic signatures (ε^{205}Tl) in the studied Zn-rich sulfide concentrates, the post-flotation waste and the metallurgical waste samples (Larox and Dorr sludges). Detailed information about the samples is available in the Supplementary Material section.

No.	Description	Tl mg/kg	Zn g/kg	Pb g/kg	Fe g/kg	ε^{205}Tl ± 0.7
1	Lisheen, Ireland – concentrate (ZnS)	169 ± 4	500 ± 38	25 ± 2	47 ± 6	-3.47
2	Pinargozu, Turkey – concentrate (ZnS)	8.64 ± 0.24	499 ± 34	47 ± 2	44 ± 6	-3.39
3	Olkusz, Poland – concentrate (ZnS)	70.1 ± 12.8	554 ± 156	18 ± 2	30 ± 10	-4.40
4	Olkusz, Poland – concentrate/reflot (ZnS+PbS)	94.8 ± 3.6	366 ± 30	147 ± 20	71 ± 6	-4.20
5	Olkusz, Poland – post-flotation waste (ZnS)	27.6 ± 3.0	116 ± 42	25 ± 5	–	-3.89
6	Larox sludge (50% Olkusz and 50% mix Lisheen/Pinargozu)	122 ± 0	180 ± 88	123 ± 2	194 ± 98	-3.63
7	Dorr sludge (50% Olkusz and 50% mix Lisheen/Pinargozu)	283 ± 34	245 ± 102	79 ± 2	135 ± 56	-3.11
	A smelter feed material (charge)*	~86	–	–	–	~−3.9

The Tl/metal concentrations are reported at the 2σ level (n = 3).
The ε^{205}Tl results assign an estimated error of ± 0.7 ε^{205}Tl (2σ) which is based on our external reproducibility of multiple separate analyses of the SRM AGV-2 (USGS, USA) (Table S3). "Reflot" means a metal-rich concentrate prepared by recycling of mine waste, i.e., by flotation. *Data obtained by a weighted mean calculation from the Olkusz, Lisheen and Pinargozu concentrate data in a mixing ratio of ~2/~1/~1, respectively; see the Supplementary Material section for details. —: not determined.

Olkusz ores with ε^{205}Tl values of −4.4 and −4.2 (samples 3 and 4) (Table 1), it can be argued that initial sulfide pre-concentration did not affect the Tl isotopic signature of the flotation product, which is mostly absent of gangue constituents. In other words, the role of gangue mineralization in total Tl isotopic composition of the Olkusz Zn/Pb deposit is probably not important.

It should also be highlighted that the identified overall ε^{205}Tl range, including the lowest ε^{205}Tl value in the concentrate from Olkusz (−4.4), is regularly observed in igneous/hydrothermal and even sedimentary rocks or phases (Prytulak et al., 2013, 2017; Nielsen et al., 2017; Howarth et al., 2018). Hettmann et al. (2014) on an example of the MVT deposit in Wiesloch (Germany) demonstrate relatively similar ε^{205}Tl values to our ore-like samples, with ε^{205}Tl = −2.7 (±0.5) for sphalerite or −1.4 for galena. In general, the authors report that the main cause for the Tl isotopic variations in sulfides and accompanying trace metal-bearing minerals like sulfosalts is mass-independent fractionation (MIF), with a nuclear volume-dependent effect as the controlling mechanism. It is assumed that the mass-dependent fractionation (MDF), which is typically associated with kinetic processes of heavy metal isotopes, including Tl, seems to be somewhat suppressed during hydrothermal processes (Hettmann et al., 2014). The theory is based on the premise that the diffusivity of Tl in the sulfide melt is possibly much

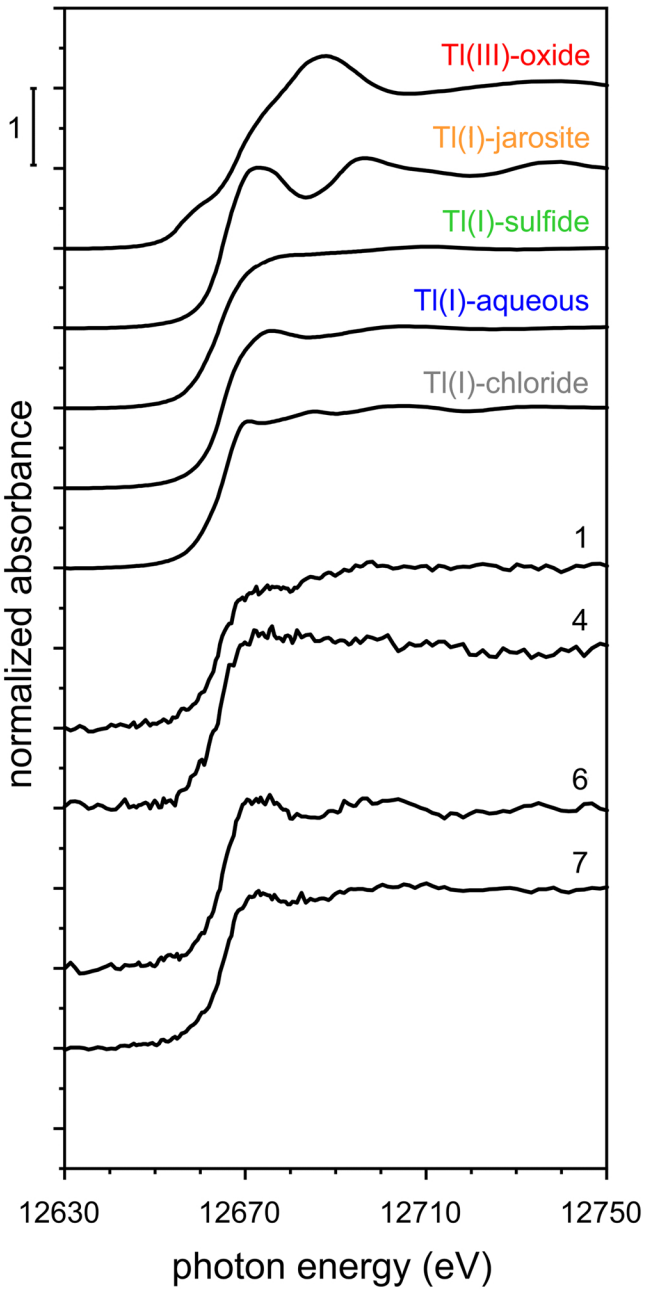

Fig. 2. Normalized Tl L_{III}-edge XANES spectra in selected sulfide concentrates (no. 1 and 4) and metallurgical wastes/sludges (no. 6 and 7), compared with reference spectra for Tl(III)-oxide (Tl_2O_3, avicenite), Tl-jarosite, Tl-sulfide ($TlAsS_2$, lorandite), aqueous Tl^+ and Tl(I)-chloride. 1 – Lisheen, Ireland; 4 – Olkusz, Poland; 6 and 7 – Larox and Dorr sludges. Detailed information about the samples is available in the Supplementary Material section.

faster than preferential (kinetically-driven) reactions of Tl isotopes over the sulfide formation. By combining all the available Tl isotopic MVT data with the ε^{205}Tl values observed in the Earth's mantle and/or bulk continental crust samples with ε^{205}Tl −2.0 (±1) on average (Nielsen et al., 2006a, 2006b, 2017), this could also be evidence for relatively low/limited stable Tl isotope fractionation during the formation of sulfides within the MVT deposits. Therefore, some consistency in Tl isotopic signatures with the primary magmatic Tl source or differentiated crust-derived melt enriched in Tl could be assumed.

3.4. Thallium concentrations and isotopic variability in processing wastes

The metallurgical sludges, with up to 283 mg Tl/kg (Table 1), indicate substantial Tl(I) accumulation, though mainly in specific newly formed oxides and gypsum (Table S6), in line with primary Tl source(s) such as sulfide concentrates (Table 1 and S4).

The calculated (weighted) mean ε^{205}Tl value corresponding to the metallurgical feed material used in the Boleslaw Zn smelter (as for November, 2020), which is a mixture of the concentrates 1, 2 and 3(4) in a ratio of ~1/~1/~2, respectively (Supplementary Material), equals −3.9. This value is analogous to that observed for a local post-flotation waste (Table 1). When ε^{205}Tl values in metallurgical sludges (−3.6 and −3.1, ±0.7) are compared with the smelter feed (−3.9, ±0.7), the data are indicative of a negligible Tl isotopic fractionation. This assumption is also consistent with only small variations in ε^{205}Tl (from −4.1 to −3.3, ±0.7) that we have first observed in all local massive ore and various waste materials from a high-temperature roasting/Waelz process (fly ash, slag and granulated waste) in the same metallurgical plant (Vaněk et al., 2018). Given the limited isotopic variability in the studied samples of only ~1 ε^{205}Tl (Table 1 and Fig. S1), including that regarding the roasting technology (Vaněk et al., 2018), we assume that sulfide ore processing does not result in significant Tl isotopic fractionation(s), i.e., in terms of a complete industrial Tl cycle. Further evidence for a conservative behavior of stable Tl isotopes can be seen from Fig. 3, which shows that all samples apparently fall in a 2σ range of a mean ε^{205}Tl value (−3.7).

Such an isotopic homogeneity is quite surprising, at least in view of a wide range of Tl concentrations (~9–280 mg/kg) (Table 1) or a very large variability in Tl isotopic ratios in different solid wastes from pyrite roasting technology, yielding ~17 ε^{205}Tl units (from −1 to +16), as recently reported by Liu et al. (2020). Therefore, our results are more similar to data by Kersten et al. (2014), who observed even an absence of Tl isotopic fractionation for a high-temperature process, albeit in relation to cement production. The authors revealed an analogy in the isotopic signature in Tl-rich FeS_2, co-combusted waste from FeS_2 roasting (as an additive) and emitted cement kiln dust (CKD), all exhibiting ε^{205}Tl ~0.

Indeed, our earlier isotopic data for fly ash and slag in the Boleslaw Zn smelter point to isotopically lighter Tl in the fly ash, corresponding to 0.8 ε^{205}Tl unit as a difference (Vaněk et al., 2018). The finding was explained by a higher rate of reaction kinetics of the ^{203}Tl isotope during evaporation, followed by the accumulation of ^{205}Tl in the remaining slag phase. From this viewpoint, the concept is synonymous to that proposed by Liu et al. (2020), who, on the basis of a Rayleigh distillation model, demonstrated marked Tl isotopic fractionation factors of $\alpha_{slag\text{-}vapor}$ = 1.0010–1.0025 between the slag and model vapor phase (Liu et al., 2020). We observed similar behavior in various emitted temperature-controlled Tl vapor and condensate samples (ε^{205} between ~−6 and −10), in comparison to the bottom ash (ε^{205} ~0) from industrial coal burning, thus, exhibiting a total variability of 10 ε^{205}Tl units (Vaněk et al., 2016). However, all the solid materials of fly and bottom ashes derived in the studied coal-fired power plant (Turów, Poland) showed much lower isotopic variability, which accounted for ~2.5 ε^{205}Tl units (Vaněk et al., 2016). At this point, again, it should be noted that we did not observe similar marked isotopic variations in any solid material or critical reaction products throughout the currently studied metallurgical technology. Moreover, all the identified Tl shifts were insignificant, on the basis of 2σ (Fig. 3).

In contrast, for stable Zn isotopes during primary Cu smelting (Krompachy, Slovakia), Bigalke et al. (2010) proved significant isotopic variations, in fly ash (δ^{66}Zn, −0.41‰) and grained slag and solid waste (0.18‰ and 0.25‰, respectively). This is congruent with data detected by Cloquet et al. (2006) for stable Cd isotopes. Comparable results are also reported by Kříbek et al. (2018) for Cu isotopes from the Cu smelter in Tsumeb (Namibia). The authors revealed isotopically lighter Cu in the fly ash (δ^{65}Cu = +0.15‰) relative to the Cu isotopic signature in the smelter charge (δ^{65}Cu = +0.28 and +0.44‰). All this information, in combination, possibly indicates the ability of lighter trace elements (Zn, Cu, Ni, Cd etc.) to be isotopically redistributed more significantly during both high- and low-temperature metallurgical operations or within anthropogenic activities in general (Wiederhold, 2015; Chrastný et al., 2015).

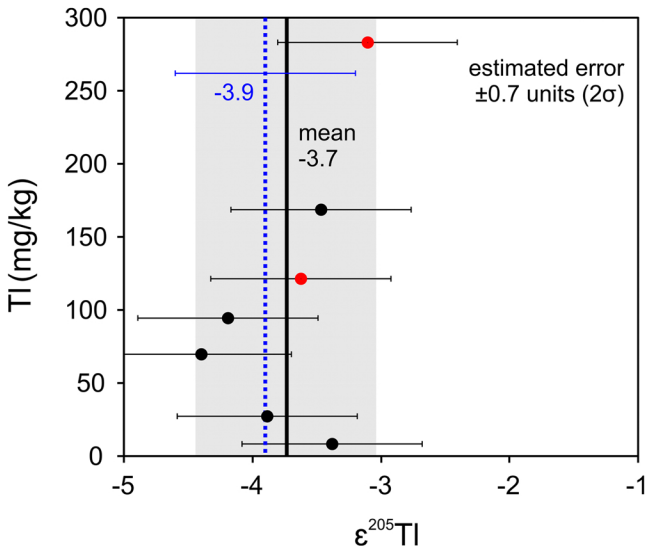

Fig. 3. Thallium concentration in the studied sulfide concentrates, the post-flotation waste and the metallurgical wastes/sludges (red points) vs. ε^{205}Tl. Black bold line depicts an unweighted mean ε^{205}Tl value calculated from all the samples (−3.7), blue dotted line depicts a calculated model ε^{205}Tl value for the metallurgical feed (−3.9). An estimated error of ± 0.7 ε^{205}Tl (2σ) is based on our external reproducibility of multiple separate analyses of the SRM AGV-2 (USGS, USA) (Table S3, Supplementary Material).

3.5. Potential link between Tl speciation and Tl isotopic data?

A combination of Tl mineralogical and speciation data and Tl isotopic compositions in the studied samples did not reveal any link between Tl forms and Tl isotopic signature. Omitting the fact that the total number of XANES and EPMA analyses was limited, apparently Tl was mainly present as Tl(I) and ZnS was a dominant Tl-host phase in all concentrate samples (Figs. 1 and S1). Thallium was also detected in other minor sulfides (FeS_2, PbS). Nevertheless, the overall distribution of Tl was relatively uniform in different sulfide minerals (≤0.2 wt%) (Table S4). Similarly, both the secondary Tl-rich minerals (mainly sulfates) and metallurgical precipitates (spinel oxides) did not indicate any important shifts in Tl concentrations, all exhibiting ≤ 0.3 wt% (Tables S5 and S6).

Regarding the absence of any relationship between Tl(I) speciation and the isotopic Tl signature, we assume that the Tl isotopes can be more efficient as qualitative tracers of the genesis of ore deposits. More specifically, Tl isotopic ratios can successfully be used as tracers of specific inter-element or mineral relationships within a specific deposit/mineralization for which, however, an accurate separation of Tl-rich minerals accompanied by selective Tl isotopic analysis is essential (Hettmann et al., 2014; Rader et al., 2018).

4. Conclusions

Contamination of the environment with Tl due to mining/processing of sulfides has widely been reported (Kazantzis, 2000; Xiao et al., 2004, 2012; Jakubowska et al., 2007; Karbowska et al., 2014; Gomez-Gonzalez et al., 2015; Liu et al., 2016, 2019; Aguilar-Carrillo et al., 2018; Garrido et al., 2020; Wei et al., 2021; Ning et al., 2021). Furthermore, it seems that similar to industrial coal burning, this activity is potentially

responsible for up to 1/4 of global anthropogenic Tl inputs (>0.5 Gg Tl/year) (John Peter and Viraraghavan, 2005).

Here, we present the first evaluation of Tl isotopic ratios over a complex cycle of sulfide processing, from the ore flotation to pyro- and hydrometallurgical stages. We found only insignificant Tl isotopic variations (on the basis of 2σ, 0.7 ε^{205}Tl) between initial smelter feed – sulfide concentrates and the waste materials from hydrometallurgical Zn extraction, in spite of relatively large differences in their Tl concentrations. The present data confirmed a very good consistency with the Tl isotopic data that we first obtained solely within roasting technology in the same plant (Vaněk et al., 2018). In combination, the results point to minimum Tl isotopic effects in terms of a total industrial process.

We found that the prevailing Tl form in all concentrates and metallurgical wastes is Tl(I), without any preferential incorporation into sulfides or Tl-containing secondary phases, mainly sulfates and spinel oxides. Therefore, we expect any reactions which alter Tl redox speciation (oxidation) and which could possibly be expected for some stages of hydrometallurgical processing to be absent. These reactions, if present, could lead to marked Tl isotopic effects (Wiederhold, 2015; Nielsen et al., 2017).

In summary, the obtained Tl isotopic data are similar and mimic the signature of the primary Tl source in all the key stages of sulfide processing. As a result, the use of Tl isotopic ratios as a source proxy or for quantifying industrial emissions may be complicated or even impossible in areas with naturally high/extreme Tl background contents. On the other hand, areas with two or more isotopically contrasting Tl sources allow for relatively easily tracing (Kersten et al., 2014; Vaněk et al., 2016; Grösslová et al., 2018), for instance, in sediments or soils which do not suffer from post-depositional isotopic redistribution effects.

CRediT authorship contribution statement

Aleš Vaněk – Methodology, Analysis, Investigation, Writing & Editing, Formal analysis, **Kateřina Vejvodová** – Analysis, Investigation, **Martin Mihaljevič** – Methodology, Analysis, Investigation, **Vojtěch Ettler** – Methodology, Analysis, Investigation, Writing, **Jakub Trubač** – Analysis, **Maria Vaňková** – Analysis, **Leslaw Teper** – Methodology, Investigation; Writing, **Jerzy Cabala** – Methodology, **Katarzyna Sutkowska** – Methodology, **Andreas Voegelin** – Analysis, Investigation, **Jörg Göttlicher** – Analysis, **Ondřej Holubík** – Analysis, **Petra Vokurková** – Analysis, **Lenka Pavlů** – Analysis, **Ivana Galušková** – Analysis, **Tereza Zádorová** - Analysis.

Declaration of Competing Interest

The authors declare that they have no known competing financial interests or personal relationships that could have appeared to influence the work reported in this paper.

Acknowledgements

This study was funded by the projects of the Czech Science Foundation (GAČR 20–08717S) and the European Regional Development Fund (CZ.02.1.01/0.0/0.0/16_019/0000845). Charles University researchers also received institutional funding from the Center for Geosphere Dynamics (UNCE/SCI/006). Polish authors were financially supported by the University of Silesia (WNP/INoZ/2020-ZB32). Furthermore, we acknowledge the assistance of Petr Drahota (XRD) and Radim Jedlička (SEM/EDS, EPMA), as well as of Chris Ash (UK) (English editing). Finally, all the anonymous reviewers are thanked for their comments and/or suggestions which improved the quality of the original manuscript version.

Appendix A. Supporting information

Supplementary data associated with this article can be found in the online version at doi:10.1016/j.jhazmat.2021.127325.

References

Aguilar-Carrillo, J., Herrera, L., Gutiérrez, E.J., Reyes-Domínguez, I.A., 2018. Solid-phase distribution and mobility of thallium in mining-metallurgical residues: environmental hazard implications. Environ. Pollut. 243, 1833–1845. https://doi.org/10.1016/j.envpol.2018.10.014.

Bigalke, M., Weyer, S., Kobza, J., Wilcke, W., 2010. Stable Cu and Zn isotope ratios astracers of sources and transport of Cu and Zn in contaminated soil. Geochim. Cosmochim. Acta 74, 6801–6813. https://doi.org/10.1016/j.gca.2010.08.044.

Chrastný, V., Čadková, E., Vaněk, A., Teper, L., Cabala, J., Komárek, M., 2015. Cadmium isotope fractionation within the soil profile complicates source identification in relation to Pb–Zn mining and smelting processes. Chem. Geol. 405, 1–9. https://doi.org/10.1016/j.chemgeo.2015.04.002.

Cloquet, C., Carignan, J., Libourel, G., Sterckeman, T., Perdrix, E., E, 2006. Tracing source pollution in soils using cadmiumand lead isotopes. Environ. Sci. Technol. 40, 2525–2530. https://doi.org/10.1021/es052232.

Dutrizac, J.E., 1997. The behavior of thallium during jarosite precipitation. Met. Mater. Trans. B 28, 765–776. https://doi.org/10.1007/s11663-997-0003-9.

Garrido, F., Garcia-Guinea, J., Lopez-Arce, P., Voegelin, A., Göttlicher, J., Mangold, S., Almendros, G., 2020. Thallium and co-genetic trace elements in hydrothermal Fe-Mn deposits of Central Spain. Sci. Total Environ. 717, 137162 https://doi.org/10.1016/j.scitotenv.2020.137162.

Gomez-Gonzalez, M.A., Garcia-Guinea, J., Laborda, F., Garrido, F., 2015. Thallium occurrence and partitioning in soils and sediments affected by mining activities in Madrid province (Spain). Sci. Total Environ. 536, 268–278. https://doi.org/10.1016/j.scitotenv.2015.07.033.

Gražulis, S., Daškevič, A., Merkys, A., Chateigner, D., Lutterotti, L., Quirós, M., Serebryanaya, N.R., Moeck, P., Downs, R.T., Le Bail, A., Crystallography, A., 2012. Open database (COD): an open-access collection of crystal structures and platform for world-wide collaboration. Nucleic Acids Res. 40, D420–D427. https://doi.org/10.1093/nar/gkr900.

Grösslová, Z., Vaněk, A., Oborná, V., Mihaljevič, M., Ettler, V., Trubač, J., Drahota, P., Penížek, V., Pavlů, L., Sracek, O., Kříbek, B., Voegelin, A., Göttlicher, J., Drábek, O., Tejnecký, V., Houška, J., Mapani, B., Zádorová, T., 2018. Thallium contamination of desert soil in Namibia: chemical, mineralogical and isotopic insights. Environ. Pollut. 239, 272–280. https://doi.org/10.1016/j.envpol.2018.04.006.

Hettmann, K., Kreissig, K., Rehkämper, M., Wenzel, T., Mertz-Kraus, R., Markl, G., 2014. Thallium geochemistry in the metamorphic Lengenbach sulfide deposit, Switzerland: Thallium-isotope fractionation in a sulfide melt. Am. Miner. 99, 793–803. https://doi.org/10.2138/am.2014.459.

Holleman, A.F., Wiberg, E., Wiberg, N., 1995. Lehrbuch der Anorganischen Chemie. Walter de Gruyter & Co.,, Berlin, NY.

Howarth, S., Prytulak, J., Little, S.H., Hammond, S.J., Widdowson, M., 2018. Thallium concentration and thallium isotope composition of lateritic terrains. Geochim. Cosmochim. Acta 239, 446–462. https://doi.org/10.1016/j.gca.2018.04.017.

Jacobson, A.R., McBride, M.B., Baveye, P., Steenhuis, T.S., 2005a. Environmental factors determining the trace-level sorption of silver and thallium to soils. Sci. Total Environ. 345, 191–205. https://doi.org/10.1016/j.scitotenv.2004.10.027.

Jacobson, A.R., Klitzke, S., McBride, M.B., Baveye, P., Steenhuis, T.S., 2005b. The desorption of silver and thallium from soils in the presence of a chelating resin with thiol functional groups. Water Air Soil Pollut. 160, 41–54. https://doi.org/10.1007/s11270-005-3860-3.

Jakubowska, M., Pasieczna, A., Zembrzuski, W., Swit, Z., Lukaszewski, Z., 2007. Thallium in fractions of soil formed on floodplain terraces. Chemosphere 66, 611–618. https://doi.org/10.1016/j.chemosphere.2006.07.098.

John Peter, A.L., Viraraghavan, T., 2005. Thallium: a review of public health and environmental concerns. Environ. Int. 31, 493–501. https://doi.org/10.1016/j.envint.2004.09.003.

Jović, V., 1998. Thallium. In: Marshall, C.P., Fairbridge, R.W. (Eds.), Encyclopedia of Geochemistry. Kluwer Academic Publishers, Dordrecht, Germany, pp. 622–623.

Karbowska, B., Zembrzuski, W., Jakubowska, M., Wojtkowiak, T., Pasieczna, A., Lukaszewski, Z., 2014. Translocation and mobility of thallium from zinc–lead ores. J. Geochem. Explor. 143, 127–135. https://doi.org/10.1007/s00128-016-1831-6.

Kazantzis, G., 2000. Thallium in the environment and health effects. Environ. Geochem. Hlth. 22, 275–280. https://doi.org/10.1023/A:1006791514080.

Kersten, M., Xiao, T., Kreissig, K., Brett, A., Coles, B.J., Rehkämper, M., 2014. Tracing anthropogenic thallium in soil using stable isotope compositions. Environ. Sci. Technol. 48, 9030–9036. https://doi.org/10.1021/es501968d.

Kříbek, B., Šípková, A., Mihaljevič, M., Majer, V., Knésl, I., Mapani, B., Penížek, V., Vaněk, A., Sracek, O., 2018. Variability of the copper isotopic composition in soil and grass affected by mining and smelting in Tsumeb, Namibia. Chem. Geol. 493, 121–135. https://doi.org/10.1016/j.chemgeo.2018.05.035.

Lide, D.R. (Ed.), 2009. CRC Handbook of Chemistry and Physics, 90th.,. CRC Press (Taylor and Francis Group), Boca Raton, FL.

Liu, J., Wang, J., Chen, Y., Xie, X., Qi, J., Lippold, H., Luo, D., Wang, C., Su, L., He, L., Wu, Q., 2016. Thallium transformation and partitioning during Pb−Zn smelting and environmental implications. Environ. Pollut. 212, 77–89. https://doi.org/10.1016/j.envpol.2016.01.046.

Liu, J., Yin, M., Luo, X., Xiao, T., Wu, Z., Li, N., Wang, J., Zhang, W., Lippold, H., Belshaw, N.S., Feng, Y., Chen, Y., 2019. The mobility of thallium in sediments and source apportionment by lead isotopes. Chemosphere 219, 864–874. https://doi.org/10.1016/j.chemosphere.2018.12.041.

Liu, J., Yin, M., Xiao, T., Zhang, C., Tsang, D.C.W., Bao, Z., Zhou, Y., Chen, Y., Luo, X., Yuan, W., Wang, J., 2020. Thallium isotopic fractionation in industrial process of pyrite smelting and environmental implications. J. Hazard. Mater. 384, 121378 https://doi.org/10.1016/j.jhazmat.2019.121378.

Nielsen, S.G., Rehkämper, M., Teagle, A.A.H., Butterfield, D.A., Alt, J.C., Halliday, A.N., 2006a. Hydrothermal fluid fluxes calculated from the isotopic mass balance of thallium in the ocean crust. Earth Planet. Sci. Lett. 251, 120–133. https://doi.org/10.1016/j.epsl.2006.09.002.

Nielsen, S.G., Rehkämper, M., Norman, M.D., Halliday, A.N., Harrison, D., 2006b. Thallium isotopic evidence for ferromanganese sediments in the mantle source of Hawaiian basalts. Nature 439, 314–317. https://doi.org/10.1038/nature04450.

Nielsen, S.G., Wasylenki, L.E., Rehkämper, M., Peacock, C.L., Xue, Z., Moon, E.M., 2013. Towards an understanding of thallium isotope fractionation during adsorption to manganese oxides. Geochim. Cosmochim. Acta 117, 252–265. https://doi.org/10.1016/j.gca.2013.05.004.

Nielsen, S.G., Rehkämper, M., Prytulak, J., 2017. Investigation and application of thallium isotope fractionation. Rev. Mineral. Geochem. 82, 759–798. https://doi.org/10.2138/rmg.2017.82.18.

Ning, Z., Liu, E., Yao, D., Xiao, T., Ma, L., Liu, Y., Li, H., Liu, C., 2021. Contamination, oral bioaccessibility and human health risk assessment of thallium and other metal (loid)s in farmland soils around a historic Tl-Hg mining area. Sci. Total Environ. 758, 143577 https://doi.org/10.1016/j.scitotenv.2020.143577.

Ostrander, C.M., Nielsen, S.G., Owens, J.D., Kendall, B., Gordon, G.W., Romaniello, S.J., Anbar, A.D., 2019. Fully oxygenated water columns over continental shelves before the Great Oxidation Event. Nat. Geosci. 12, 186–191. https://doi.org/10.1038/s41561-019-0309-7.

Ostrander, C.M., Owens, J.D., Nielsen, S.G., Lyons, T.W., Shu, Y., Chen, X., Sperling, E.A., Jiang, G., Johnston, D.T., Sahoo, S.K., Anbar, A.D., 2020. Thallium isotope ratios in shales from South China and northwestern Canada suggest widespread O_2 accumulation in marine bottom waters was an uncommon occurrence during the Ediacaran period. Chem. Geol. 557, 119856 https://doi.org/10.1016/j.chemgeo.2020.119856.

Owens, J.D., Nielsen, S.G., Horner, T.J., Ostrander, C.M., Peterson, L.C., 2017. Thallium-isotopic compositions of euxinic sediments as a proxy for global manganese-oxide burial. Geochim. Cosmochim. Acta 213, 291–307. https://doi.org/10.1016/j.gca.2017.06.041.

Peacock, C.L., Moon, E.M., 2012. Oxidative scavenging of thallium by birnessite: explanation for thallium enrichment and stable isotope fractionation in marine ferromanganese precipitates. Geochim. Cosmochim. Acta 84, 297–313. https://doi.org/10.1016/j.gca.2012.01.036.

Phillips, S.L., Perry, D.L. (Eds.), 1995. Handbook of Inorganic Compounds. CRC Press, Boca Raton, FL.

Prytulak, J., Nielsen, S.G., Plank, T., Barker, M., Elliot, T., 2013. Assessing the utility of thallium and thallium isotopes for tracing subduction zone inputs to the Mariana arc. Chem. Geol. 345, 139–149. https://doi.org/10.1016/j.chemgeo.2013.03.003.

Prytulak, J., Brett, A., Webb, M., Plank, T., Rehkämper, M., Savage, P.S., Woodhead, J., 2017. Thallium elemental behavior and stable isotope fractionation during magmatic processes. Chem. Geol. 448, 71–83. https://doi.org/10.1016/j.chemgeo.2016.11.007.

Rader, S.T., Mazdab, F.K., Barton, M.D., 2018. Mineralogical thallium geochemistry and isotope variations from igneous, metamorphic, and metasomatic systems. Geochim. Cosmochim. Acta 243, 42–65. https://doi.org/10.1016/j.gca.2018.09.019.

Rader, S.T., Maier, R.M., Barton, M.D., Mazdab, F.K., 2019. Uptake and fractionation of thallium by *Brassica juncea* in a geogenic thallium-amended substrate. Environ. Sci. Technol. 53, 2441–2449. https://doi.org/10.1021/acs.est.8b06222.

Rehkämper, M., Frank, M., Hein, J.R., Porcelli, D., Halliday, A., Ingri, J., Liebetrau, V., 2002. Thallium isotope variations in seawater and hydrogenetic, diagenetic, and hydrothermal ferromanganese deposits. Earth Planet. Sci. Lett. 197, 65–81. https://doi.org/10.1016/S0012-821X(02)00462-4.

Rehkämper, M., Frank, M., Hein, J.R., Halliday, A., 2004. Cenozoic marine geochemistry of thallium deduced from isotopic studies of ferromanganese crusts and pelagic sediments. Earth Planet. Sci. Lett. 219, 77–91. https://doi.org/10.1016/S0012-821X(03)00703-9.

Tremel, A., Masson, P., Sterckeman, T., Baize, D., Mench, M., 1997. Thallium in French agrosystems–I. thallium contents in arable soils. Environ. Pollut. 95, 293–302. https://doi.org/10.1016/S0269-7491(96)00145-5.

Vaněk, A., Grygar, T., Chrastný, V., Tejnecký, V., Drahota, P., Komárek, M., 2010. Assessment of the BCR sequential extraction procedure for thallium fractionation using synthetic mineral mixtures, assessment of the BCR sequential extraction procedure for thallium fractionation using synthetic mineral mixtures. J. Hazard. Mater. 176, 913–918. https://doi.org/10.1016/j.jhazmat.2009.11.123.

Vaněk, A., Komárek, M., Vokurková, P., Mihaljevič, M., Šebek, O., Panušková, G., Chrastný, V., Drábek, O., 2011. Effect of illite and birnessite on thallium retention and bioavailability in contaminated soils. J. Hazard. Mater. 191, 190–196. https://doi.org/10.1016/j.jhazmat.2011.04.065.

Vaněk, A., Mihaljevič, M., Galušková, I., Chrastný, V., Komárek, M., Penížek, V., Zádorová, T., Drábek, O., 2013. Phase-dependent phytoavailability of thallium – a synthetic soil experiment. J. Hazard. Mater. 250–251, 265–271. https://doi.org/10.1016/j.jhazmat.2013.01.076.

Vaněk, A., Grösslová, Z., Mihaljevič, M., Trubač, J., Ettler, V., Teper, L., Cabala, J., Rohovec, J., Zádorová, T., Penížek, V., Pavlů, L., Holubík, O., Němeček, K., Houška, J., Drábek, O., Ash, C., 2016. Isotopic tracing of thallium contamination in soils affected by emissions from coal-fired power plants. Environ. Sci. Technol. 50, 9864–9871. https://doi.org/10.1021/acs.est.6b01751.

Vaněk, A., Grösslová, Z., Mihaljevič, M., Ettler, V., Trubač, J., Chrastný, V., Penížek, V., Teper, L., Cabala, J., Voegelin, A., Zádorová, T., Oborná, V., Drábek, O., Holubík, O., Houška, J., Pavlů, L., Ash, C., 2018. Thallium isotopes in metallurgical wastes/contaminated soils: a novel tool to trace metal source and behavior. J. Hazard. Mater. 343, 78–85. https://doi.org/10.1016/j.jhazmat.2017.09.020.

Vaněk, A., Holubík, O., Oborná, V., Mihaljevič, M., Trubač, J., Ettler, V., Pavlů, L., Vokurková, P., Penížek, V., Zádorová, T., Voegelin, A., 2019. Thallium stable isotope fractionation in white mustard: implications for metal transfers and incorporation in plants. J. Hazard. Mater. 369, 521–527. https://doi.org/10.1016/j.jhazmat.2019.02.060.

Vaněk, A., Voegelin, A., Mihaljevič, M., Ettler, V., Trubač, J., Drahota, P., Vaňková, M., Oborná, V., Vejvodová, K., Penížek, V., Pavlů, L., Drábek, O., Vokurková, P., Zádorová, T., Holubík, O., 2020. Thallium stable isotope ratios in naturally Tl-rich soils. Geoderma 364, 114183. https://doi.org/10.1016/j.geoderma.2020.114183.

Vaněk, Aleš, Vejvodová, Kateřina, Mihaljevič, Martin, Ettler, Vojtěch, Trubač, Jakub, Vaňková, Maria, Goliáš, Viktor, Teper, Leslaw, Sutkowska, Katarzyna, Vokurková, Petra, Penížek, Vít, Zádorová, Tereza, Drábek, Ondřej, 2021. Thallium and lead variations in a contaminated peatland: A combined isotopic study from a mining/smelting area. Environmental Pollution 290, 117973. https://doi.org/10.1016/j.envpol.2021.117973.

Vejvodová, K., Vaněk, A., Mihaljevič, M., Ettler, V., Trubač, J., Vaňková, M., Drahota, P., Vokurková, P., Penížek, V., Zádorová, T., Tejnecký, V., Pavlů, L., Drábek, O., 2020. Thallium isotopic fractionation in soil: the key controls. Environ. Pollut. 265, 114822 https://doi.org/10.1016/j.envpol.2020.114822.

Voegelin, A., Pfenninger, N., Petrikis, J., Majzlan, J., Plötze, M., Senn, A.C., Mangold, S., Steininger, R., Göttlicher, J., 2015. Thallium speciation and extractability in a thallium- and arsenic-rich soil developed from mineralized carbonate rock. Environ. Sci. Technol. 49, 5390–5398. https://doi.org/10.1021/acs.est.5b00629.

Wei, X., Wang, J., She, J., Sun, J., Liu, J., Wang, Y., Yang, X., Ouyang, Q., Lin, Y., Xiao, T., Tsang, D.C.W., 2021. Thallium geochemical fractionation and migration in Tl-As rich soils: The key controls. Sci. Total Environ. 784, 146995 https://doi.org/10.1016/j.scitotenv.2021.146995.

Wiederhold, J., 2015. Metal stable isotope signatures as tracers in environmental geochemistry. Environ. Sci. Technol. 49, 2606–2624. https://doi.org/10.1021/es504683e.

Xiao, T., Guha, J., Boyle, D., Liu, C.Q., Chen, J., 2004. Environmental concerns related to high thallium levels in soils and thallium uptake by plants in southwest Guizhou, China. Sci. Total Environ. 318, 223–244. https://doi.org/10.1016/s0048-9697(03)00448-0.

Xiao, T., Yang, F., Li, S., Zheng, B., Ning, Z., 2012. Thallium pollution in China: a geo-environmental perspective. Sci. Total Environ. 421–422, 51–58. https://doi.org/10.1016/j.scitotenv.2011.04.008.

7.4. Effect of peat organic matter on sulphide weathering and thallium reactivity: Implications for organic environments

Vejvodová, K., Vaněk, A., Spasić, M., Mihaljevič, M., Ettler, V., Vaňková, M., Drahota, P., Teper, L., Vokurková, P., Pavlů, L., Zádorová, T., Drábek, O. (2022). Effect of peat organic matter on sulphide weathering and thallium reactivity: Implications for organic environments. Chemosphere, 299, 134380.

Chemosphere 299 (2022) 134380

Contents lists available at ScienceDirect

Chemosphere

journal homepage: www.elsevier.com/locate/chemosphere

Effect of peat organic matter on sulfide weathering and thallium reactivity: Implications for organic environments

Kateřina Vejvodová [a], Aleš Vaněk [a,*], Marko Spasić [a], Martin Mihaljevič [b], Vojtěch Ettler [b], Maria Vaňková [b], Petr Drahota [b], Leslaw Teper [c], Petra Vokurková [a], Lenka Pavlů [a], Tereza Zádorová [a], Ondřej Drábek [a]

[a] Department of Soil Science and Soil Protection, Faculty of Agrobiology, Food and Natural Resources, Czech University of Life Sciences Prague, Kamýcká 129, 165 00, Praha 6, Czech Republic
[b] Institute of Geochemistry, Mineralogy and Mineral Resources, Faculty of Science, Charles University, Albertov 6, 128 00, Praha 2, Czech Republic
[c] Institute of Earth Sciences, Faculty of Natural Sciences, University of Silesia, Bedzinska 60, 41-200, Sosnowiec, Poland

HIGHLIGHTS

- Sphalerite is less stable in peat as compared to other sulfides.
- Sphalerite, a major phase controlling the Tl flux into peat.
- Thallium showed a higher mobility and migration potential than Pb.
- Industrial acid precipitations can accelerate ZnS weathering and Tl release.

GRAPHICAL ABSTRACT

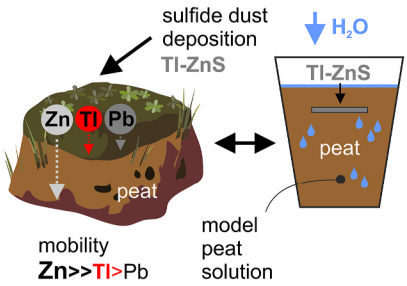

ARTICLE INFO

Handling Editor: Petra Petra Krystek

Keywords:
Contamination
Organic matter
Peat
Mobility
Weathering

ABSTRACT

Weathering of Tl-containing sulfides in a model (12-week) peat pot trial was studied to better understand their geochemical stability, dissolution kinetics, alteration products and the associated release and mobility of anthropogenic Tl in organic environments. We also present the effect of industrial acid rainwater on sulfide degradation and Tl migration in naturally acidic peat. Sphalerite (ZnS) was much less stable in peat than other Tl-containing sulfides (galena and pyrite), and thus acted as a major phase responsible for Tl mobilization. Furthermore, Tl incongruently leached out over Zn from ZnS, and accumulated considerably more in the peat solutions (≤5 μg Tl/L) and the peat samples (≤0.4 mg Tl/kg) that were subjected to acid rain watering compared to a deionized H_2O regime. This finding was in good agreement with the absence of secondary Tl-containing phases, which could potentially control the Tl flux into the peat. The behavior of Tl was not as conservative as Pb throughout the trial, since a higher peat mobility and migration potential of Tl was observed compared to Pb. In conclusion, industrial acid precipitations can significantly affect the stability of ZnS even in acidic peat/organic environments, making it susceptible to enhanced weathering and Tl release in the long term.

* Corresponding author.
E-mail address: vaneka@af.czu.cz (A. Vaněk).

https://doi.org/10.1016/j.chemosphere.2022.134380
Received 7 February 2022; Received in revised form 14 March 2022; Accepted 18 March 2022
Available online 19 March 2022

1. Introduction

Peat organic matter may behave as an efficient scavenger of trace elements (e.g., Pb, Sb, Hg and Ag) that are atmospherically deposited onto peatlands (e.g., Cabala et al., 2013; De Vleeschouwer et al., 2009, 2020; Farmer et al., 2006; Fiałkiewicz-Kozieł et al., 2018, 2020; Kylander et al., 2005; Mihaljevič et al., 2006; Novak et al., 2008; Shotyk et al., 1992, 1996, 1998, 2001, 2016a,b, 2017; Shotyk and Krachler, 2004; Smieja-Król and Bauerek, 2015; Smieja-Król et al., 2015, 2019; Vaněk et al., 2021; Weiss et al., 1999, 2002, 2007; Zuna et al., 2011, 2012). Regarding element capture, dust particle fixation, specific/non-specific sorption or even coprecipitation all have to be considered (Cabala et al., 2013; Smieja-Król et al., 2010, 2015). Furthermore, there are contaminants such as Zn, Cu, Ni or Cr which, by contrast tend to be mobile and readily migrate in peatlands (Novak and Pacherova, 2008; Smieja-Król and Bauerek, 2015; Vaněk et al., 2021; Weiss et al., 2007).

In this context, still limited geochemical data are available for thallium (Tl), a highly toxic trace element (Nriagu, 1998), and its fate in organic geosystems (fen, bog, forest floor layer, etc.) (Jacobson et al., 2005a,b; Shotyk and Krachler, 2004; Shotyk et al., 2017; Smieja-Król et al., 2015). More specifically, the stability and dissolution kinetics of Tl-rich compounds (mainly sulfides) in the presence of water-saturated particulate peat, the types of secondary alteration products, or the associated degree of Tl leaching in both the short- and the long-term, are unclear. At this point, it should be noted that sulfide ore mining and processing are among the most important sources of anthropogenic Tl in the environment (e.g., Aguilar-Carrillo et al., 2018; Cabala and Teper, 2007; Garrido et al., 2020; Gomez-Gonzalez et al., 2015; Grösslová et al., 2018; Jakubowska et al., 2007; Karbowska et al., 2014; Lis et al., 2003; Liu et al., 2016, 2019, 2020a,b, 2022; Lukaszewski et al., 2018; Vaněk et al., 2013, 2018, 2022; Wang et al., 2021; Xiao et al., 2004a, 2004b, 2012; Zhou et al., 2022).

In this study, we present combined chemical and mineralogical data on the weathering of Tl-containing sulfides subjected to model peat conditions. The contaminating material represents a Tl-rich sulfide concentrate from the flotation of Zn–Pb ores (Olkusz, Poland). Due to its grain size (<60 μm, corresponding to the clay/silt sized fraction), it can be assumed to account for the majority of fugitive dust mass flux, if it is wind-mobilized (Robson et al., 2014). From this viewpoint, the concentrate has environmental relevance for both local ore mining- and processing-related activities, and it may also serve as a model material for similar Tl-affected areas.

The following major questions were addressed in our research: (i) Does the peat organic matter significantly accelerate sulfide weathering and Tl release in a short-term period (≤12 weeks), and if so, what are the key controlling mechanisms? (ii) Does the formation of secondary Tl-containing phases potentially limit Tl mobilization and its entry into the organic environment? (iii) Could acid rainwater enhance sulfide degradation and Tl release in naturally acidic peat? These answers are clearly needed for a complex understanding of Tl behavior, its fate or geochemical cycling in polluted organic environments.

2. Experimental

2.1. Peat and contaminating sulfide material

A commercial pollutant-free ombrotrophic peat (Agro, Czech Republic) was used throughout our experiments. Basic data on its physicochemical properties are summarized in (Table 1), these were obtained using the following methods: The peat pH values were determined in H_2O and KCl solutions (v/v ratio, 1/5) and the cation exchange capacity (CEC) was calculated on the basis of the Bower Na/NH_4 acetate method (Bower et al., 1954). The total carbon and sulfur concentrations (TC, TS) were determined using the elemental CNS analyzer (Flash, 2000; Thermo Fisher Scientific, Germany). To calculate the ash content (loss of ignition), 1 g of peat sample was burned at 550 °C (% of dry sample weight).

Table 1
Basic physicochemical properties and trace element concentrations in the experimental peat used in the laboratory pot trial.

pH[a]		LOI[a]	TC[a]	TS[a]	CEC[a]	Tl	Zn	Pb
H_2O	KCl	(%)	(%)		(cmol+/kg)	(mg/kg)		
4.3	3.2	89	41.7	0.5	99	0.03 ± 0.004	13.8 ± 0.3	6.05 ± 0.7

Trace element concentrations depict means (n = 3; ±1 SD).
LOI: loss on ignition.
[a] The data depict means (n = 3; RSD ≤10%).

The Tl-rich sulfide concentrate, representing the anthropogenic model source of Tl/trace elements in the studied peat, was obtained by the flotation of Zn–Pb ores from the hydrothermal/MVT deposit at Olkusz in Poland. Its granulometry was double-checked so that the sample was sieved to <63 μm particle-sized fraction, using a stainless-steel sieve (Fritsch, Germany), and examined with scanning electron microscopy (SEM), showing the average particle size <30 μm (Fig. 1). The bulk mineralogy was determined using X-ray diffraction analysis (XRD) (X'Pert Pro diffractometer, PANalytical, the Netherlands) under the following conditions: CuKα radiation at 40 kV (30 mA), 2 theta range of 5–80°, counting time of 150 s per step (step of 0.02°), in combination with X'Pert High Score Plus 3.0 software and a Crystallography Open Database (COD) (Gražulis et al., 2012). The electron probe microanalysis (EPMA) using a JEOL JXA-8530 F (JEOL, Japan) electron probe microanalyzer with a field emission gun as an electron source and an energy dispersion spectrometer (EDS) (JEOL JED-2300 F) was used to assess the individual role of metal sulfides and their alteration products in the fixation of Tl. Complex data on the chemical and mineralogical compositions of the sulfide concentrate is given in Table 2.

2.2. Laboratory pot trial

In the pot experiment, 0.5 g of sulfide concentrate (±0.0001 g) was placed into double-layered polyamide bags (NITEX 03–1/1, Sefar AG, Switzerland; 3 × 3 cm inner bag and 5 × 5 cm outer bag with a mean mesh size of 1 μm). All the bags were sealed by welding, weighed, and stored before further use. A mass of 60 g of peat was placed into acid-washed 150 mL polypropylene pots. Rhizon pore water samplers (Rhizosphere Research Products, the Netherlands) were placed in the bottom part of each pot (Fig. 2). The bags were placed horizontally into

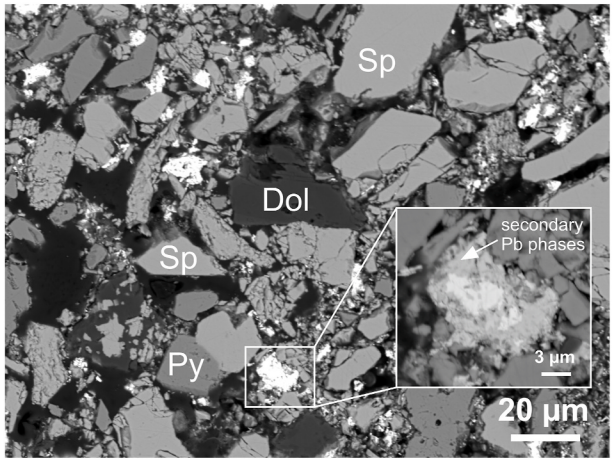

Fig. 1. Scanning electron micrograph in back-scattered electrons (SEM-BSE) of the Tl-rich sulfide concentrate used in the pot trial. Phase abbreviations: Sp – sphalerite (ZnS); Py – pyrite (FeS_2); Dol – dolomite ($CaMg(CO_3)_2$).

Table 2
Chemical and bulk mineralogical data of the Tl-rich sulfide concentrate used in the laboratory pot trial.

Total element concentrations		After Incubation[c]
(n = 3; ± 1 SD)		H_2O/SRW
Tl (mg/kg)	94.8 ± 1.8	85.9/85.6
Zn (g/kg)	366 ± 15	350/318
Pb (g/kg)	147 ± 10	–
Fe (g/kg)	71 ± 3	–
Mg (g/kg)	6 ± 0.07	0.36/0.39
Bulk mineralogy[a]	Semi-quantity	
Sphalerite (ZnS)	++++++	
Galena (PbS)	++	
Pyrite (FeS_2)	+++	
Anglesite ($PbSO_4$)	++	
Sussanite ($Pb_4(CO_3)_2(SO_4)(OH)_2$)	++	
Plumbojarosite ($PbFe_6(SO_4)_4(OH)_{12}$)	+	
Dolomite ($CaMg(CO_3)_2$)	++	
Quartz (SiO_2)	+	
Tl in sulfides (wt.%)[b]	0.04–0.20	

[a] Data obtained by X-ray diffraction analysis (Fig. S1, Supplementary Material); ++++++ major component (>50%); +++ (~20%); ++ (~5%); + (traces).
[b] Data obtained by EPMA on the basis of number of spot analyses (Table S2, Supplementary Material).
[c] Data related to the end of the pot trial (after 12 weeks) using deionized H_2O and synthetic rainwater (SRW) for peat watering/concentrate incubation; — no difference in relation to initial element concentrations.

the peat, 1 cm below the surface. All pots were then watered with either deionized H_2O (MilliQ+, Millipore, USA) or synthetic rainwater (SRW) to maintain 70% water holding capacity (WHC), corresponding to a volume of ~65 mL. This type of saturation was constant over the whole experiment. The SRW was prepared according to the protocol used in a precipitation leaching procedure (SPLP) (acid water solution – pH 4.2 ± 0.05; 60/40 wt% mixture of H_2SO_4 and HNO_3) related to industrially affected areas (EPA Method 1312, USEPA). The pots without bags were used to control the release of trace elements from the peat matrix. The experiment was run in pentaplicates for both H_2O and SRW variants (Fig. 2). This methodological approach is adopted from previous environmental studies of Ettler et al. (2012, 2016), which dealt with the reactivity and solubility of various fly ashes in different types of soils.

The peat pore solutions (~2–3 mL) were sampled after 1, 2, 3, 4, 6, 8 and 12 weeks (84 days). All samples were filtered using 0.45 μm nylon syringe filters (Nalgene, USA) and their pH and Eh values were immediately measured using a Handylab pH 11 multimeter (Schott, Germany). Subsequently, the filtrates were diluted, stabilized and stored before determination of Tl, Zn, Pb and Fe concentrations (see Section 2.3). At the end of the trial, individual bags were extracted and weighed again to quantify their mineral loss. The altered concentrate was dissolved and analyzed for individual element contents so that their role in material degradation could be selectively quantified. In order to evaluate the peat contamination resulting from the alteration (weathering) of the sulfide concentrate, peat in the pots was divided into two segments (Fig. 2) and subsequently analyzed for total Tl, Zn, Pb and Fe concentrations. A sample aliquot of 0.5 g dissolved in a mixture of concentrated HNO_3/HCl/HF (Merck Ultrapure, Germany) (3:1:0.5 ratio, ~12 mL, total volume) using a microwave system (Multiwave 5000, Anton Paar, Austria) preceded this analysis. An Analogous digestion procedure was used for the uncontaminated peat. The sulfide concentrate sample was dissolved from a mass of 0.2 g which was subjected to a mixture of concentrated HNO_3/HF (2:1 ratio, ~20 mL, total volume) in PTFE beakers (60-mL, Savillex, USA) placed on a ceramic plate (175 °C) for 48 h.

2.3. Analyses

Concentrations of Tl, Zn, Pb, Fe and Mg in individual solutions, digested peat and sulfide concentrate samples were determined using Q-ICP-MS (Xseries II, Thermo Fisher Scientific, Germany) under the standard analytical conditions. QC was ensured using the standard reference material 2711 (Montana Soil, NIST, USA). The accuracy of individual measurements was typically ≤5% RSD (Table S1, Supplementary Material).

2.4. Statistics

Statistica 13.3 software (StatSoft Inc, USA) was used to perform statistical analyses. Basic statistical parameters, such as the averages and the standard deviations were computed. One-way analysis of variance (ANOVA) and post-hoc Tukey test ($p < 0.05$) was performed for categorical variables (Tl and Zn concentrations) to compare the laboratory pot experiment variants – H_2O and SRW.

3. Results and discussion

3.1. Thallium and metal concentrations in peat solutions

Element monitoring in the peat solutions showed a gradual/time-dependent increase in Tl concentrations (Fig. 3). This trend is related to Tl leaching from sphalerite (ZnS), a major Tl-containing phase, and to a limited degree from less abundant galena (PbS) and pyrite (FeS_2) (Table 2 and S2; Fig. S1). Regarding Zn, its concentrations in the peat solutions were rather stable throughout the pot trial, suggesting different geochemical patterns between Zn and Tl, and even the incongruent dissolution of ZnS. For example, given the Tl/Zn solution ratios in

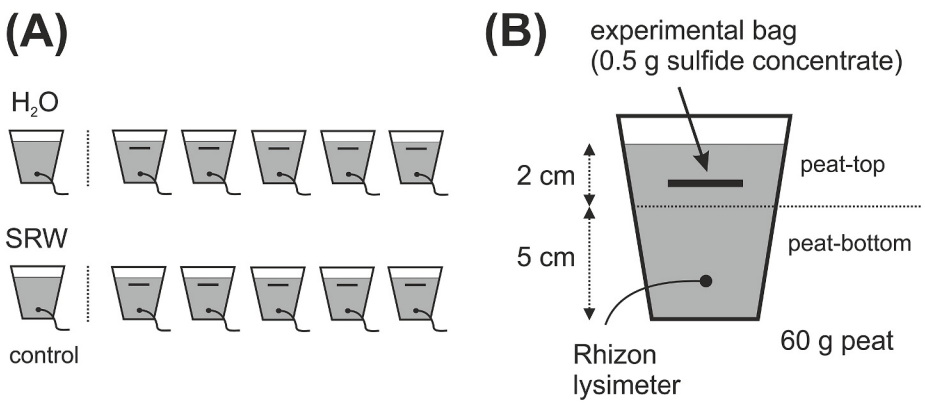

Fig. 2. The pot trial setup with bags containing sulfide concentrate – Tl/trace element source (A). Deionized H_2O (H_2O) and synthetic rainwater (SRW) were used for peat watering. Pots without bags were used as a control variant. Location of the bag, Rhizon pore solution sampler and peat segments sampled at the end of the concentrate incubation (12 weeks) (B).

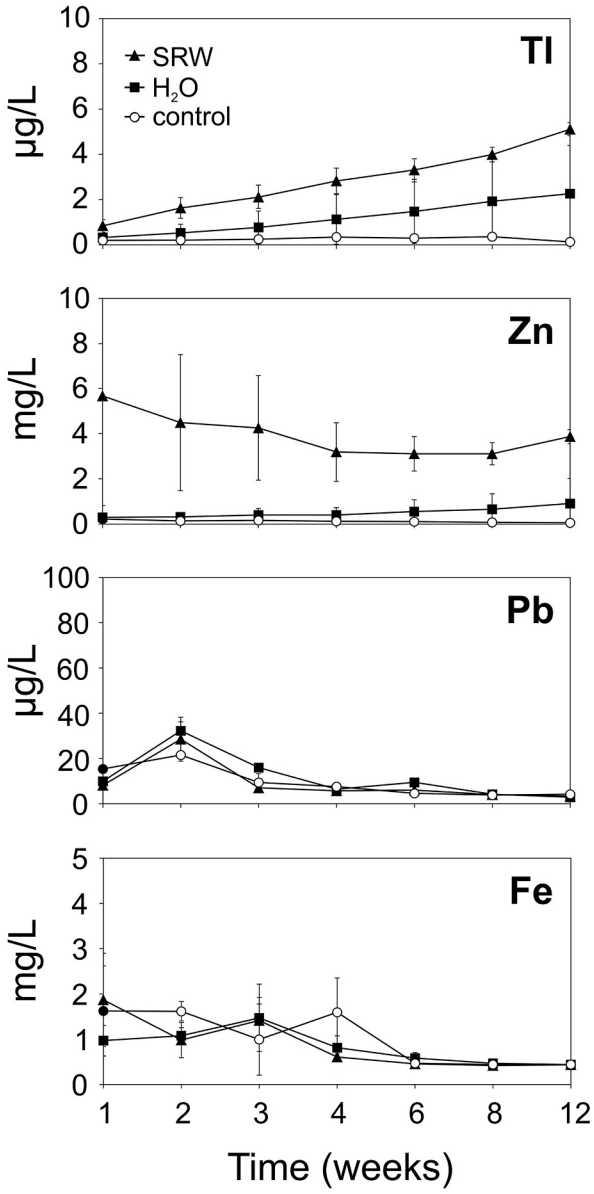

Fig. 3. Thallium, Zn, Pb and Fe concentrations in peat pore solutions over the pot trial/12 weeks (n = 5; ±1 SD); synthetic rainwater (SRW), deionized water (H_2O), control – no contamination.

the first third, or at the end of the experiment (4 and 12 weeks, respectively) relative to their concentrations present in the concentrate sample, the calculated Tl/Zn values in the solutions are 3–5 times higher. This finding indicates that Tl and Zn were not released in the same proportion as they were found in the concentrate (Fig. 3), considering their similar affinity to particulate peat estimated for both elements (Tl and Zn). Therefore, the primary cause could be heterogeneous distribution of Tl in the structure of ZnS, and/or Tl association with more soluble (unidentified) Tl species that can become enriched on the sulfide surface(s) (Table S2), resulting in relatively higher Tl release, compared to Zn.

Significantly higher Tl and Zn mobilization rates were observed for the SRW variant, as compared to H_2O, with maximum concentrations of ~5 µg Tl/L and 6 mg Zn/L. Therefore, acid-promoted and/or oxidative leaching (due O_2 or Fe^{3+}) are assumed to be the key control mechanisms for the dissolution of ZnS and enhanced Tl and Zn release (Robson et al., 2014). The finding further implies that the acid rainwater in mining/smelting-affected areas can substantially affect sulfide dust degradation, even in naturally acidic peat environments. Considering the increasing trend in Tl concentrations in the peat solutions (Fig. 3), it can be argued that the short-term Tl retention by the particulate peat matter is not considerably high (Jacobson et al., 2005a) and led to a vertical migration of Tl (see Section 3.2). In agreement with the model sorption studies compiled by Nriagu (1998), the Tl(I) complexation with most organic ligands (log $K \leq 2.0$) or fulvic and humic acids (log $K \leq 5$) is weak and probably insignificant in its fixation by peat. The only exception is Tl adsorption on the S-rich compounds, i.e., specifically bound to the –SH functional groups (Jacobson et al., 2005b). However, Martin et al. (2020), who evaluated Tl sorption types on natural organic compounds using the NICA-Donnan model, also report that quite a small portion (~15%) of total T(I) speciation can actually be complexed. Therefore, the formation of stable Tl(I) complexes on the surface of peat organic matter is not likely, and Tl is suggested to mainly associate with the exchange site positions, i.e., similar as for the organo-mineral soils (Vaněk et al., 2013, 2016, 2018). The retention of Tl in peat via the indiscriminate (or discriminate) abiotic uptake with K^+ or NH_4^+, having similar ionic properties and geochemical and sorption behavior (Kersten et al., 2014; Liu et al., 2020a,b, 2022; Vaněk et al., 2011, 2012, 2019; Voegelin et al., 2015; Wang et al., 2021; Wick et al., 2019, 2020, etc.) is questionable. However, during a batch Tl sorption study, Jacobson et al. (2005a) document that both these cations (K^+ and NH_4^+) do not act as important competitors for Tl exchange sites. This factor could be more important for living peat biota and associated biogeochemical cycling where the K-channel could be one of the key control mechanisms affecting biotic uptake and translocation of Tl (Rader et al., 2019; Vaněk et al., 2019).

Different concentration trends were observed for Pb and Fe. With the exception of a small Pb peak (~30 µg/L) found in the 2nd week of peat monitoring, both these elements showed constant, and low rate, solubilizations without any significant differences for all the SRW, H_2O and the control variants (Fig. 3). Therefore, it can be reasonably assumed that especially PbS and the identified products of its alteration such as anglesite ($PbSO_4$), plumbojarosite ($PbFe_6(SO_4)_4(OH)_{12}$) or susannite ($Pb_4(CO_3)_2(SO_4)(OH)_2$) were relatively stable in the peat and played a minor role in the Pb, Fe and Tl release (Table 2 and S3, Fig. 1). In addition, low solubilities of PbS ($K_{sp} = 10^{-13.97}$, PHREEQC database) and Pb sulfates in organic soils have previously been reported by e.g. Ettler et al. (2005) etc. The relatively low solubility of PbS in the peat environment is in line with the results presented by Smieja-Król et al. (2010), who clearly indicate its resistance in peat for at least hundreds of years. The PbS half-life in peat can further be prolonged with a decrease in Eh, which could potentially happen in deeper peat layers of natural bog sediments, even capable for authigenic PbS formation (Smieja-Król et al., 2010, 2015). Moreover, dissolved Pb, if present, tends to be strongly bound to the peat matter (see Section 3.2), where it typically forms stable surface complexes with number of primary organic and/or humic compounds (Mihaljevič et al., 2006; Novak et al., 2008; Novak and Pacherova, 2008; Smieja-Król et al., 2010, etc.). To summarize, the acidic character of the studied peat ($pH_{H2O} = 4.3$, Table 1) and the reduced stability of sulfides, which makes them more susceptible to further alterations (Vaněk et al., 2015), is not likely to have led to the significant mobilization of Pb and Fe. The generally low Fe concentrations in the peat solutions can be attributed to the low dissolution of FeS_2 (Fig. 3) supplemented by Fe^{3+} complexation by peat matter and/or the identified Fe coprecipitation with secondary Pb phases (e.g. plumbojarosite), as there was no evidence for the formation of secondary Fe (III)-oxides or Fe(III)-sulfates from the altered FeS_2 (Table 2, Fig. 1 and S1). This type of weathering behavior could be promoted by different oxidation kinetics for individual sulfides in sulfide associations. A limited oxidation of sulfides with a high electrode potential (FeS_2) relative to other sulfides such as ZnS, exhibiting low conductivity and associated higher oxidation potential, was proven by Sato (1992).

The average mass loss of the sulfide concentrate reached high values at the end of its incubation (12 weeks), which accounted for 9 ± 1 and

10.4 ± 0.8 wt% for deionized H_2O and the SRW variants, respectively. Considering this data, the approximate model-life time for the contaminating material (= at given conditions) would equal to only 2–3 years. However, in view of selective breakdown of dolomite ($CaMg(CO_3)_2$), as it is indicated by > 90-wt.% depletion of the initial Mg amount in the altered concentrate (6 g/kg relative to 0.4 g/kg, Table 2), this mineral is assumed to account for the majority of the material loss. Following the observed low Pb and Fe solubilities, the presence of Pb- and Pb–Fe sulfates and the presumption for their continuous formation, affecting the mobility of major/trace elements in oxic peat systems (surface peat layers) (Cabala et al., 2013; Smieja-Król et al., 2010, 2015; Smieja-Król and Bauerek, 2015), the predicted contaminant retention time is at least of order(s) of magnitude higher.

It should be highlighted that we did not observe any significant changes in the peat solution pH during the dissolution and/or alteration of sulfides, which in that case might be linked with the H_3O^+ consumption and associated pH increase. In fact, slightly lower pH values (~3.9–4.2) were found for the SRW variant as compared to the H_2O treatment (~4.2–4.3), indicating the more important acid effect of synthetic rainwater and/or soluble organic substances (acids). The redox potentials (Eh) of ~200–300 mV assigned relatively stable oxic conditions throughout the pot trial (data not shown), similar to those observed by e.g. Robson et al. (2014), albeit in agricultural mineral soils solely amended with ZnS microparticles.

3.2. Thallium and metal concentrations in peat

In agreement with the peat pore water data, the release of Tl, Zn, Pb and Fe is reflected by their concentration gradients in the peat itself (Fig. 4). A comparison of the contaminated peat segments with the trends found for the uncontaminated peat showed that Zn displayed the highest (up to ~70-times) enrichment (≤940 mg Zn/kg) (Fig. 4). In line with our previous results from the mining-affected peatland at Wolbrom (Poland), being a natural analogy to the present pot trial, Zn showed similar increased mobility in the peat profile (Vaněk et al., 2021).

Regarding Tl and Pb concentrations, much lower concentration gradients were observed for both elements. The Tl and Pb patterns depicted maximum ~12- and 4-times enrichments (0.4 and 25 mg/kg) in the topmost peat relative to the control variant (0.03 and 6 mg/kg), respectively (Fig. 4); this observation was consistent with the low concentrations in the peat solutions. Omitting the fact that both Tl and Pb demonstrate limited solubilizations in peat (Fig. 3) (e.g., Shotyk et al., 2016b; Shotyk and Krachler, 2004; Vaněk et al., 2021), Pb, in contrast to Tl, also tends to occur in large colloids where stable Pb-complexes with insoluble humic acids can readily form (Gao et al., 1999), lessening its migration even further. Although we did not identify statistically significant differences in peat metal concentrations between the SRW and the H_2O variants, rainwater apparently promoted sulfide degradation and vertical migration of Zn and Tl (Fig. 4), in line with the peat solution data (Fig. 3). Given the element concentrations in the contaminated bottom peat segments and the uncontaminated peat (control), we can suggest a higher migration potential of Tl relative to Pb. The prediction is in accordance with the enrichments that accounted for ~6–8 for Tl, 1–2 for Pb, and up to ~36 for Zn (Fig. 4). Regarding Fe, again, very limited leaching from the contaminating concentrate is evident, which, if present, could be related to the potential dissolution and/or alteration of FeS_2 (Fig. 4).

As such, all the data in combination with the results for the peat solutions (Fig. 3) favor the anticipated vertical migration of Zn in the experimental pots, i.e., similar to natural peat profiles (Vaněk et al., 2021; Weiss et al., 2007), as well as the more conservative behavior of Pb relative to Tl (Mihaljevič et al., 2006; Shotyk and Krachler, 2004; Shotyk et al., 2017; Smieja-Król et al., 2015). Even though we did not study metal speciation in the peat solutions, Novak and Pacherova (2008) demonstrate that the formation of Zn complexes with mobile fulvic acids (unlike humic substances) could further promote Zn vertical

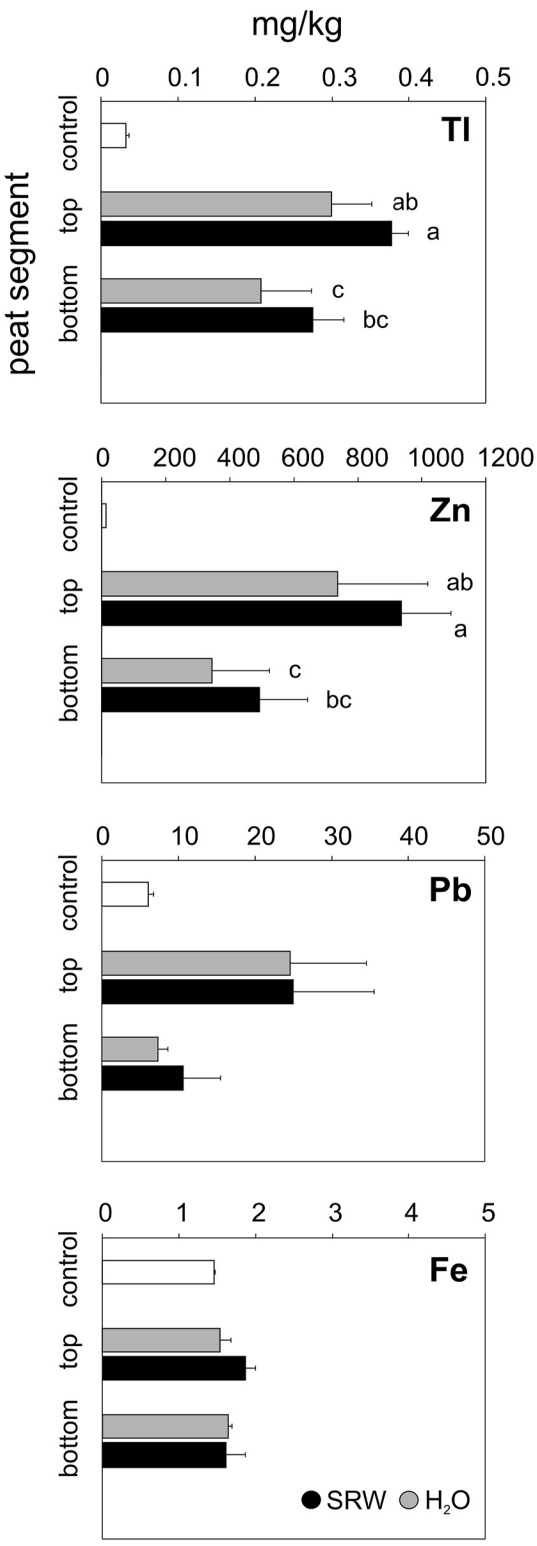

Fig. 4. Total Tl, Zn, Pb and Fe concentrations in individual peat segments (top and bottom) extracted from the experimental pots (n = 5; ±1 SD); synthetic rainwater (SRW), deionized water (H_2O), control – no contamination. Data with the same letter represent statistically identical values according to the one-way ANOVA and the post-hoc Tukey test ($p < 0.05$). Thallium and Zn was tested separately.

migration in the peat column.

3.3. Implications for organic environments

Our data do not indicate any formation of Tl-organic complexes that could potentially affect (reduce) Tl mobility in peat, in line with earlier findings from the organic environments (Jacobson et al., 2005a,b; Martin et al., 2020; Nriagu, 1998). Therefore, our results imply that mobilized Tl was adsorbed more simply in the studied peat, following the non-specific exchange reactions onto the surface of peat organic matter (Vaněk et al., 2021). When viewing Tl concentration trends in both peat solutions and peat material itself, Tl exhibits a higher migration potential compared to Pb (Figs. 3 and 4). This finding is consistent with data reported by e.g. Wojtkowiak et al. (2016) showing increased Tl concentrations in natural groundwaters derived from Tl-rich Miocene organic sediments (Poznan region, Poland). Based on trials with SRW and H_2O, it can be assumed that cyclic changes in the peat pH can result in increased degradation of specific sulfides, mainly ZnS and associated Tl leaching. Shotyk and Krachler (2004) reported that Tl in a peat bog is mostly as stable as Pb, and it tends to exhibit similar pattern(s) to Pb (and Ag) in peat profiles. This type of Pb–Tl geochemical analogy was also recently observed in a contaminated natural peatland at Wolbrom (Vaněk et al., 2021). On the contrary, the present results show that such an assumption does not need to be a rule and can differ during (industrial) acid precipitations, which may promote Tl mobilization in peat. Although, here we report only short-term data on Tl-rich sulfide weathering in a model peat system, apparently all PbS, or newly-formed (secondary) Tl-containing phases (mainly Pb-sulfates) (Table S3) did not act as controls reducing Tl entry into the peat solution/peat. This type of Tl behavior is reported for secondary Fe/Mn-oxide precipitates in various sea sediments, laterites or redoximporhic soils that all showed systematic capture of dissolved Tl(I) by secondary Mn(III,IV)-oxides (e.g. hexagonal birnessite) over its uptake by Fe(III)-oxides (Nielsen et al., 2017; Howarth et al., 2018; Ostrander et al., 2019; Owens et al., 2017; Peacock and Moon, 2012; Rehkämper et al., 2002, 2004; Vaněk et al., 2020; Vejvodová et al., 2020; Wick et al., 2019, 2020). Omitting the ability of Fe-oxides to form in peat sediments as well (Cabala et al., 2013; Smieja-Król et al., 2010, 2015), simultaneous formation of Mn-oxides seems to be unlikely or only scarce, mainly due to very low peat-pH values (~3–4) for most peatlands, resulting in limited stability and precipitation potential of Mn-oxides in general.

4. Conclusions

This study demonstrates chemical and mineralogical data on the weathering of Tl-containing sulfides in a model peat system, to gain detailed insights into: (i) geochemical stability of important carriers (sulfides) of anthropogenic Tl in organic environments, (ii) the formation of secondary Tl-containing phases, which could potentially limit Tl mobilization and associated environmental availability, and (iii) the role of acid rainwater in all Tl mobility, alteration and cycling in acid organic environments. We found that sphalerite (ZnS) was much less stable in the peat environment than other Tl-containing sulfides, namely galena and pyrite. Thus, sphalerite acted as a major primary phase responsible for Tl mobilization. We also identified an incongruent leaching of Tl over Zn throughout the 12-week pot trial, suggesting relatively higher Tl release from ZnS. Furthermore, Tl showed a greater accumulation in the peat solution and the peat that was subjected to acid rain watering, as compared to a deionized H_2O regime. The finding is in line with the fact that we did not observe any formation of secondary Tl-containing phases which could potentially control the Tl flux into the peat. In contrast to previously published results from the peat systems, our model data clearly indicate that Tl is not as conservative as Pb, resulting in a higher mobility and migration potential of Tl in comparison to Pb. In conclusion, we can state that industrial acid precipitations can significantly affect the stability of ZnS even in acidic peat/organic environments, making it susceptible to enhanced weathering and Tl release in the long term.

Author contributions statement

Kateřina Vejvodová;: Analyses, Sampling, **Vaněk Aleš**: Methodology, Data Processing, Data Interpretation, Paper Preparation/Editing, **Marko Spasić**;: Methodology, Sampling, **Martin Mihaljevič**;: Analyses, Paper Preparation/Editing, **Vojtěch Ettler**: Data Interpretation, Paper Preparation/Editing, **Maria Vaňková**;: Data Processing, Paper Editing, **Petr Drahota**: Data Interpretation, Paper Editing, **Leslaw Teper**: Data Interpretation, Paper Editing, **Petra Vokurková**;: Analyses, **Lenka Pavlů**;: Analyses, **Tereza Zádorová**;: Data Processing, **Ondřej Drábek**: Analyses

Declaration of competing interest

The authors declare that they have no known competing financial interests or personal relationships that could have appeared to influence the work reported in this paper.

Acknowledgements

This study was funded by the projects of the Czech Science Foundation (GAČR 20-08717S) and the European Regional Development Fund (CZ.02.1.01/0.0/0.0/16_019/0000845). Charles University authors also received institutional funding from the UNCE/SCI/006 project and the Polish author (Prof. Leslaw Teper) was supported by the University of Silesia (WNP/INoZ/2020-ZB32). Dr. Chris Ash is thanked for English editing of this paper. The anonymous reviewers are thanked for their valuable suggestions/comments which helped to improve the quality of the original manuscript version.

Appendix A. Supplementary data

Supplementary data to this article can be found online at https://doi.org/10.1016/j.chemosphere.2022.134380.

References

Aguilar-Carrillo, J., Herrera, L., Gutiérrez, E.J., Reyes-Domínguez, I.A., 2018. Solid-phase distribution and mobility of thallium in mining-metallurgical residues: environmental hazard implications. Environ. Pollut. 243, 1833–1845. https://doi.org/10.1016/j.envpol.2018.10.014.

Bower, C.A., Reitemeier, R.F., Fireman, M., 1954. Exchangeable cation analysis of saline and alkali soils. Soil Sci 73 (4), 251–262. https://doi.org/10.1097/00010694-195204000-00001.

Cabala, J., Teper, L., 2007. Metalliferous constituents of rhizosphere soils contaminated by Zn-Pb mining in southern Poland. Water Air Soil Pollut. 178, 351–362. https://doi.org/10.1007/s11270-006-9203-1.

Cabala, J., Smieja-Król, B., Jablonska, M., Chróst, L., 2013. Mineral components in a peat deposit: looking for signs of early mining and smelting activities in Silesia-Cracow region (Southern Poland). Environ. Earth Sci. 69, 2559–2568. https://doi.org/10.1007/s12665-012-2080-6.

De Vleeschouwer, F., Fagel, N., Cheburkin, A., Pazdur, A., Sikorski, J., Matielli, N., Renson, V., Fialkiewicz, B., Piotrowska, N., Le Roux, G., 2009. Anthropogenic impacts in North Poland over the last 1300 years - a record of Pb, Zn, Cu, Ni and S in an ombrotrophic peat bog. Sci. Total Environ. 407, 5674–5684. https://doi.org/10.1016/j.scitotenv.2009.07.020.

De Vleeschower, F., Baron, S., Cloy, J.M., Enrico, M., Ettler, V., Fagel, N., Kempter, H., Kylander, M., Li, C., Longman, J., Martinez-Cortizas, A., Marx, S., Mattielli, N., Mighall, T., Nieminen, T.M., Piotrowska, N., Pontevedra-Pombal, X., Pratte, S., Renson, V., Shotyk, W., Shuttleworth, E., Sikorski, J., Stromsoe, N., Talbot, J., von Scheffer, C., Weiss, D., Zaccone, C., Le Roux, G., 2020. Comment on: "A novel approach to peatlands as archives of total cumulative spatial pollution loads fromatmospheric deposition of airborne elements complementary to EMEP data: priority pollutants (Pb, Cd, Hg)" by Ewa Miszczak, Sebastian Stefaniak, Adam Michczyński, Eiliv Steinnes and Irena Twardowska. Sci. Total Environ. 737, 138699. https://doi.org/10.1016/j.scitotenv.2020.138699.

Ettler, V., Vaněk, A., Mihaljevič, M., Bezdička, P., 2005. Contrasting lead speciation in forest and tilled soils heavily polluted by metallurgy. Chemosphere 58, 1449–1459. https://doi.org/10.1016/j.chemosphere.2004.09.084.

Ettler, V., Mihaljevič, M., Šebek, O., Grygar, T.M., Klementová, M., 2012. Experimental in situ transformation of Pb smelter fly ash in acidic soils. Environ. Sci. Technol. 46, 10539–10548. https://doi.org/10.1021/es301474v.

Ettler, V., Petráňová, V., Vítková, M., Mihaljevič, M., Šebek, O., Kříbek, O., 2016. Reactivity of fly ash from copper smelter in an Oxisol: implication for smelter-polluted soil systems in the tropics. J. *Soils Sediments* 16, 115–124. https://doi.org/10.1007/s11368-015-1174-7.

Farmer, J.G., Graham, M.C., Yafa, C., Cloy, J.M., Freeman, A.J., MacKenzie, A.B., 2006. Use of 206Pb/207Pb ratios to investigate the surface integrity of peat cores used to study the recent depositional history and geochemical behaviour of inorganic elements in peat bogs. Global Planet. Change 53, 240–248. https://doi.org/10.1016/j.gloplacha.2006.03.006.

Fiałkiewicz-Kozieł, B., Łokas, E., Gałka, M., Kołaczek, P., De Vleeschouwer, F., Le Roux, G., Smieja-Król, B., 2020. Influence of transboundary transport of trace elements on mountain peat geochemistry (Sudetes, Central Europe). Quat. Sci. Rev. 230, 106162. https://doi.org/10.1016/j.quascirev.2020.106162.

Fiałkiewicz-Kozieł, B., De Vleeschouwer, F., Mattielli, N., Fagel, N., Palowski, B., Pazdur, A., Smieja-Król, B., 2018. Record of Anthropocene pollution sources of lead in disturbed peatlands from Southern Poland. Atmos. Environ 179, 61–68. https://doi.org/10.1016/j.atmosenv.2018.02.002.

Gao, K.Z., Pearce, J., Jones, J., Taylor, C., 1999. Interaction between peat, humic acid and aqueous metal ions. Environ. Geochem. Health 21, 13–26. https://doi.org/10.1023/A:1006592627852.

Garrido, F., Garcia-Guinea, J., Lopez-Arce, P., Voegelin, A., Göttlicher, J., Mangold, S., Almendros, G., 2020. Thallium and co-genetic trace elements in hydrothermal Fe-Mn deposits of Central Spain. Sci. Total Environ. 717, 137162. https://doi.org/10.1016/j.scitotenv.2020.137162.

Gomez-Gonzalez, M.A., Garcia-Guinea, J., Laborda, F., Garrido, F., 2015. Thallium occurrence and partitioning in soils and sediments affected by mining activities in Madrid province (Spain). Sci. Total Environ. 536, 268–278. https://doi.org/10.1016/j.scitotenv.2015.07.033.

Gražulis, S., Daškevič, A., Merkys, A., Chateigner, D., Lutterotti, L., Quirós, M., Serebryanaya, N.R., Moeck, P., Downs, R.T., Le Bail, A., 2012. Crystallography Open Database (COD): an open-access collection of crystal structures and platform for world-wide collaboration. Nucleic Acids Res 40, D420–D427. https://doi.org/10.1093/nar/gkr900.

Grösslová, Z., Vaněk, A., Oborná, V., Mihaljevič, M., Ettler, V., Trubač, J., Drahota, P., Penížek, V., Pavlů, L., Sracek, O., Kříbek, B., Voegelin, A., Gottlicher, J., Drábek, O., Tejnecký, V., Houška, J., Mapani, B., Zádorová, T., 2018. Thallium contamination of desert soil in Namibia: chemical, mineralogical and isotopic insights. Environ. Pollut. 239, 272–280. https://doi.org/10.1016/j.envpol.2018.04.006.

Howarth, S., Prytulak, J., Little, S.H., Hammond, S.J., Widdowson, M., 2018. Thallium concentration and thallium isotope composition of lateritic terrains. Geochem. Cosmochim. Acta 239, 446–462. https://doi.org/10.1016/j.gca.2018.04.017.

Jacobson, A.R., McBride, M.B., Baveye, P., Steenhuis, T.S., 2005a. Environmental factors determining the trace-level sorption of silver and thallium to soils. Sci. Total Environ. 345, 191–205. https://doi.org/10.1016/j.scitotenv.2004.10.027.

Jacobson, A.R., Klitzke, S., McBride, M.B., Baveye, P., Steenhuis, T.S., 2005b. The desorption of silver and thallium from soils in the presence of a chelating resin with thiol functional groups. Water Air Soil Pollut 160, 41–54. https://doi.org/10.1007/s11270-005-3860-3.

Jakubowska, M., Pasieczna, A., Zembrzuski, W., Swit, Z., Lukaszewski, Z., 2007. Thallium in fractions of soil formed on floodplain terraces. Chemosphere 66, 611–618. https://doi.org/10.1016/j.chemosphere.2006.07.098.

Karbowska, B., Zembrzuski, W., Jakubowska, M., Wojtkowiak, T., Pasieczna, A., Lukaszewski, Z., 2014. Translocation and mobility of thallium from zinc–lead ores. J. Geochem. Explor. 143, 127–135. https://doi.org/10.1016/j.gexplo.2014.03.026.

Kersten, M., Xiao, T., Kreissig, K., Brett, A., Coles, B.J., Rehkämper, M., 2014. Tracing anthropogenic thallium in soil using stable isotope compositions. Environ. Sci. Technol. 48 (16), 9030–9036. https://doi.org/10.1021/es501968d.

Kylander, M.E., Weiss, D.J., Martínez Cortízas, A., Spiro, B., Garcia-Sanchez, R., Coles, B. J., 2005. Refining the pre-industrial atmospheric Pb isotope evolution curve in Europe using an 8000 year old peat core from NW Spain. Earth Planet Sci. Lett. 240, 467–485. https://doi.org/10.1016/j.epsl.2005.09.024.

Lis, J., Pasieczna, A., Karbowska, B., Zembrzuski, W., Lukaszewski, Z., 2003. Thallium in soils and stream sediments of a Zn-Pb mining and smelting area. Environ. Sci. Technol. 37, 4569–4572. https://doi.org/10.1021/es0346936.

Liu, J., Wang, J., Chen, Y., Xie, X., Qi, J., Lippold, H., Luo, D., Wang, C., Su, L., He, L., Wu, Q., 2016. Thallium transformation and partitioning during Pb − Zn smelting and environmental implications. Environ. Pollut. 212, 77–89. https://doi.org/10.1016/j.envpol.2016.01.046.

Liu, J., Yin, M., Luo, X., Xiao, T., Wu, Z., Li, N., Wang, J., Zhang, W., Lippold, H., Belshaw, N.S., Feng, Y., Chen, Y., 2019. The mobility of thallium in sediments and source apportionment by lead isotopes. Chemosphere 219, 864–874. https://doi.org/10.1016/j.chemosphere.2018.12.041.

Liu, J., Yin, M., Xiao, T., Zhang, C., Tsang, D.C.W., Bao, Z., Zhou, Y., Chen, Y., Luo, X., Yuan, W., Wang, J., 2020a. Thallium isotopic fractionation in industrial process of pyrite smelting and environmental implications. J. Hazard Mater. 384, 121378. https://doi.org/10.1016/j.jhazmat.2019.121378.

Liu, J., Wei, X., Zhou, Y., Tsang, D.C.W., Bao, Z., Yin, M., Lippold, H., Yuan, W., Wang, J., Feng, Y., Chen, D., 2020b. Thallium contamination, health risk assessment and source apportionment in common vegetables. Sci. Total Environ. 703, 135547. https://doi.org/10.1016/j.scitotenv.2019.135547.

Liu, J., Ouyang, Q., Wang, L., Wang, J., Zhang, Q., Wei, X., Lin, Y., Zhou, Y., Yuan, W., Xiao, T., 2022. Quantification of smelter-derived contributions to thallium contamination in river sediments: novel insights from thallium isotope evidence. J. Hazard Mater. 424, 127594. https://doi.org/10.1016/j.jhazmat.2021.127594.

Lukaszewski, Z., Jakubowska, M., Zembrzuski, W., 2018. The mobility of thallium from bottom soil of the Silesian-Cracowian zinc-lead ore deposit region (Poland). J. Geochem. Explor. 184, 11–16. https://doi.org/10.1016/j.gexplo.2017.10.009.

Martin, L.A., Simonucci, C., Rad, S., Benedetti, M.F., 2020. Effect of natural organic matter on thallium and silver speciation. J. Environ. Sci. 93, 185–192. https://doi.org/10.1016/j.jes.2020.04.001.

Mihaljevič, M., Zuna, M., Ettler, V., Šebek, O., Strnad, L., Goliáš, V., 2006. Lead fluxes, isotopic and concentration profiles in a peat deposit near a lead smelter (Příbram, Czech Republic). Sci. Total Environ. 372, 334–344. https://doi.org/10.1016/j.scitotenv.2006.09.019.

Nielsen, S.G., Rehkämper, M., Prytulak, J., 2017. Investigation and application of thallium isotope fractionation. Rev. Mineral. Geochem. 82, 759–798. https://doi.org/10.2138/rmg.2017.82.18.

Novak, M., Pacherova, P., 2008. Mobility of trace metals in pore waters of two Central European peat bogs. Sci. Total Environ. 394, 331–337. https://doi.org/10.1016/j.scitotenv.2008.01.036.

Novak, M., Erel, Y., Zemanova, L., Bottrell, S.H., Adamova, M., 2008. A comparison of lead pollution record in Sphagnum peat with known historical Pb emission rates in the British Isles and the Czech Republic. Atmos. Environ. 42, 8997–9006. https://doi.org/10.1016/j.atmosenv.2008.09.031.

Nriagu, J.O., 1998. Thallium in the Environment. John Wiley & Sons, Inc., New York, USA.

Ostrander, C.M., Nielsen, S.G., Owens, J.D., Kendall, B., Gordon, G.W., Romaniello, S.J., Anbar, A.D., 2019. Fully oxygenated water columns over continental shelves before the Great Oxidation Event. Nat. Geosci. 12 (3), 186–191. https://doi.org/10.1038/s41561-019-0309-7.

Owens, J.D., Nielsen, S.G., Horner, T.J., Ostrander, C.M., Peterson, L.C., 2017. Thallium-isotopic compositions of euxinic sediments as a proxy for global manganese-oxide burial. Geochem. Cosmochim. Acta 213, 291–307. https://doi.org/10.1016/j.gca.2017.06.041.

Peacock, C.L., Moon, E.M., 2012. Oxidative scavenging of thallium by birnessite: explanation for thallium enrichment and stable isotope fractionation in marine ferromanganese precipitates. Geochem. Cosmochim. Acta 84, 297–313. https://doi.org/10.1016/j.gca.2012.01.036.

Rader, S.T., Maier, R.M., Barton, M.D., Mazdab, F.K., 2019. Uptake and fractionation of thallium by *Brassica juncea* in a geogenic thallium-amended substrate. Environ. Sci. Technol. 53 (5), 2441–2449. https://doi.org/10.1021/acs.est.8b06222.

Rehkämper, M., Frank, M., Hein, J.R., Porcelli, D., Halliday, A., Ingri, J., Liebetrau, V., 2002. Thallium isotope variations in seawater and hydrogenetic, diagenetic, and hydrothermal ferromanganese deposits. Earth Planet Sci. Lett. 197, 65–81. https://doi.org/10.1016/S0012-821X(02)00462-4.

Rehkämper, M., Frank, M., Hein, J.R., Halliday, A., 2004. Cenozoic marine geochemistry of thallium deduced from isotopic studies of ferromanganese crusts and pelagic sediments. Earth Planet Sci. Lett. 219, 77–91. https://doi.org/10.1016/S0012-821X(03)00703-9.

Robson, T.C., Braungardt, C.B., Rieuwerts, J., Worsfold, P., 2014. Cadmium contamination of agricultural soils and crops resulting from sphalerite weathering. Environ. Pollut. 184, 283–289. https://doi.org/10.1016/j.envpol.2013.09.001.

Sato, M., 1992. Persistency-field Eh-pH diagrams for sulfides and their application to supergene oxidation and enrichment of sulfide ore bodies. Geochem. Cosmochim. Acta 56, 3133–3156. https://doi.org/10.1016/0016-7037(92)90294-S.

Shotyk, W., Nesbitt, H.W., Fyfe, W.S., 1992. Natural and anthropogenic enrichments of trace metals in peat profiles. Int. J. Coal Geol. 20, 49–84. https://doi.org/10.1016/0166-5162(92)90004-G.

Shotyk, W., Cheburkin, A.K., Appleby, P.G., Fankhauser, A., Kramers, J.D., 1996. Two thousand years of atmospheric arsenic, antimony, and lead deposition recorded in an ombrotrophic peat bog profile, Jura Mountains, Switzerland. Earth Planet Sci. Lett. 145, E1–E7. https://doi.org/10.1016/S0012-821X(96)00197-5.

Shotyk, W., Weiss, D., Appleby, P.G., Cheburkin, A.K., Frei, R., Gloor, M., Kramers, J.D., Reese, S., Van Der Knaap, W.O., 1998. History of atmospheric lead deposition since 12,370 14C yr BP from a peat bog, Jura Mountains, Switzerland. Science 281, 1635–1640. https://doi.org/10.1126/science.281.5383.1635.

Shotyk, W., Krachler, M., 2004. Atmospheric deposition of silver and thallium since 12 370 ^{14}C years BP recorded by a Swiss peat bog profile, and comparison with lead and cadmium. J. Environ. Monit. 6, 427–433. https://doi.org/10.1039/b315084b.

Shotyk, W., Appleby, P.G., Bicalho, B., Davies, L., Froese, D., Grant-Weaver, I., Krachler, M., Magnan, G., Mullan-Boudreau, G., Noernberg, T., Shannon, B., van Bellen, S., Zaccone, C., 2016a. Peat bogs in northern Alberta, Canada reveal decades of declining atmospheric Pb contamination. Geophys. Res. Lett. 43, 9964–9974. https://doi.org/10.1002/2016GL070952.

Shotyk, W., Rausch, N., Nieminen, T.M., Ukonmaanaho, L., Krachler, M., 2016b. Isotopic Composition of Pb in peat and porewaters from three contrasting ombrotrophic bogs in Finland: evidence of chemical diagenesis in response to acidification. Environ. Sci. Technol. 50, 9943–9951. https://doi.org/10.1021/acs.est.6b01076.

Shotyk, W., Appleby, P.G., Bicalho, B., Davies, L.J., Froese, D., Grant-Weaver, I., Magnan, G., Mullan-Boudreau, G., Noernberg, T., Pelletier, R., Shannon, B., van Bellen, S., Zaccone, C., 2017. Peat bogs document decades of declining atmospheric contamination by trace metals in the Athabasca bituminous sands region. Environ. Sci. Technol. 51, 6237–6249. https://doi.org/10.1021/acs.est.6b04909.

Smieja-Król, B., Fiałkiewicz-Kozieł, B., Palowski, B., 2010. Heavy metal behaviour in peat – a mineralogical perspective. Sci. Total Environ. 408, 5924–5931. https://doi.org/10.1016/j.scitotenv.2010.08.032.

Smieja-Król, B., Bauerek, A., 2015. Controls on trace-element concentrations in the pore waters of two *Sphagnum*-dominated mires in southern Poland that are heavily

polluted by atmospheric deposition. J. Geochem. Explor. 151, 57–65. https://doi.org/10.1016/j.gexplo.2015.01.010.

Smieja-Król, B., Janeczek, J., Bauerek, A., Thorseth, I.H., 2015. The role of authigenic sulfides in immobilization of potentially toxic metals in the Bagno Bory wetland, southern Poland. Environ. Sci. Pollut. Res. 22, 15495–15505. https://doi.org/10.1007/s11356-015-4728-8.

Smieja-Król, B., Fiałkiewicz-Kozieł, B., Michalska, A., Krzykawski, T., Smołka-Danielowska, D., 2019. Deposition of mullite in peatlands of southern Poland: implications for recording large-scale industrial processes. Environ. Pollut. 250, 717–727. https://doi.org/10.1016/j.envpol.2019.04.077.

USEPA, 1994. Synthetic Precipitation Leaching Procedure (SPLP). EPA Method 1312, Washington, USA.

Vaněk, A., Chrastný, V., Teper, L., Cabala, J., Penížek, V., Komárek, M., 2011. Distribution of thallium and accompanying metals in tree rings of Scots pine (*Pinus sylvestris* L.) from a smelter-affected area. J. Geochem. Explor. 108, 73–80. https://doi.org/10.1016/j.gexplo.2010.10.006.

Vaněk, A., Komárek, M., Chrastný, V., Galušková, I., Mihaljevič, M., Šebek, O., Drahota, P., Tejnecký, V., Vokurková, P., 2012. Effect of low-molecular-weight organic acids on the leaching of thallium and accompanying cations from soil – a model rhizosphere solution approach. J. Geochem. Explor. 112, 212–217. https://doi.org/10.1016/j.gexplo.2011.08.010.

Vaněk, A., Chrastný, V., Komárek, M., Penížek, V., Teper, L., Cabala, J., Drábek, O., 2013. Geochemical position of thallium in soils from a smelter-impacted area. J. Geochem. Explor. 124, 176–182. https://doi.org/10.1016/j.gexplo.2012.09.002.

Vaněk, A., Grösslová, Z., Mihaljevič, M., Ettler, V., Chrastný, V., Komárek, M., Tejnecký, V., Drábek, O., Penížek, V., Galušková, I., Vaněčková, B., Pavlů, L., Ash, Christopher, 2015. Thallium contamination of soils/vegetation as affected by sphalerite weathering: a model rhizospheric experiment. J. Hazard Mater. 283, 148–156. https://doi.org/10.1016/j.jhazmat.2014.09.018.

Vaněk, A., Grösslová, Z., Mihaljevič, M., Trubač, J., Ettler, V., Teper, L., Cabala, J., Rohovec, J., Zádorová, T., Penížek, V., Pavlů, L., Holubík, O., Němeček, K., Houška, J., Drábek, O., Ash, C., 2016. Isotopic tracing of thallium contamination in soils affected by emissions from coal-fired power plants. Environ. Sci. Technol. 50 (18), 9864–9871. https://doi.org/10.1021/acs.est.6b01751.

Vaněk, A., Grösslová, Z., Mihaljevič, M., Ettler, V., Trubač, J., Chrastný, V., Penížek, V., Teper, L., Cabala, J., Voegelin, A., Zádorová, T., Oborná, V., Drábek, O., Holubík, O., Houška, J., Pavlů, L., Ash, C., 2018. Thallium isotopes in metallurgical wastes/contaminated soils: a novel tool to trace metal source and behavior. J. Hazard Mater. 343, 78–85. https://doi.org/10.1016/j.jhazmat.2017.09.020.

Vaněk, A., Holubík, O., Oborná, V., Mihaljevič, M., Trubač, J., Ettler, V., Pavlů, L., Vokurková, P., Penížek, V., Zádorová, T., Voegelin, A., 2019. Thallium stable isotope fractionation in white mustard: implications for metal transfers and incorporation in plants. J. Hazard Mater. 369, 521–527. https://doi.org/10.1016/j.jhazmat.2019.02.060.

Vaněk, A., Voegelin, A., Mihaljevič, M., Ettler, V., Trubač, J., Drahota, P., Vaňková, M., Oborná, V., Vejvodová, K., Penížek, V., Pavlů, L., Drábek, O., Vokurková, P., Zádorová, T., Holubík, O., 2020. Thallium stable isotope ratios in naturally Tl-rich soils. Geoderma 364, 114183. https://doi.org/10.1016/j.geoderma.2020.114183.

Vaněk, A., Vejvodová, K., Mihaljevič, M., Ettler, V., Trubač, J., Vaňková, M., Goliáš, V., Teper, L., Sutkowska, K., Vokurková, P., Penížek, V., Zádorová, T., Drábek, O., 2021. Thallium and lead variations in a contaminated peatland: a combined isotopic study from a mining/smelting area. Environ. Pollut. 290, 117973. https://doi.org/10.1016/j.envpol.2021.117973.

Vaněk, A., Vejvodová, K., Mihaljevič, M., Ettler, V., Trubač, J., Vaňková, M., Teper, L., Cabala, J., Sutkowska, K., et al., 2022. Evaluation of thallium isotopic fractionation during the metallurgical processing of sulfides: An update. J. Hazard Mater. 424, Part A, 127325. https://doi.org/10.1016/j.jhazmat.2021.127325.

Vejvodová, K., Vaněk, A., Mihaljevič, M., Ettler, V., Trubač, J., Vaňková, M., Drahota, P., Vokurková, P., Penížek, V., Zádorová, T., Tejnecký, V., Pavlů, L., Drábek, O., 2020. Thallium isotopic fractionation in soil: the key controls. Environ. Pollut. 265, 114822. https://doi.org/10.1016/j.envpol.2020.114822.

Voegelin, A., Pfenninger, N., Petrikis, J., Majzlan, J., Plötze, M., Senn, A.C., Mangold, S., Steininger, R., Göttlicher, J., 2015. Thallium speciation and extractability in a thallium- and arsenic-rich soil developed from mineralized carbonate rock. Environ. Sci. Technol. 49 (9), 5390–5398. https://doi.org/10.1021/acs.est.5b00629.

Wang, J., Wang, L., Wang, Y., Tsang, D.C.W., Yang, X., Beiyuan, J., Yin, M., Xiao, T., Jiang, Y., Lin, W., Zhou, Y., Liu, J., Wang, L., Zhao, M., 2021. Emerging risks of toxic metal(loid)s in soil-vegetables influenced by steel-making activities and isotopic source apportionment. Environ. Int. 146, 106207. https://doi.org/10.1016/j.envint.2020.106207.

Weiss, D., Shotyk, W., Appleby, P.G., Kramers, J.D., Cheburkin, A.K., 1999. Atmospheric Pb deposition since the Industrial Revolution recorded by five Swiss peat profiles; enrichment factors, fluxes, isotopic composition, and sources. Environ. Sci. Technol. 33, 1340–1352. https://doi.org/10.1021/es980882q.

Weiss, D., Shotyk, W., Boyle, E.A., Kramers, J.D., Appleby, P.G., Cheburkin, A.K., 2002. Comparative study of the temporal evolution of atmospheric lead deposition in Scotland and eastern Canada using blanket peat bogs. Sci. Total Environ. 292, 7–18. https://doi.org/10.1016/s0048-9697(02)00025-6.

Weiss, D.J., Rausch, N., Mason, T.F.D., Coles, B.J., Wilkinson, J.J., Ukonmaanaho, L., Arnold, T., Nieminen, T.M., 2007. Atmospheric deposition and isotope biogeochemistry of zinc in ombrotrophic peat. Geochem. Cosmochim. Acta 71, 3498–3517. https://doi.org/10.1016/j.gca.2007.04.026.

Wick, S., Peña, J., Voegelin, A., 2019. Thallium sorption onto manganese oxides. Environ. Sci. Technol. *53* (22), 13168–13178. https://doi.org/10.1021/acs.est.9b04454.

Wick, S., Baeyens, B., Fernandes, M.M., Göttlicher, J., Fischer, M., Pfenninger, N., Plötze, M., Voegelin, A., 2020. Thallium sorption and speciation in soils: role of micaceous clay minerals and manganese oxides. Geochem. Cosmochim. Acta 288, 83–100. https://doi.org/10.1016/j.gca.2020.07.037.

Wojtkowiak, T., Karbowska, B., Zemrzuski, W., Siepak, M., Lukaszewski, Z., 2016. Miocene colored waters: a new significant source of thallium in the environment. J. Geochem. Explor. 161, 42–48. https://doi.org/10.1016/j.gexplo.2015.09.014.

Xiao, T., Guha, J., Boyle, D., Liu, C.Q., Chen, J., 2004a. Environmental concerns related to high thallium levels in soils and thallium uptake by plants in southwest Guizhou, China. Sci. Total Environ. 318, 223–244. https://doi.org/10.1016/S0048-9697(03)00448-0.

Xiao, T., Guha, J., Boyle, D., Liu, C.Q., Zheng, B., Wilson, G.C., Rouleau, A., Chen, J., 2004b. Naturally occurring thallium: a hidden geoenvironmental health hazard? Environ. Int. 30, 501–507. https://doi.org/10.1016/j.envint.2003.10.004.

Xiao, T., Yang, F., Li, S., Zheng, B., Ning, Z., 2012. Thallium pollution in China: a geo-environmental perspective. Sci. Total Environ. 421–422, 51–58. https://doi.org/10.1016/j.scitotenv.2011.04.008.

Zhou, Y., He, H., Wang, J., Liu, J., Lippold, H., Bao, Z., Wang, L., Lin, Y., Fang, F., Huang, Y., Jiang, Y., Xiao, T., Yuan, W., Wei, X., Tsang, D.C.W., 2022. Stable isotope fractionation of thallium as novel evidence for its geochemical transfer during lead-zinc smelting activities. Sci. Total Environ. 803, 150036. https://doi.org/10.1016/j.scitotenv.2021.150036.

Zuna, M., Mihaljevič, M., Šebek, O., Ettler, V., Handley, M., Navrátil, T., Goliáš, V., 2011. Recent lead deposition trends in the Czech Republic as recorded by peat bogs and tree rings. Atmos. Environ. 45, 4950–4958. https://doi.org/10.1016/j.atmosenv.2011.06.007.

Zuna, M., Ettler, V., Šebek, O., Mihaljevič, M., 2012. Mercury accumulation in peatbogs at Czech sites with contrasting pollution histories. Sci. Total Environ. 424, 322–330. https://doi.org/10.1016/j.scitotenv.2012.02.049.

7.5. Understanding stable Tl isotopes in industrial processes and the environment: A review

Vejvodová, K., Vaněk, A., Drábek, O., Spasić, M. (2022). Understanding stable Tl isotopes in industrial processes and the environment: A review. Journal of Environmental Management, 315, 115151.

Journal of Environmental Management 315 (2022) 115151

Contents lists available at ScienceDirect

Journal of Environmental Management

journal homepage: www.elsevier.com/locate/jenvman

Review

Understanding stable Tl isotopes in industrial processes and the environment: A review

Kateřina Vejvodová *, Aleš Vaněk, Ondřej Drábek, Marko Spasić

Department of Soil Science and Soil Protection, Faculty of Agrobiology, Food and Natural Resources, Czech University of Life Sciences Prague, Kamýcká 129, 165 00, Praha 6, Czech Republic

ARTICLE INFO

Keywords:
Industrial waste
Soil
Isotopic fractionation
Mn-oxides
Hyperaccumulator

ABSTRACT

In this review, a compilation of the current knowledge on stable thallium (Tl) isotopes (^{205}Tl and ^{203}Tl) in specific industrial processes, soils and plants is presented. An overview of the processes that may control Tl concentration and Tl isotope fractionation is compiled, while also overviewing the ability of Tl isotopic ratios to be used as a 'fingerprint' in source apportionment. Thallium isotopic compositions not only depend on their origin, but also on soil processes that may occur over time. One of the most important phases affecting the fractionation of stable Tl isotopes in soils (or sediments) was systematically identified to be specific Mn(III,IV)-oxides (mainly birnessite), due to their potential ability of oxidative Tl sorption, i.e., indicative of redox Tl reactions to be critical controlling factor. It has been established that the Brassica family is a hyperaccumulator of Tl, with clear demonstrations of Tl isotopic fractionation occurring up the translocation pathway. A clear pattern, so far, was observed with Tl isotopic compositions in plants grown on soils that were contaminated and those grown on uncontaminated soils, indicating the importance of the growing medium on Tl uptake, translocation, and isotopic fractionation.

1. Introduction

1.1. Thallium in the environment

While there is some understanding about the chemistry and the toxicity of thallium (Tl), there are still gaps in the geochemistry of the element and very limited information about Tl isotopes and isotopic fractionation in plants.

It is naturally found in the environment with a mean Tl concentration in the Earth's crust ranging between 0.1 and 1.7 mg/kg. It is mostly associated with Tl-bearing sulphides (pyrite (FeS_2), galena (PbS), sphalerite (ZnS), chalcopyrite ($CuFeS_2$), realgar (As_4S_4)), Mn-oxides and silicates (biotite ($K(Mg,Fe)_3AlSi_3O_{10}(OH)_2$), muscovite ($KAl_2(AlSi_3O_{10})(OH)_2$), K-feldspar ($KAlSi_3O_8$)) Fe-(hydr)oxide (hematite (Fe_2O_3) and goethite (α-$Fe^{3+}O(OH)$), illite ($K_{0.65}Al_{2.0}$ $[Al_{0.65}Si_{3.35}O_{10}](OH)_2$) and jarosite $KFe^{3+}_3(SO_4)_2(OH)_6$) (Nriagu, 1998; Kaplan and Mattigod, 1998; Lis et al., 2003; Peter and Viraraghavan, 2005; Karbowska, 2016; Garrido et al., 2020; Aguilar-Carrillo et al., 2020; Lin et al., 2020; Đorđević et al., 2021; Zhuang et al., 2021; Migaszewski and Gałuszka, 2021). Furthermore, Tl may be incorporated into the structure of minerals via redox reactions, sorption or substitution of cations. Thallium can be found in hutchinsonite ($PbTlAs_5S_9$), lorandite ($TlAsS_2$), urbanite ($TlAs_2SbS_5$) and crookesite ($(Cu,Tl,Ag)_2Se$), avicennite (Tl_2O_3), jarosite ($KFe^{3+}_3(SO_4)_2(OH)_6$), pharmacosiderite (secondary mineral that occurs in the oxidized zones of Fe-bearing sulphide/hydrothermal deposits and the newly discovered thalliomelane ($Tl(Mn^{4+}_{7.5}Cu^{2+}_{0.5})O_{16}$) (Nriagu, 1998; Herrmann et al., 2018; Aguilar-Carrillo et al., 2020; Đorđević et al., 2021; Gołębiowska et al., 2021).

Thallium has two oxidation states, monovalent and trivalent, with monovalent Tl predominating in most environments (Rader et al., 2018). In certain instances, such as highly oxidising conditions, the formation of trivalent Tl can arise (Peter and Viraraghavan, 2005; Belzile and Chen, 2017; Migaszewski and Gałuszka, 2021). Thallium can exhibit both lithophile and chalcophile natures, which controls its presence and ability to sorb efficiently to K-feldspar, illite, and Mn-oxides. Monovalent Tl can be substituted for elements such as K and Rb in silicates (Rader et al., 2018).

There are several mechanisms that are responsible for Tl sorption onto micaceous clay minerals (e.g. illite) and Mn-oxides (Mn(III,IV)-oxides, birnessite, todorokite). Illite has been noted on multiple

* Corresponding author.
E-mail address: vejvodova@af.czu.cz (K. Vejvodová).

https://doi.org/10.1016/j.jenvman.2022.115151
Received 6 January 2022; Received in revised form 28 March 2022; Accepted 21 April 2022
Available online 29 April 2022

occasions as a great scavenger of Tl in soils, brought about mainly by the similarity of Tl^+ to K^+, immobilizing Tl via interlayer fixation and surface complexation (e.g. cation exchange reactions) (Voegelin et al., 2015; Zhuang et al., 2021). Thallium has been extensively proven to have an analogy to K due to similar ionic radii of the elements (1.59 Å for Tl and 1.51 Å for K), which can lead to inter-layer Tl–K replacements (Shannon, 1976; Heinrichs et al., 1980; Vaněk et al., 2011; Voegelin et al., 2015; Antić-Mladenović et al., 2017; Wick et al., 2018). It was shown that cation selectivity coefficients proved that illite was able to strongly adsorb Tl^+, due to the affinity Tl has with Cs and Rb (Martin et al., 2018). It was shown that micaceous clay minerals could control the short-term solubility of Tl via cation exchange, however in the longer run the geogenic Tl is held via structural fixation. As mentioned before, the competition of K^+ adsorption onto edges of the clay minerals affects Tl mobility. The adsorption of Tl onto the frayed edges of illite displayed Tl^+ was found to be highly dependent on the adsorption competition with K^+ and NH_4^+, where both cations are able to decrease the adsorption of Tl^+ onto illite, while the opposite was observed for Na^+ and Ca^{2+} (Wick et al., 2018). Increase in dissolved K^+ concentrations in soil water may lead to the release of Tl into the solution (Wick et al., 2020).

The adsorption of Tl to Mn-oxides (e.g. non-/poorly-crystalline Mn (III,IV)-oxides, birnessite) has also been proved, with results proving that Tl has a greater affinity to Mn-oxides, with little affinity towards Fe oxides (Vaněk et al., 2009; Cruz-Hernández et al., 2019; Wick et al., 2020; Zhuang et al., 2021). There are three mechanisms of Tl uptake by Mn-oxides. The first one is the oxidation of Tl(I) and the complexation of Tl(III) by birnessite. The second is the sorption of hydrated Tl(I) by triclinic birnessite or todorokite, and lastly, the incorporation of dehydrated Tl^+ into the structures, of for example, cryptomelane (potassium manganese oxide ($K(Mn_7^{4+}Mn^{2+})O_{16}$)) (Peacock and Moon, 2012; Wick et al., 2019; Cruz-Hernández et al., 2019; Aguilar-Carrillo et al., 2020; Zhuang et al., 2021). Cruz-Hernández et al. (2019) observed that the sorption/oxidation of Tl to birnessite increased with increasing pH, it was also independent of the particle size or vacancy, indicating that the negative electrostatic charge has an important role in the reactions. In a study by Aguilar-Carrillo et al. (2020), birnessite was shown to favourably uptake Tl(I) via irreversible surface adsorption mechanism. The study also investigated the behaviour between jarosite and Tl(I). The results show that Tl incorporation into the jarosite structure occurs via the substitution of K in the A site of the formula $AB_3(TO_4)_2(OH)_6$ (where A, B and T sites allow for the incorporation/substitution of anions or cations). In the structure of the jarosite, there is an expansion of the FeO_6 octahedra, caused by the incorporation of Tl (due to the ionic radius of Tl^+). Once Tl is incorporated in the jarosite structure it forms Tl (I)-jarosite which, under the presence of high Tl concentrations, can in turn form the mineral dorallcharite ($TlFe_3(SO_4)_2(OH)_6$). In the results observed by Garrido et al. (2020) the X-ray adsorption near edge structure (XANES) results show that Tl(I) is bound to jarosite-type minerals, while Herrmann et al. (2018) discovered up to 10% of Tl(I) for K substitution in jarosite. However, from the two (birnessite and jarosite), birnessite has been stated to be more effective in Tl(I) immobilization. Birnessite has also shown to sorb Tl(III), where it forms an inner-spere complex on the surface of birnessite, verifying the efficiency of Mn-oxides in adsorbing Tl (Peacock and Moon, 2012; Wick et al., 2020; Aguilar-Carrillo et al., 2020; Zhuang et al., 2021).

The sources of Tl, like many other trace elements, can be lithogenic and anthropogenic, with the latter being the dominant source of Tl in the environment, with concentrations found to reach up to thousands of mg/kg (Xiao et al., 2004; Cabala and Teper, 2007; Bačeva et al., 2014; Wei et al., 2020). Sulphide ore mining and ferrous and non-ferrous smelting, coal combustion and cement production all potentially represent important anthropogenic sources of Tl in the environment (Peter and Viraraghavan, 2005; Karbowska et al., 2018). In soils, Tl from geogenic origins can be found to be associated with aluminosilicates and crystallized mineral fractions (Gomez-Gonzalez et al., 2015; Vaněk et al., 2015) while Tl from anthropogenic origins is usually associated with more labile fractions (exchangeable Tl) (Al-Najar et al., 2005; Yang et al., 2005; Lin et al., 2020).

1.2. Stable thallium isotopes

There are two stable Tl isotopes, with atomic masses of 203 and 205 (in abundance of ~30% and 70%, respectively) and varying Tl isotope ratios in the environment, which can be shown in Table 1 and Fig. 1 (Nielsen and Rehkämper, 2012; Nielsen et al., 2017). Thallium isotopes were first successfully measured by Rehkämper and Halliday (1999) using multiple collector inductively coupled plasma mass spectrometry (MC-ICP-MS). They developed a new chemical and mass spectrometric procedure that allowed for the determination of Tl isotopic elements in environmental samples, as the precision of Tl isotopic measurements by thermal ionization mass spectrometry (TIMS) was limited by Tl having only two stable and naturally occurring isotopes. The new high-precision MC-ICP-MS is capable of recognizing small variations in stable isotope compositions of Tl in various environmental samples. The Tl isotopic ratio ($^{205}Tl/^{203}Tl$) in the studied sample is determined relative to the reference material NIST SRM 997 (National Institute of Standards and Technology) ($\epsilon^{205}Tl = 0$). Heavy Tl isotopes refer to ^{205}Tl, while ^{203}Tl is a light isotope. Regarding Tl isotopes, some isotopic fractions can be heavier than the other is, and depends on the proportion and abundance of ^{205}Tl in one sample compared to that of another. External normalization/standard sample bracketing (NIST SRM 997) is employed to eliminate the mass bias drift. The $^{208}Pb/^{206}Pb$ ratio is commonly used for internal correction of the raw $^{205}Tl/^{203}Tl$ ratio. The isotope composition is then calculated using the following equation:

$$\epsilon^{205}Tl = 10^4 \times (^{205}Tl/\,^{203}Tl_{sample} - {}^{205}Tl/\,^{203}Tl_{NIST997})/\,(^{205}Tl/\,^{203}Tl_{NIST997})$$

The annotation used to describe Tl isotope ratios is ϵ-notation (variations in parts per 10,000) due to the Tl isotopic system being first developed as a cosmochemical radiogenic isotope system (Nielsen and Rehkämper, 2012; Nielsen et al., 2017). The ϵ-notation also proves useful with regards to the variability of stable Tl isotope ratios, as data are presented usually as whole figures with only one decimal point. The ϵ-notation also allows for the comparison between terrestrial and cosmochemical data. However, for the correct and precise measurement of Tl isotope ratios, the sample matrix must undergo separation to isolate Tl and remove any Pb in the sample (which interferes with results). The fundamentals of Tl separation are as described by Rehkämper and Halliday (1999), however, several modifications have been made throughout the years by Nielsen et al. (2004, 2007) and Baker et al. (2009). The separation processes for separating Tl from the sample matrix is dependent on trivalent Tl in acidic conditions to produce anionic complexes with halogens (Cl^- or Br^-) which are able to partition to anion exchange resins. Whereas for monovalent Tl, this does not apply, as it does not form anionic complexes, thus, samples must be prepared in oxidising conditions by adding water saturated in Br_2 to the digested samples, in order to make sure that all the present Tl is in the trivalent state. The sample is then washed with different acids until Br_2 is no longer present. The last step of the separation involves the removal of Tl from the resin using reducing agents (0.1 M HCl with dissolved SO_2 gas) (Nielsen et al., 2004, 2007; Baker et al., 2009; Nielsen and Rehkämper, 2012).

Ever since the development of the MC-ICP-MS, multiple studies have been conducted to measure Tl isotopic ratios in varying environments. Creating an isotope-based source identification, allowing to distinguish the source of an element into the studied environment with the use of mixing models, especially in scenarios with more than one source. However, such mixing models cannot be used to provide data on the precise contributions of multiple anthropogenic sources, as sometimes more sources or processes can blur the source signals, making it harder to identify the exact source input. While many other isotopes were

Table 1
Tl isotopic compositions in industrial materials, soils, rocks and plants.

Material	ϵ^{205}Tl	Country	Source
Loess	−2.3 to −1.8		Nielsen et al. (2005)
Continental crust	−2		
Calcareous and siliceous clays	−1 to +7		Rehkämper et al. (2004)
Ocean crust alteration	−2 to −14		Rehkämper et al. (2004); Nielsen et al. (2006c)
Black-smoker fluids	−2.5 to −1.1		Nielsen et al. (2006c)
Altered ocean crust	−1 to −16		
Meteorites	−20 to +30		Nielsen et al. (2006a)
Cement kiln dust	−0.2	Lengerich, Germany	Kersten et al. (2014)
Meggen pyrite	−0.4		
Soil profile	−0.9 to −4.2		
Green cabbage	−2.5 to −5.4	Lanmuchang, China	
Arable soil	+0.5		
Raw pyrite ore	+1.3	Guangdong	Liu et al. (2020a)
Fluidized-bed furnace slag	+16.2	Province, China	
Boiler fly ash	+8.3		
Cyclone fly ash	+2.2		
Electrostatic precipitation fly ash	−1.1		
Amphibole (magmatic stage 1)	−2.1 to −2.9	Ilimaussaq complex, Greenland	Hettmann et al. (2014)
Amphibole (magmatic stage 2)	−2.6 to −2.9		
Amphibole (magmatic stage 3)	−3.7 to +5.8		
Astrophyllite (late magmatic)	+1.0 to +1.8		
Unweathered greywacke (India)	−2.3	India	Howarth et al. (2018)
Lighter greywacke (India)	−1.3		
Soft weathered greywacke (india)	−2.4		
Weathered greywacke (india)	−2.1		
Red weathered greywacke (india)	−1.9		
Base of laterite	−1.1		
Nodular laterite base	−0.5		
Nodular laterite	+0.3		
Semi-indurated laterite	−1.2		
Massive laterite	+3.5		
Indurated laterite cap	−1.0		
Basaltic saprolite	+6.2		
Sandstone	−4.2	Bingham Canyon	Fitzpayne et al. (2018)
Silicified limestone	−2.9		
Latite porphyry	−8.8 to −2.9		
Silicified limestone breccia	+1.3		
Quartzite	−3.4 to +0.9		
Lamprophyre	−3.6		
Monzonite	−1.3		
Recrystallised calcareous sandstone	−3.3		
Silicified limestone	+0.2		
Quartzite breccia	−2.3 to +7.2		
Veined limestone	−6.5	Narneys Canyon/	Fitzpayne et al.
Quartzite breccia	−16.4 to +6.0	Melco	(2018)
Quartzite	−3.1		

Table 1 (*continued*)

Material	ϵ^{205}Tl	Country	Source
Dolomitic nodule	0.0		
Andesite	−5.1 to −1.0	Collahuasu Formation, northern	Baker et al. (2010)
Dacite	−3.5 to +0.1	Chile	
Rhyolite	−3.4 to −1.3		
Altered oceanic crust composites	0.0 to −4.4		Prytulak et al. (2013)
Amazonite	−0.1 to +3.5		Rader et al. (2018)
Feldspar	−5.1 to +9.4		
Chalcopyrite	−1.0 to +17.8		
Chlorite	−6.2		
Muscovite	+3.8 to +5.3		
Biotite	−7.1 to +0.4		
Phlogopite	−12.1 to +18.0		
Galena	+4.4		
Orthoclase	−4.4 to +4.4		
Covellite	+4.4		
Jarosite	+2.9		
Microcline	−1.6		
Sanidine	+3.0		
Hyalophane	−4.3		
Baumhauerite	+2.0		
Hutchinsonite	−1.0		
Parapierrotite	+1.6		
Cryptomelane/ hollandite	+11.4		
Hendricksite	−1.9		
Soil	−0.4 to +3.8	Rosh Pinah, Namibia	Grösslová et al., 2018
Flotation tailing	+6.1 to +6.3		
Flotation tailing (<0.05 mm)	+3.6		
Flotation tailing (0.05–0.25 mm)	+14.6		
Flotation tailing (>0.25 mm)	+4.8		
Bottom ash	0.0	'Black triangle'	Vaněk et al. (2016)
Fly ash	−2.5 to −2.8	Czechia	
Coal pyrite	−5.5		
Volatile Tl fractions	−6.2 to −10.3		
Forest soils	−3.9 to +0.4	Olkusz district, Poland	Vaněk et al. (2018)
Meadow soils	−1.9 to −2.7		
Zn ore	−3.8		
Post-flotation Zn–Fe residue	−3.9		
Fly ash	−4.1		
Slag	−3.3		
Granulated waste	−3.6		
Final refinement waste	−4.8		
Sinapis alba L. root	−2.8 to −10.6		Vaněk et al. (2019)
Sinapis alba L. stem	−1.8 to −4.2		
Sinapis alba L. leaf	−2.5 to −4.9		
Sinapis alba L. shoot	−3.0 to −3.8		
Meadow soils	+1.6 to +8.7	Erzmatt, Switzerland	Vaněk et al. (2020)
Forest soils	+0.8 to +8.7		

(*continued on next page*)

Table 1 (*continued*)

Material	ϵ^{205}Tl	Country	Source
Brassica juncea L. stem	+2 to +5		Rader et al. (2019)
Brassica juncea L. leaves	0 to +1		
Brassica juncea L. seed pods	0 to −5		
Brassica juncea L. flowers and flower stems	−0.9 to −5		
Soils	+0.02 to +4.0	Kluky, Czech Republic	Vejvodová et al. (2020)
Mn-oxide nodules	+14.4		
K-feldspar	+1.4		
Soil clay	+4.6		
Peat	−1.1 to −3.6	Wolbrom, Poland	Vaněk et al. (2021)
Clayey sand	−1.5		
Chalk rock	+0.5		
Metallurgical waste	−3.1 to −3.6	Poland	Vaněk et al. (2022)
Post flotation waste	−3.9		
Zn-rich sulfides	−4.4 to −3.4		
Acidic wastes	−4.6	Guangdong Province, China	Liu et al. (2022)
Smelter clinkers	1.1		
Sediments	−3.8 to 1.0		
Raw material	−0.9	Guangdong Province, China	Zhou et al. (2022)
Return fines (sinter)	−1.0		
Electrostatic precipitator dust	−2.0		
Lime neutralizing slag	−2.4		
Acid sludge	−4.6		
clinker	1.1		

widely studied, the isotopes of Tl were studied to a lesser degree. With the more precise MC-ICP-MS, the ability to determine Tl isotopes and their ratios in varying environments (ranging from marine environments, arc lava genesis, soil, plants and many industrial wastes) were proved successful (Nielsen et al., 2004, 2005, 2006a, 2006b, 2006c, 2007, 2009, 2017; Rehkämper and Nielsen et al., 2004; Prytulak et al., 2013; Kersten et al., 2014; Vaněk et al., 2016, 2018, 2019, 2020; Vejvodová et al., 2020). This allows for a better understanding of Tl behaviour and fractionation in different environments, providing useful insight as to the origins of Tl and the processes that control its concentration and availability (Kersten et al., 2014; Wang et al., 2021).

Regarding Tl isotopic fractionation in the environment, there are several types of fractionations that determine the fate of Tl isotopes. Equilibrium and kinetically driven processes control mass-dependent isotopic fractionations of Tl isotopes (Wiederhold, 2015). Thallium isotopic fractionation via the nuclear field shift effect (effect related to mass independent fractionation), was found to be <0.1% in T(I)–Tl(III) redox systems and ligand exchange systems of Tl(III) (Wiederhold, 2015). Redox conditions and bonding environment play a significant role and controls Tl isotopic fractionation. In oxidising environments, Tl (I) oxidises to Tl(III), which leads to the enrichment of heavy ^{205}Tl in Mn-oxides (especially birnessite) and ferromanganese nodules and crusts, however Fe(III) oxides probably do not significantly sorb Tl or even isotopically redistribute it (Peacock and Moon, 2012). Higher ϵ^{205}Tl values observed by Rader et al. (2018) in sulphides indicate that the presence of covalent bonds and high oxidation states could favour ^{205}Tl.

Environmental processes believed to cause variations in the isotopic ratios between environmental samples are evaporation/condensation, redox processes, dissolution/precipitation, adsorption/desorption, and biological cycling (Wiederhold, 2015; Vaněk et al., 2016; Liu et al., 2020a). Regarding soils and plants, Kersten et al. (2014) conducted the first study involving the use of Tl isotopes to provide useful insights into the origins (anthropogenic/geogenic) of Tl into soils and plants. The study provided a supply of information into a whole new field of studies along with several questions, which lead to further research conducted, in order to understand the processes that control Tl isotopic fractionation. This was followed by multiple other papers being published on the same or similar topic (with isotopic compositions of industrial wastes, soils and plants compiled in Table .1 and Fig. 1) (e.g. Grösslová et al., 2018; Rader et al., 2018, 2019; Vaněk et al., 2016, 2018, 2019, 2020, 2021; Vejvodová et al., 2020; Liu et al., 2020a, 2022; Wang et al., 2021; Zhou et al., 2022).

This paper compiles the information currently available about Tl isotopic compositions throughout the industrial processes, and in soils and plants. The review provides an overview of the processes that control isotopic fractionation and the use of Tl stable isotopes as a source or geochemical indicator (proxy).

2. Thallium and Tl isotopes in industrial processes

High temperature processes can potentially volatilize Tl, therefore, processes associated with coal combustion, cement production and mining and smelting operations are important sources of environmental Tl contamination. An estimate of 2000–5000 tons of Tl per year is mobilized, with approximately 1000 tons deriving from coal combustion (Galván-Arzate and Santamaria, 1998; Kazantzis, 2000; Peter and Viraraghavan, 2005; Antón et al., 2012; Xiao et al., 2012; Kersten et al., 2014; Vaněk et al., 2016). This is due to the high concentrations found in certain sulphides, such as pyrite and sphalerite. During pyrite roasting, the temperatures in the fluidized furnace ranges around 850 °C which does not lead to significant volatilization of Tl, as the boiling point of Tl_2O is 1080 °C. Therefore, Tl is still present in the roasting calcines that are then used in the raw mix of cement production. In the cement production, the Tl is volatilized and circulated through dust that enters the gas-suspension preheaters that heats the raw mix. During the circulation, Tl compounds are evaporated to form volatile Tl(I) chloride (TlCl boiling temperature is 806 °C) (Kersten et al., 2014).

In Zn ore processing, Tl must be eliminated from the Zn circuit. The use of the jarosite process has become widely used to eliminate Tl in Zn circuits, as jarosite is a scavenger for Tl (Dutrizac, 1997). The process involves the formation of jarosite precipitate that removes and stabilizes Tl in Zn operations by the substitution of alkali metals for Tl^+, therefore preventing the further contamination of Tl in Zn processing (Dutrizac, 1997; Aguilar-Carrillo et al., 2020). High Tl concentrations in electrostatic dusts and acidic waste compared to Pb–Zn ore materials were observed, suggesting that the ore roasting (at temperatures of 1000–1200 °C) could play a significant role in the transformation and mobilization of Tl. As volatilization of Tl occurs, because of alteration and decomposition of the minerals (e.g. pyrite, sphalerite, galena), it leads to the release of Tl and its condensation on the surface of fine particles of the waste materials (Liu et al., 2016).

Large differences in Tl concentrations were found in industrial waste samples with slags containing 1 mg/kg and final refinement wastes containing 568 mg/kg of Tl. Regarding the isotope signatures, fly ash was found to be isotopically lighter with ε^{205}Tl −4.1 compared to the slag (ε^{205}Tl −3.3), however there were no significant differences between the two materials (Vaněk et al., 2018). Interestingly, the results were similar to a previous study by Vaněk et al. (2016) where the fly ash (ε^{205}Tl between −2.50 and −2.8) was also found to be isotopically lighter compared to the bottom ash (ε^{205}Tl ~0), however in the previous study there was a significant difference between the materials. This was brought about by the high evaporation of Tl from the pyrite that was exposed to oxidising conditions, whereas, in this case the Tl freely entered the smelter emissions. When fly ash and bottom ash from a coal-fired power plant were analysed by Vaněk et al. (2016), the presence of isotopically lighter Tl (ε^{205}Tl ~ −2.5 to −2.8) was found in the fly ash and heavier Tl (ε^{205}Tl ~ 0.0) in the bottom ash. The differences in the Tl isotopic compositions of the waste materials from the coal-fired power plant were significant and could have been the result of Tl

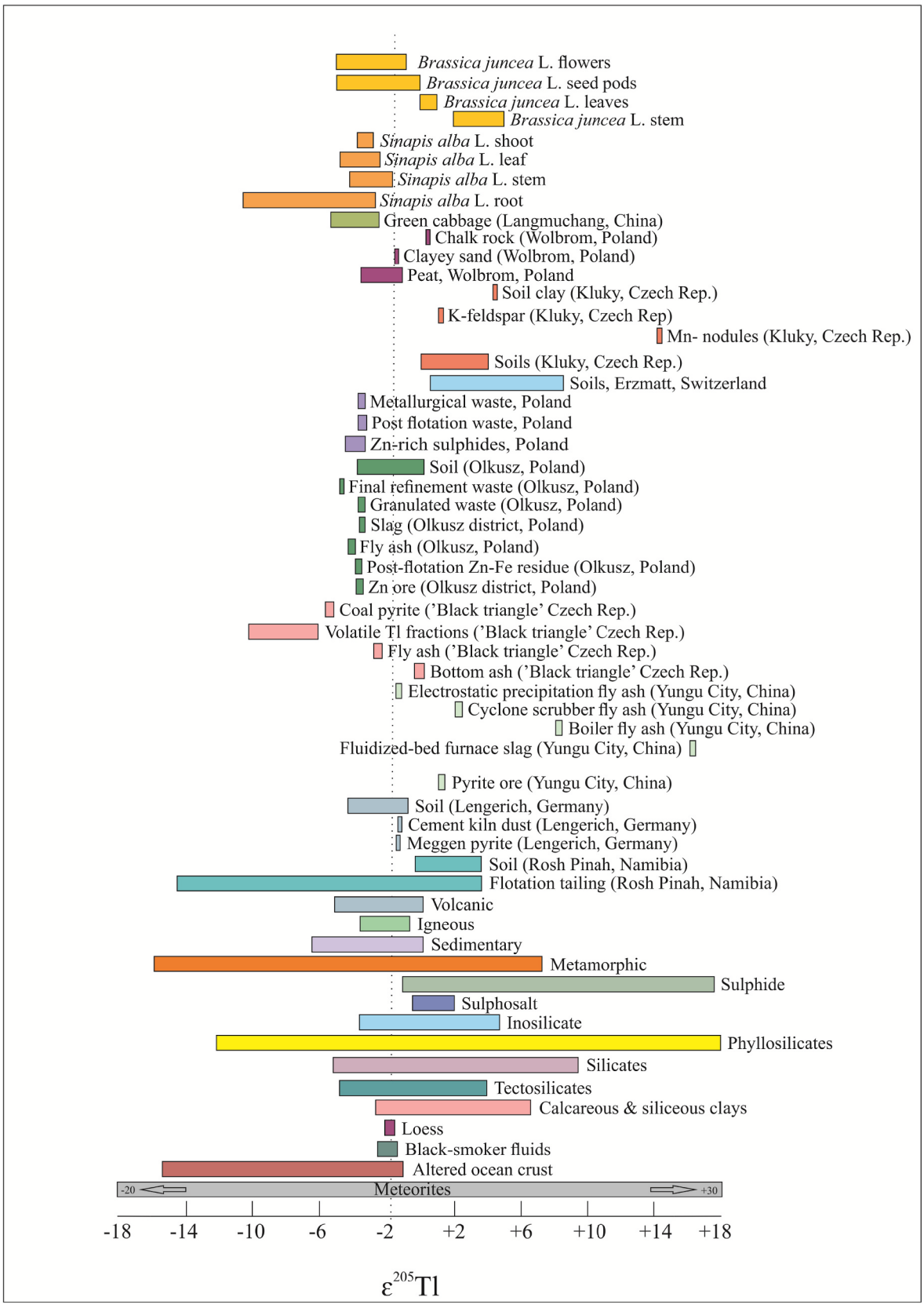

Fig. 1. Thallium isotope variations in different reservoirs. The dashed line $\varepsilon^{205}Tl = -2$ depicts the Tl isotopic composition of the Earth's mantle. Adapted from Kersten et al. (2014); references therein can be found in Table 1.

evaporation from the Tl-rich pyrite under high temperatures which could volatilize the Tl present in the samples. Also, as mentioned before, sulphides may accumulate Tl, therefore any pyrite in the feed coal and the high processing temperatures could have an influence over the lighter fractions of Tl emissions. The results also show that the process seems to mostly be driven by kinetic isotope fractionation (Vaněk et al., 2016). In the study by Vaněk et al. (2016), they also conducted a model thermo-desorption experiment with sulphide that showed great volatilization of Tl that had a mean of ε^{205}Tl −6.4, which is similar to the model pyrite evaporates. At 700 °C there was 1% of volatile Tl fraction (ε^{205}Tl −6.2), at 900 °C there was 4% of volatile Tl fraction (ε^{205}Tl −10.3), and at 300–900 °C there was 78% of Tl condensate (ε^{205}Tl −6.2).

Substantial variations and Tl isotopic fractionation between pyrite ore (ε^{205}Tl ~ +1.3) and waste materials (ε^{205}Tl ~ −1.1 to +16.2) were noted during pyrite smelting in sulphuric acid production (Liu et al., 2020a). The processing led to smaller grain sizes of waste materials, with elevated concentrations of Tl and enrichments of isotopically lighter (compared to the furnace slag) Tl (ε^{205}Tl −1.1 to +8.3) that was contradictory to the heavy isotopes found in the furnace slag (ε^{205}Tl ~ +16.2). The study predicts that Tl isotope fractionation is controlled by Rayleigh-type fractionation and adsorption of volatilized Tl by particles of various grain sizes. The Rayleigh-type fractionation allows to demonstrate the evolution of stable isotopes from a homogenous pool. It has been suggested that the high temperature causes lighter ^{203}Tl isotope to enter the vapour phase, leaving the heavier ^{205}Tl isotope to become enriched in the slags, through processes of evaporation and condensation lead to isotopic fractionation, with kinetic isotope fractionation as a possible controlling factor (Liu et al., 2020a). In the fluidized-bed furnace of a sulphuric acid production plant, where temperatures reach 800–1000 °C, high amounts of Tl bound in pyrite begin to volatilize, while the remaining Tl can become concentrated in Fe-oxides (Yang et al., 2009; Liu et al., 2020a). The Tl vapour generated is recovered creating Tl with an isotopic composition relatively similar to the pyrite ore. After enduring such high temperatures, the temperatures drop to 400–450 °C in the boiler, then to 300–350 °C in the cyclone scrubber and finally to 150–200 °C in the electrostatic precipitation unit. The result of the changes in temperatures allows for the condensation of Tl from the vapour phases onto the fly ash particles where processes of adsorption and accumulation occur. The isotopic fractionation caused by different temperatures in different parts of the furnace, leads to isotopic variability of different fly ash samples, from the evaporation and condensation. The reducing particle sizes led to an increase in sorption capacity for volatile Tl, thereby enriching fly ash in light Tl isotopes, while heavy Tl isotopes remain enriched in the slag (Chen et al., 2013; Liu et al., 2020a).

In a study by Vaněk et al. (2022), the Tl isotopic ratios from a set of Tl-rich sulphide concentrates and wastes from hydrometallurgical Zn extraction were analysed. Thallium was found exclusively as Tl(I) and the Tl isotopic variability ranged between ε^{205}Tl −3.1 and −4.4. There was little to no evidence of initial sulphide pre-concentrations (ε^{205}Tl −4.4 and −4.2) affecting the isotopic compositions of the flotation product (ε^{205}Tl −3.9). The results of the Tl isotopic variability in the processing wastes (ε^{205}Tl −3.6 and −3.1), compared to the smelter feed (ε^{205}Tl −3.9), show insignificant isotopic fractionation, which was consistent with previous results found by Vaněk et al. (2018). This points to little or no influence of gangue mineralization on the Tl isotopic compositions and that the processing of the sulphide ores leads to insignificant Tl isotopic fractionation.

When comparing ores from various studies, each ore tends to have its own Tl isotopic signature, based upon the sulphide melt, deposit type, temperature, pressure, and the original matrix. For example, Liu et al. (2020a) determined Tl composition of ε^{205}Tl ~ +1.3, while Kersten et al. (2014) observed ε^{205}Tl ~ −0.4 for Meggen pyrite, Wickham (2014) found ε^{205}Tl ~ −1.3 for ore-stage pyrite and Vaněk et al. (2016) found ε^{205}Tl ~ −5.5 for Tl-rich coal pyrite. Grösslová et al. (2018) studied flotation tailings that had an average ^{205}Tl value of ε^{205}Tl ~ +6.2 which represents a possible reference of local mineralization, as the flotation tailings did not undergo any smelting or chemical processes. Hettmann et al. (2014) found values of ε^{205}Tl −2.7 for sphalerite and ε^{205}Tl −1.4 for galena. It was found that the principle behind the Tl isotopic variations in the sulphides was mass-independent fractionation involving a nuclear volume-dependent effect (Hettmann et al., 2014). In the study by Rader et al. (2018) the studied sulphides displayed ε^{205}Tl ranging between +1.6 and + 17.8, with 3 out of 6 samples showing a normal distribution of ε^{205}Tl values (ε^{205}Tl = +4.0 to +6.0). In a paper written by Zhou et al. (2022), studying Pb–Zn smelting, they observed significant variations in Tl isotopic composition of the raw material and different waste materials (shown in Table 1), these large variations attribute to the possibility of Tl isotopic fractionation during the entire smelting processes. The combination of the results and the application of the Rayleigh fractionation model proved the enrichment of heavy Tl isotopes in the waste slags and that volatile fractions formed during high-temperature processes were enriched in light Tl isotopes (Zhou et al., 2022).

The data from all the different industrial processes differ from one another, due to different raw materials and their properties and different temperatures and processes used, leading to unique Tl isotopic compositions for individual raw and waste materials.

3. Thallium isotopes in soils/sediments

Kersten et al. (2014) laid the groundwork for the first study revolving around applications of stable Tl isotope ratios to determine anthropogenic and geogenic Tl inputs into soils. The results displayed two separate Tl pools: one with high Tl concentrations and heavy isotope composition (ε^{205}Tl > -1.0) and one with low Tl concentrations and light Tl isotope compositions (ε^{205}Tl < -3.0). This suggests that heavier isotopic compositions are derived from anthropogenic origins, while light isotopic signatures represent the geogenic origins.

In naturally Tl-rich meadow and forest soils (Cambisols) studied by Vaněk et al. (2020) the isotope composition was the lightest in the C horizon (ε^{205}Tl ~ + 0.8 to + 2.6), becoming significantly heavier in the B horizon (ε^{205}Tl ~ + 8.7) and decreasing in the horizons above (ε^{205}Tl ~ + 2.5). The mineralogy of the soil was determined as quartz, K-feldspar, muscovite or illite, chlorite and illite/smectite and the bed associated with micaceous minerals had a ε^{205}Tl value of +1.6. Therefore, the enrichment of the heavy ^{205}Tl was ascribed to continuous mobilization and immobilization of Tl that was controlled by the redox cycles involving the parent material and soil forming processes. Heavy Tl isotope fractions from weathering of Tl(III)-containing phases and Tl(I) remobilization lead to the enrichment of ^{205}Tl into other phases, such as into illite. The systematic oxidative Tl uptake by Mn-oxides probably lead to a positive Tl isotopic shift. Vejvodová et al. (2020) observed a similar enrichment of heavier Tl isotopes between the A and B soil horizons of Cambisols, mainly composed of quartz, K-feldspar and plagioclase, ranging from ε^{205}Tl ~ +3.5 to +4. The soil samples also showed increased total Tl concentrations in the B horizon (1.6–3 mg/kg) compared to the A and C horizons, 13 to 1 mg/kg and 2 mg/kg, respectively. The horizons above and below were composed of lighter Tl isotope signatures (ε^{205}Tl −0 to +2) that were similar to the underlying bedrock (ε^{205}Tl + 1.6). The enrichment on heavy Tl isotopes can be explained by the presence of heavier Tl in the clay and Mn-oxide nodules (3 mg/kg Tl; ε^{205}Tl ~ +4.6 and 5 mg/kg Tl; +8.2, respectively), that underwent redox-reactions, resulting in heavier Tl isotopes in the middle profile.

The geochemical process that plays a role and controls Tl isotopic fractionation in soils is associated with Mn-oxides, where a positive relationship between Mn-oxide concentration and the degree of Tl isotopic fractionation is clearly observed (Vejvodová et al., 2020). With many studies proving Mn-oxides to play a role in the fractionation of Tl isotopes (Nielsen et al., 2013; Kersten et al., 2014; Vaněk et al., 2016,

2018; Howarth et al., 2018). A shift in Tl(I)–Tl(III) or vice versa is suggested as a major key control in Tl isotopic fractionation in soils (Wiederhold, 2015; Rader et al., 2018; Vejvodová et al., 2020).

Grösslová et al. (2018) observed different soil (Arenosols) profiles from an area contaminated with dust from flotation tailings (Zn–Pb ore deposits) and noticed that total Tl concentrations and ^{205}Tl decreased with depth (0.5–7.6 mg/Kg Tl; ε^{205}Tl ~ −0.4 to 3.8). The upper soil layers displaying a resemblance to the flotation wastes (13–27 mg/kg Tl; ε^{205}Tl ~ +6.1 to +6.3), therefore confirming the anthropogenic influence on the soil contamination. However, within soil horizons, the isotopic fractionation that is brought about through certain chemical processes cannot be fully derived from the anthropogenic source alone, therefore, there is some influence of geogenic Tl.

Two profiles (profile A and B, sampled at different distances (A closer and B further) from a Pb–Zn smelter in Guangdong Province, China) studied by Liu et al. (2022), displayed Tl isotopic compositions similar to that of the waste materials, and when recalculated, approximately 80% of the Tl was attributed by the smelter. The isotopic compositions of acid wastes (result of removal of SO_2 smoke) (ε^{205}Tl = −4.6), background sediments (ε^{205}Tl = +1.3) and smelter slag (ε^{205}Tl = +1.1) (Liu et al., 2020a; Zhou et al., 2022) indicate that the wastes play a major role in Tl input to the sediments (profile A ε^{205}Tl −2.4 to +1.2; profile B ε^{205}Tl −3.8 to +2.4).

Soils studied by Vaněk et al. (2018) displayed variations in the Tl isotope signature between the upper and lower horizons, with ^{205}Tl increasing with depth. The surface organic layers displayed light Tl isotopes that matched with anthropogenic origins (waste material ε^{205}Tl ~ −3.8). However, the soil profile depicts two Tl pools: anthropogenic and geogenic, with a higher predominance of the anthropogenic pool. The increase in the ^{205}Tl down the soil profile (up to ε^{205}Tl~ +0.4), does not reflect geogenic Tl inputs, as underlying soils have much lower Tl concentrations. In peat samples studied by Vaněk et al. (2021), the ability of peat to be used as an archive of atmospheric deposition was questioned. The peat samples had an isotopic variability of ε^{205}Tl ~ −3.6 to −1.1. The results showed that Tl was not present in industrial emissions over 250 years ago and that Tl is predominantly from local anthropogenic (ε^{205}Tl ~ −3 to −4) and geogenic/background (ε^{205}Tl~ 0 to −1) origins.

Therefore, processes related to sorption and precipitation likely controlled the heavier Tl isotopic composition. This highlights that there are isotopic processes that can lead to changes in primary isotopic data, which can complicate the source apportion.

4. Thallium isotopes in plants

Multiple studies have shown that the Brassica family is a hyper accumulator of Tl as the translocation of Tl into the brassica species were proven successful, with *Iberis intermedia* L, *Sinapis alba* L, *Brassica napus* L, *Biscutella laevigata* L, *Brassica oleracea* L. *var. capitata* L. as proven brassica Tl hyper accumulating species (Tremel et al., 1997; Xiao et al., 2004; Al-Najar et al., 2003, 2005; Scheckel et al., 2004, 2007; Krasnodębska-Ostręga et al., 2012; Jia et al., 2013; Grösslová et al., 2015; Ning et al., 2015; Liu et al., 2017, 2020b; Vaněk et al., 2010, 2011, 2013, 2015, 2019, 2020; Holubík et al., 2020, 2021). Other studies have also confirmed the accumulating and translocation abilities of the mustard plant (Krasnodębska-Ostręga et al., 2008, 2012; Holubík et al., 2020). Some studies have shown Brake fern (*Pteris vittata* L.) and green cabbage (*Brassica oleracea* L. *var. capitata* L.) to be hyper accumulators of Tl (Xiao et al., 2004; Jia et al., 2013; Wei et al., 2020). *Iberis intermedia* L. had highest concentrations of Tl in its leaves and was present as Tl(I). What was also noted was a link between vein sizes in leaves and Tl concentrations, with Ca being correlated with the distribution of Tl (Scheckel et al., 2004, 2007).

In green cabbage, approximately 80% of Tl concentrations were found in the leaves (Jia et al., 2013) with Tl concentrations in green cabbage accumulating in the cytosol and vacuole (Ning et al., 2015). Concentrations of Tl in vegetables grown on contaminated soils in China show that the Tl concentrations in green cabbage surpass that of other studied crops (e.g. Carrot, chilli, rice). The high Tl concentrations within the studied crops is believed to be due to the affinity/similarity Tl has with K and also displays a correlation between Tl, Ca and Mg (high Ca and Mg concentrations in plants were shown to increase uptake of Tl) (Xiao et al., 2004). Concentrations of Tl in green cabbage reached up to 500 mg/kg (dry weight), with higher accumulation in later growth stages, exceeding Tl concentrations of the soil (maximum Tl concentration in soil was 124 mg/kg) (Xiao et al., 2004). Higher concentrations of Tl in plants could be explained from the continuous release of mobile Tl, during erosion and weathering of primary sulphide mineralization, mining activity, coal use and farming activities. Indian mustard (*Brassica juncea* L.) studied by Rader et al. (2019), also observed considerably higher concentrations of Tl in the plants (3.8 mg/kg) than in the soils (0.1 mg/kg). Thallium was found in higher concentrations in plants compared to that of Hg and As, while the opposite effect was observed in soils, therefore indicating a preferential uptake of Tl. The study by Rader et al. (2019) along with the study by Grösslová et al. (2015) show that the bioaccessibility of Tl was heavily dependent on the mineralogy of the soils, especially on the K-feldspars and Mn-oxides, that when present in soils, can render Tl immobile.

Regarding Tl isotopes in plants, the number of studies are limited and the isotopic compositions in different parts of the plant is shown in Fig. 1 with ϵ^{205}Tl isotopic compositions ranging from −10.6 to +5. Studies have shown that plants prefer the uptake and accumulate lighter Tl due to the greater presence and plant availability of Tl(I) (Kersten et al., 2014). The pioneering study on Tl isotopes in plants showed an enrichment of light Tl isotopes in the soil-root interface, but that there was further fractionation along the translocation pathway from the roots (ϵ^{205}Tl −2.5) to the young leaves (ϵ^{205}Tl −5.4) (Kersten et al., 2014). The elevated concentration of Tl in the plants is explained by the high Tl levels in the rhizosphere, with the mobility controlled by many factors including water, pH, organic matter, mineralogy, speciation and cation exchange capacity. Thallium concentrations in the leaves of the green cabbage showed very high bioaccumulation, reaching 1000 mg/kg, compared to 30 mg/kg in the soil; with the distribution of Tl concentrations following the order old leaves > young leaves > stems > roots (Kersten et al., 2014). The distribution is slightly similar to that observed by Grösslová et al. (2015), where Tl was found distributed in the mustard plant (*Sinapis alba* L.) in the order stem > leaf > root. The study by Grösslová et al. (2015) also proved a strong correlation between Tl uptake by plant and the mineralogy of the soil, with results showing the influence of pH on secondary Tl phases. Soil mineralogy affected the bioavailability of Tl in the soils, with Mn(III, IV) oxides decreasing plant uptake of Tl and poorly-crystalline Fe(III) oxides or Ca-carbonates could promote Tl mobilization. Quantity and quality of soil organic matter (SOM) could be critical in controlling Tl bioaccumulation and soils that have lower pH were found to reduce the stability of secondary Tl phases in the rhizosphere, and therefore can be broken down by root exudates (Grösslová et al., 2015).

With regards to Tl isotopes in plants, the white mustard (*Sinapis alba* L.) favoured the uptake of light Tl isotopes (Vaněk et al., 2019), just like the study conducted by Kersten et al. (2014). However, a Tl isotope shift was observed during translocation in plants, with increases of heavy ^{205}Tl in the shoots (ε^{205}Tl < -2.5) when compared to the roots (ε^{205}Tl < -5.9). Mustard displayed substantial fractionation of Tl isotopes during the translocation between different tissues (ϵ^{205}Tl variation reaching −8 units). The ε^{205}Tl values in the shoots is dependent on the isotope fractionation that occurs during translocation, but also on the Tl isotope composition of the whole plant. With that being said, the heavier Tl isotopes found in above ground biomasses of plants, leads to the roots usually containing light Tl isotopic compositions (Vaněk et al., 2019).

The role of K^+ plays a dominant role in the Tl cycle, but there are other possible reasons for heavier Tl isotope enrichment during translocation. Other possibilities include Tl(I) complexation by specific

organic ligands that prefer the heavy ^{205}Tl isotope, and the association with S-coordinated Tl(I) (Vaněk et al., 2019). The results showed that when comparing the spectra of TlAsS2 with the plant parts, they did not closely match, meaning that S-coordinated Tl was not involved in the uptake of Tl and its fractionation. The XANES spectroscopy did show that the plant Tl spectra matched the spectra for Tl(I)-acetate and aqueous Tl^+, indicating the presence of O-coordinated Tl(I) as free Tl^+ or associated with O-containing functional groups.

In Indian mustard plants (*Brassica juncea* L.) studied by Rader et al. (2019) ^{205}Tl values were higher in the younger stages of plant development such as the earlier development of the stem ($\varepsilon^{205}Tl \sim +2.5$) compared to later developed plant parts such as flower and flower stems ($\varepsilon^{205}Tl \sim -0.2$) and seed pods ($\varepsilon^{205}Tl \sim -1.8$). This signifies the level of translocation that occurs within the plant during plant growth, with biological processes that occur during the plant development controlling the isotopic patterns (Rader et al., 2019).

The differences in translocation found in the mustard plants by Vaněk et al. (2019), Kersten et al. (2014) and Rader et al. (2019), could be due to different Tl concentrations in the growing medium (one in hydroponic systems, the other in contaminated soils and the other in Tl amended soils, respectively). The hydroponic systems had Tl concentrations of 0.1, 0.05 and 0.01 mg/L, the contaminated soils had 30 mg/kg of Tl and the Tl amended soils had concentrations of 0.1 mg/kg, 0.02 mg/kg and 20 mg/kg. Therefore, the origins and concentrations of Tl and its isotopic compositions in the growing medium seems to play a role in the uptake and translocation of Tl isotopes into plants.

The Tl isotopic composition helps in understanding the apportionment of Tl during uptake and translocation, and the behaviour of Tl in different plant species. It provides insight into the preference of light Tl isotopes in plants, and using the isotopic composition, helps to understand the fractionation that occurs along the translocation pathways. Different plants fractionate Tl differently, as described above, which could be correlated to the concentration of Tl in the soils, the source of the |Tl and the mineralogy of the soil, which can affect mobility and bioaccessibility of Tl. As mentioned by Rader et al. (2019) the use of isotopes helps in understanding the behaviour of Tl during both anthropogenic and geogenic processes and its uptake and redistribution in plants. Knowing which plants have the ability to uptake Tl and redistribute it in its above ground biomass helps in understanding which plants could be used in phytomining and bioprospecting processes.

5. Conclusion and perspectives

While there are numerous papers focused on Tl and slightly less on Tl isotopes, there is still a crucial need to understand Tl and its isotopic compositions in different anthropogenically affected environments and plants. Thus far, micaceous clays, especially illite, and Mn-oxides have been unequivocally confirmed as scavengers of Tl and control its mobility within soils. The Tl isotopic composition within soils were successfully traced back to the origins when comparing the isotopic values with parent materials and industrial (by)products, with plants grown in both contaminated and uncontaminated soils displaying different translocation behaviour, which also provide useful information as to the origins of Tl.

Most of the research agrees with one another in the processes involved in the fractionation of Tl in soils. One of the biggest controlling soil processes of Tl is the presence of Mn-oxides. It was shown in multiple studies, that Tl(I)–Tl(III) shifts are key controls in Tl isotopic fractionation. Additional insights into the exact Tl isotopic composition for exact phases of both geogenic and anthropogenic materials (Mn-nodules, micaceous clays, spectrum of Tl-rich waste materials) could be useful in better understanding of what roles they have within respective environments. Also, how and to which degree they can affect the isotopic fractionation of Tl. Chemical analysis used to identify Tl concentrations in specific phases would also prove useful in broadening the knowledge surrounding Tl isotopic fractionation. In other words, the verification of single extractions used for identification of specific Tl chemical fractions, which do not suffer from artificial method-related isotopic redistribution is a big deal in the future research. Through their application, the use of Tl isotopes in determining the source of the pollution can be an advantageous tool in implementing appropriate remediation measures. The use of isotopic fractionation data could be used to assess the progress of different environmental processes regarding immobilization or plant uptake of Tl. For example, Tl behaves differently depending on its source, so soils contaminated with anthropogenic Tl would behave differently from geogenic Tl, due to different Tl speciation and with Tl from anthropogenic sources likely to be more associated with labile fractions in soils and pose a higher risk for plants. That being said, the understanding on Tl isotopic fractionation and translocation within plants requires a better understanding, therefore, further research is required to get a better comprehension of all the processes involved in this field of studies.

Declaration of competing interest

The authors declare that they have no known competing financial interests or personal relationships that could have appeared to influence the work reported in this paper.

Acknowledgements

This study was funded by the projects of the Czech Science Foundation (GAČR 20-08717S) and the European Regional Development Fund (CZ.02.1.01/0.0/0.0/16_019/0000845).

References

Aguilar-Carrillo, J., Herrera-García, L., Reyes-Domínguez, I.A., Gutiérrez, E.J., 2020. Thallium (I) sequestration by jarosite and birnessite: structural incorporation vs surface adsorption. Environ. Pollut. 257, 113492. https://doi.org/10.1016/j.envpol.2019.113492.

Al-Najar, H., Schilz, R., Römheld, V., 2003. Plant availability of thallium in the rhizosphere of hyperaccumulator plants: a key factor for assessment of phytoextraction. Plant Soil 249, 97–105. https://doi.org/10.1023/A:1022544809828.

Al-Najar, H., Kaschl, A., Schulz, R., Römheld, V., 2005. Effect of thallium fractions in the soil and pollution origins on Tl uptake by hyperaccumulator plants: a key factor for the assessment of phytoextraction. Int. J. Phytoremediation 7, 55–67. https://doi.org/10.1080/16226510590915837.

Antić-Mladenović, S., Frohne, T., Kresović, M., Stärk, H.-J., Savić, D., Ličina, V., Rinklebe, J., 2017. Redox-controlled release dynamics of thallium in periodically flooded arable soil. Chemosphere 178, 268–276. https://doi.org/10.1016/j.chemosphere.2017.03.060.

Antón, M.A.L., Spears, D.A., Somoano, M.D., Tarazona, M.R.M., 2012. Thallium in coal: analysis and environmental implications. Fuel 105, 13–18. https://doi.org/10.1016/j.fuel.2012.08.004.

Bačeva, K., Stafilov, T., Šajn, R., Tănăselia, C., Makreski, P., 2014. Distribution of chemical elements in soils and stream sediments in the area of abandoned Sb-As-Tl Allchar mine, Republic of Macedonia. Environ. Res. 133, 77–89. https://doi.org/10.1016/j.envres.2014.03.045.

Baker, R.G.A., Rehkämper, M., Hinkley, T.K., Nielsen, S.G., Toutain, J.P., 2009. Investigation of thallium fluxes from subaerial volcanism- Implication for the present and past mass balance of thallium in the oceans. Geochem. Cosmochim. Acta 73, 6340–6359. https://doi.org/10.1016/j.gca.2009.07.014.

Baker, R.G.A., Rehkämper, M., Ihlenfeld, C., Oates, C.J., Coggon, R., 2010. Thallium isotope variations in an ore-bearing continental igneous setting: collahuasi Formation, northern. Chile. Geochem. Cosmochim. Acta 74, 4405–4416. https://doi.org/10.1016/j.gca.2010.04.068.

Belzile, N., Chen, Y., 2017. Thallium in the environment: a critical review focused on natural waters, soils, sediments and airborne particles. Appl. Geochem. 84, 218–243. https://doi.org/10.1016/j.apgeochem.2017.06.013.

Cabala, J., Teper, L., 2007. Metalliferous constituents of rhizosphere soils contaminated by Zn-Pb mining in southern Poland. Water, Air, Soil Pollut. 178, 351–362. https://doi.org/10.1007/s11270-006-9203-1.

Chen, Y.H., Wang, C.L., Liu, J., Wang, J., Qi, J.Y., Wu, Y.J., 2013. Environmental exposure and flux of thallium by industrial activities utilizing thallium-bearing pyrite. Sci. China Earth Sci. 56, 1502–1509. https://doi.org/10.1007/s11430-013-4621-6.

Cruz-Hernández, Y., Villalobos, M., Marcus, M.A., Pi-Puig, T., Zanella, R., Martínez-Villegas, N., 2019. Tl(I) sorption behaviour on birnessite and its implications for mineral structural changes. Geochem. Cosmochim. Acta 248, 356–369. https://doi.org/10.1016/j.gca.2019.01.020.

Đorđević, T., Drahota, P., Kolitsch, U., Majzlan, J., Peřestá, S., Kiefer, S., Stöger-Pollach, M., Tepe, N., Hofmann, T., Mikuš, T., Tasev, G., Serafimovski, T., Boev, I., Boev, B., 2021. Synergetic Tl and as retention in secondary minerals: an example of extreme arsenic and thallium pollution. Appl. Geochem. 135, 105114. https://doi.org/10.1016/j.apgeochem.2021.105114.

Dutrizac, J.E., 1997. The behaviour of thallium during jarosite precipitation. Metall. Mater. Trans. B 28, 765–776. https://doi.org/10.1007/s11663-997-0003-9.

Fitzpayne, A., Prytulak, J., Wilkinson, J.J., Cooke, D.R., Bakers, M.J., Wilkinson, C.C., 2018. Assessing thallium elemental systematics and isotope ratio variations in porphyry ore systems: a case study of the bingham canyon district. Minerals 8, 548. https://doi.org/10.3390/min8120548.

Galván-Arzate, S., Santamaría, A., 1998. Thallium toxicity. Toxicol. Lett. 99, 1–13. https://doi.org/10.1016/S0378-4274(98)00126-X.

Gomez-Gonzalez, M.A., Garcia-Guinea, J., Laborda, F., Garrido, F., 2015. Thallium occurrence and partitioning in soils and sediments affected by mining activities in Madrid province (Spain). Sci. Total Environ. 536, 268–278. https://doi.org/10.1016/j.scitotenv.2015.07.033.

Garrido, F., Garcia-Guinea, J., Lopez-Arce, P., Voegelin, A., Göttlicher, J., Mangold, S., Almendros, G., 2020. Thallium and co-genetic trace elements in hydrothermal Fe-Mn deposits of Central Spain. Sci. Total Environ. 717, 137162. https://doi.org/10.1016/j.scitotenv.2020.137162.

Gołębiowska, B., Pieczka, A., Zubko, M., Voegelin, A., Göttlicher, J., Rzepa, G., 2021. Thalliomelane, $TlMn^{4+}_{7.5}Cu^{2+}_{0.5}O_{16}$, a new member of the coronadite group from the preglacial oxidation zone at Zalas, southern Poland. Am. Mineral. 106, 2020–2027. https://doi.org/10.2138/am-2021-7577.

Grösslová, Z., Vaněk, A., Mihaljevič, M., Ettler, V., Hojdová, M., Zádorová, T., Pavlů, L., Penížek, V., Vaněčková, B., Komárek, M., Chrastný, V., Ash, C., 2015. Bioaccumulation of thallium in a neutral soil as affected by solid-phase association. J. Geochem. Explor. 159, 208–212. https://doi.org/10.1016/j.gexplo.2015.09.009.

Grösslová, Z., Vaněk, A., Oborná, V., Mihaljevič, M., Ettler, V., Trubač, J., Drahota, P., Penížek, V., Pavlů, L., Sracek, O., Kříbek, B., Voegelin, A., Göttlicher, J., Drábek, O., Tejnecký, V., Houška, J., Mapani, B., Zádorová, T., 2018. Thallium contamination of desert soil in Namibia: chemical, mineralogical and isotopic insights. Environ. Pollut. 239, 272–280. https://doi.org/10.1016/j.envpol.2018.04.006.

Heinrichs, H., Schulz-Dobrick, B., Wedepohl, K.H., 1980. Terrestrial geochemistry of Cd, Bi, Tl, Pb, Zn and Rb. Geochem. Cosmochim. Acta 44, 1519–1533. https://doi.org/10.1016/0016-7037(80)90116-7.

Herrmann, J., Voegelin, A., Palatinus, L., Mandold, S., Majzlan, J., 2018. Secondary Fe-as-Tl mineralization in soils near buus in the Swiss jura mountains. J. Mineral. 30, 887–898. https://doi.org/10.1127/ejm/2018/0030-2766.

Hettmann, K., Marks, M.A.W., Kreissig, K., Zack, T., Wenzel, T., Rehkämper, M., Jacob, D.E., Markl, G., 2014. The geochemistry of Tl and its isotopes during magmatic and hydrothermal processes: the peralkaline Ilimaussaq complex, southwest Greenland. Chem. Geol. 366, 1–13. https://doi.org/10.1016/j.chemgeo.2013.12.004.

Holubík, O., Vaněk, A., Mihaljevič, M., Vejvodová, K., 2020. Higher Tl bioaccessibility in white mustard (hyper-accumulator) grown under the soil than hydroponic conditions: a key factor for the phytoextraction use. J. Environ. Manag. 255, 109880. https://doi.org/10.1016/j.jenvman.2019.109880.

Holubík, O., Vaněk, A., Mihaljevič, M., Vejvodová, K., 2021. Thallium uptake/tolerance in a model (hyper)accumulating plant: effect of extreme contaminant loads. Soil Water Res. 16, 129–135. https://doi.org/10.17221/167/2020-SWR.

Howarth, S., Prytulak, J., Little, S.H., Hammond, S.J., Widdowson, M., 2018. Thallium concentration and thallium isotope composition of lateritic terrains. Geochem. Cosmochim. Acta 239, 446–462. https://doi.org/10.1016/j.gca.2018.04.017.

Jia, Y., Xiao, T., Zhou, G., Ning, Z., 2013. Thallium at the interface of soil and green cabbage (Brassica oleracea L. var. capitata L.): soil-plant transfer and influencing factors. Sci. Total Environ. 450–451, 140–147. https://doi.org/10.1016/j.scitotenv.2013.02.008.

Kaplan, D.I., Mattigod, S.V., 1998. Aqueous geochemistry of thallium. In: Nriagu, J.O. (Ed.), Thallium in the Environment, vol. 2. Wiley & Sons, New York, pp. 15–29.

Karbowska, B., 2016. Presence of thallium in the environment: sources of contaminations, distribution and monitoring. Environ. Monit. Assess. 188, 1–19. https://doi.org/10.1007/s10661-016-5647-y.

Karbowska, B., Rębiś, T., Milczarek, G., 2018. Electrode modified by reduced graphene oxide for monitoring of total thallium in grain products. Int. J. Environ. Res. Publ. Health 15, 653. https://doi.org/10.3390/ijerph15040653.

Kazantzis, G., 2000. Thallium in the environment and health effects. Environ Geochem Hlth 22, 275–280. https://doi.org/10.1023/A:1006791514080.

Kersten, M., Xiao, T., Kreissig, K., Brett, A., Coles, B.J., Rehkämper, M., 2014. Tracing anthropogenic thallium in soil using stable isotope compositions. Environ. Sci. Technol. 48, 9030–9036. https://doi.org/10.1021/es501968d.

Krasnodębska-Ostręga, B., Asztemborska, M., Strusińska, K., Golimowski, J., 2008. Determination of thallium form in plants extracts by anion exchange chromatography with inductively coupled plasma mass spectrometry detection (IC-ICP-MS). J. Anal. At. Spectrom. 23, 1632–1635. https://doi.org/10.1039/b804456b.

Krasnodębska-Ostręga, B., Sadowska, M., Ostrowska, S., 2012. Thallium speciation in plant tissue-Tl(III) found in Sinapis alba L. grown in soil polluted with tailing sediment containing thallium minerals. Talanta 93, 326–329. https://doi.org/10.1016/j.talanta.2012.02.042.

Lin, J., Yin, M., Wang, J., Liu, J., Tsang, D.C.W., Wang, Y., Lin, M., Li, H., Zhou, Y., Song, G., Chen, Y., 2020. Geochemical fractionation of thallium in contaminated soils near a large-scale Hg-Tl mineralised area. Chemosphere 239, 124775. https://doi.org/10.1016/j.chemosphere.2019.124775.

Lis, J., Pasieczna, A., Karbowska, B., Zembrzuski, W., Lukaszewski, Z., 2003. Thallium in soils and stream sediments of a Zn-Pb mining and smelting area. Environ. Sci. Technol. 37, 4569–4572. https://doi.org/10.1021/es0346936.

Liu, J., Wang, J., Chen, Y., Xie, X., Qi, J., Lippold, H., Luo, D., Wang, C., Su, L., He, L., Wu, Q., 2016. Thallium transformation and partitioning during Pb-Zn smelting and environmental implications. Environ. Pollut. 212, 77–89. https://doi.org/10.1016/j.envpol.2016.01.046.

Liu, J., Luo, X., Wang, J., Xiao, T., Chen, D., Sheng, G., Yin, M., Lippold, H., Wang, C., Chen, Y., 2017. Thallium contamination in arable soils and vegetables around steel plant- A newly-found significant source of Tl pollution in South China. Environ. Pollut. 224, 445–453. https://doi.org/10.1016/j.envpol.2017.02.025.

Liu, J., Yin, M., Xiao, T., Zhang, C., Tsang, D.C.W., Bao, Z., Zhou, Y., Chen, Y., Luo, X., Yuan, W., Wang, J., 2020a. Thallium isotopic fractionation in industrial process of pyrite smelting and environmental implications. J. Hazard Mater. 384, 121378. https://doi.org/10.1016/j.jhazmat.2019.121378.

Liu, J., Wei, X., Zhou, Y., Tsang, D.C.W., Bao, Z., Yin, M., Lippold, H., Yuan, W., Wang, J., Feng, Y., Chen, D., 2020b. Thallium contamination, health risk assessment and source apportionment in common vegetables. Sci. Total Environ. 703, 135547. https://doi.org/10.1016/j.scitotenv.2019.135547.

Liu, J., Ouyang, Q., Wang, L., Wang, J., Zhang, Q., Wei, X., Lin, Y., Zhou, Y., Yuan, W., Xiao, T., 2022. Quantification of smelter-derived contributions to thallium contamination in river sediments: novel insights from thallium isotope evidence. J. Hazard Mater. 424, 127594. https://doi.org/10.1016/j.jhazmat.2021.127594.

Martin, L.A., Wissocq, A., Benedetti, M.F., Latrille, C., 2018. Thallium (Tl) sorption onto illite and smectite: implications for Tl mobility in the environment. Geochem. Cosmochim. Acta 230, 1–16. https://doi.org/10.1016/j.gca.2018.03.016.

Migaszewski, Z.M., Gałuszka, A., 2021. Abundance and fate of thallium and its stable isotopes in the environment. Rev. Environ. Sci. Biotechnol. 20, 5–30. https://doi.org/10.1007/s11157-020-09564-8.

Nielsen, S.G., Rehkämper, M., Baker, J., Halliday, A.N., 2004. The precise and accurate determination of thallium isotope compositions and concentrations for water samples by MC-ICPMS. Chem. Geol. 204, 109–124. https://doi.org/10.1016/j.chemgeo.2003.11.006.

Nielsen, S.G., Rehkämper, M., Porcelli, D., Andersson, P., Halliday, A.N., Swarzenski, P. W., Latkoczy, C., Günther, D., 2005. Thallium isotope composition of the upper continental crust and rivers – an investigation of the continental sources of dissolved marine thallium. Geochem. Cosmochim. Acta 19, 2007–2019. https://doi.org/10.1016/j.gca.2004.10.025.

Nielsen, S.G., Rehkämper, M., Halliday, A.N., 2006a. Large thallium isotopic variations in iron meteorites and evidence for lead-205 in the early solar system. Geochem. Cosmochim. Acta 70, 2643–2657. https://doi.org/10.1016/j.gca.2006.02.012.

Nielsen, S.G., Rehkämper, M., Norman, M.D., Halliday, A.N., Harrison, A.N., 2006b. Thallium isotopic evidence for ferromanganese sediments in the mantle source of Hawaiian basalts. Nature 439, 314. https://doi.org/10.1038/nature04450. -314.

Nielsen, S.G., Rehkämper, M., Teagle, D.A.H., Butterfield, D., Halliday, A.N., 2006c. Hydrothermal fluid fluxes calculated from the isotopic mass balance of thallium in the ocean crust. Earth Planet Sci. Lett. 251, 120–133. https://doi.org/10.1016/j.epsl.2006.09.002.

Nielsen, S.G., Rehkämper, M., Brandon, A.D., Norman, M.D., Turner, S., O'Reilly, S.Y., 2007. Thallium isotopes in Iceland and Azores lavas- Implications for the role of altered crust and mantle geochemistry. Earth Planet Sci. Lett. 264, 332–345. https://doi.org/10.1016/j.epsl.2007.10.008.

Nielsen, S.G., Mar-Gerrison, S., Gannoun, A., LaRowe, D., Klemm, V., Halliday, A.N., Burton, K.W., Hein, J.R., 2009. Thallium isotope evidence for a permanent increase in marine organic carbon export in the early Eocene. Earth Planet Sci. Lett. 278, 297–307. https://doi.org/10.1016/j.epsl.2008.12.010.

Nielsen, S.G., Rehkämper, M., 2012. Thallium isotopes and their application to problems in earth and environmental science. In: Baskaran, M. (Ed.), Handbook of Environmental Isotope Geochemistry: Advances in Isotope Geochemistry, Part 2. Springer, Berlin, pp. 247–269.

Nielsen, S.G., Wasylenki, L.E., Rehkämper, M., Peacock, C.L., Xue, Z., Moon, E.M., 2013. Towards an understanding of thallium isotope fractionation during adsorption to manganese oxides. Geochem. Cosmochim. Acta 117, 252–265. https://doi.org/10.1016/j.gca.2013.05.004.

Nielsen, S.G., Rehkämper, M., Prytulak, J., 2017. Investigation and application of thallium isotope fractionation. Rev. Mineral. Geochem. 82, 759–798. https://doi.org/10.2138/rmg.2017.82.18.

Ning, Z., He, I., Xiao, T., Márton, L., 2015. High accumulation and subcellular distribution of thallium in green cabbage (*Brassica Oleracea* L. *Var Capitata* L. Int. J. Phytoremediation 17, 1097–1104. https://doi.org/10.1080/15226514.2015.1045133.

Nriagu, J., 1998. Thallium in the Environment. Wiley, New York.

Peacock, C.L., Moon, E.M., 2012. Oxidative scavenging of thallium by birnessite: explanation for thallium enrichment and stable isotope fractionation in marine ferromanganese precipitates. Geochem. Cosmochim. Acta 84, 297–313. https://doi.org/10.1016/j.gca.2012.01.036.

Peter, A.L.J., Viraraghavan, T., 2005. Thallium: a review of public health and environmental concerns. Environ. Int. 31, 493–501. https://doi.org/10.1016/j.envint.2004.09.003.

Prytulak, J., Nielsen, S.G., Plank, S.G., Plank, T., Barker, M., Elliott, T., 2013. Assessing the utility of thallium and thallium isotopes for tracing subduction zone inputs to the Mariana arc. Chem. Geol. 345, 139–149. https://doi.org/10.1016/j.chemgeo.2013.03.003.

Rader, S.T., Mazdab, F.K., Barton, M.D., 2018. Mineralogical thallium geochemistry and isotope variations from igneous, metamorphic, and metasomatic systems. Geochem. Cosmochim. Acta 243, 42–65. https://doi.org/10.1016/j.gca.2018.09.019.

Rader, S.T., Maier, R.N., Barton, M.D., Mazdab, F.K., 2019. Uptake and fractionation of thallium by *Brassica juncea* in geogenic thallium-amended substrate. Environ. Sci. Technol. 53, 2441–2449. https://doi.org/10.1021/acs.est.8b06222.

Rehkämper, M., Halliday, A.N., 1999. The precise measurement of Tl isotopic compositions by MC-ICPMS: application to the analysis of geological materials and meteorites. Geochem. Cosmochim. Acta 63, 935–944. https://doi.org/10.1016/S0016-7037(98)00312-3.

Rehkämper, M., Frank, M., Hein, J.R., Halliday, A., 2004. Cenozoic marine geochemistry of thallium deduced from isotopic studies of ferromanganese crusts and pelagic sediments. Earth Planet Sci. Lett. 219, 77–91. https://doi.org/10.1016/S0012-821X(03)00703-9.

Scheckel, K.G., Lombi, E., Rock, S.A., McLaughlin, M.J., 2004. In Vivo synchrotron study of thallium speciation and compartmentation in *Iberis Intermedia*. Environ. Sci. Technol. 38, 5059–5100. https://doi.org/10.1021/es049569g.

Scheckel, K.G., Hamon, R., Jassogne, L., Rivers, M., Lombi, E., 2007. Synchrotron X-ray absorption-edge computed microtomography imaging of thallium compartmentalization in *Iberis intermedia*. Plant Soil 290, 51–60. https://doi.org/10.1007/s11104-006-9102-7.

Shannon, R.D., 1976. Revised effective ionic radii and systematic studies of interatomic distances in halides and chalcogenides. Acta Crystallogr. A32, 751–767. https://doi.org/10.1107/S056773947600155.

Tremel, A., Masson, P., Garroud, H., Donard, O.F.X., Baize, D., Mench, M., 1997. Thallium in French agrosystems-II. Concentration of thallium in field-grown rap and some other plant species. Enviorn Pollut 97, 161–168. https://doi.org/10.1016/S0269-7491(97)00060-2.

Vaněk, A., Chrastný, V., Mihaljevič, M., Drahota, P., Grygar, T., Komárek, M., 2009. Lithogenic thallium behavior in soils with different land use. J. Geochem. Explor. 102, 7–12. https://doi.org/10.1016/j.gexplo.2008.10.004.

Vaněk, A., Komárek, M., Chrastný, V., Bečka, D., Mihaljevič, M., Šebek, O., Panušková, G., Schusterová, Z., 2010. Thallium uptake by white mustard (Sinapis alba L.) grown on moderately contaminated soils- Agro-environmental implications. J. Hazard Mater. 182, 303–308. https://doi.org/10.1016/j.jhazmat.2010.06.030.

Vaněk, A., Komárek, M., Vorkurková, P., Mihaljevič, M., Šebek, O., Panušková, G., Chrastný, V., Drábek, O., 2011. Effect of Illite and birnessite on thallium retention and bioavailability in contaminated soils. J. Hazard Mater. 191, 170–176. https://doi.org/10.1016/j.jhazmat.2011.04.065.

Vaněk, A., Mihaljevič, M., Galušková, I., Chrastný, V., Komárek, M., Penížek, V., Zádorová, T., Drábek, O., 2013. Phase-dependent phytoavailability of thallium- a synthetic soil experiment. J. Hazard Mater. 250–251, 265–271. https://doi.org/10.1016/j.jhazmat.2013.01.076.

Vaněk, A., Grösslová, Z., Mihaljevič, M., Ettler, V., Chrastný, V., Komárek, M., Tejnecký, V., Drábek, O., Penížek, V., Galušková, I., Vaněčková, B., Pavlů, L., Ash, C., 2015. Thallium contamination of soils/vegetation as affected by sphalerite weathering: a model rhizospheric experiment. J. Hazard Mater. 283, 148–156. https://doi.org/10.1016/j.jhazmat.2014.09.018.

Vaněk, A., Grösslová, Z., Mihaljevič, M., Trubač, J., Ettler, V., Teper, L., Cabala, J., Rohovec, J., Zádorová, T., Penížek, V., Pavlů, L., Holubík, O., Němeček, K., Houška, J., Drábek, O., Ash, C., 2016. Isotopic tracing of thallium contamination in soils affected by emissions from coal-fired power plants. Environ. Sci. Technol. 50, 9864–9871. https://doi.org/10.1021/acs.est.6b01751.

Vaněk, A., Grösslová, Z., Mihaljevič, M., Ettler, V., Trubač, J., Chrastný, V., Penížek, V., Teper, L., Cabala, J., Voegelin, A., Zádorová, T., Oborná, V., Drábek, O., Holubík, O., Houška, J., Pavlů, L., Ash, C., 2018. Thallium isotopes in metallurgical wastes/contaminated soils: a novel tool to trace metal source and behavior. J. Hazard Mater. 343, 78–85. https://doi.org/10.1016/j.jhazmat.2017.09.020.

Vaněk, A., Holubík, O., Odborná, V., Mihaljevič, M., Trubač, J., Ettler, V., Pavlů, L., Vokurková, P., Penížek, V., Zádorová, T., Voegelin, A., 2019. Thallium stable isotope fractionation in white mustard: implications for metal transfers and incorporation in plants. J. Hazard Mater. 369, 521–527. https://doi.org/10.1016/j.jhazmat.2019.02.060.

Vaněk, A., Voegelin, A., Mihaljevič, M., Ettler, V., Trubač, J., Drahota, P., Vaňková, M., Oborná, V., Vejvodová, K., Penížek, V., Pavlů, L., Drábek, O., Vokurková, P., Zádorová, T., Holubík, O., 2020. Thallium stable isotope ratios in naturally Tl-rich soils. Geoderma 364, 114183. https://doi.org/10.1016/j.geoderma.2020.114183.

Vaněk, A., Vejvodová, K., Mihaljevič, M., Ettler, V., Trubač, J., Vaňková, M., Goliáš, V., Teper, L., Sutkowska, K., Vokurková, P., Penížek, V., Zádorová, T., Drábek, O., 2021. Thallium and lead variations in a contaminated peatland: a combined isotopic study from a mining/smelting area. Environ. Pollut. 290, 117973. https://doi.org/10.1016/j.envpol.2021.117973.

Vaněk, A., Vejvodová, K., Mihaljevič, M., Ettler, V., Trubač, J., Vaňková, M., Teper, L., Cabala, J., Sutkowska, K., Voegelin, A., Göttlicher, J., Holubík, O., Vokurková, P., Pavlů, L., Galušková, I., Zádorová, T., 2022. Evaluation of thallium isotopic fractionation during the metallurgical processing of sulphides: an update. J. Hazard Mater. 424, 127325. https://doi.org/10.1016/j.jhazmat.2021.127325. Part A.

Vejvodová, K., Vaněk, A., Mihaljevič, M., Ettler, V., Trubač, J., Vaňková, M., Drahota, P., Vorkurková, P., Penížek, V., Zádorová, T., Tejnecký, V., Pavlů, L., Drábek, O., 2020. Thallium isotopic fractionation in soil: the key controls. Environ. Pollut. 265, 114822. https://doi.org/10.1016/j.envpol.2020.114822. Part A.

Voegelin, A., Pfenninger, N., Petrikis, J., Majzlan, J., Plötze, M., Senn, A.-C., Mangold, S., Steininger, R., Göttlicher, J., 2015. Thallium speciation and extractability in a thallium- and arsenic-rich soil developed from mineralized carbonate rock. Environ. Sci. Technol. 49, 5390–5398. https://doi.org/10.1021/acs.est.5b00629.

Wang, L., Jin, Y., Weiss, D.J., Schleicher, N.J., Wilcke, W., Wu, L., Guo, Q., Chen, J., O'Connor, D., Hou, D., 2021. Possible application of stable isotope compositions for the identification of metal sources in soil. J. Hazard Mater. 407, 124812. https://doi.org/10.1016/j.jhazmat.2020.124812.

Wei, X., Zhou, Y., Tsang, D.C.W., Song, L., Zhang, C., Yin, M., Liu, J., Viao, T., Zhang, G., Wang, J., 2020. Hyperaccumulation and transport mechanism of thallium and arsenic in brake ferns (*Pteris vittata* L.): a case study from mining area. J. Hazard Mater. 388, 121756. https://doi.org/10.1016/j.jhazmat.2019.121756.

Wick, S., Baeyens, B., Fernandes, M.M., Voegelin, A., 2018. Thallium adsorption onto illite. Environ. Sci. Technol. 52, 571–580. https://doi.org/10.1021/acs.est.7b04485.

Wick, S., Peña, J., Voegelin, A., 2019. Thallium sorption onto manganese oxides. Environ. Sci. Technol. 53, 13168–13178. https://doi.org/10.1021/acs.est.9b04454.

Wick, S., Baeyens, B., Fernandes, M.M., Göttlicher, J., Gischer, M., Pfenninger, N., Plötze, M., Voegelin, A., 2020. Thallium sorption and speciation in soils: role of micaceous clay minerals and manganese oxides. Geochem. Cosmochim. Acta 288, 83–100. https://doi.org/10.1016/j.gca.2020.07.037.

Wickham, K., 2014. Thallium Isotope Implications for the Metalliferous Source of Carlin-Type Gold Deposits in Northern Nevada. Master's Thesis, University of Nevada, Reno, NV, USA.

Wiederhold, J.G., 2015. Metal stable isotope signatures as tracers in environmental geochemistry. Environ. Sci. Technol. 49, 2606–2624. https://doi.org/10.1021/es504683e.

Xiao, T., Guha, J., Boyle, D., Liu, C.Q., Chen, J., 2004. Environmental concerns related to high thallium levels in soils and thallium uptake by plants in southwest Guizhou, China. Sci. Total Environ. 318, 223–244. https://doi.org/10.1016/S0048-9697(03)00448-0.

Xiao, T., Yang, F., Li, S., Zheng, B., Ning, Z., 2012. Thallium pollution in China: a geo-environmental perspective. Sci. Total Environ. 421–422, 51–58. https://doi.org/10.1016/j.scitotenv.2011.04.008.

Yang, C., Chen, Y., Peng, P., Li, C., Chang, X., C, X., 2005. Distribution of natural and anthropogenic thallium in the soils in an industrial pyrite slag disposing area. Sci. Total Environ. 341, 159–172. https://doi.org/10.1016/j.scitotenv.2004.09.024.

Yang, C., Chen, Y., Peng, P., Li, C., Chang, X., Wu, Y., 2009. Trace element transformations and partitioning during the roasting of pyrite ores in the sulphuric acid industry. J. Hazard Mater. 167, 835–845. https://doi.org/10.1016/j.jhazmat.2009.01.067.

Zhou, Y., He, H., Wang, J., Liu, J., Lippold, H., Bao, Z., Wang, L., Lin, Y., Fang, F., Huang, Y., Jiang, Y., Xiao, T., Yuan, W., Wei, X., Tsang, D.C.W., 2022. Stable isotope fractionation of thallium as novel evidence for its geochemical transfer during lead-zinc smelting activities. Sci. Total Environ. 803, 150036. https://doi.org/10.1016/j.scitotenv.2021.150036.

Zhuang, W., Liu, M., Song, J., Ying, S.C., 2021. Retention of thallium by natural minerals: a review. Sci. Total Environ. 777, 146074. https://doi.org/10.1016/j.scitotenv.2021.146074.